# Valorization of Biorefinery Side Streams and Systemic Analysis of the Adaptation towards Anaerobiosis – Studies with *Corynebacterium glutamicum*

DISSERTATION

Von der Fakultät Energie-, Verfahrens- und Biotechnik der Universität Stuttgart zur Erlangung der Würde eines Doktors der Naturwissenschaften (Doctor rerum naturalium, Dr. rer. nat.) genehmigte Abhandlung

Vorgelegt von

**Julian Lange**

aus Aalen

Hauptberichter: Prof. Dr.-Ing. Ralf Takors

Mitberichter: Prof. Dr. Bernhard Hauer

Tag der mündlichen Prüfung: 04.07.2018

University of Stuttgart
Germany

Institut für Bioverfahrenstechnik

(Institute of Biochemical Engineering)

2018

**German Title:**

Verwertung von Bioraffinerienebenströmen und die systemische Analyse einer Anpassung von Aerobiose zu Anaerobiose – Untersuchungen mit *Corynebacterium glutamicum*

*To my love Vanessa,*
*my daughter Luna,*
*my Parents,*
*and my Family*

*"Being clever was when you looked at how things were and used the evidence to work out something new."*

Christopher John Francis Boone
Protagonist in
*The Curious Incident of the Dog in the Night-time*
by Mark Haddon

The experimental work (with exception of RNA-sequencing analysis) framing this manuscript was conducted under leadership and supervision of Prof. Dr.-Ing. Ralf Takors and Dr. Bastian Blombach at the Institute of Biochemical Engineering (University of Stuttgart, Germany) within the time span of 2014-2017.

The project was supported by a grant from the Ministry of Science, Research and the Arts of Baden-Württemberg (Az: 33-7533-10-5/84/1) as part of the BBW ForWerts Graduate Program.

Parts of this work have been published in peer-reviewed journals.

**Lange, J.**, Müller, F., Takors, R., and Blombach, B. (2018) Harnessing novel chromosomal integration loci to utilize an organosolv-derived hemicellulose fraction for isobutanol production with engineered *Corynebacterium glutamicum*. *Microb. Biotechnol*. **11**: 257–263.

**Lange, J.**, Müller, F., Bernecker, K., Dahmen, N., Takors, R., and Blombach, B. (2017) Valorization of pyrolysis water: a biorefinery side stream, for 1,2-propanediol production with engineered *Corynebacterium glutamicum*. *Biotechnol. Biofuels* **10**: 277.

**Lange, J.**, Takors, R., and Blombach, B. (2017) Zero-growth bioprocesses – a challenge for microbial production strains and bioprocess engineering. *Eng. Life Sci.* **17**: 27–35.

**Lange, J.**, Münch, E., Müller, J., Busche, T., Kalinowski, J., Takors, R., and Blombach, B. (2018) Deciphering the adaptation of *Corynebacterium glutamicum* in transition from aerobiosis via microaerobiosis to anaerobiosis. *Genes*. **9**: 297.

Excerpts of this research have additionally been presented at international conferences as posters (*) or talks (°).

* **Lange, J.**, Busche, T., Kalinowski, J., Takors, R., Blombach, B. (09/2017) Facing a gradual shift from aerobiosis to anaerobiosis – the regulatory perspective in *Corynebacterium glutamicum*. *ProkaGENOMICS 2017: 7th European Conference on Prokaryotic and Fungal Genomics, Göttingen, Germany.*

° **Lange, J.** (09/2017) Exploiting biorefinery side streams for the microbial production of chemicals. *2nd Bioeconomy Congress, Hohenheim, Germany.*

* **Lange, J.**, Busche, T., Kalinowski, J., Takors, R., Blombach, B. (12/2016) Systems biology provides holistic insights into *Corynebacterium glutamicum*'s adaptation towards anaerobiosis. *Stuttgart Research Center Systems Biology (SRCSB) Workshop, Stuttgart, Germany.*

* **Lange, J.**, Müller, F., Bernecker, K., Busche, T., Kalinowski, J., Takors, R., Blombach, B. (10/2016) Development and systemic optimization of lignocellulose-based production processes with *Corynebacterium glutamicum*. *2nd Status Seminar Bioeconomy Baden-Württemberg, Stuttgart, Germany.*

* **Lange, J.**, Busche, T., Kalinowski, J., Takors, R., Blombach, B. (09/2016) Deciphering the response of *Corynebacterium glutamicum* to oxygen deprivation. *VAAM – Mechanisms of Gene Regulation Meeting 2016, Bad Bergzabern, Germany.*

* **Lange, J.,** Busche, T., Kalinowski, J., Takors, R., and Blombach, B. (12/2016) A systems biology-motivated approach to improve dual-phase production processes with *Corynebacterium glutamicum*. *Chemie Ing. Tech.* 88: 1408–1408. *DECHEMA ProcessNet Congress 2016, Aachen, Germany*

* **Lange, J.**, Busche, T., Kalinowski, J., Takors, R., Blombach, B. (06/2016) Advancing zero-growth production strategies with *Corynebacterium glutamicum* through systems biology. *Metabolic Engineering 11 Conference, Kobe, Japan.*

* **Lange, J.**, Busche, T., Kalinowski, J., Takors, R., Blombach, B. (05/2016) Transition from aerobiosis to anaerobiosis – deciphering the adaptation of *Corynebacterium glutamicum* to various oxygen availabilities. *DECHEMA Himmelfahrtstagung 2016. Koblenz, Germany.*

* **Lange, J.**, Busche, T., Kalinowski, J., Takors, R., Blombach, B. (03/2016) Transition from aerobiosis to anaerobiosis – deciphering the adaptation of *Corynebacterium glutamicum* to various oxygen availabilities. *VAAM Annual Conference 2016, Jena, Germany.*

* **Lange, J.**, Takors, R., Blombach, B. (10/2015) Transition from aerobiosis to anaerobiosis - enlightening the weak spot of dual-phase production processes with *Corynebacterium glutamicum*. *1st Status Seminar Bioeconomy Baden-Württemberg, Hohenheim, Germany.*

# ACKNOWLEDGEMENTS

Three years of research involves many contributors from inside and outside of the scientific community. With this short paragraph I want to offer my appreciation to friends and colleagues involved in the success of the overall project. Apart from the named persons I am grateful for the many further contributors, who are, due to the lack of space, not mentioned here, but supported the ongoing research and perpetually encouraged me during the entire time frame.

First, I want to mention Prof. Dr.-Ing. Ralf Takors, my doctoral advisor, who leads the Institute of Biochemical Engineering (IBVT) and provided this well-equipped and professionally organized workplace as platform for the practical realization of my scientific energy. Also, I direct my thankfulness to the Co-examiner Prof. Dr. Bernhard Hauer and examination chair Prof. Dr. Stephan Nußberger.

The most important contributor concerning the project, research topic, scientific daily routine and publishing is Dr. Bastian Blombach, who leads the group *Molecular Biotechnology* at the IBVT with his profoundly inspirational and motivating personality. His expert knowledge in *Corynebacterium glutamicum*, industrial biotechnology and experimental design significantly directed the progression of the project. Thank you, Basti, for the opportunity to participate in numeral conferences and faith to represent the institute and research. I want to thank the whole directory board (Prof. Dr. Thomas Rausch, PhD Ines Petersen, Anni Mandel and Jean Maples) of the BBW-ForWerts graduate school for excellent organization of method courses, workshops and summer schools and for enabling the evaluation of the project in annual meetings of my Thesis Advisory Committee (TAC) [comprising Prof. Dr.-Ing. Ralf Takors, Prof. Dr. Bernhard Eikmanns and

Dr. Bastian Blombach]. The graduate program truly broadened my view of bioeconomy through a marvelously heterogeneous and international group. I want to thank Prof. Dr. Bernhard Eikmanns from the Institute of Microbiology and Biotechnology at the Ulm University, who delivered plasmids, willingly participated in the TAC meetings and took the burden to travel to Stuttgart. He contributed with his expertise in *C. glutamicum* and microbiology to evaluate the project's progression and to generate new ideas and problem solution strategies.

No research can be adequately successful without fruitful collaboration. Therefore, I appreciate the cooperation with Prof. Dr. J. Kalinowski and Dr. Tobias Busche at the Center for Biotechnology (CeBiTec) at the University of Bielefeld, who willingly accepted me as temporary researcher in their laboratory, made RNA-sequencing of my experimental samples possible and supported me during interpretations. Prof. Dr. J. Kalinowski also kindly provided strains of *C. glutamicum*. Furthermore, I thank Prof. Dr. Nicolaus Dahmen (Institute of Catalysis Research and Technology (IKFT) at the Karlsruhe Institute of Technology (KIT)) and Dr.-Ing. Susanne Zibek (Fraunhofer Institute for Interfacial Engineering and Biotechnology (IGB), Stuttgart) for providing the renewable resources from the bioliq® plant and organosolv processing, respectively.

I am grateful for the experimental contribution of especially Felix Müller and Johanna Rapp but also of Kerstin Bernecker and Jan Müller to the overall project by their master theses and research associate occupations, respectively.

For GC analytic, molecular biology and coffee/cafeteria discussions, I thank Dr. Bernd Nebel, Maike Lenz and Dr. Julia Halder from the Institute of Technical Biochemistry at the University of Stuttgart and Dr. Johannes Maier from the Department of Biochemistry University of Stuttgart.

Mira Lenfers-Lücker and Eugenia Münch I thank for assistance during HPLC analytics, Andreas Schwentner, Salaheddine Laghrami, and Andreas Freund for bioprocess conceptions and Joana Simen and Michaela Graf, who lend their support during analysis, evaluation and interpretation of the RNA-sequencing results. I thank our good soul of the IBVT administration Silke Reu, who was patient with cheeky PhD students and complicated travel organizations, contract and financial

issues.

Last but not least, I want to thank my love Vanessa, my parents, my whole family and friends who backed me up within the entire timeframe of the work. They distracted me during hard times of the project and had an open ear (and questioning looks) during my scientific monologs that non-experts can hardly grasp.

Thank you.

# AUTHORS' CONTRIBUTIONS AND CO-WORKERS

I personally conducted the experimental work, interpreted the results, created figures and tables and drafted the manuscript. I was assisted by Felix Müller, Johanna Rapp, Jan Müller and Kerstin Bernecker at the practical realization and Dr. Tobias Busche during RNA-sequencing. Dr. Bastian Blombach conceptualized the project and supported the experimental design, interpretation of the experiments and manuscript writing. Prof. Dr. Nicolaus Dahmen, Dr.-Ing. Susanne Zibek, Prof. Dr. J. Kalinowski and Prof. Dr. Bernhard Eikmanns provided the pyrolysis water, the hemicellulose fraction, *C. glutamicum* Δ*oxyR* and the plasmid pK19Δ*ramB*, respectively. Prof. Dr.-Ing. Ralf Takors enabled access to facilities and laboratory equipment.

# CONTENTS

# FIGURE DIRECTORY

# TABLE DIRECTORY

# SUPPLEMENTARY FIGURES

# SUPPLEMENTARY TABLES

# NOMENCLATURE

**Table 1.1. Abbreviations and descriptions**.

| Abbreviation | Description |
|---|---|
| 1G | First-generation |
| 2G | Second-generation |
| 2x YT | 2x yeast tryptone |
| 6PG-DH | Phosphogluconate dehydrogenase |
| A | Volumetric enzyme activity |
| a | Specific enzyme activity |
| α | $CDW/OD_{600}$ correlation coefficient |
| a-value | Average value of two $log_2TPM$ values used for m-value calculation |
| ABC | ATP-binding cassette or annual basis carbon |
| *aceA* | Isocitrate lyase (gene) |
| *aceB* | Malate synthase (gene) |
| *aceE* | E1p subunit of the pyruvate dehydrogenase complex (gene) |
| Acetyl-CoA | Acetyl-coenzyme A |
| ACN | Aconitate hydratase |
| *adhA* | Alcohol dehydrogenase (gene) |
| ADP | Adenosine diphosphate |
| AK | Acetate kinase |
| *alaT* | Alanine aminotransferase (gene) |
| *ald* | Acetaldehyde dehydrogenase (gene) |
| AMP | Adenosine monophosphate |
| *araA* | L-Arabinose isomerase (gene) |
| *araB* | L-Ribulokinase (gene) |
| *araC* | L-Ribulose-5-phosphate 4-epimerase (gene) |
| ArcBA | Two-component regulatory system (anoxic redox control) |
| *aspT* | Aspartate aminotransferase (gene) |
| ATP | Adenosine triphosphate |
| *atpBEFHAGDC* | $H^+$-ATPase (genes) |
| β | Buffer capacity |
| *B. subtilis* | *Bacillus subtilis* |
| BHI | Brain heart infusion |
| BHIS | BHI medium supplemented with 91 g $L^{-1}$ sorbitol |
| BLAST | Basic local alignment search tool |
| BSA | Bovine serum albumin |
| c | Concentration |
| *C. glutamicum* | *Corynebacterium glutamicum* |
| CDW | Cell dry weight |
| CeBiTec | Center for Biotechnology |
| CER | $CO_2$ evolution rate |
| cf. | Confer |
| CgLP | *Corynebacterium glutamicum* landing pad |
| *chrSA* | Two-component system involved in heme resistance |
| Cm | Chloramphenicol |
| C-mol | Carbon-mol |

| Abbreviation | Description |
|---|---|
| COG | Clusters of orthologous genes |
| Crp | cAMP receptor protein |
| CS | Citrate synthase |
| *cspA* | Cold-shock protein A (gene) |
| d | Diameter |
| D | Dilution factor |
| Δ | Delta |
| DAD | Diode array detector |
| DECHEMA | Deutsche Gesellschaft für chemisches Apparatewesen, Chemische Technik und Biotechnologie e.V. |
| $dH_2O$ | Deionized water |
| DHAP | Dihydroxyacetone phosphate |
| Dld | Quinone-dependent D-lactate dehydrogenase |
| DMSO | Dimethyl sulfoxide |
| DNA | Deoxyribonucleic acid |
| DNAP | DNA-polymerase |
| DO | Dissolved oxygen concentration |
| DOOR | Devoid of oxygen respiration |
| DP | Degree of polymerization |
| DTT | Dithiotreitol |
| ε | Extinction coefficient |
| *E. coli* | *Escherichia coli* |
| e.g. | Exempli gratia (for example) |
| EDTA | Ethylenediamine tetraacetic acid |
| EF-TU | Elongation factor TU |
| EMP | Embden-Meyerhof-Parnas |
| *et al.* | Et aliae (and others) |
| f | Femto (in combination with SI units) |
| F6P | Fructose-6-phosphate |
| *farR* | Transcriptional regulator, GntR-family (gene) |
| *FBP* | Fructose-1,6-bisphosphatase |
| *fbp* | Fructose-1,6-bisphosphatase (gene) |
| FDA | U.S. food and drug administration or fructose-bisphosphate aldolase |
| *fda* | Fructose-bisphosphate aldolase (gene) |

| Abbreviation | Description |
|---|---|
| FID | Flame ionization detector |
| FLD | Fluorescence detector |
| Fmoc | 9-Fluorenylmethoxy-carbonyl chloride |
| Fnr | DNA-binding transcriptional dual regulator (fumarate and nitrate reduction) |
| *fucO* | Propanediol oxidoreductase/ lactaldehyde reductase (gene) |
| FUM | Fumarate hydratase |
| *fum* | Fumarate hydratase (gene) |
| Fur | Ferric uptake regulator |
| g | Gram |
| G6P-DH | Glucose-6-phosphate dehydrogenase |
| GAP or GA3P | Glyceraldehyde-3-phosphate |
| *gapA* | Glyceraldehyde-3-phosphate dehydrogenase (gene) |
| GC | Gas chromatography |
| *gdh* | Glutamate dehydrogenase (gene) |
| *genR* | Transcriptional activator of gentisate catabolism (gene) |
| *gldA* | Glycerol dehydrogenase (gene) |
| *gltA* | citrate synthase (gene) |
| Glu | L-Glutamate |
| *glyA* | Serine hydroxymethyltransferase (gene) |
| *gnd* | 6-Phosphogluconate dehydrogenase (gene) |
| h | Hours |
| HF | Hemicellulose fraction |
| HMF | Hydroxymethylfurfural |
| HPLC | High performance liquid chromatography |
| HT | Heat treated |
| HTH | Helix turn helix |
| i.e. | Id est (that is to say) |
| IBVT | Institute of Biochemical Engineering |
| ICD | Isocitrate dehydrogenase |
| ICL | Isocitrate lyase |
| *iclR* | Activator of putative hydroxyquinol pathway genes (gene) |

| Abbreviation | Description |
|---|---|
| IGB | Fraunhofer Institute for Interfacial Engineering and Biotechnology |
| IKFT | Institute of Catalysis Research and Technology |
| Ile | L-Isoleucine |
| *ilvC* | Acetohydroxyacid isomeroreductase (gene) |
| *ilvD* | Dihydroxyacid dehydratase (gene) |
| *ilvE* | Transaminase B (gene) |
| *ivlBN* | Acetohydroxyacid synthase (gene) |
| Kan | Kanamycin |
| KBBE | Knowledge-based bioeconomy |
| $K_D$ | Dissociation constant |
| KIT | Karlsruhe Institute of Technology |
| *kivd* | 2-Ketoacid decarboxylase (gene) |
| $K_M$ | Michaelis Menten constant |
| L | Liter |
| *L. lactis* | *Lactococcus lactis* |
| LCA | Life cycle assessment |
| LDH | Lactate dehydrogenase |
| *ldhA* | Lactate dehydrogenase (gene) |
| Leu | L-Leucine |
| *leuA* | 2-Isopropylmalate synthase (gene) |
| *leuB* | 3-isopropylmalate dehydrogenase (gene) |
| *leuCD* | 3-isopropylmalate dehydratase (gene) |
| *leuCD* | 3-Isopropylmalate dehydratase (gene) |
| m | Meter |
| M | Molar (mol $L^{-1}$) |
| µ | Micro (in combination with SI units) |
| m | Milli (in combination with SI units) |
| *M. tuberculosis* | *Mycobacterium tuberculosis* |
| m-value | $log_2$TPM, $log_2$-fold change |
| MalE | Malic enzyme |
| *malE* | Malic enzyme (gene) |
| max | Maximal (superscript) |
| MDH | Malate dehydrogenase |
| *mdh* | Malate dehydrogenase (gene) |
| ME | Malic enzyme |
| min | Minutes |
| *mmpLR* | Putative transcriptional regulator, TetR-family (gene) |
| MOPS | 3-(N-morpholino) propane sulphonic acid |
| MQ | Menaquinone |
| $MQH_2$ | Menaquinol |
| MQO | Malate:quinone oxidoreductase |
| mRNA | Messenger RNA |
| MS | Mass spectrometry or malate synthase |
| MSG | Monosodium glutamate |
| n | Amount of substance |
| n | Nano (in combination with SI units) |
| N | Rotational speed |
| $\Delta n^C$ | Net amount of substance in C-mol |
| $NAD^+$ | Nicotinamide adenine dinucleotide (oxidized) |
| NADH | Nicotinamide adenine dinucleotide (reduced) |
| $NADP^+$ | Nicotinamide adenine dinucleotide phosphate (oxidized) |
| NADPH | Nicotinamide adenine dinucleotide phosphate (reduced) |
| *narKGHJI* | Respiratory nitrate reductase (genes) |
| $N_C$ | Number of carbon atoms |
| *ndh* | NADH dehydrogenase (gene) |
| *nusA* | Putative transcriptional termination/antitermination factor |
| *nusB* | Transcription termination factor |
| ω | Omega |
| *o*- | *Ortho*- |
| o/d | Overday |
| o/n | Overnight |
| ODHC | Oxoglutarate dehydrogenase complex |
| ODx | Oxaloacetate decarboxylase |
| OPA | *Ortho*-Phthaldialdehyde |

| Abbreviation | Description |
|---|---|
| *opcA* | Subunit of the glucose-6-phosphate dehydrogenase (gene) |
| ORF | Open reading frame |
| *oriV* | Origin of vegetative replication |
| ORP | Oxygen-reduction potential |
| OTR | Oxygen transfer rate |
| *oxyR* | Hydrogen peroxide sensing regulator (gene) |
| p | Pressure |
| p | Pico (in combination with SI units) |
| $^{P}$ | Product (superscript) |
| 1,2-PDO | 1,2-Propanediol, propylene glycol |
| PCA | Protocatechuic acid |
| *pck* | Phosphoenolpyruvate carboxykinase (gene) |
| PCR | Polymerase chain reaction |
| PCx | Pyruvate carboxylase |
| PDHC | Pyruvate dehydrogenase complex |
| PEG | Polyethylene glycol |
| PEP | Phosphoenolpyruvate |
| PEPCk | PEP carboxykinase |
| PEPCx | PEP carboxylase |
| PFK | 6-Phosphofructokinase |
| *pfk* | 6-Phosphofructokinase (gene) |
| PGI | Phosphoglucoisomerase |
| PGK | 3-Phosphoglycerate kinase |
| *pgk* | 3-Phosphoglycerate kinase (gene) |
| $pK_a$ | Logarithmic acid dissociation constant |
| pp. | Pages |
| *ppc* | Phosphoenolpyruvate carboxylase (gene) |
| PPP | Pentose phosphate pathway |
| PQO | Pyruvate:quinone oxidoreductase |
| *pqo* | Pyruvate:quinone oxidoreductase (gene) |
| PTA | Phosphotransacetylase |
| *pta* | Phosphotransacetylase (gene) |
| *ptnAB* | Membrane bound transhydrogenase (gene) |

| Abbreviation | Description |
|---|---|
| PTS | Phosphotransferase system |
| $P_{tuf}$ | Promoter of the *C. glutamicum* elongation factor EF-TU (cg0587) |
| PW | Pyrolysis water |
| *pyc* | Pyruvate carboxylase (gene) |
| PYK | Pyruvate kinase |
| $Q_{CO2}$ | Volumetric $CO_2$ evolution rate |
| $Q_{O2}$ | Volumetric $O_2$ evolution rate |
| $q_P$ | Biomass specific product formation rate |
| $Q_P$ | Volumetric product formation rate |
| $q_S$ | Biomass specific substrate uptake rate |
| $^{R}$ | Resistant (superscript) |
| $R^2$ | Coefficient of determination |
| *ramB* | Master regulator of carbon metabolism (gene) |
| *rbsR* | Repressor of ribose uptake and uridine utilization genes (gene) |
| rcf | Relative centrifugal force |
| *rho* | Transcription termination factor Rho |
| RIN | RNA integrity number |
| *ripA* | Repressor of iron protein genes (gene) |
| RNA | Ribonucleic acid |
| RNAP | RNA-polymerase |
| ROS | Reactive oxygen species |
| RPKM | Reads per kilobase |
| rpm | Revolutions (or rotations) per minute |
| *rpoA* | DNA-directed RNA polymerase, α subunit |
| rRNA | Ribosomal RNA |
| RT | Room temperature |
| s | Seconds (SI-unit) |
| $_{S}$ | Substrate (subscript) |
| σ-factors | Sigma factors |
| *S. cerevisiae* | *Saccharomyces cerevisiae* |
| *sacB* | Levansucrase (gene) |
| SCS | Succinyl-CoA synthetase |
| SD | Standard deviation |

| Abbreviation | Description |
|---|---|
| SDG | Sustainable development goals |
| SDH | Succinate dehydrogenase |
| *sdhABCD* | Succinate dehydrogenase (gene) |
| *serA* | Phosphoglycerate dehydrogenase (gene) |
| *serB* | Phosphoserine phosphatase (gene) |
| *sig* | Genes of sigma factors (*sigA*, *sigB*, *sigC*, *sigD*, *sigE*, *sigH*, *sigM*) |
| sp. | Species |
| Spec | Spectinomycin |
| *sucCD* | Succinyl-CoA synthetase (gene) |
| *sugR* | Transcriptional regulators of sugar metabolism |
| *sutR* | Bacterial regulatory protein (gene) |
| t | Time |
| T | Temperature |
| TAC | Thesis Advisory Committee |
| TAE | Tris-acetate and EDTA |
| TC | Total carbon |
| TCA | Tricarboxylic acid cycle |
| TES | Trace element solution |
| *tex* | Transcriptional accessory protein |
| TIC | Total inorganic carbon |
| TOC | Total organic carbon |
| TPI | Triosephosphate isomerase |
| *tpi* | triosephosphate isomerase (gene) |
| TPM | Transcripts per million |
| $T_{rrnB}$ | Terminator of the *E. coli rrnB* operon |
| V | Volume |
| % (v/v) | Volume per volume percent |
| VAAM | Vereinigung für Allgemeine und Angewandte Mikrobiologie |
| Val | L-Valine |
| $V_L$ | Liquid volume |
| vs. | Versus |
| vvm | Volume per volume per minute |
| % (w/v) | Weight per volume percent |
| WT | Wild type |
| $x$ | Biomass (superscript) |
| *X. campestris* | *Xanthomonas campestris* |
| *xylA* | Xylose isomerase (gene) |
| *xylB* | Xylulokinase (gene) |
| $y_{CO2}$ | Exhaust gas $CO_2$ fraction |
| $y_{O2}$ | Exhaust gas $O_2$ fraction |
| $Y_{P/S}$ | Product/substrate yield |
| $Y_{X/S}$ | Biomass/substrate yield |
| $Y_{X/S}^*$ | Apparent biomass/substrate yield |
| *znr* | Putative transcriptional regulator, ArsR-family (gene) |
| *zur* | Putative transcriptional regulator, FUR-family (gene) |
| *zwf* | Subunit of the glucose-6P dehydrogenase (gene) |

# SUMMARY

In near future, the world faces a shortage of fossil fuels, a growing population and the impact of the global climate change. Consequentially, our economy must change from being mainly non-regenerative and built on fossil resources to a bio-based economy (bioeconomy) that exploits renewable resources in a sustainable manner. An integral part of bioeconomic strategies are biorefineries, which operate analogously to petrochemical refineries but depend on novel technologies to efficiently convert complex lignocellulosic materials. Industrial biotechnology employs living organisms that inherently convert renewable resources. Microorganisms are therefore considered as one important piece of the many faceted *bioeconomy vision* that we, our children and grandchildren must realize and continually develop in future.

The main body of this thesis is organized into the paragraphs *motivation and objectives*, *background*, *material and methods*, *results and discussion* (themed into three parts), and *open questions and future directives*. The three topical divisions of the *results and discussion* section are experimentally self-contained and alleviate perception, readability and understanding.

**Part I**. In this thematic section, a biorefinery side stream – pyrolysis water – that arises during fast pyrolysis of lignocellulosic residues is assayed for microbial cultivation and fermentative 1,2-propanediol production (Figure 1.1, Part I). We established an appropriate pretreatment procedure and demonstrated the suitability of pyrolysis water as substrate for cultivations of *Corynebacterium glutamicum*. The bacterium proliferated with growth rates up to $0.36 \pm 0.04\ h^{-1}$ consuming the major contents acetate and acetol. Acetol was for the first time demonstrated to be a suitable substrate for *C. glutamicum*.

To convert acetol to 1,2-propanediol as exemplary product, the glycerol dehydrogenase from *Escherichia coli* was introduced into *C. glutamicum*. 1,2-Propanediol was produced in a growth-coupled biotransformation with the accordingly engineered strain PDO1. The bioconversion was further improved in PDO2 (*C. glutamicum* Δ*pqo* Δ*aceE* Δ*ldhA* Δ*mdh* pJUL*gldA*) under oxygen limitation. In a most advanced two phase aerobic/microaerobic fed-batch process with pyrolysis water as substrate, this strain secreted 18.3 ± 1.2 mM 1,2-propanediol with a yield of 0.96 ± 0.05 mol 1,2-propanediol per mol acetol and showed an overall volumetric productivity of 1.4 ± 0.1 mmol 1,2-propanediol $L^{-1}$ $h^{-1}$. In its entirety this part accesses a novel value chain and valorizes pyrolysis water in a process towards 1,2-propanediol formation. The developed bioprocess operated at maximal product yield and reached the so far highest overall volumetric productivity for microbial 1,2-propanediol production with an engineered producer strain.

**Part II**. This section is also directly related to biorefineries and valorizes a hemicellulose fraction originating in beech wood organosolv processing (Figure 1.1, Part II). This complex resource was for the first time used in microbial cultivations and isobutanol production with engineered *C. glutamicum*. In a systematic approach, novel loci for the chromosomal integration of genetic information were identified and termed *C. glutamicum* landing pads (CgLPs). Two of the 16 proposed loci were harnessed to introduce synthetic operons for L-arabinose and L-xylose metabolization. Under aerobic conditions the engineered strain CArXy displayed fast growth with rates up to 0.34 ± 0.02 $h^{-1}$ on the hemicellulose fraction. A further developed isobutanol producer strain CIsArXy, which additionally expresses genes of the native L-valine biosynthetic and the heterologous Ehrlich pathway, could manufacture 7.2 ± 0.2 mM isobutanol at a carbon molar yield of 0.31 ± 0.02 C-mol isobutanol per C-mol substrate (L-arabinose + D-xylose) in a zero-growth production scenario.

**Part III**. Industrial biotechnology struggles with stagnating yields and productivities in the development of microbial production processes (Figure 1.1, Part III). In large scale production bacteria face various gradients during their turbulent cell trajectory through the bioreactor. Among the inhomogeneities, oxygen plays a key role, as it directly effects the bacterium's energy conservation and triggers major metabolic rearrangements. The adaptation of *C. glutamicum* to such altering oxygen availabilities is poorly understood. In this study, we conceived a triple-phase fermentation system that pictures a gradual

decimation of the dissolved oxygen and embraces a shift from aerobiosis via microaerobiosis to anaerobiosis. The distinct process phases were bordered by the bacteria's physiologic response such as a respectively decimating growth rate ($0.40 \pm 0.01$, $0.21 \pm 0.00$, $0.09 \pm 0.01$ $h^{-1}$), biomass substrate yield ($0.52 \pm 0.04$, $0.29 \pm 0.02$, $0.16 \pm 0.01$ g CDW per g glucose) or fermentation product yield (e.g. $0.03 \pm 0.01$, $0.49 \pm 0.03$, $1.39 \pm 0.05$ mol lactate per mol glucose). We could therewith define the initiation of the microaerobic phase by the first occurrence of secreted fermentation products. During the process, successive samples were drawn at six points in time and analyzed via RNA-sequencing, for metabolites and for enzyme activities. Transcriptional alterations of almost 50 % (1421 genes) of the entire protein coding genes pictured the dramatic environmental and physiological changes. Overall, these caused an upregulation of fermentative pathways, a rearrangement of respiration, a putative metabolic inhibition of the pentose phosphate pathway by NADPH and mitigation of the basic cellular mechanisms such as cell division, transcription and translation. Interestingly, growth rate and the total amount of RNA per cell showed a clear linear correlation suggesting a minimal RNA level at extrapolated non-growth conditions of $8.8 \pm 0.7$ fg per cell. Sigma factor $\sigma^B$ and $\sigma^D$ were found changed in progression of oxygen scarcity and may contribute to the effects. To investigate the regulatory regime, 18 transcriptionally altered transcriptional regulators were deleted in the chromosome of *C. glutamicum* (single deletions) but showed no direct effect on proliferation in tightly oxygen restricted conditions. Disruption of the transcriptional redox regulator OxyR, resulted in a slightly reduced growth under microaerobiosis, which was hypothetically allocated to a decreasing expression of the cytochrome *bd* oxidase. The gathered knowledge could in future provide the basis for a better understanding of *C. glutamicum*'s adaptation to varying oxygen availabilities and generated targets for rational strain engineering.

In its entirety, this thesis demonstrates the suitability of *C. glutamicum* as qualified biocatalyst in biorefineries and contributes to a better understanding of the bacterium's adaptation towards anaerobiosis. This knowledge generates targets to improve industrial bioprocesses and could even be projected to pharmaceutical applications.

**Part I** Valorization of pyrolysis water for 1,2-propanediol production with engineered *C. glutamicum*

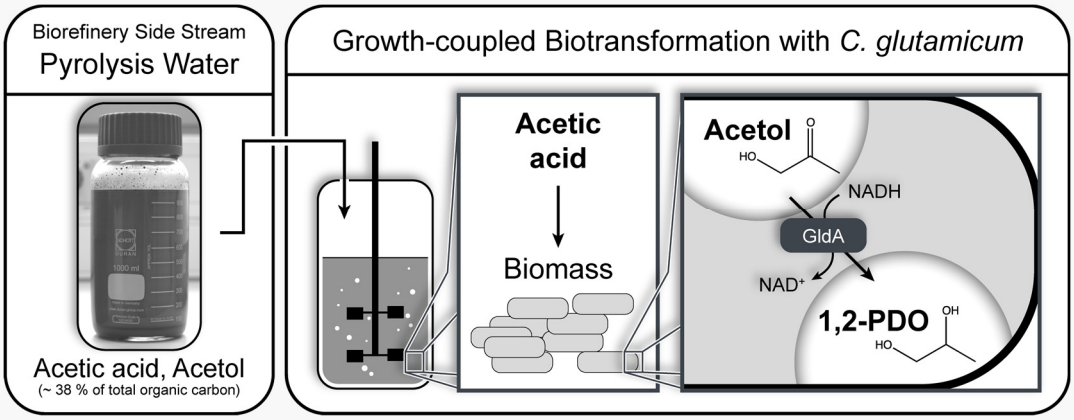


**Part II** Harnessing novel chromosomal integration loci to utilize a hemicellulose fraction for isobutanol production with engineered *C. glutamicum*

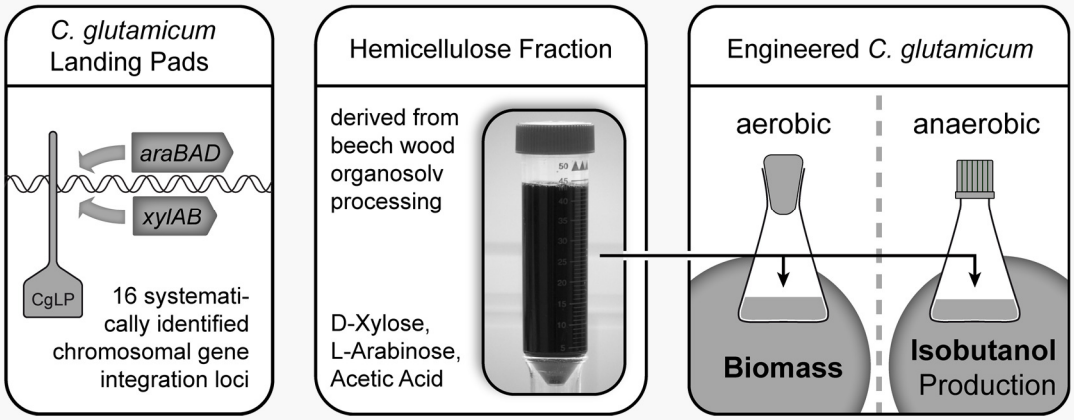


**Part III** Systemic decipherment of *C. glutamicum*'s response to self-enforcing oxygen deprivation

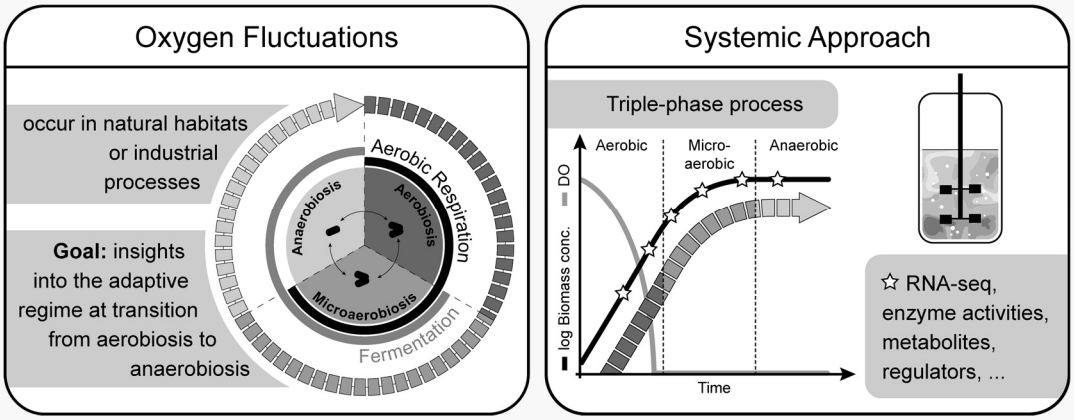


**Figure 1.1. Graphical abstracts** of the three major topical divisions of this thesis.

# ZUSAMMENFASSUNG

Die Knappheit fossiler Ressourcen, die wachsende Weltbevölkerung und der Klimawandel formieren sich zu den großen Problemen unserer Zukunft. Daraus entsteht die unabdingbare Notwendigkeit unsere individuelle Lebensweise, sowie die Weltwirtschaft aus einem hauptsächlich von fossilen Ressourcen dominierten System, in eine Bioökonomie zu wandeln, welche nachwachsende Rohstoffe nachhaltig nutzt. Ein integraler Bestandteil derartiger Strategien sind Bioraffinerien, welche analog zu petrochemischen Raffinerien, eine Rohstoffkonversionsplattform darstellen. Im Gegensatz zu Ölraffinerien verwenden diese jedoch kein fossiles Öl als Rohstoff, sondern machen nachwachsende Materialien, wie die Lignocellulose, mit neuen Technologien nutzbar. Die industrielle Biotechnologie, als aufstrebende Säule solcher Ansätze, bedient sich lebender Organismen, welche seit Jahrmillionen erfolgreich die Eigenschaft entwickelt haben, komplexe Bio-Materialien abzubauen. Insbesondere der Einsatz von Mikroorganismen wird als ein wichtiger Bestandteil der Bioökonomie betrachtet. Um ein Leben mit unseren Standards auf dem Planeten Erde auch in Zukunft gewährleisten zu können, gilt es die bio-basierte Ökonomie Schritt für Schritt zu entwickeln und zu realisieren und dabei Fehler vergangener Zeitalter zu vermeiden.

Diese Dissertationsschrift gliedert sich in die Kapitel *Motivation und Fragestellungen*, *Hintergründe*, *Material und Methoden*, *Ergebnisse und Diskussion* (aufgeteilt in drei themenspezifische Teile), sowie *Offene Fragen und Ausblick*. Die drei themengebundenen Hauptteile der Arbeit sind experimentell eigenständig und erleichtern das Verständnis und die Nachvollziehbarkeit der Forschung.

**Teil I**. In diesem Abschnitt wird Pyrolysewasser, als Bioraffinerie-Nebenstrom, auf

die Eignung zur mikrobiellen Kultivierung und Produktion von 1,2-Propandiol analysiert. Der Rohstoff entsteht bei der schnellen Pyrolyse von lignocellulose-haltigen Materialien und fällt in signifikant hohen Mengen an. Mit einer speziell entwickelten Vorbehandlung von Pyrolysewasser war es *Corynebacterium glutamicum* möglich, mit hohen Raten bis zu $0{,}36 \pm 0{,}04\ h^{-1}$ auf dem neuen Substrat zu wachsen. Das Bakterium assimilierte dabei vor allem die Hauptkomponenten Acetat und Acetol. Insbesondere Acetol konnte erstmalig als geeignete Kohlenstoffquelle für *C. glutamicum* demonstriert und als ideales Substrat für die 1,2-Propandiol Produktion identifiziert werden. Über die heterologe Expression der Glycerin-Dehydrogenase aus *Escherichia coli* im Stamm PDO1 wurde die Herstellung des Beispielprodukts in einer reduktiven und wachstumsgekoppelten Katalyse ermöglicht. Die Produktion konnte sowohl durch die Konstruktion des Stammes PDO2 (*C. glutamicum* Δ*pqo* Δ*aceE* Δ*ldhA* Δ*mdh* pJUL*gldA*), als auch durch die sauerstofflimitierten Kultivierungsbedingungen gesteigert werden. Bei optimierter, zweiphasig aerob/mikroaerober Produktion mit dem Substrat Pyrolysewasser, wurden $18{,}3 \pm 1{,}2$ mM 1,2-Propandiol mit einem Ertrag von $0{,}96 \pm 0{,}05$ mol 1,2-Propandiol pro mol Acetol und einer gesamtvolumetrischen Produktivität von $1{,}4 \pm 0{,}1$ mmol 1,2-Propanediol $L^{-1}\ h^{-1}$ hergestellt. In der Gesamtheit legt dieser Teil der Abhandlung eine neuartige Wertschöpfungskette dar und offenbart dabei erstmalig die mikrobielle Umwandlung von Pyrolysewasser zu 1,2-Propandiol. Der entwickelte Bioprozess erreichte die in der Theorie maximal mögliche Produktausbeute und die bisher höchste mikrobiell erzielte volumetrische Produktivität mit genetisch manipulierten Organismen.

**Teil II**. In dieser thematischen Einheit wurde eine, aus Buchenholzverflüssigung generierte (Organosolv-Verfahren), Hemicellulosefraktion mikrobiell genutzt. Das komplexe Substrat wurde erstmalig für mikrobielle Kultivierungen und Isobutanolproduktion mit gentechnisch verändertem *C. glutamicum* eingesetzt. In einem systematischen Ansatz konnten zuerst neuartige Loci für eine Integration von genetischem Material ins Chromosom von *C. glutamicum* identifiziert und als *C. glutamicum* landing pads (CgLPs) klassifiziert werden. Zwei der 16 vorgeschlagenen Loci wurden daraufhin für die Integration von synthetischen Operons für die L-Arabinose und D-Xylose Verstoffwechslung ausgewählt. Beim Einsatz der Hemicellulosefraktion konnten unter aeroben Bedingungen, mit dem dementsprechend ausgerüsteten Stamm (CArXy), Wachstumsraten bis $0{,}34 \pm 0{,}02\ h^{-1}$ erreicht werden. Aufbauend auf diesen

Ergebnissen wurde der Stamm CIsArXy kloniert, welcher zusätzlich die Gene des nativen L-Valin Biosyntheseweges und den heterologen Ehrlich-Stoffwechselweg exprimiert. So konnten 7,2 ± 0,2 mM Isobutanol bei einem Produktertrag von 0,31 ± 0,02 C-mol Isobutanol pro C-mol Substrat (L-Arabinose + D-Xylose) in einem Bioprozess mit ruhenden Zellen dargestellt werden. Auch in diesem Abschnitt wurde eine neuartige Wertschöpfungskette als potentieller Teil einer Bioraffinerie, in Form einer Machbarkeitsstudie, erforscht.

**Teil III**. Im systembiologisch geprägten letzten Abschnitt der Abhandlung werden stagnierende Erträge und Produktivitäten, trotz immer besser werdender Methoden, als Grundprobleme moderner industrieller Biotechnologie diskutiert. Dies geschieht am Beispiel der sauerstoffbezogenen Inhomogenitäten großer Bioreaktoren, sowie zweiphasig aerob/anaerober Bioprozesse. Mikrobielle Produzenten erfahren, einerseits beim Durchwandern ihrer Trajektorie im Bioreaktor, als auch bei Zweiphasenbioprozessen harsche Sauerstoffgradienten, welche von aerob über mikroaerob bis anaerob reichen. Da Sauerstoff einen der wichtigsten Parameter bakterieller Energiekonservierung darstellt, werden dabei massive metabolische Anpassungen ausgelöst, welche bei industriellen Prozessen mit einer Verringerung von Produktausbeuten, Produktivitäten und Zellviabilitäten einhergehen. Diese Mechanismen sind jedoch, insbesondere für *C. glutamicum*, kaum im Detail verstanden. In diesem Forschungsprojekt wurde deshalb ein Dreiphasenprozess konzipiert, welcher den Übergang von aeroben zu mikroaeroben und anaeroben Bedingungen graduell abzeichnet. Den einzelnen Phasen konnten distinkte physiologische Antworten zugeordnet werden. Diese zeichneten sich in der dezimierenden Wachstumsrate (0,40 ± 0,01, 0,21 ± 0,00, 0,09 ± 0,01 $h^{-1}$), dem abnehmenden Biomasseertrag (0,52 ± 0,04, 0,29 ± 0,02, 0,16 ± 0,01 g Biotrockenmasse pro g Glukose) und der veränderten Produktbildungsrate (z. B. 0,03 ± 0,01, 0,49 ± 0,03, 1,39 ± 0,05 mol Laktat pro mol Glukose) ab. Zum ersten Mal konnte damit der genaue physiologische Zustand einer mikroaeroben Phase gegen aerobe und anaerobe Bedingungen abgegrenzt werden. Während des Prozesses wurden phasenübergreifend 6 Proben gezogen, um eine Analyse des Transkriptoms (RNA-Sequenzierung), intrazellulärer Metabolite und Enzymaktivitäten zu ermöglichen. Die dramatische physiologische Veränderung zeigte sich in einer Anpassung der Transkription von etwa 50 % (1421 Gene) aller

proteincodierenden Gene. In der Gesamtheit bewirkte dies eine Verstärkung der fermentativen Stoffwechselwege, eine Reorganisation der Respiration, eine über NADPH putativ metabolisch gesteuerte Inhibition des Pentosephosphatweges und eine Abschwächung globaler Zellmechanismen wie Zellteilung, Transkription und Translation. Es konnte die Abnahme der Wachstumsrate in direkten linearen Zusammenhang mit einer Reduktion der zellulären Gesamt-RNA-Konzentration gestellt werden. Nach Extrapolation wurde demzufolge ein minimaler Gehalt an zellulärer RNA mit $8{,}8 \pm 0{,}7$ fg pro Zelle unter stationär-anaeroben Bedingungen postuliert. Die Sigmafaktoren $\sigma^B$ und $\sigma^D$ zeigten eine transkriptionelle Änderung bei fortschreitendem Sauerstoffmangel und könnten an der generellen physiologischen Steuerung beteiligt sein. Um die regulatorische Hierarchie der Anpassung zu untersuchen, wurden insgesamt 18 transkriptionell veränderte Regulatoren im Chromosom von *C. glutamicum* als Einzeldeletionen eliminiert. Diese zeigten jedoch keinen direkten Wachstumsphänotyp bei Sauerstoffmangel. Eine Deletion des transkriptionellen Redox-Regulators OxyR löste hingegen eine leicht abgeschwächte Wachstumsrate unter sauerstofflimitierten Kultivierungsbedingungen aus, welche möglicherweise mit der Regulation der Cytochrom *bd* Oxidase verknüpft werden kann. Das in diesem Teil der Arbeit gewonnene, vertiefte Verständnis und die eindeutige Korrelation sauerstoffassoziierter Umweltbedingungen mit metabolischen und transkriptionellen Reaktionen, stellt eine gute Basis für weitere Untersuchungen mit *C. glutamicum* dar und generiert neue Ziele für die Verbesserung industrieller Produktionsorganismen und -prozesse.

In der Gesamtheit, demonstriert diese Dissertation die Eignung von *C. glutamicum* als Biokatalysator für zukünftige Bioraffinerien mit neuartigen Substraten und bündelt wertvolle Informationen über dessen physiologische Anpassung an alternierende Sauerstoffbedingungen. Das gewonnene Wissen gibt somit neue Anstöße für die Verbesserung bestehender industrieller Bioprozesse und könnte auch auf andere pharmazeutisch relevante Applikationen übertragen werden.

# CHAPTER 1: MOTIVATION AND OBJECTIVES

Today, with a world population of more than 7 billion people, we consume about 600 EJ $a^{-1}$ primary energy (Henrich *et al.*, 2015). About 80 % of this energy is currently delivered by fossil resources and only 10 % from bioenergy. With the prospectively rising energy demand, a large gap, not only concerning energy but also other material products such as bulk or fine chemicals and feed or food, must be filled with new technologies. A knowledge-based bioeconomy is one visionary answer to this issue and brings sustainable technologies that preserve the global natural capital. This study gives indications about the possibility to access so far unexploited or neglected biorefinery side streams with *Corynebacterium glutamicum* (Part I and Part II) and systemically analyzes issues in current production scenarios in industrial biotechnology to provide solutions in future bioprocess improvement. Thereby, the study of the microbial adaptation towards enforced oxygen scarcity intends to deliver insights to the physiological response at systems-level with a focus on transcriptomic and regulatory mechanisms (Part III). The following objectives were addressed in this study:

Part I (p. 104 pp.)

- Investigate pyrolysis water, derived as side stream from fast pyrolysis of wheat straw, as potential substrate for *C. glutamicum*
- Cultivate *C. glutamicum* on this resource
- Conceive bioprocesses exploiting major carbon sources of pyrolysis water
- Implement a novel value chain using pyrolysis water to produce 1,2-propanediol as exemplary bulk chemical

Part II (p. 123 pp.)

- Provide novel solutions to the bottleneck of chromosomal loci for integration of genetic information in metabolic engineering strategies
- Equip *C. glutamicum* with heterologous pathways for the utilization of the pentoses L-arabinose and D-xylose
- Exploit of a hemicellulose fraction derived from beech wood organosolv processing as neglected material stream
- Cultivate *C. glutamicum* on the hemicellulose fraction using major carbon contents
- Conceptualize a value chain using hemicellulose to produce isobutanol as exemplary second-generation biofuel

Part III (p. 138 pp.)

- Development of a defined system to study gradual transitions from aerobic via microaerobic to anaerobic cultivation conditions with *C. glutamicum*
- Propose a comprehensive and accessible definition of microaerobiosis
- Study the distinct features of each phase harnessing RNA-sequencing, metabolomics and enzyme analyzing technologies
- Illuminate the regulatory regime of *C. glutamicum* in response to the altering oxygen availabilities
- Compile future targets to enhance *C. glutamicum*'s robustness to oxygen shifts in industrial bioprocesses via metabolic engineering

The theoretical background and state of the art in the light of these objectives is summarized in the following section and is fully addressed in the *results and discussion*.

# CHAPTER 2: BACKGROUND

## 2.1. Project framework

This thesis is an integral part of the national research strategy bioeconomy 2030 in Germany (Bundesministerium für Bildung und Forschung (BMBF), 2010). The overarching goal is to advance politics, innovation and research supporting a knowledge-based and internationally competitive role of Germany in bioeconomic directions. One of the forerunners in Germany is Baden-Württemberg, where a strategic bioeconomy approach for the establishment of a research and innovation network in the field of bioeconomy was formulated (Ministry of Science Research and the Arts (MWK) of Baden-Württemberg, 2013). Analysis of the entire system by gathering experts from agricultural and other biological sciences, forestry, environmental and engineering sciences, social and economic sciences, biodiversity research and ethics was intended to form a consortium for the assessment, development and realization of a bioeconomy in Baden-Württemberg. Among the other fields (*microalgae*, *biogas* and the integrative competence network *modelling*), the research field *lignocellulose* focuses on the development and improvement of production, conversion and valorization of lignocellulosic biomasses. Therein, this project with the title "Development and optimization of microbial lignocellulose-based fermentation processes to produce bulk chemicals and biofuels"[1] is attributed to the action field 3 (conversion technologies and

[1] Translated from the German title "Entwicklung und Optimierung mikrobieller Lignocellulose-basierter Fermentationsverfahren zur Herstellung von Bulk-Chemikalien und Treibstoffen"; original title "Entwicklung und Optimierung mikrobieller lignocellulose-basierter Fermentationsverfahren zur Herstellung von Isobutanol mit *Corynebacterium glutamicum*"; Project ID: TP844.

value chains) and action field 4 (product development and novel products). We demonstrate the biochemical conversion of lignocellulose-derived side streams of biorefineries by microbial fermentation into an exemplary material product (1,2-propanediol, Part I, p. 104 pp.) and a biofuel (isobutanol, Part II, p. 123 pp.). Because biotechnological processes need continuous optimization to stay or become competitive and profitable, holistic and systemic investigations as demonstrated in this study (Part III, p. 138 pp.) gather the understanding needed in a knowledge-based bioeconomy (KBBE).

## 2.2. Industrial biotechnology

The entire body of the thesis can be allocated to the field of industrial biotechnology. In general, this domain, aims in the context of this thesis, to generate microbial bioprocesses to manufacture products or reduce wastes (Doran, 1995; Baltz *et al.*, 1999). Particularly in the field of bioeconomy, which will be discussed in the following section (cf. 2.3, p. 16), industrial biotechnology (often referred to as *white biotechnology* (Hatti-Kaul *et al.*, 2007)) offers a green alternative to classical chemical engineering, which inherently relies on fossil resources. Three major fields of the biosciences are essentially involved in the development of such bioprocesses and are the underlying essence of the project: metabolic engineering, bioprocess engineering and systems biology (Figure 2.1). Lee and Kim summarized the systems strategies in the development of industrial production scenarios and connect the three domains to a functional value chain (Lee and Kim, 2015).

**Metabolic engineering** (Stephanopoulos, 1999; Nielsen *et al.*, 2013) is a bio-discipline that aims on the improvement of bacterial production hosts by analyzing and manipulating metabolic fluxes to a desired product and eventually to improve properties and productivities of the process. This pathway streamlining can be accomplished using recombinant DNA technologies of modern genetics. In this study (Part I, p. 104 pp.; Part II, p. 123 pp.), we make use of such technologies to specifically manipulate the bacterial host's genetic setup to expand the substrate spectrum (here towards the pentoses L-arabinose and D-xylose) and to redirect the metabolism towards desired products (here isobutanol and 1,2-propanediol). With our current microbial producer strains and biotechnological processes, we already push towards the technical and biological limits. In order to become competitive to established chemical processes and thereby be sustainable, economic and profitable, novel knowledge-based approaches are needed. Further understanding of microbial consortia, for example in heterogenic conditions in large scale bioprocesses, is essential for increasing process efficiencies. An emerging field that holistically gathers information of such complex phenomena and involves quantitative analysis of large systems with the use of *OMICS* technologies (for example transcriptomics, metabolomics, fluxomics, proteomics, genomics) by guidance of computational biology and mathematical models is **systems biology** (Ideker *et al.*, 2001; Kitano, 2002; Aderem, 2005; Williamson, 2005; Takors *et al.*, 2007; Vidal, 2009; Nielsen, 2017). Such studies often concentrate on

> *"**Metabolic engineering** is the directed improvement of cellular properties through the modification of specific biochemical reactions or the introduction of new ones, with the use of recombinant DNA technology."*
>
> (Stephanopoulos, 1999)

> *"**Systems biology** studies biological systems by systematically perturbing them (biologically, genetically, or chemically); monitoring the gene, protein, and informational pathway responses; integrating these data; and ultimately, formulating mathematical models that describe the structure of the system and its response to individual perturbations."*
>
> (Ideker *et al.*, 2001)

the basic understanding of microbial systems. In this thesis (Part III, p. 138 pp.), we aim at the deciphering of the adaptation of *C. glutamicum* to fluctuations in oxygen availability (aerobic, microaerobic, anaerobic) in a systemic approach. Such fundamental research provides the basis for future bioprocess development (Hansen *et al.*, 2017), which is driven by the field of **bioprocess engineering** (Shuler and Kargi, 1992; Villadsen *et al.*, 2011). Analogously to chemical engineering, bioprocess engineering designs, develops and analyzes the technical framework of a production scenario, but involves biocatalysts instead of abiotic materials. Most prominent in Part I (p. 104 pp.) of this thesis, bioprocesses were optimized regarding feeding and oxygen transfer rates resulting in an overall improvement of the productivities of engineered strains.

> *"**Bioprocess engineering** is the application of engineering principles to design, develop, and analyze processes using biocatalysts"*
>
> (Shuler and Kargi, 1992)

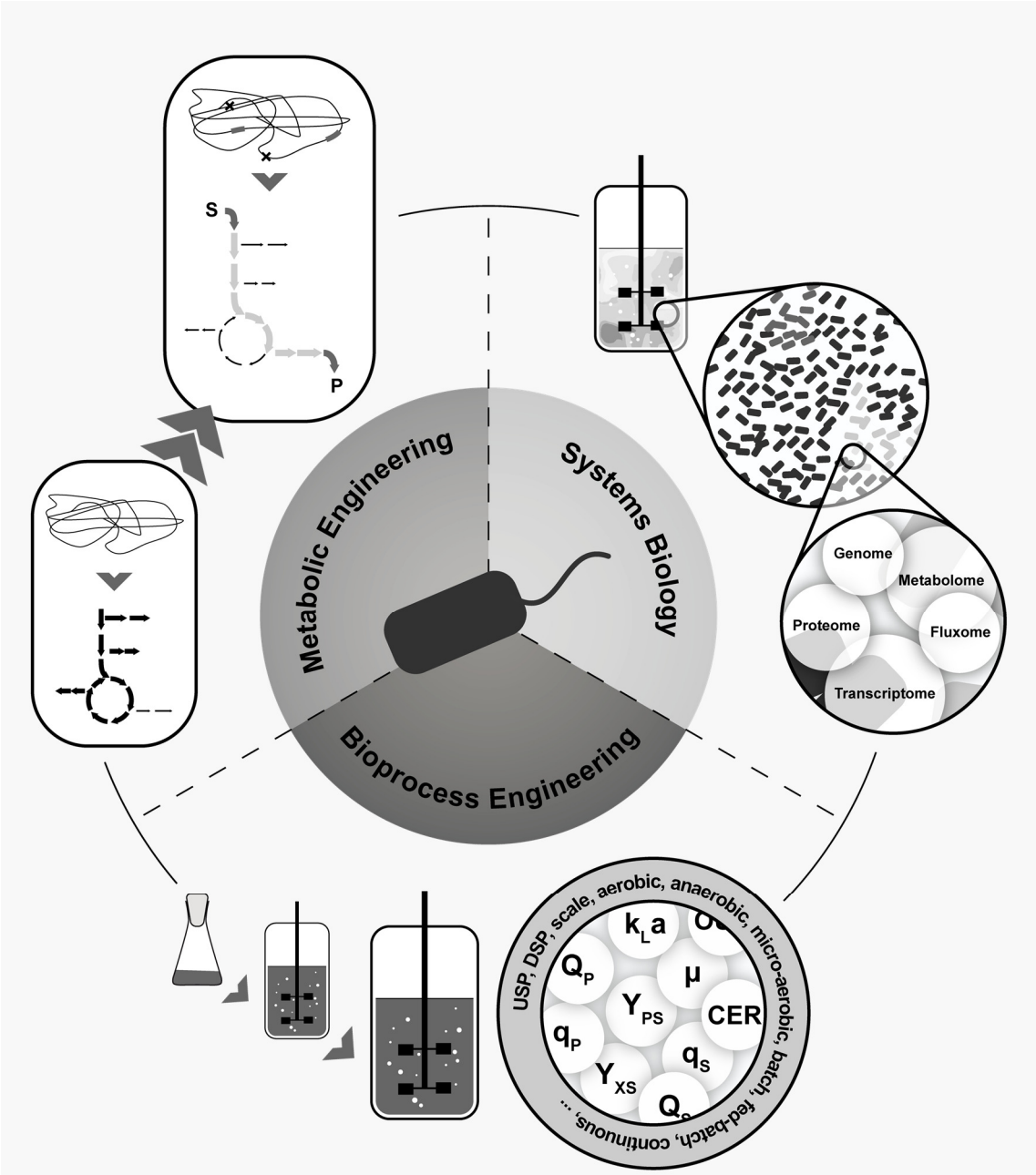


**Figure 2.1. Metabolic engineering, systems biology and bioprocess engineering**. For metabolic engineering strategies, an exemplary streamlining of a metabolic pathway (arrows) is shown by genetic manipulation of the chromosome (wavy line) that enables the conversion of a novel substrate (S) to a desired product (P). Systems biology is exemplarily explained by the investigation of population heterogeneities in large scale bioreactors. *OMICS* technologies like metabolomics, transcriptomics, fluxomics and others are harnessed to develop a comprehensive picture of such complex phenomena and generate the basis for process and strain optimization. Bioprocess engineering is pictured by scale up development and described by process parameters such as volumetric productivity, yields, growth rates, carbon emission rates and others. Process operation modes (aerobic, anaerobic, batch, fed-batch, …) as well as upstream and downstream processing are exemplary topics within this field.

# 2.3. Bioeconomy

## 2.3.1. Perspective and definition

Major societal and global challenges, such as a shortage of fossil fuel and energy resources, a growing world population (estimated 9 billion by 2050) and the rising impact


**Figure 2.2. Sustainable development goals** (SDG) proposed by the United Nations (The General Assembly, 2015). At least half of these goals will be majorly contributed to by bioeconomic strategies.

**Goal 1**. End poverty in all its forms everywhere. **Goal 2**. End hunger, achieve food security and improved nutrition and promote sustainable agriculture. **Goal 3**. Ensure healthy lives and promote well-being for all at all ages. **Goal 4**. Ensure inclusive and equitable quality education and promote lifelong learning opportunities for all. **Goal 5**. Achieve gender equality and empower all women and girls. **Goal 6**. Ensure availability and sustainable management of water and sanitation for all. **Goal 7**. Ensure access to affordable, reliable, sustainable and modern energy for all. **Goal 8**. Promote sustained, inclusive and sustainable economic growth, full and productive employment and decent work for all. **Goal 9**. Build resilient infrastructure, promote inclusive and sustainable industrialization and foster innovation. **Goal 10**. Reduce inequality within and among countries. **Goal 11**. Make cities and human settlements inclusive, safe, resilient and sustainable. **Goal 12**. Ensure sustainable consumption and production patterns **Goal 13**. Take urgent action to combat climate change and its impacts. **Goal 14**. Conserve and sustainably use the oceans, seas and marine resources for sustainable development. **Goal 15**. Protect, restore and promote sustainable use of terrestrial ecosystems, sustainably manage forests, combat desertification, and halt and reverse land degradation and halt biodiversity loss. **Goal 16**. Promote peaceful and inclusive societies for sustainable development, provide access to justice for all and build effective, accountable and inclusive institutions at all levels. **Goal 17**. Strengthen the means of implementation and revitalize the Global Partnership for Sustainable Development. Icons downloaded from: http://www.un.org/sustainable development/news/communications-material/.

of the climate change, generate the urgency to change our current economy in near future (Directorate-General for Research and Innovation (European Commission), 2012). The bioeconomy, also bio-based economy, is a vision that tackles these problems by using naturally regrowing resources in a sustainable manner. Thereby, our dependence on fossil resources is continually decimated, the net emission of greenhouse gasses reduced and the global climate change mitigated. Eventually, a bioeconomy must rebuild our natural capital, improve the quality of life, reduce waste and balance global harvest, production and consumption (Directorate-General for Research and Innovation (European Commission), 2012; El-Chichakli *et al.*, 2016). Unifying all aspects of a bioeconomy and formulate a common definition is a difficile task. At the current standpoint, no such definition is available and variations are proposed around the globe. A representative definition is given here (cf. right). Bioeconomy is a highly innovative and interdisciplinary field, which is followed by more than 40 countries around the world with dedicated strategies (The Bioeconomy Council, 2015) and already contributed to 13 % of the world trade in 2014 with products from agriculture and forestry, food, bioenergy, biotechnology and green chemistry (El-Chichakli *et al.*, 2016). Leaders in bioeconomy are the European Union, Japan and the United States of America (El-Chichakli *et al.*, 2016). The European Commission published a strategy that highlights the importance of bioeconomy for the European Union (Directorate-General for Research and Innovation (European Commission), 2012). One primary goal is the assurance of sustainability, which itself is discussed controversially due to a lack of unified definition and measurability. The term sustainable should therefore be regarded and mentioned cautiously. The United Nations proposed 17 sustainable development goals (SDGs, Figure 2.2) in the 2030 agenda, where the bioeconomy will practically contribute to at least half of these. Biotechnology for the production of sustainable biopharmaceuticals (SDG 3) or switching from oil based to bio-based chemical production (SDG 12) are selected examples. Especially, white biotechnology benefits from advances in metabolic

> *"**Bioeconomy** […] [is] the knowledge-based production and utilization of biological resources, innovative biological processes and principles to sustainably provide goods and services across all economic sectors"*
>
> (The Bioeconomy Council, 2015)

engineering and systems biology and will be a key player for the development of new processes using biotransformation and fermentation of renewable resources (Octave and Thomas, 2009; Nielsen *et al.*, 2013; Chen and Liu, 2016). One integral part of bioeconomic strategies, are biorefineries that are discussed in the following paragraph. A problem that many bioeconomic strategies share is the ignorance of the importance to globally decrease the high levels of present consumption as principal cause of resource depletion (Mills, 2015). This effort can be weighed of equal importance to the development of a sustainable economy and must be clearly enforced politically in future agendas.

*"**Green chemistry** is the design of chemical products and processes that reduce or eliminate the generation of hazardous substances."*

*United States Environmental Protecting Agency*

Within the scope of this thesis, the focus lies on the utilization of biological resources with microorganisms and the development of novel value chains, technologies and products and thus covers only selected aspects of the entire bioeconomy concept.

### 2.3.2. Biorefineries and next generation biomasses

As mentioned above biorefineries operate analogously to petrochemical refineries and are one central technology in a future bioeconomy that accomplishes the transformation of biomass into energy (biofuels, heat, electricity, …), molecules (bulk and fine chemicals, cosmetics, pharmaceuticals, …), materials (plastics, composites, …) but also food or feed (Octave and Thomas, 2009). The top 10 biorefinery-derived products were suggested by Bozell and Petersen and include for example ethanol, furans, succinate, sorbitol and others (Bozell and Petersen, 2010). Biorefineries are systematically developed, analyzed and defined in the International Energy Agency (IEA) Bioenergy Task 42, and have been extensively analyzed and are reviewed in literature (Octave and Thomas, 2009; Cherubini, 2010;

*"**Biorefinery** is the sustainable processing of biomass into a spectrum of marketable products and energy."*

(de Jong and Jungmeier, 2015)

Rabaçal *et al.*, 2017). Biorefineries need to replace crude-oil refineries once the fossil resources are depleted. As transportation is the major sector for an increasing oil demand, the production of biofuels as substitute is in particular focus (Fatih Demirbas, 2009) and is further discussed in the paragraph 2.8 (p. 46). Currently, about 4 % of crude-oil is used worldwide for chemical and plastic production (Cherubini and Ulgiati, 2010), which must also be substituted by green chemicals in future. There is a need to develop innovative conversion technologies, because of the complex consistence of renewable biomasses, which in contrast to crude oil, are highly variable, have a much lower grade of reduction and thus a higher oxygen and water content (Figure 2.3, p. 24). The biomass processing technologies were classified into mechanical pretreatments (extraction, fractionation, separation) and thermochemical, chemical, enzymatic and microbial conversions (fermentation). In order to stay efficient and profitable a zero-waste biorefinery is desirable, where all side streams are fully valorized (Ferreira, 2017). In the presented thesis, two examples will be given that address this issue by microbial processing of biorefinery side streams that evoke from thermochemical processing of lignocellulose. The analysis of the efficiency and sustainability of biorefineries is an important future aspect to fulfill the requirements within a bioeconomy. Selected tools accomplishing such difficult analyses are for example life cycle assessments (LCA) or annual basis carbon (ABC) methods (Cherubini and Ulgiati, 2010; Silva *et al.*, 2017). These methods take indirect factors or material and energy steams into account but are still are highly variable due to different assumptions. As it is proposed and demonstrated in this thesis (Part I, p. 104 pp.; Part II, p. 123 pp.) microbes in white biotechnology will play an integral role in biorefinery strategies (Octave and Thomas, 2009). Bacteria and yeast due to their flexibility towards a variety of feedstocks are in focus of future industrial biotechnology (Rumbold *et al.*, 2010; Wendisch *et al.*, 2016). An overview of current advances of microbial biotechnology as integral part of biorefineries is for example given in literature (Kamm, 2015).

Biomasses[2] as suitable substrates for biorefineries were for example defined in a directive of the European Parliament and the Council of the European Union and classified based on their origin into: woody plants, herbaceous plants, aquatic plants, and wastes (Williams *et al.*, 2001; McKendry, 2002a). Due to ethical reasons, the biomasses stated as such were considered, as they do not directly compete with food or feed and share plentiful abundance at negative, no or low cost. An indirect competition occurs for example with respect to arable land. For this reason, a future strategy is the production of energy crops such as perennial grasses (e.g. *Miscanthus* sp., switchgrass, or reed canary grass) or tree species (e.g. willow, poplar) on marginal lands and in short rotation coppices (Valentine *et al.*, 2012; López-Bellido *et al.*, 2014). In theory, there is enough biomass available to satisfy our economic demands (Valdivia *et al.*, 2016). Already 14 % of the world's primary energy consumption is currently obtained from such biomasses (Ferreira, 2017). A critical obstacle to overcome is the access, harvest and transportation of biomasses. As an example, todays biofuel production plants have a transportation cost of roughly 75 US$ per ton, which even exceeds the value of transported terrestrial biomasses (~ 60 US$ per ton at the farm gate) (Valdivia *et al.*, 2016). Reduction of transportation cost can be achieved by creating centralized markets with homogenous supply routes or decentralized processing of biomasses into energy dense materials, as will be discussed later with respect to fast pyrolysis and the bioliq® concept (2.5.2, p. 24).

> *"'**Biomass**' means the biodegradable fraction of products, waste and residues from biological origin from agriculture (including vegetal and animal substances), forestry and related industries including fisheries and aquaculture, as well as the biodegradable fraction of industrial and municipal waste"*
>
> (The European Parliament and The Council of the European Union, 2009)

[2] The reader may notice that the term biomass is also used in different context as description of the bacterial cell dry weight for example in biomass concentration, biomass specific substrate uptake or product formation rate ($q_S$ or $q_P$) and the biomass/substrate yield ($Y_{X/S}$).

# 2.4. Lignocellulose

## 2.4.1. Abundance and potential as resource for bioeconomy

Nature produces over 200 billion tons of biomass per year by capturing solar energy via photosynthesis and carbon in form of atmospheric $CO_2$ (Tschan *et al.*, 2012). Woody biomass is regarded as the most abundant renewable resource with 90 % of the global carbon in standing biomass (Sauer *et al.*, 2014). Estimations of the energetic capacity of all currently standing and harvestable biomass on our planet proposed a potential resource of about 100 times of our current annual energy demand (Ferreira, 2017). Especially lignocellulose, as major structural element of all woody biomasses, holds the lion share of renewable materials on our planet and is regarded as sound resource for biorefineries. As it does not compete directly with food or feed, lignocellulose is regarded as a second-generation (2G) bioresource with leading potential (Valentine *et al.*, 2012). Lignocellulose deduced building blocks for chemical industry were compiled by the U.S. Department of Energy (DOE) in two volumes for sugar (cellulose, hemicellulose) and lignin (Werpy and Petersen, 2004; Holladay *et al.*, 2007) but also for example by Isikgor and Becer, who propose over 200 lignocellulose-derived chemicals (Isikgor and Becer, 2015). The named chemicals can be either produced biotechnologically or chemically. In particular, in the sector of biofuels a dogmatic change will be necessary from established first-generation (1G) biofuels (such as ethanol from sugar cane or starch) to 2G (such as ethanol from straw) as discussed below (cf. 2.8, p. 46). Among suitable agricultural residues, straw was classified as being most abundant and relevant in Europe (Möller *et al.*, 2007; BioBoost, 2015). An overview of the availability of bioresources in the EU was analyzed in 2015 and determined total accessible amount of 150 Mio. t of straw representing 37 % (w/w) of all assessed biomasses followed by forest residues of 118 Mio. t and 29 % (w/w) (BioBoost, 2015). The difficulty in the shift from 1G resources, where technologies for conversion are long since established, to 2G biomass lies in its recalcitrance and complexity of composition (cf. 2.4.2, p. 22). An abundance of conversion strategies (Sánchez and Cardona, 2008) were developed including thermochemical treatments like pyrolysis (cf. 2.5.2, p. 24) or organosolv (cf. 2.5.1, p. 23) but also microorganisms were explored and engineered (Liao *et al.*, 2016). In the presented study, biorefinery side streams that originate in forestry (beech wood) and

agriculture (wheat straw) are valorized in novel value chains as proof of principle [cf. Part I (p. 104 pp.) and Part II (p. 123 pp.].

### 2.4.2. Structure

Lignocellulose is the major constituent of the plant cell wall and comprises approximately 30-50 % cellulose, 15-35 % hemicellulose and 10-30 % lignin (Sauer *et al.*, 2014). Due to partially crystalline and highly crosslinked structures of the polymers, lignocellulose is a biopolymer highly recalcitrant towards biological degradation (Himmel *et al.*, 2007). **Cellulose** is a high molecular weight (about 200-2000 kDa, degree of polymerization (DP) 5000-15000) homopolysaccharide of β-1,4-linked glucose entities and can form various crystalline structures (Sannigrahi *et al.*, 2010; Rajendran and Taherzadeh, 2014). Biologically, cellulose is hydrolyzed to monomers by the action of two classes of enzymes (endoglucanases and cellobiohydrolases) (Aristidou and Penttilä, 2000). **Hemicellulose** is a branched heteropolymer of amorphous structure (about 2-20 kDa, DP between 70-200) and is composed of hexoses (D-glucose, D-mannose and D-galactose), pentoses (D-xylose and L-arabinose) and various side chains (acetyl, arabinofuranosyl and methyl glucuronosyl) (Aristidou and Penttilä, 2000; Jacobs and Dahlman, 2001; Sannigrahi *et al.*, 2010; Stickel *et al.*, 2014). It links cellulose fibers in the primary plant cell wall and crosslinks these microfibrils with lignin (Rubin, 2008). The principal enzymes for biological degradation are xylanases and xylosidases among galactosidases, arabinofuranosidases and others (Stickel *et al.*, 2014). In contrast to cellulose, hemicellulose is due to the loose structure easily hydrolysable by dilute acid or base (Aristidou and Penttilä, 2000). **Lignin** is a phenolic macromolecule (about 2-80 kDa, DP (milled wood lignin) < 12) present in the secondary cell wall of woody plants and thus functions as a reinforcement of the of the structural integrity and links contiguous cells (Kirk and Farrell, 1987; Crestini *et al.*, 2011; Chen, 2014; Rajendran and Taherzadeh, 2014; Tolbert *et al.*, 2014). The macromolecule is irregularly synthesized by polymerization and thus exhibits a complex and covalently crosslinked structure (carbon-carbon and carbon-oxygen (ether) bonds), which is highly recalcitrant to digestion. The basic phenolic monomers are *p*-coumaryl alcohol, coniferyl alcohol and sinaply alcohol. Before the evolution of white-rot fungi, lignin could not be biologically digested and was thus the source material of coal in the Cambrian of the earth's history (Floudas *et al.*,

2012). Enzymatic degradation of lignin is a specialty of the kingdom of fungi. It is targeted for depolymerization to quinones through oxidative reactions catalyzed by laccases and peroxidases (Rajendran and Taherzadeh, 2014).

## 2.5. Biomass pretreatment

As discussed above, lignocellulose is highly recalcitrant to decomposition. Enzymatic degradation at a current state fails to provide a biorefinery platform that fully digest lignocellulose. Although commercial strategies for cellulose and hemicellulose hydrolysis exist, especially lignin has not been enzymatically degraded in an economic manner. For these reasons enzymatic conversion technologies will not be included in this thesis but were addressed elsewhere (Sun and Cheng, 2002; Van Dyk and Pletschke, 2012; Stickel *et al.*, 2014). Fast degradation of lignocellulosic biomasses can be achieved by thermochemical processing. Excellent overviews of feasible lignocellulose pretreatment procedures can be found in literature (Sánchez and Cardona, 2008; P. Kumar *et al.*, 2009; Alvira *et al.*, 2010). In this study, pyrolysis and organosolv as an example of hydrothermal processing are discussed. While fast pyrolysis aims at the rapid liquefaction of lignocellulose into bio-oils, organosolv is a method to fractionate lignocellulose into its major macromolecules cellulose, hemicellulose and lignin.

### 2.5.1. Elemental analysis

To understand the nature of the converted biomasses the consideration of an elemental analysis is worthwhile (Figure 2.3; Table S 1, p 210). For fast pyrolysis as well as organosolv no dramatic alteration towards the original substrate can be found after processing with respect to atomic constituency (Bridgwater, 2017). However, the composition of lignocellulosic biomasses deviates significantly from fossil crude oil. As an example, the elemental analysis of petroleum, a primary product of oil refining, is depicted in comparison to biomasses relevant to this study (wheat straw, beech wood) and liquefied fractions through pyrolysis and organosolv processing. The most striking difference is the oxygen content, which poses special challenges in the decomposition and further use in the chemistry. Generally speaking, crude oil derived platform chemicals

such as ethylene, benzene and others, have a much higher reduction grade and thus less oxygen content than biomass. Alternatively, this could also be considered as a beneficial characteristic and could enable a future to shift from an often hazardous oxidation chemistry, to a greener reduction chemistry that relies on platform chemicals of lower reduction grade (Bozell and Petersen, 2010; Cherubini and Ulgiati, 2010).

### 2.5.2. Fast pyrolysis and the bioliq® process

Lignocellulose can be thermochemically converted to an energy dense and liquid bio-oil by **fast pyrolysis**. In general, this process is a thermochemical conversion carried out in the absence of oxygen at temperatures around 500 °C with high heating rates and gas residence of only a few seconds before an instant cooling is affiliated. By these characteristics it differs from gasification and combustion that both occur under oxygen atmosphere at higher temperatures (Sondreal *et al.*, 2001; McKendry, 2002b; A. Kumar *et al.*, 2009; Kirubakaran *et al.*, 2009). Between these technologies, the biomass energy conversion efficiencies varies from 20-40 % (combustion power plant), 40-50 % (integration of gasification and combustion/heat recovery) and up to 80 % (fast pyrolysis to bio-crude) (McKendry, 2002b). The instant cooling of the pyrolysis vapors generates

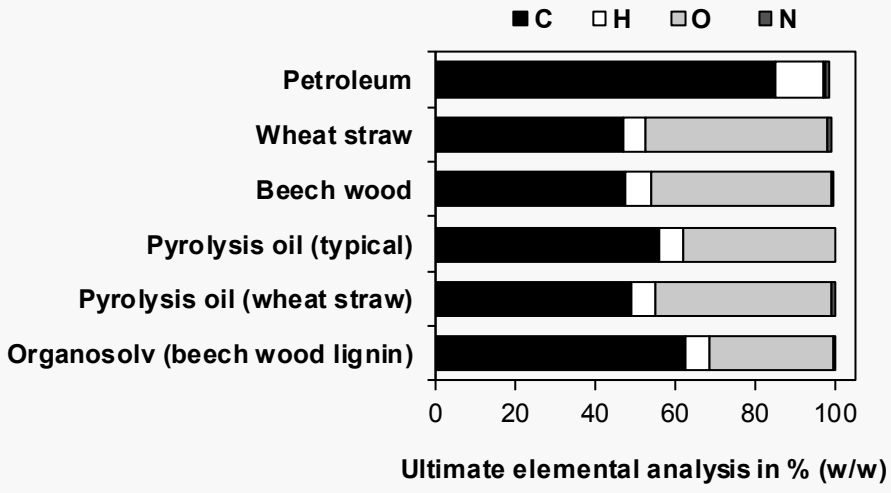


**Figure 2.3. Elemental analysis of crude and pretreated biomasses in comparison to petroleum**. Representative values from literature are given and drawn as % (w/w). In order to visualize the petroleum analysis, average values from the range given in Table S 1 (p. 210) are shown.

three products: liquid condensate phase (bio-oil), solid phase (char), and gaseous phase consisting of non-condensable gasses (Bridgwater, 2017). The heating value of bio-oil (22 MJ $kg^{-1}$) is approximately half of that of fossil crude oil (Pfitzer *et al.*, 2016). A tabular compilation of typical ingredients is given in literature (Diebold, 2000). The bio-oil composition yet varies remarkably depending on the processing technology, the converted biomasses and thermochemical parameters such as temperature (Demirbas, 2007; Arnold *et al.*, 2017). Among the major components are acids (acetate, formate, …), alcohols (methanol, ethanol, …), esters (methyl formate, methyl acetate, …), ketones (acetone, hydroxyacetone, …), aldehydes (formaldehyde, acetaldehyde, …), phenols (phenol, 1,4-dihydroxybenzol, …), sugars (levoglucosan, glucose, …), furans, guaiacols, syringols, alkenes, other aromatics and miscellaneous oxygenates. Additionally, water insoluble contents (mostly lignin-derived oligomers, but also resins and fatty acids) are occurring constituents (Oasmaa *et al.*, 2015; Dahmen *et al.*, 2016). The energy dense characteristic of bio-oil makes it a transportable form of converted biomass. Bio-oils can be used in various applications, from heat generation (state-of-the-art today), as refinery feed after catalytic upgrading or for synthetic fuel (synfuel) production as developed within the bioliq® process at the KIT (Karlsruhe Institute of Technology, Germany). Overall, fast pyrolysis is discussed as suitable strategy to efficiently convert lignocellulose and provide heat, electricity, biofuels and green chemicals in a bioeconomy. The contemplation of latest general (Arnold *et al.*, 2017; Bridgwater, 2017; Dhyani and Bhaskar, 2017; Meier, 2017), technological (Venderbosch and Prins, 2010) and environmental and economic (Roy and Dias, 2017) reviews are recommended for detailed information. Bio-oil characteristics with their causes and effects are comprehensively listed in literature (Bridgwater, 2012).

> *"**Fast pyrolysis** is a high temperature process in which the feedstock is rapidly heated in the absence of air, vaporises and condenses to a dark brown mobile liquid which has a heating value of about half that of conventional fuel oil."*
>
> (Bridgwater, 2000)

It is important to consider the **stability** issue of bio-oils. In the prevalent short reaction times and rapid quenching during fast pyrolysis, a thermodynamic equilibrium is not reached. Intermediate products reside at minima of the Gibbs free energy but can quickly

undergo further reactions even under mild conditions. Therefore, the chemical composition of pyrolysis changes during storage (Boucher, Chaala, Pakdel, *et al.*, 2000). A subjection to heat enhances a change in color and viscosity, which originates in secondary reactions (polymerization, condensation, etherification and esterification reactions including the Maillard reaction) (Diebold, 2000; Oasmaa and Peacocke, 2010; Pfitzer *et al.*, 2016). Due to the high water content in bio-oils, phase separation is a common issue and restricts direct usage as fuel (Boucher, Chaala, Pakdel, *et al.*, 2000; Oasmaa and Peacocke, 2010; Oasmaa *et al.*, 2015). The addition of pyrolysis water to bio-oil was also shown to dramatically lower its stability and promote this phase separation (Boucher, Chaala, Pakdel, *et al.*, 2000). Therefore, stepwise condensation procedures were developed as for example demonstrated in the bioliq® plant to yield more stable bio-oil fractions.

The **bioliq® pilot plant** (Eggenstein-Leopoldshafen, Germany) manufactured the pyrolysis batches applied in this study (Dahmen, Dinjus, *et al.*, 2012; Dahmen, Henrich, *et al.*, 2012; Dahmen *et al.*, 2016; Henrich *et al.*, 2016; Pfitzer *et al.*, 2016). Bioliq® means "biomass-to-liquid" and currently relies on straw as renewable resource. The availability of this resources along with wood residues and the potential for fuel, energy and heat generation was systematically analyzed for Baden-Württemberg (Leible *et al.*, 2007). Overall the intention of the bioliq® process is the production of synthetic biofuels based on lignocellulosic residues (Dahmen *et al.*, 2016). From a logistic perspective lignocellulose is intended to be converted in regionally distributed plants (decentralized) towards the highly energy dense biosyncrude – a slurry of bio-oil and char. Such biosyncrudes contain up to 85 % of the initial biomass energy and can be transported in an efficient way to a centralized gasification site, where synfuels or chemicals can be manufactured (Pfitzer *et al.*, 2016). The products of the bioliq® process are according to mass balance: liquid (34 % (w/w) bio-oil with 15 % (w/w) water content, 25 % (w/w) PW with 80 % (w/w) water content), solid (20 % (w/w) char and ash) and pyrolysis gas (20 % (w/w), non-condensable) (Dahmen *et al.*, 2016). The bio-oil retains about 60 % of the original energy of the biomass (Pfitzer *et al.*, 2016). Besides bio-oil, representing the actual value product, aqueous condensates, here referred to as PW, generally arise during fast pyrolysis as a low-value side-product.

The **aqueous condensate (pyrolysis water)** is generated in large quantities of up to

30 % (w/w), in the bioliq® process, in particular from conversion of ash rich and low-quality biomass like wheat straw (Dahmen *et al.*, 2016; Pfitzer *et al.*, 2016). A full description of analyzed constituents of PW is given in the appendix (Table S 21, p. 239). Such side streams are formed due to bio-oil instabilities and phase separation and jeopardize the overall efficiency of the conversion process (Dahmen, Henrich, *et al.*, 2012; Oasmaa *et al.*, 2015). PW retains about 15 % of the total energy of the initial biomass but valorization is discussed controversially. Notably, the high water content restrict further use as biofuel and renders extraction of hydrocarbons or gasification due to the low heating value inefficient (Xu *et al.*, 2011; Dahmen, Henrich, *et al.*, 2012). Whilst some studies clearly consider PW as waste stream and discuss disposal strategies (Xu *et al.*, 2009, 2011), others highlight the energy and organic compound content (Pfitzer *et al.*, 2016). In general, PW attracted minor consideration but valorization was for example proposed: by upgrading the biomass feed prior to pyrolysis (D. Chen *et al.*, 2017); biogas production after struvite recovery (Shanmugam *et al.*, 2017), by mixing with bio-slurries (biosyncrude) prior to gasification (Dahmen *et al.*, 2016); by blending of bio-oil fuels (Boucher, Chaala, and Roy, 2000; Boucher, Chaala, Pakdel, *et al.*, 2000); through green chemical production of hydrogen, alkanes (from C1 to C6) or polyols (ethylene glycol, 1,2-propanediol, 1,4-butanediol) (Vispute and Huber, 2009); biochemically by fermentation (Lian *et al.*, 2012; Wang *et al.*, 2013); or even in food applications such as liquid smoke flavors (Theobald *et al.*, 2012; Oasmaa *et al.*, 2015). Also extraction of hydrocarbons from pyrolysis water with the use of activated carbon or distillation was performed, with the goal of easier wastewater disposal (Xu *et al.*, 2011). The environmental parameters of pyrolysis water were analyzed in literature as well as on- or off-site wastewater treatment (Xu *et al.*, 2009).

Besides the chemical strategies, **biotechnological valorization** of fast pyrolysis fractions was proposed and is reviewed in literature (Arnold *et al.*, 2017). The major challenges to utilize such fractions is the general toxicity, a complex composition and low concentration of accessible molecules for microbes (Arnold *et al.*, 2017). In particular, the occurrence of sugar monomers, such as levoglucosan, was a driver to investigate the suitability of bio-oils for microbial cultivations. It is my personal convincement that chemical utilization as discussed above will be the more efficient and meaningful for bio-oils. Therefore, in this thesis we focused on the microbial use of the fast pyrolysis side

stream PW that so far received only limited consideration. Two examples for a fermentative use of pyrolysis water with either *Cryptococcus curvatus* or *E. coli* are known (Lian *et al.*, 2012; Wang *et al.*, 2013). Lian *et al.* demonstrated the lipid formation from acetate within PW with the oleaginous yeast *C. curvatus* ATCC 20509 with a lipid yield of 0.11 g lipid per g acetate within the PW. Their pretreatment procedure involved the following consecutive steps: neutralization, evaporation at 80 °C, dilution, and detoxification with activated carbon. During evaporation acetol (35 g $L^{-1}$) and glycolaldehyde was lost, yet intended, to circumvent their strong inhibitory effect on yeast proliferation. Wang *et al.* achieved succinate production with engineered *E. coli* MG-PYC and a maximum titer 0.38 g succinate $L^{-1}$ on pretreated 20 % (v/v) PW. The PW used in this study did not originate as side product directly from pyrolysis but by adding water to bio-oil and harvest a water fraction through centrifugation. In both studies toxicity of PW restricted its utilization – an issue that was addressed in this thesis as well.

In this work, we conceived an approach for growth-coupled biotransformation of the major carbon contents of PW to manufacture 1,2-propanediol (1,2-PDO, propylene glycol) with *Corynebacterium glutamicum* (cf. Part I, p. 106).

### 2.5.3. Organosolv processing

Organosolv processing or pretreatment of lignocellulosic residues is known since the 1970s as more eco-friendly alternative to kraft and sulfite pulping and traditionally accomplishes the extraction of lignin from the material by organic solvents or their water mixtures (Kleinert, 1971). The difference between organosolv pulping and pretreatment lies in the grade of delignification, which is higher in pulping (Brosse *et al.*, 2017). Most commonly utilized organic solvents are ethanol or methanol, but also other alcohols (ethylene glycol, glycerol, butanol, …), ethers, organic acids, ketones (for example acetone), phenols or more recently also ionic liquids were applied (Brosse *et al.*, 2017). The spent solvents can be recovered by distillation

***Organosolv pretreatment** involves organic solvents or their aqueous solutions, inorganic catalysts and temperatures between 100-250 °C to fractionate lignocellulose into solids (cellulose, lignin) and liquids (hemicellulose).*

*The Author*

(Zhao *et al.*, 2009). With the urgency of biomass valorization in a bioeconomy, organosolv pretreatment is another emerging option to overcome the recalcitrance of lignocellulose. The method is summarized in recommended literature (Duff and Murray, 1996; Zhao *et al.*, 2009, 2017; Brosse *et al.*, 2017). In contrast to fast pyrolysis, organosolv processing fractionizes the lignocellulose into solid cellulose, pure dry lignin and an aqueous hemicellulose solution (Duff and Murray, 1996). The process involves first the heating of a mixture of lignocellulose (solid liquid ratio between 1:4 to 1:10 (w/w)), organic solvents such as ethanol with concentrations of 35-70 % (w/v), water and inorganic catalysts like sulfuric acid to 180-210 °C for 30-90 min. Thereby, cellulose is fractionized as solid and a black liquor remains, containing extracted hemicellulose and lignin. The organic solvent is then recovered by distillation and lignin precipitated by addition of water and eventually filtered from the black liquor comprising hemicellulose-derived entities (Zhao *et al.*, 2009). **Cellulose** can be enzymatically saccharified and used for fermentation purposes (Zhao *et al.*, 2017). Exemplary applications of the high purity **lignin** are plastics and thermoplastic elastomers, functionalized fibers, polymeric foams and membranes, biofuels and other green chemicals (Brosse *et al.*, 2011; Ragauskas *et al.*, 2014; Liu *et al.*, 2015). Alternatively, lignin can be processed for example by fragmentation combined with hydrogenation and thermal depolymerization processes such as pyrolysis (Sannigrahi *et al.*, 2010; de Wild *et al.*, 2012; Liu *et al.*, 2015). The general role of lignin as cumulating renewable resource in lignocellulose biorefineries is discussed in literature with a proposed spectrum of thinkable products (Holladay *et al.*, 2007). The black residual liquor of organosolv pretreatment will henceforth be referred to as **hemicellulose fraction (HF)** and comprises sugars (monomers such as D-xylose, L-arabinose, D-glucose, D-mannose, D-galactose and oligomeric forms), weak acids, furan derivatives, phenolic residues and other extractives (Zhao *et al.*, 2009). It represents the fraction with most diverse composition and lowest value of the overall process. The complexity as well as the presence of toxic entities restricts a straightforward use of the HF. Potential application for fermentation and production of chemicals such as xylitol, furfural or other green chemicals were proposed, but await a practical realization (Zhao *et al.*, 2009; Brosse *et al.*, 2017). The HF due to its sophisticated composition is another example, why hemicelluloses in biorefinery strategy are still commonly wasted (Gírio *et al.*, 2010).

In the presented thesis, we assessed HF as potential substrate for *C. glutamicum*, demonstrate the bacterium's robustness and furthermore realized the production of an exemplary 2G biofuel – isobutanol – in engineered strains (cf. Part II, p. 123).

### 2.5.4. Lignocellulose decomposition releases toxic and inhibitory products

A major drawback that is shared among all lignocellulose pretreatment procedures is the formation of inhibitory or toxic side products. A list of typical inhibitors for *E. coli* such as 5-hydroxymethyl furfural, furfural, acetol or acetate is given in literature (Jarboe *et al.*, 2011). The toxic compounds can be grouped into weak acids, alcohols, furan derivatives, phenolic compounds and alkali metals and trace minerals. They strongly restrict the usability of lignocellulose-derived fractions for microbial cultivation purposes. Comprehensive summaries as well as measures for inhibitor removal are given in literature (Palmqvist and Hahn-Hägerdal, 2000a, 2000b; Klinke *et al.*, 2004; Sánchez and Cardona, 2008; Mills *et al.*, 2009; Jönsson *et al.*, 2013). Klinke *et al.* provide a detailed list of inhibitory substances and their effect on growth, production yield and productivity among various bacteria and yeasts and Sánchez and Cardona a recommended tabular compilation of detoxification routines.

Lignocellulose pretreatment results in the formation of **weak acids** such as acetate, formate, levulinate and others (Mills *et al.*, 2009). They account for the high buffering capacity of processing fractions. The weak acids can inhibit bacterial growth directly by promoting a low pH. They also act indirectly by diffusing through the cell membrane into the cytosol in form of the undissociated acid evoking intracellular pH reduction, metabolic inhibition and proton motive force disruption (Palmqvist and Hahn-Hägerdal, 2000b). Among others, acetate, which is predominantly formed from deacetylation of hemicellulose and to some extent lignin, is the major weak acid with concentrations in the range of 1-10 g $L^{-1}$ (Klinke *et al.*, 2004; Mills *et al.*, 2009).

Low molecular weight **alcohols** such as ethanol and methanol are abundant in lignocellulosic hydrolysates. As an example, pyrolysis water contains about 1.6 % (w/w) methanol (Table S 21, p. 239). Methanol toxicity can be allocated to an alteration of membrane fluidity (Sonmez *et al.*, 2013) or intracellular accumulation of the degradation

products formaldehyde or formate (Leßmeier and Wendisch, 2015).

In particular problematic is the occurrence of **furan derivatives**, mostly furfural (from pentoses) and hydroxymethylfurfural (HMF; from hexoses), as a result of sugar dehydration during the pretreatment procedure with typical concentrations between 0-5 g $L^{-1}$ (Almeida *et al.*, 2009; Mills *et al.*, 2009). Their degradation can promote the formation of formate and levulinate as previously discussed inhibitors. Both furfural and HMF were shown to provoke growth inhibition, lag-phase prolongation, and reduce fermentation rates in bacteria and yeast (Almeida *et al.*, 2009). Furfural is considered the most toxic entity of lignocellulose degradation and can cause DNA damage, inhibit glycolytic enzymes or hamper membrane integrity in its reduced form (Mills *et al.*, 2009). Numerous microorganisms and yeast have the native potential to modify the derivatives to their less toxic forms such as 2-furoic acid and furfuryl alcohol, respectively, and thereby mitigate the toxicity (Almeida *et al.*, 2009; Tsuge *et al.*, 2014).

Degradation of lignin is the source of **phenolic compounds** as acids, aldehydes and alcohols being found in pretreatment fractions with monomeric concentrations between 0-3 g $L^{-1}$ (Mills *et al.*, 2009). The most prominent entities are 4-hydroxybenzaldehyde, 4-hydroxybenzoic acid, vanillin, dihydroconiferyl alcohol, coniferyl aldehyde, syringaldehyde, and syringic acid (Klinke *et al.*, 2004). It was shown that toxicity mainly originates in the disruption of the cell membrane or interaction with yet unidentified intracellular hydrophobic structures. In general, low molecular weight phenols are less toxic than high molecular weight polyphenolics (Klinke *et al.*, 2004). Aldehydes cause the formation of reactive oxygen species and thus evoke oxidative damage (Almeida *et al.*, 2009).

**Alkali metals and trace minerals**, which are released from the plant cell wall during pretreatment, can be stress stimuli and elevate the osmotic pressure of cultivation broths (Jönsson *et al.*, 2013). An inhibitory effect was shown for $Ca^{2+}$, $Mg^{2+}$, $K^{+}$, $Na^{+}$, $NH_4^{+}$, $Cl^{-}$, $SO_4^{2-}$ and $HPO_4^{-}$ for *S. cerevisiae* (Maiorella *et al.*, 1984).

To overcome the toxicity a variety of physicochemical and biological strategies were developed (Palmqvist and Hahn-Hägerdal, 2000a; Jönsson *et al.*, 2013). Physicochemical strategies involve for example evaporation, extraction, ion exchange, active coal, treatment with reducing agents and overliming (increasing the pH to 9-10 with $Ca(OH)_2$)

(Olsson and Hahn-Hägerdal, 1996; Palmqvist and Hahn-Hägerdal, 2000a). Biological alternatives are treatment with enzymes (laccases, peroxidases) (Jönsson *et al.*, 1998; Zibek *et al.*, 2010) and bioprocess or metabolic engineering strategies to enhance strain robustness (Almeida *et al.*, 2009). As an example, anaerobic conditions were shown to be beneficial for *C. glutamicum* (Sakai *et al.*, 2007) as well as early stationary conditions in *S. cerevisiae* (Narayanan *et al.*, 2017). Furfural and HMF degradation was genetically enhanced in *E. coli* and *S. saccharomyces* (Petersson *et al.*, 2006; Liu and Moon, 2009; Miller *et al.*, 2009, 2010; Ishii *et al.*, 2013; Song *et al.*, 2017). Pre-adaptation or long-term evolution of > 2 years in *E. coli* (Geddes *et al.*, 2011) can be alternatively fruitful approaches to improve strain resistance and production performance. Functional metagenomics were recently performed and identified an enormous genetic potential to counteract toxicity of lignocellulose-derived inhibitors (Forsberg *et al.*, 2015). Relevant to the experimental work conducted here is also the previously demonstrated positive effect of reduced glutathione (GSH) on cultivations with lignocellulose hydrolysates in *S. cerevisiae* (Ask *et al.*, 2013).

Although in the last decade progress was made, a breakthrough to advance the tolerance of microorganisms towards inhibitors and toxic entities in lignocellulosic hydrolysates was not yet achieved (Huang *et al.*, 2016). In this study, we apply a fed-batch process to minimize the toxic effect of pyrolysis water as substrate (Figure 4.4, p. 118), which is a common strategy to circumvent initial high concentrations of growth and production inhibitors (Almeida *et al.*, 2009). Alternatively, genetic engineering to provide low molecular weight thiols was followed (cf. 4.2.3, p. 115).

# 2.6. *Corynebacterium glutamicum*

## 2.6.1. Discovery, taxonomy and characterization

This study is rooted on *C. glutamicum*, one of the most relevant biotechnological workhorse. It was originally isolated in 1957 under the original name *Micrococcus glutamicus* No. 534 and exhibits exceptional glutamate production (Kinoshita *et al.*, 1957, 1958). Ten years later until it was renamed and classified to *Corynebacterium glutamicum* (Abe *et al.*, 1967). The bacterium belongs to the class *Actinobacteria* and is non-spore forming, Gram-positive, has a high GC content (53-58 mol %), forms a typical "V-shape" during cell separation and shows an irregular rod-shaped morphology that is often referred to as "coryneform" (Liebl, 2005) (Figure 2.4). *C. glutamicum* is non-acid fast, immotile, biotin auxotrophic, catalase positive and facultatively anaerobic (Liebl, 2005; Nishimura *et al.*, 2007). Under anaerobic conditions it proliferates in the presence of nitrate (Nishimura *et al.*, 2007), whereas in the absence of this terminal electron acceptor only marginal growth was found (Michel *et al.*, 2015). *Corynebacterineae* possess an exceptionally stable cell wall structure that incorporates lipophilic mycolic acids – a unique feature of this suborder (Liebl, 2005). *C. glutamicum* can be isolated from soil, soil contaminated with bird feces, sewage, manure, vegetables, and fruits (Tauch, 2008) and thrives with growth rates up to 0.46 $h^{-1}$ (single cells 0.62 $h^{-1}$) in minimal medium with D-glucose as sole carbon source (Grünberger *et al.*, 2012; Unthan, Grünberger, *et al.*, 2014). Most commonly applied strains are *C. glutamicum* ATCC 13032 or *C. glutamicum* R. For both the genome was sequenced (Ikeda and Nakagawa, 2003; Kalinowski *et al.*, 2003; Yukawa *et al.*, 2007). A recent study compares 26 different *C. glutamicum* strains and resolves a pan-genomic description at the species level (Yang

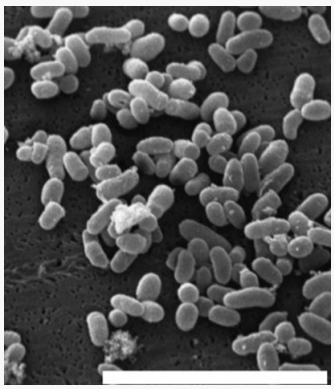

**Figure 2.4. Scanning electron micrograph of *C. glutamicum* WT** with an average length of 1.43 µm. The graphic was withdrawn from literature (Möker *et al.*, 2004). White bar marks 10 µm.

and Yang, 2017). Besides non-pathogenic representatives, the genus *Corynebacterium* also includes pathogens such as *C. diphtheriae* or *C. jeikeium* (Barksdale, 1970; Tauch, 2008). Knowledge about *C. glutamicum* can thus be projected also to pathogenic relatives and provides valuable information for pharmaceutical applications.

### 2.6.2. Industrial biotechnology

Since its first discovery, *C. glutamicum* has manifested as a generally recognized as safe (GRAS) industrial workhorse besides *E. coli*, *Bacillus subtilis* and *Saccharomyces cerevisiae* (Becker and Wittmann, 2015). Originally, it was solely a specialist for the amino acid production such as monosodium glutamate (MSG) and L-lysine, which reached a market size of approximately 3.1 and 2.2 million tons per year in 2015, respectively (Ajinomoto Co., 2016). Intensive research overcame this specialization, gave rise to sound development of metabolic engineering (Suzuki and Inui, 2013) and synthetic biology (Woo and Park, 2014) tools and access to systems biology with *OMICS* technologies (Wendisch *et al.*, 2006; Burkovski, 2015) and genome scale metabolic models (Kjeldsen and Nielsen, 2009; Shinfuku *et al.*, 2009; Zhang *et al.*, 2017). The production scope thus expanded towards various natural and non-natural compounds such as L-amino acids (L-alanine, L-valine, …) and D-amino acids (D-serine, D-lysine, …), organic acids (D-lactate, succinate, …), alcohols (ethanol, isobutanol, 1,2-propanediol, …), vitamins (pantothenate), pyrazines, diamines (cadaverine, diaminopentane, …), pyrimidines (ectoines), terpenoids (astaxanthin, β-carotene, …) and polymers (P(3HB), polygalacturonic acid, …) (reviewed in (Becker and Wittmann, 2012, 2015; Heider and Wendisch, 2015)). Most advanced production processes reached exceptionally high productivities of 4 g L-lysine $L^{-1}$ $h^{-1}$ (Becker *et al.*, 2011) and high titers such as 216 g L-alanine $L^{-1}$ in anaerobic zero-growth productions (Yoto *et al.*, 2012; Lange, Takors, *et al.*, 2017). Beyond small molecules, *C. glutamicum* is also discussed as host for biotechnological and pharmaceutical protein production (Vertès, 2013; Freudl, 2015, 2017). With the demand to integrate into bioeconomy and biorefinery processes the substrate spectrum was expanded from native substrates (glucose, fructose, sucrose, mannose, ribose, acetate, lactate, …) towards novel carbon sources (starch, arabinose, xylose, lactose, galactose, cellobiose, glycerol, …) (Blombach and Seibold, 2010; Becker and Wittmann, 2012, 2015; Leßmeier *et al.*, 2015).

### 2.6.3. Central metabolism

Intensive reviews of the central metabolism of *C. glutamicum* (Figure 2.5) are available in literature and represented the anchor for the given brief summary (Eikmanns, 2005; Yokota and Lindley, 2005; Bott and Eikmanns, 2013). The backbone of the central metabolism of *C. glutamicum* form sugar uptake, glycolysis, pentose phosphate pathway (PPP) and the tricarboxylic acid cycle (TCA). A remarkable role play anaplerotic reactions at the phosphoenolpyruvate (PEP)-pyruvate-oxaloacetate node that intertwines glycolysis and TCA (Sauer and Eikmanns, 2005). Classical **sugar uptake systems** in *C. glutamicum* with three phosphotransferase systems (PTS) accomplish the major phosphorylative uptake of fructose, glucose and sucrose (Postma *et al.*, 1993; Yokota and Lindley, 2005; Galinier and Deutscher, 2017). Assimilated sugars enter classical **glycolysis** at the level of glucose-6-phosphate or fructose-1,6-bisphosphate. Interestingly, glycolysis and **PPP** have a remarkable ratio. Under aerobic conditions around 69 % of the carbon flux is directed through the PPP (Bartek *et al.*, 2011), whereas for *E. coli* it was determined between only 20-30 % (Szyperski, 1995; Fischer and Sauer, 2003). Under anaerobiosis the PPP is almost inactive with a low flux of 5 % (Radoš *et al.*, 2014), which is in accordance to *S. cerevisiae* (8 %) or *E. coli* (5 %) (Nissen *et al.*, 1997; Sauer *et al.*, 1999; Villadsen *et al.*, 2011). The PPP is divided into an oxidative, where glucose-6-phosphate is converted to ribulose-5-phosphate, and a reductive branch that realizes reversible interconversion reactions employing transketolases and transaldolases. The major function of the oxidative branch (Figure 3.4, p. 98) is the delivery of reducing equivalents in form of NADPH to generate anabolic reduction power for the synthesis of cellular building blocks (Yokota and Lindley, 2005). The heart of the metabolism being active regardless of the carbon or energy source is the **TCA**, which serves as anabolic but also for catabolic purposes for energy generation. It is the connecting circle between glycolysis, biosynthesis, fermentation and respiration and thus fuels the cell with energy by providing ATP and reducing equivalents. Its primary substrate is acetyl-coenzyme A (acetyl-CoA), which is provided by the oxidation of pyruvate in the pyruvate dehydrogenase complex (PDHC). Acetyl-CoA is fully oxidized to $CO_2$ in the TCA (Bott and Eikmanns, 2013). The PDHC as multienzyme complex is a central target for strain engineering to enhance pyruvate availability in PDHC deficient strains or PDHC mutants with reduced activity (Eikmanns and Blombach, 2014). Depending on carbon source or

environmental conditions, parts of the TCA are shutdown or enforced. For example the glyoxylate shunt is activated, where substrates such as acetate enter the metabolism at the state of acetyl-CoA (Eikmanns, 2005). As intermediates of the TCA are constantly withdrawn for biosynthesis, the cycle must be replenished by anaplerotic reactions. The **PEP-pyruvate-oxaloacetate node** accomplishes this task using C3 (PEP and pyruvate) carboxylating reactions (Sauer and Eikmanns, 2005). It is also the origin of gluconeogenesis by working in reverse direction via C4 (oxaloacetate and malate) decarboxylation and thus directly links the glycolysis with the TCA. At least five enzymes, catalyze the reactions and thereby either fixate $CO_2$ [PEP carboxylase (PEPCx), pyruvate carboxylase (PCx)] or produce $CO_2$ [PEP carboxykinase (PEPCk), oxaloacetate decarboxylase (ODx), malic enzyme (ME)]. The coexistence of a PEPCx and a PCx is a notable feature of *C. glutamicum* and not present in most other organisms (Eikmanns, 2005; Sauer and Eikmanns, 2005).

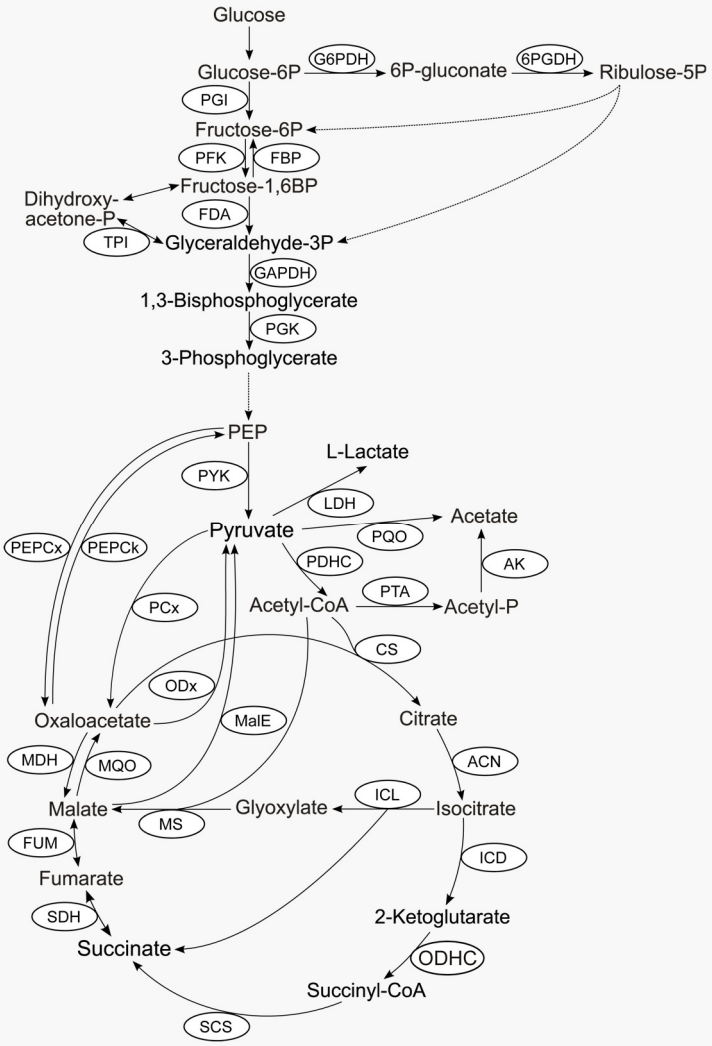


**Figure 2.5. Central metabolism of *C. glutamicum***. A selection of glycolysis, PPP, TCA and the PEP pyruvate-oxaloacetate node is vizualized. Enzymes are given including the gene(s) and name in parenthesis: 6PGDH (*gnd*; 6-phosphogluconate dehydrogenase), ACN (*acnA*; aconitate hydratase), AK (*ackA*; acetate kinase), CS (*gltA*; citrate synthase), FBP (*fbp*; fructose-1,6-bisphosphatase), FDA (*fda*; fructose-bisphosphate aldolase), FUM (fum; fumarate hydratase), G6PDH (*zwf*, *opcA*; glucose-6P dehydrogenase), GAPDH (*gapA*; glyceraldehyde-3-phosphate dehydrogenase), ICD (*icd*; isocitrate dehydrogenase), ICL (*aceA*; isocitrate lyase), LDH (*ldhA*; L-lactate dehydrogenase), MalE (*malE*; malic enzyme), MDH (*mdh*; malate dehydrogenase), MQO (*mqo*; malate:quinone oxidoreductase), MS (*aceB*; malate synthase), ODHC (*odhA*, *sucB*; E1o and E2o subunits oxoglutarate dehydrogenase complex, ODx (*odx*; oxaloacetate decarboxylase), PCx (*pyc*; pyruvate carboxylase), PDHC (*aceE*, *sucB* and *lpd*; E1p, E2 and E3 pyruvate dehydrogenase complex subunits), PEPCk (*pck*; phosphoenolpyruvate carboxykinase), PEPCx (*ppc*; phosphoenolpyruvate carboxylase), PFK (pfk; 6-phosphofructokinase), PGI (*pgi*; phosphoglucoisomerase), PGK (*pgk*; 3-phosphoglycerate kinase), PQO (*pqo*; pyruvate:quinone oxidoreductase, PTA (*pta*; phosphotransacetylase), PYK (*pyk*; pyruvate kinase), SCS (*sucCD*; succinyl-CoA synthetase), SDH (*sdhA*, *sdhB* and *sdhCD*; succinate dehydrogenase), and TPI (*tpi*; triosephosphate isomerase). Graphic represents an extended version to literature (Eikmanns and Blombach, 2014).

### 2.6.4. Fermentative capacity and anaerobic phenotype

Under anaerobic conditions and in the absence of nitrate as terminal electron acceptor *C. glutamicum* exhibits a mixed acid fermentation of D-glucose to L-lactate, acetate and succinate (Dominguez *et al.*, 1993; Inui, Murakami, *et al.*, 2004). Transcriptomic data of the shift from aerobiosis to anaerobiosis are available but will be discussed elsewhere (cf. Part III, p. 138) (Inui *et al.*, 2007; Yamamoto *et al.*, 2011; Sun *et al.*, 2016). Although classically it was believed that growth under such oxygen deprived conditions was not feasible (Bott and Niebisch, 2005), newer studies could prove marginal growth on selected carbon sources (Michel *et al.*, 2015). Under non-growth anaerobic conditions *C. glutamicum* exhibits a high robustness; a feature which is exploited for high cell density production of low energy demanding products (Jojima, Inui, *et al.*, 2015). Products such as organic acids (e.g. succinic acid, lactic acid), alcohols (e.g. ethanol, isobutanol) or amino acids (e.g. alanine, valine) can be secreted with exceptionally high productivities in resting state production scenarios (cf. 2.11.3, p. 58) (Lange, Takors, *et al.*, 2017).

### 2.6.5. Respiratory chain

Comprehensive summaries of the respiratory repertoire of *C. glutamicum* are given in literature (Bott and Niebisch, 2003, 2005; Matsushita, 2013). Suitable terminal electron acceptors are either oxygen or nitrate. The respiratory chain consists of at least eight primary dehydrogenases and four cytochrome oxidases as shown in Figure 2.6 (Bott and Niebisch, 2005). The dehydrogenases accomplish the electron transfer from NADH or directly from metabolites and carbon sources to menaquinone (MQ). The reduced menaquinol ($MQH_2$) functions as electron carrier towards terminal cytochrome oxidases, where $MQH_2$ is re-oxidized and an electrochemical proton gradient conserves the energy across the cell membrane (Matsushita, 2013). In the absence of nitrate three major cytochrome oxidases transfer electrons to molecular oxygen: First, the cytochrome $bc_1$ and $aa_3$ oxidases assemble to the cytochrome $bc_1$-$aa_3$ supercomplex (encoded by: *ctaE-qcrCAB*, *ctaCF*, *ctaD*), which is the major oxidase active under aerobic conditions (Niebisch, 2002). Second, the cytochrome *bd* oxidase (encoded by *cydAB*), which exhibits a lower energy conservation but higher affinity towards oxygen (Kusumoto *et*

*al.*, 2000; Bott and Niebisch, 2003). The cytochrome *bd* oxidase is thus activated under oxygen limited conditions (Kabus *et al.*, 2007; Koch-Koerfges *et al.*, 2013). A recent study reports that activation of the cytochrome *bd* oxidase is coordinated by the sigma factor $\sigma^C$ (Toyoda and Inui, 2016b). The regulator OxyR was also shown to regulate to the *cydA* promoter in response to peroxide stress conditions (Milse *et al.*, 2014). Koch-Koerfges *et al.* were able to construct a DOOR (devoid of oxygen respiration) mutant strain, where both cytochrome oxidases were disrupted (Koch-Koerfges *et al.*, 2013). Most interestingly, the DOOR strain proliferated as aerobic fermenting phenotype producing L-lactate, succinate and acetate with reduced biomass yield and proton motive force. Similar aerobically fermenting phenotypes were also published in *E. coli* (Bekker *et al.*, 2009; Portnoy *et al.*, 2010).

### 2.6.6. Regulatory network

Understanding the regulatory network of a host for industrial biotechnology provides the basis to modulate the native metabolism towards desired products. Regulators and sigma factors (σ-factors) were intensely studied and reviewed in literature for *C. glutamicum* (Arndt and Eikmanns, 2008; Frunzke and Bott, 2008; Brinkrolf *et al.*,

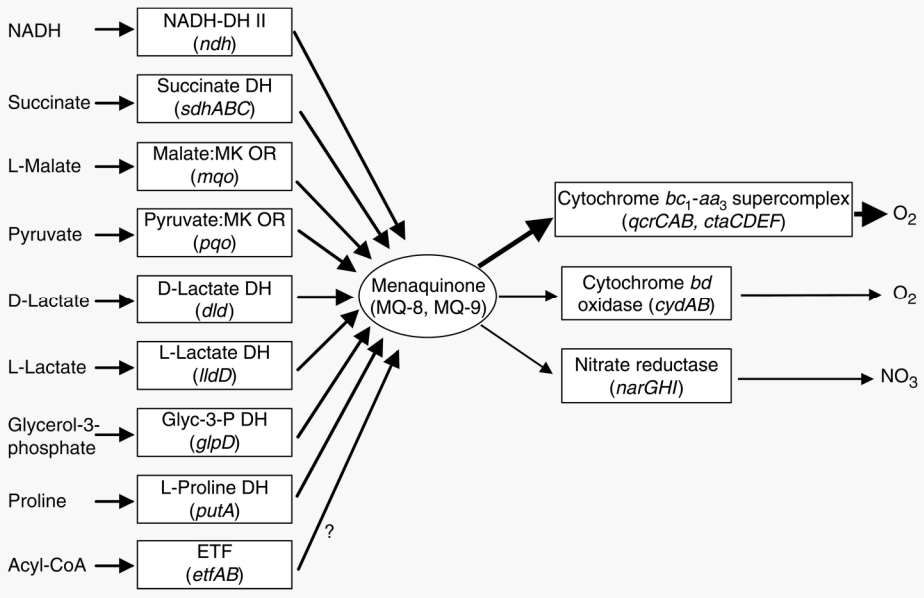


**Figure 2.6. Overview over the respiratory chain of *C. glutamicum***. Graphic withdrawn from literature (Bott and Niebisch, 2003).

2010; Schröder and Tauch, 2010; Toyoda and Inui, 2016a) but also in comparison to its close non-pathogenic and pathogenic relatives (Brune *et al.*, 2005; Schröder and Tauch, 2010). In total 159 genes encoding transcriptional regulators and 7 σ-factors (primary factor is $\sigma^A$) were annotated (Schröder and Tauch, 2010). The transcriptional regulators were classified into local regulators (e.g. RipA, SufR, CysR, …), master regulators (e.g. RamA, RamB, DtxR, …) and a global regulator (GlxR). Complex regulatory phenomena of metabolic pathways such as the TCA involve for example also post transcriptional regulation using a phosphorylation dependent modulation (Bott, 2007) or protein degradation targeting via the pupylation system (Küberl *et al.*, 2014). The potential of modulating σ-factors in industrial strain development revealed promising perspectives (Taniguchi and Wendisch, 2015; Taniguchi, 2016).

## 2.6.7. Suitability for biorefinery

### 2.6.7.1 Toxic components and diverse carbon sources

Driven by the inherent characteristics of *C. glutamicum* and the high standard of knowledge about its physiology, it is regarded as potential host to integrate into biorefineries (Jojima *et al.*, 2013). Among these properties are the high resistance towards typical lignocellulose-derived inhibitory or toxic entities, especially under oxygen deprivative conditions (Sakai *et al.*, 2007), and a broad substrate flexibility (Becker and Wittmann, 2015). Sakai *et al.* demonstrated that ethanol productivity in a resting state anaerobic process was, in comparison to *E. coli* and *S. cerevisiae*, little effected by the presence of typical lignocellulose-derived substances such as organic acids, furans and phenols (Sakai *et al.*, 2007). It was also shown that *C. glutamicum* possesses native detoxification mechanisms for inhibitors such as furfural by conversion to the less problematic intermediates furfuryl alcohol and 2-furonic acid (Tsuge *et al.*, 2014). Due to the complexity of lignocellulose-derived substrates bacteria face an abundance of potential carbon sources in parallel. It is known that the *C. glutamicum* shows little preference within such substrate mixtures and is capable of broad co-utilization (Arndt and Eikmanns, 2008; Blombach and Seibold, 2010). This fact is a clear advantage to other organisms, as sequential consumption of substrates due to carbon catabolite repression is known for numerous microbes such as *E. coli*, *B. subtilis* or *S. cerevisiae* (Gancedo, 1998; Deutscher, 2008; Görke and Stülke, 2008). *C. glutamicum* cannot naturally metabolize

prominent substrates from lignocellulose pretreatment such as L-arabinose or D-xylose (Zahoor *et al.*, 2012) but was shown to possess a broad degradation machinery for aromatic compounds and abundant organic acids (Shen *et al.*, 2012; Kallscheuer *et al.*, 2015; Leßmeier *et al.*, 2015). A tabular summary of engineered *C. glutamicum* strains in comparison to *E. coli*, *Pseudomonas* sp. and yeast with broadened substrate spectrums is reviewed elsewhere (Wendisch *et al.*, 2016). Due to the further relevance in this study, the pentoses L-arabinose and D-xylose along with engineering strategies will be further discussed in the following paragraph.

#### 2.6.7.2 L-Arabinose and D-xylose as carbon source for growth and production in engineered *C. glutamicum*

*C. glutamicum* ATCC 13032 does not harbor native metabolic pathways for L-arabinose or D-xylose metabolization. Motivated by the pentoses' abundance in lignocellulosic biomass, the bacterium was genetically engineered to provide assimilating pathways (Figure 4.9, p. 135).

It was found that *C. glutamicum* encodes a native and functional xylulokinase (XylB, cg0147) but lacks the essential xylose isomerase (XylA) (Kawaguchi *et al.*, 2006). Kawaguchi *et al.* demonstrated that heterologous production of XylA from *E. coli* is sufficient for aerobic growth on **D-xylose** as sole carbon source and moreover enabled anaerobic, parallel consumption of D-glucose and the pentose (Kawaguchi *et al.*, 2006). Improvements of this so-called *isomerase pathway* were achieved comparing various combinations of the XylA and XylB enzymes from different organisms. Meiswinkel *et al.* identified the construct of *xylA* (*Xanthomonas campestris*) and *xylB* (*C. glutamicum*) as being the most potent allowing a maximum growth rate of 0.20 $h^{-1}$ on D-xylose (Meiswinkel *et al.*, 2013). Apart from the presented *isomerase pathway*, the more carbon efficient *Weimberg* pathway, is considered more recently as an attractive alternative, also to prevent frequently occurring sequential consumption behaviors on parallel supply of D-xylose with other carbon sources (Radek *et al.*, 2014, 2016). Uptake of D-xylose was shown to be feasible also by the D-glucose phosphotransferase system (PTS) encoded by *ptsG* (Wang, Cai, *et al.*, 2014).

Another prominent pentose in hemicellulose is **L-arabinose**. Kawaguchi *et al.* enabled for the first time a parallel consumption of D-glucose and L-arabinose under anaerobic

conditions by heterologously providing an L-arabinose isomerase (AraA), L-ribulokinase (AraB) and 5-phosphate 4-epimerase (AraD) (Kawaguchi *et al.*, 2008). The close relative *C. glutamicum* ATCC 31831 is able to natively proliferate on L-arabinose through the expression of an *araBDA* operon and an L-arabinose transporter (AraE), which are both regulated by an LacI-type transcriptional regulator (AraR) (Kawaguchi *et al.*, 2009; Kuge *et al.*, 2015). The expression of the transporter gene *araE* was, besides L-arabinose uptake, also shown to be beneficial for D-xylose assimilation, which is in accordance to observations in *E. coli* and *B. subtilis* (Krispin and Allmansberger, 1998; Hasona *et al.*, 2004; Sasaki *et al.*, 2009). The maximum growth rate, substrate consumption rate and biomass/substrate yield on L-arabinose as sole carbon source in the absence of AraE and using pVWEx1-*araBAD* were 0.31 $h^{-1}$, 3.7 mmol L-arabinose per g CDW per h and 0.38 g CDW per g L-arabinose, respectively (Schneider *et al.*, 2011).

Engineered strains that allowed parallel utilization of D-glucose, L-arabinose, D-xylose and cellobiose were also constructed (Sasaki *et al.*, 2008, 2009). Under anaerobic conditions a co-utilization of these four carbon sources was impressively demonstrated (Sasaki *et al.*, 2009). Laboratory evolution approaches could further enhance xylose and/or cellobiose uptake and metabolization (Lee *et al.*, 2016; Radek *et al.*, 2017).

Overall, engineered *C. glutamicum* manifested as suitable candidate to use to utilize pentoses from pretreated lignocellulosic residues for the production of value-added products (Gopinath *et al.*, 2012) such as organic acids (L-lactate, succinate, 3-hydroxypropionate, …) (Kawaguchi *et al.*, 2009; Chen *et al.*, 2014; Wang, Zhang, *et al.*, 2014; Jo *et al.*, 2017; Z. Chen *et al.*, 2017), amino acids (L-glutamate, L-lysine, L-ornithine, putrescine, …) (Gopinath *et al.*, 2011; Schneider *et al.*, 2011; Meiswinkel *et al.*, 2013), 1,5-diaminopentane (Buschke *et al.*, 2011, 2013), ethanol (Jojima, Noburyu, *et al.*, 2015) or xylitol (Kim *et al.*, 2010; Sasaki *et al.*, 2010; Dhar *et al.*, 2016; Radek *et al.*, 2016). Besides these advances, the bacterium's suitability for biorefineries benefits from the acceptance of acetate as carbon source – a major component in such biomasses. In this thesis, we conducted cultivations of engineered *C. glutamicum* on realistic lignocellulose hydrolysates implying a parallel supply of L-arabinose, D-xylose and acetate (cf. 4.6, p. 128).

## 2.7. 1,2-Popanediol

1,2-propanediol (1,2-PDO, or propylene glycol) is a C3 dialcohol, has an estimated global production capacity of > 1.5 million tons per year and can be considered as medium-value bulk chemical due to a broad spectrum of applications (Zeng and Sabra, 2011). The diol is mainly used as eco-friendly chemical in antifreeze, heat transfer and de-icing fluids, but also for example in dyes, food (E#1520), pharmaceuticals or cosmetics (Zhou *et al.*, 2008; Zeng and Sabra, 2011; Sabra *et al.*, 2016).

Established commercial strategies produce 1,2-PDO from natural gas by conversion via propylene to 1,2-PDO (Johnson and Taconi, 2007). The production of 1,2-PDO based on renewable resources has been broadly exploited by chemical routes. Mostly, the biodiesel production by-product glycerol is converted by hydrogenolysis (Dasari *et al.*, 2005; Suppes *et al.*, 2005) but also combinatory approaches for example fermentation of glucose to lactate and subsequent chemical conversion to 1,2-PDO are proposed scenarios (Varadarajan and Miller, 1999). An alternative chemical strategy involving of the intermediate acetol was shown as well (Dasari *et al.*, 2005). Typical molar yields in the chemical conversions using glycerol [mol 1,2-PDO per mol glycerol] as substrate range from > 0.73 (Dasari *et al.*, 2005), 0.79 (Liu *et al.*, 2012), 0.92 (Suppes *et al.*, 2005) or directly from lignocellulosic material 0.39 C-mol 1,2-PDO C-mol total substrate (Zhou *et al.*, 2012). Glycerol dependent chemical processes have been broadly commercialized but apply temperatures of 200 °C and pressures of 200 psi (Bozell and Petersen, 2010).

As biochemical alternative to the chemical route, aerobic as well as anaerobic production under mild reaction conditions was achieved (reviewed in (Bennett and San, 2001; Saxena *et al.*, 2010)). A variety of either natural (e.g. *Clostridium thermosaccharolyticum, Lactobacillus buchneri*) or engineered (e.g. *C. glutamicum*, *E. coli*, *S. cerevisiae*, *Pichia pastoris*) microbial hosts were constructed and evaluated for 1,2-PDO production with a broad substrate spectrum (e.g. glucose, glycerol, and lactate) (Cameron and Cooney, 1986; Altaras and Cameron, 2000; Oude Elferink *et al.*, 2001; Clomburg and Gonzalez, 2011; Jung *et al.*, 2011; Barbier *et al.*, 2012; Siebert and Wendisch, 2015). A list of the relevant production scenarios and correspondent parameters is given in Table 2.1 in comparison to the most advanced process developed in this study (for more specific description cf. 3.14.8 Part I, p. 106). Very recently, the

cyanobacterium *Synechococcus elongatus* PCC 7942 was engineered for photosynthetic production of 1,2-PDO from $CO_2$ with a titer of approximately 2.0 mM (Li and Liao, 2013). In general, product yields were generally limited through by-product formation such as acetol, dihydroxyacetone or glycerol and partial substrate use for biomass generation. Thus, the maximal theoretical yield of 1.49 mol 1,2-PDO per mol glucose or 0.87 mol 1,2-PDO per mol glycerol could by far not be reached (Sabra *et al.*, 2016). In dominant production scenarios with engineered strains (Figure 2.9, p. 54), dihydroxyacetone phosphate is converted to methylglyoxal by the methylglyoxal synthase (MgsA), which is further reduced to acetol or lactaldehyde by the alcohol dehydrogenase (YqhD) and/or the glycerol dehydrogenase (GldA). The *E. coli* GldA, which is mostly harnessed in heterologous systems, finally converts acetol to R-1,2-PDO with the use of NADH as cofactor at 100 % stereoselectivity (Cameron *et al.*, 1998). The enzyme was functionally overexpressed also in *C. glutamicum* (Niimi *et al.*, 2011; Siebert and Wendisch, 2015). Remarkably, a production in these studies was clearly growth decoupled and arose only upon stationary phase initiation; a fact which was not further discussed. A drawback of the stated pathway is the occurrence of methylglyoxal as intermediate which is highly cytotoxic (cf. 2.10, p. 52). It was proposed that mycothiol (MSH) overproduction in engineered *C. glutamicum* could mitigate methylglyoxal sensitivity and enhance 1,2-PDO production (Siebert and Wendisch, 2015). To circumvent this issue, a fully synthetic pathway to produce 1,2-PDO from lactate in an enantioselective manner was proposed involving a lactoyl-CoA transferase (Pct, *Megasphaera elsdenii*), CoA-dependent lactaldehyde dehydrogenase (PduP, *Salmonella enterica*) and lactaldehyde reductase (YahK, *E. coli*) (Niu and Guo, 2015). In the presented study, engineered *C. glutamicum* does not encounter methylglyoxal as similar metabolite during the production of 1,2-PDO as the product is formed in a one-step reduction of acetol as direct precursor.

**Table 2.1. Comparison of selected microbial 1,2-PDO producers** in comparison to the process of this study (cf. 4.3.2, p. 120). YE, yeast extract. PW, pyrolysis water. $Y_{P/S}$, product yield. $O_P$, volumetric productivity. Table according to published work (Lange, Müller, *et al.*, 2017).

| Organism | Strain, genotype, plasmid | Substrate(s) | Oxygen-ation | Titer, mM | $Y_{P/S}$, mol mol$^{-1}$ | Process time, h | $Q_P$, mmol L$^{-1}$ h$^{-1}$ | Reference |
|---|---|---|---|---|---|---|---|---|
| **_C. glutamicum_ ATCC 13032** | **PDO2 [Δ_pqo_ Δ_aceE_ Δ_ldhA_ Δ_mdh_ + pJUL_gldA_]** | **PW (acetol), YE** | **aerobic/ microaerobic** | **18** | **0.96** | **13** | **1.40** | **This study [a]** |
| *C. glutamicum* ATCC 13032 | Δ*hdpA* Δ*ldh* + pEKEx3-*mgsA-yqhD-gldA* | Glucose | aerobic | 63 | 0.34 | 51 | 1.24 | (Siebert and Wendisch, 2015) |
| *Clostridium thermosacch-arolyticum* ATCC 31960 | | Glucose, YE | anaerobic | 119 | 0.47 | 28 [b] | 4.25 | (Cameron and Cooney, 1986) |
| *E. coli* MG1655 | Δ*ackA-pta* Δ*ldhA* Δ*dhaK* + pTHKLcfgldA mgsAyqhD | Glycerol, tryptone, YE | anaerobic | 74 | 0.26 | 72 | 1.02 | (Clomburg and Gonzalez, 2011) |
| *E. coli* MG1655 | NLD294 (Δ*ldhA*) + pNEA36 [*mgs*, *gldA*, *fucO*] | Glucose, YE | anaerobic | 59 | 0.45 | 60 | 0.99 | (Altaras and Cameron, 2000) |
| *Lactobacillus buchneri* (LMG 6892T) | | Lactate | anaerobic | 8 | 0.45 [c] | 55 | 0.14 | (Oude Elferink *et al.*, 2001) |
| *Saccharomyces cerevisiae* YPH499 | pESC-URA-*mgs* & *gldA* + pESC-LEU-*gdh* & *GUP1* | Glycerol, YE, amino acids | aerobic | 29 | 0.26 | 96 | 0.30 | (Jung *et al.*, 2011) |

[a] parameters calculated based on the acetol found in PW

[b] assigned from published graphic

[c] used the given 16.5 mM of consumed lactate as basis for calculation

# 2.8. Biofuels

## 2.8.1. A global perspective of 1G and 2G biofuels

Among other flagship targets until 2020, the European Commission proposed to reduce the greenhouse gas emissions by at least 20 % compared to 1990 (European Commission, 2010), to have a 20 % share of renewables in the total energy consumption and 10 % biofuels of the overall consumption of petrol and diesel in transportation (European Commission, 2007). The ongoing realization of such regulations can be seen for example in the 66$^{th}$ annual report of BP p.l.c. with a continuous increase of the global biofuel production in the last 10 years by 14 % until 2016 and current global production of around 82.3 billion tons of oil equivalent (Figure 2.7) (BP p.l.c., 2017). These impressing numbers were realized with 1G biofuels mainly from ethanol by fermentation or biodiesel from rape seed oil. In Europe bioethanol production peaked with 5.3 billion liters in 2014 (Flach *et al.*, 2016) and was around 58.0 billion liters in 2016 in the U.S. (Renewable Fuels Association, 2016). Bio-ethanol is traditionally produced by yeast

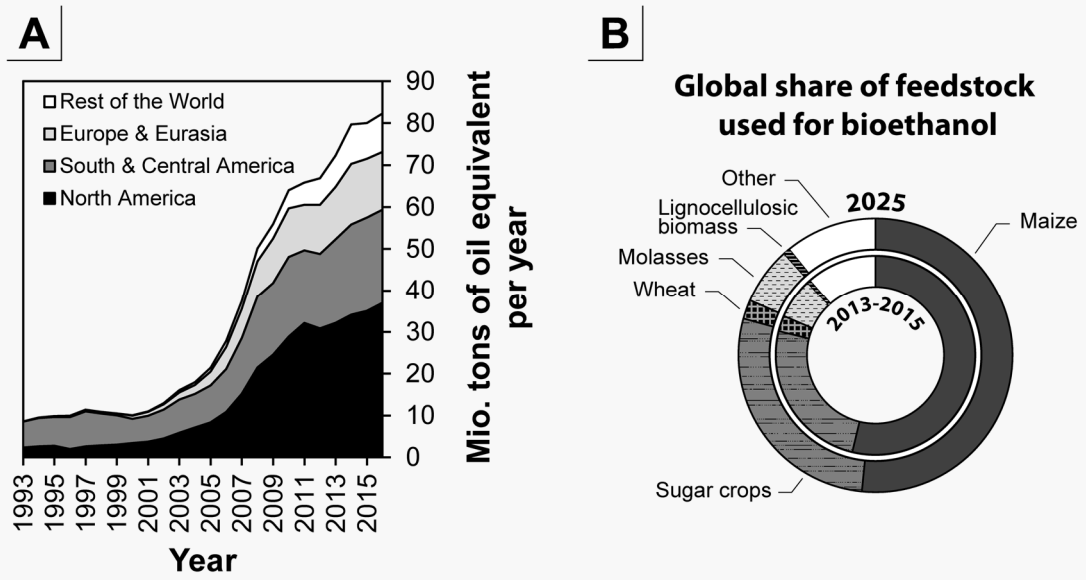


**Figure 2.7 Global biofuel production**. **A**. 1G biofuel production (ethanol, biodiesel) until 2016. Graphic based on literature (BP p.l.c., 2017). 1 ton of ethanol or biodiesel equals 0.68 or 0.88 tons of oil equivalent, respectively. **B**. Global share of feedstock for bioethanol production between 2013-2015 (inner ring) and projected until 2025 (outer ring). Data derived from the OECD-FAO agricultural outlook in the expanded biofuels chapter (OECD-FAO, 2016).

fermentation but bacterial native or engineered producer derivatives were also implemented (Dien *et al.*, 2003; Alper and Stephanopoulos, 2009). As a drawback, 1G biofuels directly compete with food and feed by the use of biomasses such as maize, sugar crops, wheat, molasses and others. Therefore, with respect to sustainability and ethics, they are considered critically (Mohr and Raman, 2013). A future change towards 2G biofuels is thus necessary to guarantee a future food security (Hahn-Hägerdal *et al.*, 2006). Currently, between 2013 and 2015 only 0.4 % of the total biomass resources used for ethanol production were lignocellulosic. For 2025 a reluctant increase to roughly 0.7 % is expected (OECD-FAO, 2016). This hesitancy in development is caused mainly by the lignocellulose recalcitrance as discussed above (cf. 2.4, p. 21) but also by a narrow price competitiveness range. It was proposed that lignocellulosic biofuels demand a price within the range of 70-85 US$ per barrel (Valdivia *et al.*, 2016), which is hardly competitive to the low current oil prices of 51.3 US$ per barrel (OPEC, 2017). Nonetheless, genetic strain engineering for the use of hemicellulose, which is commonly wasted in bioethanol production (Gírio *et al.*, 2010), reaches profitability (Zaldivar *et al.*, 2001; Balat, 2011). Pilot and commercial plants were built in recent years for example by POET-DSM Advanced Biofuels in Emmetsburg (USA), Raízen Energia Participacoes S/A using Iogen technology in Costa Pinto (Brazil), Abengoa Bioenergy Biomass of Kansas (ABBK) in Hugoton (USA), SEKAB in Örnsköldsvik (Sweden), Borregaard LignoTech in Sarpsborg (Norway) or Clariant using sunliquid® technology in Straubing (Germany). A techno-economic review as well as general reflection of 2G lignocellulosic ethanol is recommended at this point (Gnansounou and Dauriat, 2010; Valdivia *et al.*, 2016). Typical lignocellulose-rich energy crops such as switchgrass, poplar or *Miscanthus* sp. besides agrobiological wastes such as corn stover will provide a sound basis for production and have a future potential to save between 51-100 % of greenhouse gas emissions in comparison to petrol (Sanderson, 2006). The 2G biofuel vision is slowly picking up pace and will be a major future goal.

### 2.8.2. A next generation biofuel: isobutanol

Although ethanol is the most prominent microbially manufactured biofuel, it has several drawbacks such as a lower density than gasoline (~ 70 % of gasoline), high vapor pressure and high hygroscopy (Smith *et al.*, 2010). Longer chain alcohols (C4 and C5)

**Table 2.2. Yields of prominent microbial isobutanol production processes** in comparison to this study. Exemplary studies are listed and the isobutanol yield calculated per supplemented substrate. The cultivation condition with respect to oxygen availability and maximum theoretical yields (grey) are given.

| Substrate | Yield | | | Condition | Organism | Reference |
|---|---|---|---|---|---|---|
| | mol mol$^{-1}$ | g g$^{-1}$ | C-mol C-mol$^{-1}$ | | | |
| HF | - | - | 0.29 [a] | anaerobic | *C. glutamicum* | This study (cf. 4.8, p. 132) |
| Glucose | 0.77 | 0.32 | 0.51 | anaerobic | *C. glutamicum* | (Blombach *et al.*, 2011) |
| Glucose | 0.78 | 0.32 | 0.52 | anaerobic | *C. glutamicum* | (Yamamoto *et al.*, 2013) |
| Glucose | 1.00 | 0.41 | 0.66 | anaerobic | *E. coli* | (Bastian *et al.*, 2011) |
| Glucose | 0.85 | 0.35 | 0.57 | anaerobic | *E. coli* | (Atsumi *et al.*, 2008) |
| Glucose | 0.04 | 0.016 | 0.03 | semi-anaerobic | *S. cerevisiae* | (Matsuda *et al.*, 2013) |
| Xylose | 0.0004 | 0.0002 | 0.0003 | aerobic | *S. cerevisiae* | (Brat and Boles, 2013) |
| Glucose | 0.86 | 0.35 | 0.57 | aerobic | *E. coli* | (Bastian *et al.*, 2011) |
| Glucose | 1.00 | 0.41 | 0.66 | anaerobic | *E. coli* | (Bastian *et al.*, 2011) |

[a] referred to the consumed pentoses L-arabinose and D-xylose

maximum theoretical yields

such as 1-butanol, isobutanol, 2-methyl-1-butanol or 3-methyl-1-butanol have superior properties as they are less volatile, corrosive and hygroscopic (Atsumi *et al.*, 2008). Additionally, these alcohols are more compatible with existing engines, pipelines and infrastructure (Blombach *et al.*, 2011). Therefore, such alcohols are considered next-generation biofuels and could in future complement ethanol. In this study, isobutanol is in focus and will be exemplarily discussed in the following. Besides the classical application as biofuel, isobutanol can be for instance converted to isobutene a precursor for chemical synthesis of rubber and specialty chemicals and thus represents a platform for manifold applications (Blombach *et al.*, 2011).

Microbial isobutanol production in engineered strains was firstly achieved by Atsumi *et al.* in 2008 and is summarized by Chen and Liao in a current review (Atsumi *et al.*, 2008; Chen and Liao, 2016). Various organisms such as *E. coli* (Atsumi *et al.*, 2008; Bastian *et al.*, 2011; Desai *et al.*, 2014), *C. glutamicum* (Smith *et al.*, 2010; Blombach *et al.*, 2011; Yamamoto *et al.*, 2013), *S. cerevisiae* (Lee *et al.*, 2012; Brat and Boles, 2013; Matsuda *et al.*, 2013), *Geobacillus thermoglucosidasius* (Lin *et al.*, 2014), *Clostridium cellulolyticum* (Higashide *et al.*, 2011), *Clostridium thermocellum* (Lin *et al.*, 2015) or *Klebsiella pneumoniae* (Gu *et al.*, 2017) were cultivated on a broad spectrum of defined

substrates (e.g. glucose, xylose, cellobiose, cellobionic acid, isobutyraldehyde, cellulose) and realistic hydrolysates (e.g. corn stover, lignocellulose hydrolysate) also in microbial consortia of *E. coli* with fungi like *Trichoderma reesei* (Minty *et al.*, 2013) or *Neurospora crassa* (Desai *et al.*, 2015). A summary of the yields of prominent producers in comparison to yields achieved in this study (cf. 4.8, p. 132) is given in Table 2.2. Alternatively, $CO_2$ as carbon source has been exploited by lithoautotrophic, electromicrobial conversion with *Ralstonia eutropha* (H. Li *et al.*, 2012) or via photosynthesis with cyanobacteria *Synechococcus elongates* (Atsumi *et al.*, 2009) and *Synechocystis* sp. (Varman *et al.*, 2013).

Three studies investigate the **isobutanol production with *C. glutamicum*** via keto acid pathways (Smith *et al.*, 2010; Blombach *et al.*, 2011; Yamamoto *et al.*, 2013). Smith *et al.* demonstrated that *C. glutamicum* exhibits a superior tolerance towards isobutanol compared to *E. coli*, which is additionally enhanced by anaerobiosis (Smith *et al.*, 2010; Yamamoto *et al.*, 2013). In the presented thesis, we took advantage of this beneficial property and used isobutanol producer strains originating in the published *C. glutamicum* Iso7 [*C. glutamicum* Δ*aceE* Δ*pqo* Δ*ilvE* Δ*ldhA* Δ*mdh* (pJC4*ilvBNCD-pntAB*) (pBB1*kivd-adhA*)] (Blombach *et al.*, 2011). In this strain, the chromosomal inactivation of the pyruvate:quinone oxidoreductase (Pqo), the lactate dehydrogenase (LdhA), and the malate dehydrogenase (Mdh) minimize the formation of lactate, acetate and succinate as undesired side product under anaerobic conditions. The deletion of *aceE* encoding the E1p subunit of the pyruvate dehydrogenase complex enhances pyruvate availability as central precursor for isobutanol production. A drawback of this manipulation is the requirement of acetate or ethanol as additional substrate (Blombach, Arndt, *et al.*, 2009). To eliminate metabolic sideways, the transaminase B (IlvE) was inactivated, resulting in an auxotrophy for branched chain amino acids (leucine, isoleucine, valine) but also enhanced isobutanol production. A pathway reinforcement was realized by constitutive expression of the genes encoding the acetohydroxyacid synthase (IlvBN), acetohydroxyacid isomeroreductase (IlvC), dihydroxyacid dehydratase (IlvD) of *C. glutamicum*. The isobutanol production branches at the intermediate 2-ketosiovalerate by providing a 2-ketoacid decarboxylase (Kivd) of *Lactococcus lactis*. Kivd produces isobutyraldehyde, which is finally converted to isobutanol by the native alcohol dehydrogenase (AdhA) of *C. glutamicum*. As the chromosomal *adhA* is a bottleneck in

the pathway, it was enforced by the plasmid-based expression. Redox imbalances were overcome by introduction of a membrane bound transhydrogenase (PntAB) of *E. coli*.

In the presented thesis, a realistic substrate from beech wood organosolv pretreatment was assayed for production of isobutanol as exemplary biofuel in engineered *C. glutamicum* (cf. 4.8, p. 132).

## 2.9. Low molecular weight thiols

In their natural and industrial environment bacteria face a variety of stress stimuli and reactive chemicals such as pH or osmotic stress, reactive oxygen species (ROS), reactive nitrogen species, chlorine compounds (e.g. HOCl), metalloids, toxic metabolites (e.g. methylglyoxal) and other reactive electrophiles (e.g. aldehydes) (Loi *et al.*, 2015). Most living organisms have developed low molecular weight thiols that function as redox buffer, protect enzymes against oxidation via S-thiolation, scavenge reactive chemicals and are cofactors in enzyme complexes with defensive function (Masip *et al.*, 2006; Van Laer *et al.*, 2013). Among these are cysteine and coenzyme A (all organisms), glutathione (GSH; eukaryotes, Gram-negative bacteria), mycothiol (MSH; *Actinomycetes*),

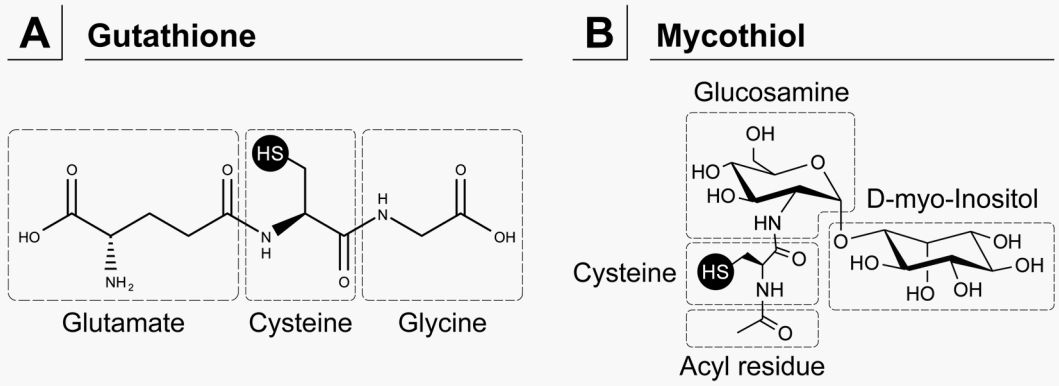


**Figure 2.8. Structure of low molecular weight thiols: glutathione and mycothiol** in their reduced and monomeric conformation. **A**. Glutathione (GSH) is synthesized from the amino acids L-glutamate, L-cysteine and L-glycine in eukaryotes and Gram-negative bacteria. **B**. Mycothiol (MSH) constitutes D-myo-inositol, glucosamine, L-cysteine and an acetyl group and is known only in *Actinomycetes*. The reactive thiol group is highlighted (black circle). MSH structure withdrawn and modified from literature (Rawat and Av-Gay, 2007).

bacillithiol (BSH; *Firmicutes*) and others (Fahey, 2013; Loi *et al.*, 2015). All entities share a reactive thiol group as common feature, which, dependent on their redox potential, can be present in the oxidized (-SH) state or reduced (-S-S-) form as disulfide.

Relevant for this study is GSH and MSH, which both were shown to have beneficial effects on bacterial resistance towards typical inhibitors in lignocellulose hydrolysates or toxic metabolites such as furfural or methylglyoxal before. The tripeptide **GSH** (γ-L-glutamyl-L-cysteinyl-glycine; Figure 2.8) is the most dominant low molecular weight thiol with a standard redox potential of the GSH/GSSG couple of -240 mV at pH 7.0 and reaches astonishingly high intracellular concentrations up to millimolar levels (Loi *et al.*, 2015). In *E. coli*, for example, it represents the second most prominent intracellular metabolite with concentrations of 17 mM GSH (Bennett *et al.*, 2009). A comprehensive review about GSH functions in bacteria is available in literature (Masip *et al.*, 2006). GSH is synthesized from L-glutamate, L-cysteine and L-glycine by the two cytosolic and ATP-dependent enzymes: γ-glutamylcysteine synthetase (encoded by *gshA*), and glutathione synthetase (encoded by *gshB*). The only known enzyme for degradation of GSH is the γ-glutamyl transpeptidase (Masip *et al.*, 2006). Murata and Kimura were the first to clone the *gshAB* operon, which was the foundation for the construction of production strains summarized by Li *et al.* (Murata and Kimura, 1982; Li, Wei, *et al.*, 2004). The heterologous production of GSH in the Gram-positive organism *L. lactis* enhanced resistance towards oxidative stress (Li *et al.*, 2003; Li, Hugenholtz, *et al.*, 2004). It was described that GSH chemically reacts with lignocellulose-derived inhibitors (Kim and Hahn, 2013). In *C. glutamicum* the alternative low molecular weight thiol **MSH** or 1-*O*-2-[[(2R)-2-(acetylamino)-3-mercapto-1-oxopropyl]amino]-2-deoxy-α-D-glucopyranosyl]-D-*myo*-inositol (Figure 2.8) functions analogously to GSH and is also produced in millimolar concentrations (Newton *et al.*, 2008; Van Laer *et al.*, 2013). It was first identified in *Actinobacteria* in 1993 and shown to be the major low molecular weight thiol in this class (Newton *et al.*, 1993, 1996). The general occurrence, biosynthesis, function and chemistry is discussed in recommended reviews (Newton and Fahey, 2002; Jothivasan and Hamilton, 2008; Newton *et al.*, 2008). Biosynthesis of MSH is catalyzed in four consecutive steps involving a glycosyltransferase (MshA), GlcNAc-Ins N-deacetylase (MshB), an ATP-dependent mycothiol ligase (MshC) and a mycothiol synthase (MshD) (Newton and Fahey, 2002). Feng *et al.* were the first to identify and

delete the *mshABCD* operon in *C. glutamicum* (Feng *et al.*, 2006). It was shown that deletion of this operon provoked a strong sensitivity to methylglyoxal (Liu *et al.*, 2013), whereas overproduction of MSH by expression of the first gene *mshA* of the biosynthesis pathway enhanced resistance towards inhibitors such as methylglyoxal or furfural (Liu *et al.*, 2014).

As discussed below, we briefly investigated the influence and potential positive effect of low molecular weight thiols on cultivations of *C. glutamicum* on pretreated lignocellulose (cf. 4.2.3, p. 115).

## 2.10. Methylglyoxal, acetol and 1,2-PDO – intertwined metabolic pathways

Methylglyoxal or 2-oxopropanal is a cytotoxic metabolite that inevitably forms in side reactions of glycolysis from triose-phosphate intermediates. Its history and role in the general physiology has been summarized extensively (Cooper, 1984; Kalapos, 1999). Methylglyoxal can be formed from dihydroxyacetone phosphate spontaneously or catalyzed by the methylglyoxal synthase (MgsA), which is inhibited by inorganic phosphate (Hopper and Cooper, 1971). Even low millimolar concentrations can lead to cell death (Grant *et al.*, 2003), which can be attributed to the reactiveness of the aldehyde, the coupled decline of intracellular potassium concentrations and by the formation of free radicals. To alleviate the inhibitory effects bacteria developed several methylglyoxal detoxification systems (Cooper, 1984). Relevant to this study is the glyoxylase I (lactoylglutathione lyase) / glyoxylase II (hydroxyacylglutathione hydrolase) system encoded by *gloA* and *gloB* in *E. coli*, respectively (Ferguson *et al.*, 1998; Grabar *et al.*, 2006; O'Young *et al.*, 2007). In this system (Figure 2.9), methylglyoxal initially reacts spontaneously with GSH forming a hemithioacetal, which is subsequently converted to *S*-lactoylglutathione by GloA (MacLean *et al.*, 1998). GloB then catalyzes the conversion to D-lactate and releases GSH (Vander Jagt, 1993). D-lactate is a known substrate for many prokaryotes including *C. glutamicum* (Kato *et al.*, 2010). An alternative, though less affine route, involves the glyoxylase III (GloC) and the glycerol dehydrogenase (GldA) converting methylglyoxal via lactaldehyde to D-lactate (Tang *et al.*, 1979; Subedi

*et al.*, 2008, 2011). The enzyme GldA with its exceptionally broad substrate spectrum (Lee and Whitesides, 1986) is frequently exploited for 1,2-PDO production as discussed above (cf. 2.7, p. 43). Interestingly, it was proposed that acetol as intermediate of acetone degradation pathways can function as direct precursor of methylglyoxal catalyzed by an acetol dehydrogenase (Taylor *et al.*, 1980). Taylor *et al.* found such enzyme activity in natural isolates that may belong to the group of *Corynebacteriaceae*. It is thus likely that *C. glutamicum* exhibits similar enzymes. *Vice versa*, methylglyoxal can be converted to acetol by aldehyde reductases, as described for example in the yeast *Hansenula mrakii* (Inoue *et al.*, 1992). The methylglyoxal, acetol and 1,2-PDO metabolism are thus strongly connected metabolites.

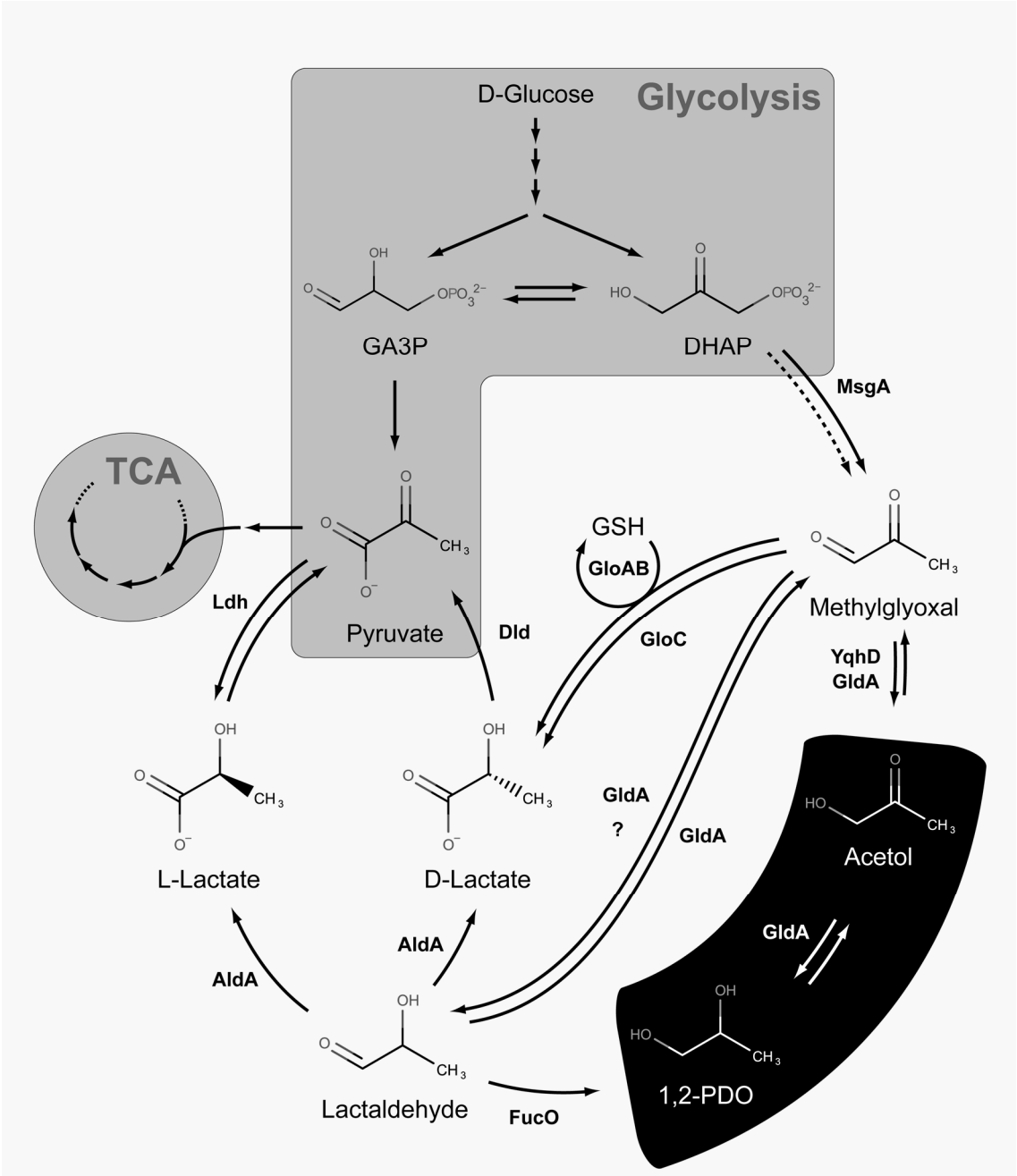


**Figure 2.9. Methylglyoxal, acetol and 1,2-PDO synthesizing and degrading pathways** in the condensed context of the central metabolism (glycolysis and TCA, grey shade). AldA (aldehyde dehydrogenase), DHAP (dihydroxyacetone phosphate), Dld (quinone-dependent D-lactate dehydrogenase), FucO (propanediol oxidoreductase/ lactaldehyde reductase), GA3P (glyceraldehyde-3-phosphate), GldA (glycerol dehydrogenase), GloAB [glyoxylase I (lactoylglutathione lyase) / glyoxylase II (hydroxyacylglutathione hydrolase) system], GloC (glyoxylase III), Ldh (lactate dehydrogenase), MgsA (methylglyoxal synthase), YqhD (aldehyde reductase). Shaded in black is the biotransformation reaction exploited in this study for 1,2-PDO production from acetol as major constituent of pyrolysis water (cf. Part I, p. 106). Graphic based on summarized literature (Kalapos, 1999; Subedi *et al.*, 2008; Siebert and Wendisch, 2015).

# 2.11. The role of oxygen in natural habitats and industrial environments on facultatively anaerobic bacteria

The following introduction is mainly based on a previously published review (Lange, Takors, *et al.*, 2017).

## 2.11.1. Facultative microbes master fluctuations in oxygen availability

Whereas anaerobic bacteria can only thrive under strict absence of oxygen, facultative bacteria developed strategies to survive in both aerobic and anaerobic environments. Transitions between aerobiosis and anaerobiosis occur frequently in natural habitats such as soil, water, biofilms or the intestine (de Beer *et al.*, 1994; Unden *et al.*, 1994; Wishner *et al.*, 1998; Silver *et al.*, 1999; Albenberg *et al.*, 2014) but also in industrial process in large scale reactors or zero-growth production scenarios (Alvaro R. Lara *et al.*, 2006; Lange, Takors, *et al.*, 2017). This demands a physiological *summersault*, which is met by rearrangement of the energy conservation from aerobic to anaerobic respiration (e.g. nitrate) or fermentation at the absence of external electron acceptors (Unden *et al.*, 1994). Oxygen as terminal electron acceptor has been widely studied and is here referred to selected literature (Borisov and Verkhovsky, 2015). A general strategy of the microbes is the maximization of energy conservation under the prevalent conditions. Under oxygen excess, aerobic respiration is preferred ($\Delta G^{0'}$ = -2870 kJ per mol glucose), over anaerobic respiration ($\Delta G^{0'}$ = -858 kJ per mol glucose with nitrate) and fermentation (e.g. *E. coli*: $\Delta G^{0'}$ = -218 kJ per mol glucose) (Unden and Bongaerts, 1997; Tran and Unden, 1998). Fermentation represents the least effective strategy conserving only 2 mol ATP per mol of glucose through substrate level phosphorylation. The oxygen-dependent respiratory chain of *C. glutamicum* (cf. 2.6.5, p. 38) or *E. coli* contain typical cytochrome oxidases such as the *bo*-, *bc*$_1$-*aa*$_3$- or *bd*-type oxidases with varying affinities for oxygen (Ingledew and Poole, 1984; Bunn and Poyton, 1996; Bott and Niebisch, 2005; Partridge *et al.*, 2007). They enable a maximal exploitation of aerobic respiration even under low oxygen availabilities such as microaerobiosis. For a summary of further terminal oxidases in other organisms please refer to secondary literature (Poole and Cook, 2000). As biochemical means, *E. coli* developed the cytochrome *bd* oxidase ($K_D$ = 0.28 µM; $K_M$ = 0.003-2 µM),

whose oxygen affinity is about a thousand times higher compared to the cytochrome *bo*$_3$ oxidase ($K_D$ > 300 μM; $K_M$ = 0.016-2.9 μM) (Borisov and Verkhovsky, 2015). Besides, the cytochrome *bd* oxidase holds a catalase activity and irreversibly reacts with $H_2O_2$ (Borisov and Verkhovsky, 2015; Borisov *et al.*, 2015). Defective mutants have been shown to be sensitive towards $H_2O_2$ for example in *E. coli* (Wall *et al.*, 1992). The role of the cytochrome *bd* oxidase can be further considered also for other organisms in literature (Borisov *et al.*, 2011, 2015). Interestingly, despite their central role, a non-lethal and complete disruption of the entire oxygen-dependent respiratory chain was shown previously, and resulted in aerobic fermenting phenotypes for example in *E. coli* (Bekker *et al.*, 2009) and *C. glutamicum* (Koch-Koerfges *et al.*, 2013). Under strict anaerobiosis and absence of external electron acceptors, fermentation provokes growth rate, biomass yield and $CO_2$ evolution rate (CER) reduction and increasing NADH/$NAD^+$ ratios (de Graef *et al.*, 1999; Molenaar *et al.*, 2000; Inui, Murakami, *et al.*, 2004). The formation of fermentation products is maximized under strict anaerobiosis, where growth is minimal and noteworthy the glucose uptake rate is elevated (Varma and Palsson, 1994; de Graef *et al.*, 1999; Inui *et al.*, 2007). A dependence of the glucose uptake rate to the cellular redox state was previously studied also in *C. glutamicum* (Tsuge *et al.*, 2015). Anaerobic elevation of substrate uptake rates is exploited by industrial biotechnology in zero-growth production processes as will be discussed later (cf. 2.11.3, p. 58). Between aerobiosis and anaerobiosis intermediate states summarized by microaerobiosis are prevalent and allow aerobic respiration and fermentation in parallel (cf. 2.11.4, p. 64) evoking a growth coupled secretion of fermentation products (Ju *et al.*, 2005).

### 2.11.2. Oxygen-dependent regulatory mechanisms

Given the importance oxygen plays in microbial energy conservation, it is not surprising that sophisticated mechanisms and regulators evolved sensing either the cellular redox state or oxygen itself and coordinate the effective physiological response (Bunn and Poyton, 1996; Green and Paget, 2004). Such mechanisms were profoundly studied for nitrogen fixation of symbiotic or free-living microorganisms, anoxygenic photosynthesis of non-sulfur bacteria but also of pathogenic infection mechanisms and biofilm formation (Patschkowski *et al.*, 2000; Starck *et al.*, 2004; Fuchs *et al.*, 2007, 2012; Grahl and Cramer, 2010; Trunk *et al.*, 2010; Potzkei *et al.*, 2012; Sousa and Pereira, 2014;

Fei *et al.*, 2016). These, however, will not be discussed here. In *E. coli* known key players of oxygen-dependent regulation were identified and harness a directly oxygen sensing iron-sulfur cluster protein Fnr (Jordan *et al.*, 1997; Khoroshilova *et al.*, 1997), the two-component systems ArcBA (Bekker *et al.*, 2010) and DipB/DipA (Sawers, 1999) and the chemotaxis system Aer (Bibikov *et al.*, 1997; Gosink *et al.*, 2006). As dual-regulator Fnr directly senses molecular oxygen, activates genes of the anaerobic metabolism and ultimately inhibits functions involved in aerobic respiration (Kang *et al.*, 2005). ArcB and ArcA form a membrane bound and cytosomal two-component system, respectively, where ArcB senses the redox state of the quinone pool and phosphorylates the cognate response regulator ArcA in the absence of oxygen (Georgellis *et al.*, 2001). The interplay between Fnr and ArcBA allows a physiological fine tuning of the cellular metabolism (Gunsalus and Park, 1994; Patschkowski *et al.*, 2000; Partridge *et al.*, 2007). More indirectly the metabolic flux network is influenced by intracellular metabolite concentrations and cofactor availability such as NADH or $NAD^+$ (Berríos-Rivera *et al.*, 2002). For *E. coli* mechanistic models at systems-level for the Fnr cycle at transitions from aerobiosis to anaerobiosis and the general response towards oxygen are available in literature (Tolla and Savageau, 2010; Ederer *et al.*, 2014). For other *Actinobacteria* such as *Mycobacterium smegmatis* or *M. tuberculosis* other mechanisms for example harnessing oxygen responsive two component systems are known (Mayuri *et al.*, 2002; O'Toole *et al.*, 2003; Sousa *et al.*, 2007).

Such deep mechanistic knowledge about the regulatory and metabolic network is so far not known for *C. glutamicum*. Most important works summarize the transcriptomic shift from aerobiosis to anaerobiosis (Inui *et al.*, 2007; Yamamoto *et al.*, 2011) also with respect to a genome wide metabolic model verification (Shinfuku *et al.*, 2009). Intermediate oxygen limited states were also investigated (Sun *et al.*, 2016). Two studies propose the involvement of the sigma-factor (σ-factor) $\sigma^B$ and $\sigma^C$ in response to microaerobic conditions (Ehira *et al.*, 2008; Ikeda *et al.*, 2009). Also recent studies addressed the influence of large scale inhomogeneities in dissolved oxygen under scale-down conditions (Limberg, Joachim, *et al.*, 2017; Limberg, Schulte, *et al.*, 2017). As a drawback the studies often neglect intermediate phases of oxygen limitation, use producer strains, failed to explain metabolic fluxes such as a shutdown of the pentose phosphate pathway under anaerobiosis (Radoš *et al.*, 2014) and most importantly could not identify

a regulatory mechanism underlying the adaptation. These disadvantages were addressed in Part III of this study (cf. p. 138).

### 2.11.3. Industrial zero-growth production processes

Industrial biotechnology strives for high yields and productivities. For energy demanding products, microbial processes mostly operate at aerobic states, whereas anaerobiosis with enhanced substrate uptake and product formation rates is often exploited for low-value products (Weusthuis *et al.*, 2011). Innovative approaches with facultatively anaerobic bacteria such as *E. coli* and *C. glutamicum* combine aerobic growth, for fast accumulation of the biocatalyst, with anaerobic production at high yield in zero-growth production processes (Jojima, Inui, *et al.*, 2015; Lange, Takors, *et al.*, 2017). Such processes have advantages like the uncoupling of growth and production, extended production periods, enabling of production at high cell densities and minimization of power input and thus enhance the overall productivities (Vemuri *et al.*, 2002b). In our published summary (Lange, Takors, *et al.*, 2017), we categorized such processes into two-stage (two separate vessels; e.g. (Inui, Murakami, *et al.*, 2004)), dual-phase (one single vessel, abrupt shift; e.g. (Vemuri *et al.*, 2002b)) and triple-phase (one single vessel, gradual oxygen reducing intermediate states; e.g. (Li *et al.*, 2013)) bioprocesses (Figure 2.10). A table summarizing the most relevant production scenarios including products, substrates, producer strains, titers, product/substrate yields ($Y_{P/S}$) and volumetric productivities ($Q_P$) is shown below (Table 2.3). Zero-growth production has the advantage of prolonged product formation periods as impressively demonstrated with *C. glutamicum* for 267 h as immobilized cells in a repetitive batch approach for succinate production (Shi *et al.*, 2014), 360 h with a constant volumetric productivity of acetate, lactate and succinate (Okino *et al.*, 2005) or succinate production for 576 h by a cell recycling approach (Jojima *et al.* 2016). Moreover, non-growth conditions in general enhance the bacteria's resistance towards toxic entities or products (Jenkins *et al.*, 1988; Steels *et al.*, 1994; Sakai *et al.*, 2007).

As discussed above facultatively anaerobic and industrially relevant bacteria such as *E. coli* and *C. glutamicum* can grow at oxygen scarcity using anaerobic respiration or fermentation (*E. coli* (Ingledew and Poole, 1984; Clark, 1989); *C. glutamicum* (Bott and Niebisch, 2005; Nishimura *et al.*, 2007; Michel *et al.*, 2015)), which represents a

bottleneck for the development of zero-growth production approaches. As a result, the absence of alternative terminal electron acceptors from the cultivation medium or metabolic engineering is mandatory. Whereas for *C. glutamicum* it is sufficient to cultivate at absence of nitrate, *E. coli* was engineered by defined deletions for example in the succinate producer strain *E. coli* AFP111, which comprises a disruption of the pyruvate formate lyase and lactate dehydrogenase (Donnelly *et al.*, 1998; Singh *et al.*, 2011).

A common drawback in the development of zero-growth production processes is that fast transitions from aerobiosis to anaerobiosis as prevalent in dual-phase approaches can lead to deficiencies in cell viability, product yield and formation rates (Lange, Takors, *et al.*, 2017). The artificially fast transitions were also investigated for mycobacterial pathogens and caused reduced viability or even cell death for example of *Mycobacterium smegmatis* or *M. tuberculosis* (Wayne and Lin, 1982; Wayne and Hayes, 1996; Dick *et*

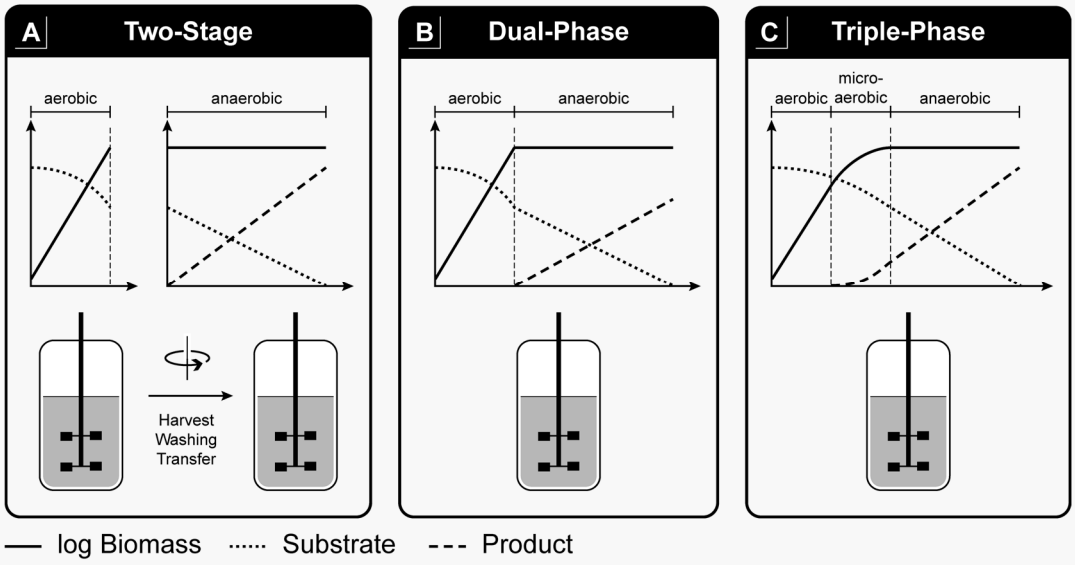


**Figure 2.10. Schematic visualization of three zero-growth production scenarios** provoked by oxygen scarcity. The biomass (solid; semi-logarithmic), substrate (dotted) and product (dashed) concentrations are shown. **A**. The two-stage bioprocesses involve two separated cultivation batches for aerobic growth and anaerobic production. To achieve high biomass concentrations in the second stage, cells are harvested, washed and transferred into fresh medium. **B**. Dual-phase processes realize both such stages in a single bioreactor but imply an instant transition from aerobiosis to anaerobiosis. **C**. The most advanced triple-phase process embraces the three separate phases aerobiosis, microaerobiosis and anaerobiosis in a single bioreactor. Graphic similarly published (Lange, Takors, *et al.*, 2017).

*al.*, 1998). Interestingly, it was found that slower transitions in two-stage (Wu *et al.*, 2007; Blombach *et al.*, 2011) and triple-phase (Hong and Lee, 2000; Martínez *et al.*, 2010; Wang *et al.*, 2011; Zhu *et al.*, 2011; Li *et al.*, 2013; Wieschalka *et al.*, 2013) processes could compensate this problem by priming the bacteria for the following oxygen scarcity. In a lactate dehydrogenase-deficient strain of *C. glutamicum* it was shown that a progressive deoxygenation enhanced product titers by up to 640 % (Kaboré *et al.*, 2016). The beneficial effect was attributed to the low aerated intermediate state, often referred to as microaerobiosis discussed in the following section. Obviously, this phase plays an essential role in the physiological adaptation and preparation of the enzymatic machinery to complete anaerobic conditions (Martínez *et al.*, 2010; Blombach and Eikmanns, 2011; Blombach *et al.*, 2011).

**Table 2.3. Literature summary of relevant zero-growth production processes**. Sorting was chosen based on the mode of operation (**A**: two-stage, **B**: dual-phase, **C**: triple-phase) and product identity. All utilized carbon sources (disregarding $CO_2$ or bicarbonate) are listed in the substrate column. Substrate specific product yields ($Y_{P/S}$) are given exclusively for the anaerobic production phase. The volumetric productivity ($Q_P$) is either mentioned for the anaerobic production phase with respect to two-stage processes (A) or for the entire process/anaerobic production phase for the dual-phase (B) and triple-phase (C) approaches. Table analogously published (Lange, Takors, *et al.*, 2017).

**A TWO-STAGE**

| Product | Substrate [a] | Organism | Strain | Titer, mM | $Y_{P/S}$, mol mol$^{-1}$ | $Q_P$, mmol L$^{-1}$ h$^{-1}$ anaerobic | Reference |
|---|---|---|---|---|---|---|---|
| Succinate | D-glucose, yeast extract, tryptone | *E. coli* | AFP111 pTrc99A-pyc | - | 1.46 | - | (Vemuri *et al.*, 2002a) |
| | D-glucose, yeast extract, tryptone | *E. coli* | SBS550MG (pHL413) | 129 | 1.6 | 5.4 [b] | (Sánchez *et al.*, 2006) |
| | D-glucose, acetate | *E. coli* | NZN111 | 95 | 1.28 | 9.6 | (Wu *et al.*, 2007) |
| | D-glucose | *C. glutamicum* R | Δ*ldhA*-pCRA717 | 1,240 | 1.40 | 27.1 | (Okino, Noburyu, *et al.*, 2008) |
| | D-glucose, yeast extract, tryptone | *E. coli* | NZN111 | 65 | 0.87 | 0.7 | (Wu *et al.*, 2009) |
| | D-glucose, formate | *C. glutamicum* | BOL-3/pAN6-*gap* | 1,134 | 1.67 | 21.4 | (Litsanov *et al.*, 2012) |
| | D-glucose | *C. glutamicum* | NC-3-1 | 957 | 1.43 | 19.9 [b] | (Xu *et al.*, 2016) |
| D-Lactate | D-glucose | *C. glutamicum* R | Δ*ldhA*/pCRB204 | 1,336 | 1.73 | 44.5 [b] | (Okino, Suda, *et al.*, 2008) |
| Xylitol | D-glucose, xylose | *C. glutamicum* R | CtXR7 | 1,091 | - | 51.9 | (Sasaki *et al.*, 2010) |
| L-Alanine | D-glucose | *C. glutamicum* R | Δ*ldhA* Δ*ppc* Δ*alr* + *alaD* + *gapA* | 1,097 | 1.68 | 34.3 [b] | (Jojima *et al.*, 2010) |
| | D-glucose | *C. glutamicum* R | GLY3/pCRD500 | 2,430 | 1.84 [b] | 50.6 [b] | (Yamamoto *et al.*, 2012) |
| L-Valine | D-glucose | *C. glutamicum* R | BN$^{GE}$C$^{TM}$DLD/ΔLDH | 1,940 | 0.63 | 40.4 [b] | (Hasegawa *et al.*, 2012) |
| | D-glucose | *C. glutamicum* R | Val-9 | 1,280 | 0.88 | 53.3 [b] | (Hasegawa *et al.*, 2013) |
| Isobutanol | D-glucose, yeast extract, L-valine, L-leucine, L-isoleucine | *C. glutamicum* | Iso7 | 82 | 0.77 | 2.7 [b] | (Blombach *et al.*, 2011) |
| | D-glucose | *C. glutamicum* R | IBU8 | 505 | 0.78 | 8.4 [b] | (Yamamoto *et al.*, 2013) |
| Ethanol | D-glucose, pyruvate | *C. glutamicum* R | *ldhA-ppc*- pCRA723 | 146 [b] | 1.48 [b] | 48.6 | (Inui, Kawaguchi, *et al.*, 2004) |

**B DUAL-PHASE**

| Product | Substrate | Organism | Strain | Titer, mM | $Y_{P/S}$, mol $mol^{-1}$ | $Q_P$, mmol $L^{-1}$ $h^{-1}$ overall / anaerobic | Reference |
|---|---|---|---|---|---|---|---|
| Succinate | D-glucose, yeast extract, tryptone | *E. coli* | AFP-111/pTrc99A-*pyc* | 840 | 1.73 | 11.2 [b] / - | (Vemuri *et al.*, 2002b) |
| | D-glucose, acetate, yeast extract | *E. coli* | NZN111 | 239 | 1.13 | 3.7 [b] / 5.9 | (Wu *et al.*, 2007) |
| | D-glucose | *E. coli* | AFP111 | 857 | 1.63 | 10.1 [b] / 16.0 | (Jiang *et al.*, 2010) |
| | D-glucose, yeast extract, tryptone | *E. coli* | SBS550MG (pHL413) | 115 | 1.25 | - / 7.6 | (Martínez *et al.*, 2010) |
| | D-glucose, yeast extract, tryptone | *E. coli* | SD111 | 844 | 1.67 | 13.2 [b] / 14.1 | (Wang *et al.*, 2010) |
| D,L-Alanine | D-glucose, yeast extract, casamino acids, L-isoleucine | *E. coli* | *pfl pps poxB ldhA aceEF* pTrc99A-*alaD* | 988 | 2.02 | 20.6 [b] / 44.9 | (Smith *et al.*, 2006) |
| Isobutanol | D-glucose, acetate, yeast extract, L-valine, L-leucine, L-isoleucine | *C. glutamicum* | Iso7 | 175 | 0.48 | 3.6 [b] / 4.4 | (Blombach *et al.*, 2011) |

**C TRIPLE-PHASE**

| Product | Substrate | Organism | Strain | Titer, mM | $Y_{P/S}$, mol mol$^{-1}$ | $Q_P$, mmol L$^{-1}$ h$^{-1}$ overall / anaerobic | Reference |
|---|---|---|---|---|---|---|---|
| Succinate | D-glucose, yeast extract, tryptone | *E. coli* | NZN111(pTrcML) | 24 | 0.47 [b] | 0.6 [b] / 0.8 [b] | (Hong and Lee, 2000) |
| | D-glucose, yeast extract, tryptone | *E. coli* | SBS550MG (pHL413) | 167 | 1.55 | - / 11.0 | (Martínez *et al.*, 2010) |
| | D-glucose, yeast extract, tryptone | *E. coli* | SBS550MG (pHL413) | 538 | 1.60 | - / 21.5 [b] | (Zhu *et al.*, 2011) |
| | Sucrose, yeast extract, tryptone | *E. coli* | SBS550MG pHL413 pUR400 | 178 | 3.33 | 3.6 / 3.9 [b] | (Wang *et al.*, 2011) |
| | D-glucose, yeast extract, tryptone | *E. coli* | YL106/pSCsfcA | 722 | 1.14 | 18.0 / 8.5 [b] | (Li *et al.*, 2013) |
| | D-glucose, acetate, L-alanine | *C. glutamicum* | ELB-P | 330 | 1.02 | - / 5.5 [b] | (Wieschalka *et al.*, 2013) |

[a] substrates applied in the anaerobic production phase

[b] calculated from given data within the reference

### 2.11.4. Microaerobiosis – a poorly characterized intermediate state

When considering transitions from oxygen-excess to oxygen-scarcity, the poorly characterized microaerobic state functions as interphase between aerobiosis and strict anaerobiosis. With respect to current knowledge, microaerobiosis has been insufficiently described and defined and was only poorly distinguishable from the aerobic and anaerobic phase. Still, intermediate states were successfully applied empirically for example to improve industrial production in triple-phase processes that implement a low aerated microaerobic interphase (Hong and Lee, 2000; Martínez *et al.*, 2010; Wang *et al.*, 2011; Zhu *et al.*, 2011; Li *et al.*, 2013; Wieschalka *et al.*, 2013). Microaerobiosis is on the other hand discussed as negative impact factor on cell viability in large-scale bioreactors, where bacteria face changing oxygen availabilities due to insufficient power input and mixing (Alvaro R Lara *et al.*, 2006; Buchholz, Graf, Freund, *et al.*, 2014; Lemoine *et al.*, 2015). Such fluctuations go hand in hand with reduced productivities and product yields (Oosterhuis and Kossen, 1984; Bylund *et al.*, 1998; Sandoval-Basurto *et al.*, 2005; Lemoine *et al.*, 2015; Limberg, Schulte, *et al.*, 2017).

Currently, microaerobiosis is mostly referred to as low DO conditions between 0-5 % (Chen *et al.*, 2003; Alfenore *et al.*, 2004; Martínez *et al.*, 2010; Zhu *et al.*, 2011; Biswas *et al.*, 2012; S. Li *et al.*, 2012; Wieschalka *et al.*, 2012; Yamauchi *et al.*, 2014). More explicitly, Kaboré *et al.* define microaerobic conditions by constantly limiting oxygen transfer rates (OTR) and used this definition as process control for enhanced succinate and acetate production in *C. glutamicum* (Kaboré *et al.*, 2016). Alternatively, a fuzzy logic control, which integrates input signals DO and $CO_2$ exhaust gas concentration and thus controls the air flow rate, could maintain defined conditions with a DO between 1 and 0.1 ppm (Nakano *et al.*, 2000). In this approach the microaerobiosis was maintained for 830 h in a xylitol production process with *Candida magnolia*. Microaerobiosis was also characterized *in situ* by determination of metabolic states via online fluorescence of NAD(P)H of denitrifying *Pseudomonas aeruginosa* (Ju *et al.*, 2005). Indirect process control by redox probes to analyze the oxygen-reduction potential (ORP) is a wide-spread method in wastewater treatment processes (Hewitt, 1950; Oktyabrsky and Smirnova, 1989; Goncharuk *et al.*, 2010). Redox probes were also applied with monitoring function in two-stage (Inui *et al.*, 2007) and dual-phase (Wimpenny and Firth, 1972) processes.

In summary, an unbiased and common definition of microaerobiosis, in particular with respect to physiological states of the microbes, is not available. On the analytical side, no robust method or biosensor system was yet found to deliver a clear signal or description. A deeper investigation of this transition state with *C. glutamicum* is performed in this thesis (cf. Part III, p. 138).

# CHAPTER 3: MATERIAL AND METHODS

## 3.1. Bacterial strains, plasmids and oligonucleotides

A full list of used bacterial strains, plasmids and oligonucleotides, corresponding systematic names (IDs), relevant characteristics or sequences and sources, references or purposes are given in Table 3.1. DNA oligonucleotides were manufactured by the biomers.net GmbH (Ulm, Germany).

**Table 3.1. List of bacterial strains, plasmids and oligonucleotides**. For oligonucleotides the prerequisite homologous region for isothermal assembly (underlined) and restriction sites (bold) are given and refer to the respective features or enzymes named in parenthesis, respectively. Alternative systematic names (IDs) are given for backtracking of bacterial strains and plasmids in laboratory journals.

| Strain, plasmid, or oligo-nucleotide | ID | Relevant characteristics or sequence | Source, reference or purpose |
|---|---|---|---|
| **Strains** | | | |
| *Escherichia coli* DH5α | | F$^-$ Φ80*lacZ*ΔM15 Δ(*lacZYA-argF*) U169 *endA1 recA1 hsdR17* (rk$^-$, mk$^+$) *supE44 thi-1 gyrA96 relA1 phoA* | (Hanahan, 1983) |
| *Corynebacterium glutamicum* ATCC 13032 | | Wild type | American Type Culture Collection |
| *C. glutamicum* Δ*pqo* Δ*aceE* Δ*ldhA* Δ*mdh* | | *C. glutamicum* with genetic deletions of the pyruvate:quinone oxidoreductase (Pqo), the E1p subunit of the pyruvate dehydrogenase complex (encoded by *aceE*), the lactate dehydrogenase (LdhA), and the malate dehydrogenase (Mdh) | (Radoš *et al.*, 2015) |

| Strain, plasmid, or oligo-nucleotide | ID | Relevant characteristics or sequence | Source, reference or purpose |
|---|---|---|---|
| *C. glutamicum* Δ*aceE* Δ*pqo* Δ*ilvE* Δ*ldhA* Δ*mdh* | | *C. glutamicum* with genetic deletions of the E1p subunit of the pyruvate dehydrogenase complex (encoded by *aceE*), the pyruvate:quinone oxidoreductase (Pqo), transaminase B (IlvE), the lactate dehydrogenase (LdhA), and the malate dehydrogenase (Mdh) | (Blombach *et al.*, 2011) |
| *C. glutamicum* Δ*pqo* Δ*ilvE* Δ*ldhA* Δ*mdh* | JL8.1.1 | *C. glutamicum* Δ*aceE* Δ*pqo* Δ*ilvE* Δ*ldhA* Δ*mdh* with restored pyruvate dehydrogenase complex (encoded by *aceE*) | This study |
| PDO1 | | *C. glutamicum* + pJUL*gldA* | This study |
| PDO2 | JL19.C1 | *C. glutamicum* Δ*pqo* Δ*aceE* Δ*ldhA* Δ*mdh* + pJUL*gldA* | This study |
| CArXy | JL14.1.11 | *C. glutamicum* Δ*pqo* Δ*ilvE* Δ*ldhA* Δ*mdh* CgLP4::($P_{tuf}$-*xylAB*-$T_{rrnB}$) CgLP12::($P_{tuf}$-*araBAD*-$T_{rrnB}$) | This study |
| CIsArXy | JL21.C2 | CArXy harboring the plasmids pJC4*ilvBNCD-pntAB* and pBB1*kivd-adhA*, $Kan^R$, $Cm^R$ | This study |
| *C. glutamicum* Δcg3303 | JL23.2.24 | Markerless deletion of cg3303 by homologous recombination with pJULΔcg3303 | This study |
| *C. glutamicum* Δcg2320 | JL31.3.25 | Markerless deletion of cg2320 by homologous recombination with pJULΔcg2320 | This study |
| *C. glutamicum* Δcg2965 | JL29.1.2 | Markerless deletion of g2965 by homologous recombination with pJULΔcg2965 | This study |
| *C. glutamicum* Δcg2746 | JL32.1.6 | Markerless deletion of cg2746 by homologous recombination with pJULΔcg2746 | This study |
| *C. glutamicum* Δ*sutR* | JL22.2.2 | Markerless deletion SutR (cg0993) by homologous recombination with pJULΔ*sutR* | This study |
| *C. glutamicum* Δcg1327 | JL24.1.11 | Markerless deletion of cg1327 by homologous recombination with pJULΔcg1327 | This study |
| *C. glutamicum* Δ*znr* | JL25.1.14 | Markerless deletion of Znr (cg2500) by homologous recombination with pJULΔ*znr* | This study |
| *C. glutamicum* Δ*zur* | JL26.2.4 | Markerless deletion of Zur (cg2502) by homologous recombination with pJULΔ*zur* | This study |
| *C. glutamicum* Δ*farR* | JL27.1.10 | Markerless deletion of FarR (cg3202) by homologous recombination with pJULΔ*farR* | This study |
| *C. glutamicum* Δ*ripA* | JL28.2.4 | Markerless deletion RipA (cg1120) by homologous recombination with pJULΔ*ripA* | This study |
| *C. glutamicum* Δcg2648 | JL33.2.4 | Markerless deletion of cg2648 by homologous recombination with pJULΔcg2648 | This study |
| *C. glutamicum* Δ*iclR* | JL34.1.3 | Markerless deletion of IclR (cg3388) by homologous recombination with pJULΔ*iclR* | This study |
| *C. glutamicum* Δ*cspA* | JL35.1.23 | Markerless deletion of CspA (cg0215) by homologous recombination with pJULΔ*cspA* | This study |

| Strain, plasmid, or oligo-nucleotide | ID | Relevant characteristics or sequence | Source, reference or purpose |
|---|---|---|---|
| *C. glutamicum* Δ*rbsR* | JL36.1.4 | Markerless deletion of RbsR (cg1410) by homologous recombination with pJULΔ*rbsR* | This study |
| *C. glutamicum* Δ*genR* | JL37.1.20 | Markerless deletion of GenR (cg3352) by homologous recombination with pJULΔ*genR* | This study |
| *C. glutamicum* Δcg0150 | JL38.1.4 | Markerless deletion of cg0150 by homologous recombination with pJULΔcg0150 | This study |
| *C. glutamicum* Δ*mmpLR* | JL39.1.20 | Markerless deletion of MmpLR (cg1053) by homologous recombination with pJULΔ*mmpLR* | This study |
| *C. glutamicum* Δ*ramB* | JL30.1.3 | Markerless deletion of RamB (cg0444) by homologous recombination with pK19Δ*ramB* | This study |
| *C. glutamicum* Δ*oxyR* | | Markerless deletion of OxyR (cg2109) | (Milse *et al.*, 2014) |
| **Plasmids** | | | |
| pJC4 | | Hybrid shuttle vector from fusion of the native plasmid pHM1519 (*C. glutamicum*) and pACYC177 (*E. coli*), $Kan^R$ | (Cordes *et al.*, 1992) |
| pK19*mobsacB* | | For chromosomal integration and deletion of genetic information (*lacZ*α, RP4 *mob*, $oriV_{E.\ coli}$, $sacB_{B.\ subtilis}$, $Kan^R$) | (Schäfer *et al.*, 1994) |
| pJUL*gldA* | pJUL38.1 | pJC4::($P_{tuf}$-*gldA*-$T_{rrnB}$) plasmid expressing the *E. coli* glycerol dehydrogenase (GldA) under control of the constitutive *C. glutamicum* EF-TU promoter ($P_{tuf}$) and closed by the *E. coli rrnB* terminator ($T_{rrnB}$), $Kan^R$ | This study |
| pEKEx3-$xylA_{Xc}$-$xylB_{Cg}$ | | Vector for expression of the genes encoding XylA (xylose isomerase) of *Xanthomonas campestris* and XylB (xylulokinase) of *C. glutamicum*, $Spec^R$ | (Meiswinkel *et al.*, 2013) |
| pVWEx1-*araBAD* | | Vector for expression of the genes encoding AraB (L-ribulokinase), AraA (L-arabinose isomerase) and AraD (L-ribulose-5-phosphate 4-epimerase) of *E. coli* MG1655, $Kan^R$ | (Schneider *et al.*, 2011) |
| pBB1*kivd-adhA* | | Constitutive expression of the genes encoding Kivd (2-ketoacid decarboxylase) of *Lactococcus lactis* and AdhA (alcohol dehydrogenase) of *C. glutamicum*, $Cm^R$ | (Blombach *et al.*, 2011) |
| pJC4*ilvBNCD-pntAB* | | Constitutive expression of the genes encoding IlvBN (acetohydroxyacid synthase), IlvC (acetohydroxyacid isomeroreductase), IlvD (dihydroxyacid dehydratase) of *C. glutamicum* and PntAB (membrane bound transhydrogenase) of *E. coli*, $Kan^R$ | (Blombach *et al.*, 2011) |
| pJUL*aceE* | | pK19*mobsacB*::*aceE*, for restoration of the *aceE* gene in *C. glutamicum* Δ*aceE* Δ*pqo* Δ*ilvE* Δ*ldhA* Δ*mdh*, $Kan^R$ | This study |
| pJUL*xylAB* | pJUL35.X10 | For integration of *xylAB* into CgLP4, pK19*mobsacB*::(Flank1-$P_{tuf}$-*xylAB*-$T_{rrnB}$-Flank2), $Kan^R$ | This study |

| Strain, plasmid, or oligo-nucleotide | ID | Relevant characteristics or sequence | Source, reference or purpose |
|---|---|---|---|
| pJUL*araBAD* | pJUL36.X7 | For integration of *araBAD* into CgLP12, pK19*mobsacB*::(Flank1-$P_{tuf}$-*araBAD*-$T_{rrnB}$-Flank2), $Kan^R$ | This study |
| pJULΔcg3303 | pJUL46.2 | For deletion of cg3303, pK19*mobsacB*::(Flank1-Flank2), $Kan^R$ | This study |
| pJULΔcg2320 | pJUL47.1 | For deletion of cg2320, pK19*mobsacB*::(Flank1-Flank2), $Kan^R$ | This study |
| pJULΔcg2965 | pJUL48.1 | For deletion of cg2965, pK19*mobsacB*::(Flank1-Flank2), $Kan^R$ | This study |
| pJULΔcg2746 | pJUL49.1 | For deletion of cg2746, pK19*mobsacB*::(Flank1-Flank2), $Kan^R$ | This study |
| pJULΔ*sutR* | pJUL54.1 | For deletion of *sutR* (cg0993), pK19*mobsacB*::(Flank1-Flank2), $Kan^R$ | This study |
| pJULΔcg1327 | pJUL55.1 | For deletion of cg1327, pK19*mobsacB*::(Flank1-Flank2), $Kan^R$ | This study |
| pJULΔ*znr* | pJUL56.1 | For deletion of *znr* (cg2500), pK19*mobsacB*::(Flank1-Flank2), $Kan^R$ | This study |
| pJULΔ*zur* | pJUL57.1 | For deletion of *zur* (cg2502), pK19*mobsacB*::(Flank1-Flank2), $Kan^R$ | This study |
| pJULΔ*farR* | pJUL58.2 | For deletion of *farR* (cg3202), pK19*mobsacB*::(Flank1-Flank2), $Kan^R$ | This study |
| pJULΔ*ripA* | pJUL59.1 | For deletion of *ripA* (cg1120), pK19*mobsacB*::(Flank1-Flank2), $Kan^R$ | This study |
| pJULΔcg2648 | pJUL60.1 | For deletion of cg2648, pK19*mobsacB*::(Flank1-Flank2), $Kan^R$ | This study |
| pJULΔ*iclR* | pJUL61.7 | For deletion of *iclR* (cg3388), pK19*mobsacB*::(Flank1-Flank2), $Kan^R$ | This study |
| pJULΔ*cspA* | pJUL62.1 | For deletion of *cspA* (cg0215), pK19*mobsacB*::(Flank1-Flank2), $Kan^R$ | This study |
| pJULΔ*rbsR* | pJUL63.1 | For deletion of *rbsR* (cg1410), pK19*mobsacB*::(Flank1-Flank2), $Kan^R$ | This study |
| pJULΔ*genR* | pJUL64.1 | For deletion of *genR* (cg3352), pK19*mobsacB*::(Flank1-Flank2), $Kan^R$ | This study |
| pJULΔcg0150 | pJUL65.1 | For deletion of cg0150, pK19*mobsacB*::(Flank1-Flank2), $Kan^R$ | This study |
| pJULΔ*mmpLR* | pJUL66.1 | For deletion of *mmpLR* (cg1053), pK19*mobsacB*::(Flank1-Flank2), $Kan^R$ | This study |
| pK19Δ*ramB* | | For deletion of *ramB* (cg0444), based on pK19*mobsacB*, $Kan^R$ | (Gerstmeir *et al.*, 2004) |
| **Oligonucleotides** | | 5' → 3' | |
| P1.1 | 56-JL | GACGCCGCAGGG**TCTAGA**CCACAGGGTAG CTGGTAGTTTG | Fw primer $P_{tuf}$ for pJUL*gldA* (pJC4, **XbaI**) |

| Strain, plasmid, or oligo-nucleotide | ID | Relevant characteristics or sequence | Source, reference or purpose |
|---|---|---|---|
| P1.2 | 13-JL | CCACAGGGTAGCTGGTAGTTTG | Fw primer $P_{tuf}$ for pJUL*kivd-adhA*, pJUL*xylAB* pJUL*araBAD*, and pJUL*araE* |
| P2 | 14-JL | CATGGTATGTCCTCCTGGACTTC | Rv primer $P_{tuf}$ |
| gldA1 | 58-JL | GAAGTCCAGGAGGACATACCATGGACCGC ATTATTCAATC | Fw primer *gldA* ($P_{tuf}$) |
| gldA2 | 59-JL | CTTCTCTCATCCGCCAAAACAGCAGGCAAT TTTGCGTTC | Rv primer *gldA* ($T_{rrnB}$) |
| T1 | 29-JL | CTGTTTTGGCGGATGAGAGAAG | Fw primer $T_{rrnB}$ |
| T2 | 57-JL | GATATCCATCACACTG**GCGGCCGC**AGGAG AGCGTTCACCGACAAAC | Rv primer $T_{rrnB}$ (pJC4, **NotI**) |
| gldAseq1 | 64-JL-seq | GATCGACGGTACGCAAC | Fw sequencing primer pJUL*gldA* |
| gldAseq2 | 65-JL-seq | GGGTGGTAAAGGATGTCG | Rv sequencing primer pJUL*gldA* |
| gldAseq3 | 66-JL-seq | GCAACCTGGTTTGAAGC | Fw sequencing primer pJUL*gldA* |
| gldAseq4 | 67-JL-seq | GTGTTCGCTTCAATCACG | Rv sequencing primer pJUL*gldA* |
| aceE1 | aceEkomp1* | ACGC**GTCGAC**CACCAAAAGGACATCAGACC | Fw primer for pJUL*aceE* (**SalI**) (= delaceE1) (Schreiner *et al.*, 2005) |
| aceE2 | aceEkomp2* | TGCG**GTCGAC**GCGGGATTTATCTGTCCC | Rv primer for pJUL*aceE* (**SalI**) |
| aceE3 | aceE200-* | CGGAGGAGACCAACGAGTGGATGGATTCA C | Fw primer to verify *aceE* restoration |
| aceE4 | ace12 rev* | GTGGGTCACGTCCGAAGAAGTGCTCAC | Rv primer to verify *aceE* restoration |
| aceEseq1* | | CCGTGGCATCAAGGACACC | Sequencing primer pJUL*aceE* |
| aceEseq2* | | GGCTACCTGCCAGAGCGTCGTG | Sequencing primer pJUL*aceE* |
| ara1 | 19-JL | GATTACGCCAAGCTT**GCATGC**GAACGTTGA AGACTCCGTCAAAC | Fw primer for Flank1 in pJUL*araBAD* (pK19*mobsacB*, **PaeI**) |
| ara2 | 20-JL | CTACCAGCTACCCTGTGGAATATGCCGATT GCAAGAAACGAGAAG | Rv primer for Flank1 in pJUL*araBAD* ($P_{tuf}$) |
| ara3 | 21-JL | GTCCAGGAGGACATACCATGGCGATTGCAA TTGGCCTC | Fw primer *araBAD* ($P_{tuf}$) |
| ara4 | 22-JL | GTGCTGATTTCAACATTTTTTGACTGGTCCT ACTCAGGAGAGCGTTC | Rv primer *araBAD* (Flank2) |
| ara5 | 23-JL | GAACGCTCTCCTGAGTAGGACCAGTCAAAA AATGTTGAAATCAGCAC | Fw primer for Flank2 in pJUL*araBAD* (*araBAD*) |

| Strain, plasmid, or oligo-nucleotide | ID | Relevant characteristics or sequence | Source, reference or purpose |
|---|---|---|---|
| ara6 | 24-JL | GCGGCAGCGTGAA**GCTAGC**GCGCTTCTTT GAAGAGTCTC | Rv primer for Flank2 in pJUL*araBAD* (pK19*mobsacB*, **NheI**) |
| xyl1 | 11-JL | GAATGGCGCGATAA**GCTAGC**CCGTTCGGC TGACTCCTTC | Fw primer for Flank1 in pJUL*xylAB* (pK19*mobsacB*, **NheI**) |
| xyl2 | 33-JL | CAAACTACCAGCTACCCTGTGGCATCAAAA AATCCGCCGTTCCTTG | Rv primer for Flank1 in pJUL*xylAB* ($P_{tuf}$) |
| xyl3 | 15-JL | GAAGTCCAGGAGGACATACCATGAGCAACA CCGTTTTCATC | Fw primer *xylAB* ($P_{tuf}$) |
| xyl4 | 16-JL | CGCATCCAAACTCACTTAGTCAATATTATTG AAGCATTTATCAGGG | Rv primer *xylAB* (Flank2) |
| xyl5 | 17-JL | CCTGATAAATGCTTCAATAATATTGACTAAG TGAGTTTGGATGCGGAAG | Fw primer for Flank2 in pJUL*xylAB* (*xylAB*) |
| xyl6 | 18-JL | GCGGCAGCGTGAA**GCTAGC**CTCACTAGTA CGCGGATAAATG | Rv primer for Flank2 in pJUL*xylAB* (pK19*mobsacB*, **NheI**) |
| araseq1 | 38-JL-seq | GGTTCCAGTTTCTGACGC | Sequencing primer pJUL*araBAD* |
| araseq2 | 46-JL-seq | GACTCGCCAGGACAGC | Sequencing primer pJUL*araBAD* |
| araseq3 | 47-JL-seq | CCGGCGCTGCAACGTC | Sequencing primer pJUL*araBAD* |
| araseq4 | 48-JL-seq | GCGATAAAGTTGCCGCAC | Sequencing primer pJUL*araBAD* |
| araseq5 | 49-JL-seq | CGATATGCGCCAATTCGC | Sequencing primer pJUL*araBAD* |
| araseq6 | 50-JL-seq | CGGCGAATATGAGTGGG | Sequencing primer pJUL*araBAD* |
| araseq7 | 51-JL-seq | CTGCGGCGCTAACTGAC | Sequencing primer pJUL*araBAD* |
| araseq8 | 39-JL-seq | CCGTGAAGTCACTCATG | Sequencing primer pJUL*araBAD* |
| xylseq1 | 36-JL-seq | GATTCGCAGGATCTTCCC | Sequencing primer pJUL*xylAB* |
| xylseq2 | 42-JL-seq | CGGACTTCAACGTCGTGG | Sequencing primer pJUL*xylAB* |
| xylseq3 | 43-JL-seq | CGGACTTTGCCAACGGC | Sequencing primer pJUL*xylAB* |
| xylseq4 | 44-JL-seq | CACTGAGCTGAGCACGC | Sequencing primer pJUL*xylAB* |
| xylseq5 | 45-JL-seq | GCCTGACGAGCTGCAC | Sequencing primer pJUL*xylAB* |

| Strain, plasmid, or oligo-nucleotide | ID | Relevant characteristics or sequence | Source, reference or purpose |
|---|---|---|---|
| xylseq6 | 37-JL-seq | CCAAGCGAACCGTCCTC | Sequencing primer pJUL*xylAB* |
| pK19seqfw | pK19-fow | TAATGCAGCTGGCACGAC | Fw Sequencing primer pK19*mobsaB* derivatives (Shah *et al.*, 2016) |
| pK19seqrv | pK19-rev* | TAATGGTAGCTGACATTCATCCG | Rv Sequencing primer pK19*mobsaB* derivatives |
| iso1 | kivdfow* | AACTGCAGAACCAATGCATTGGAGGAGACA CAACATGTATACAGTAGGAGATTACCTAT | Fw primer verifies pBB1*kivd-adhA* (Blombach *et al.*, 2011) |
| iso2 | kivd2rev* | CCAATGCATTGGTTCTGCAGTTTTATGATTT ATTTTGTTCAGCAAAT | Rv primer verifies pBB1*kivd-adhA* (Blombach *et al.*, 2011) |
| iso3 | Ptac check* | CACTCCCGTTCTGGATAATG | Fw primer verifies pJC4*ilvBNCD-pntAB* (Blombach *et al.*, 2011) |
| iso4 | pntAB check rev* | CCCAAATTCATGTGCCGCTTC | Rv primer verifies pJC4*ilvBNCD-pntAB* |
| Δcg3303-1 | 86-JL | GAAACAGCTATGACCATGATTACGCC**AAGC TT**GCCGTCGCAGCACATTGG | Fw primer Flank1 in pJULΔcg3303 (pK19*mobsacB*, **HindIII**) |
| Δcg3303-2 | 87-JL | CCCCAGTACCATGCAGCTG | Rv primer Flank1 in pJULΔcg3303 (Flank2) |
| Δcg3303-3 | 88-JL | CTTCGCGCAGCTGCATGGTACTGGGGATCA TTATCTCCTGTTCTTGAACTGAAG | Fw primer Flank2 in pJULΔcg3303 (Flank1) |
| Δcg3303-4 | 89-JL | GTGCTTGCGGCAGCGTGAA**GCTAGC**CCGA GTTCTCCCGTCAGC | Rv primer Flank2 in pJULΔcg3303 (pK19*mobsacB*, **NheI**) |
| Δcg2320-1 | 90-JL | AACAGCTATGACCATGATTACGCC**AAGCTT** GCTGCGGGGATCACTAAA | Fw primer Flank1 in pJULΔcg2320 (pK19*mobsacB*, **HindIII**) |
| Δcg2320-2 | 91-JL | AAAGAGCTTTTCAGAACACTTGGCAAACCT CAC | Rv primer Flank1 in pJULΔcg2320 (Flank2) |
| Δcg2320-3 | 92-JL | TTGCCAAGTGTTCTGAAAAGCTCTTTCATCC | Fw primer Flank2 in pJULΔcg2320 (Flank1) |
| Δcg2320-4 | 93-JL | CCTGAGTGCTTGCGGCAGCGTGAA**GCTAG C**GCAACAGTAGATGGAGCTG | Rv primer Flank2 in pJULΔcg2320 (pK19*mobsacB*, **NheI**) |
| Δcg2965-1 | 94-JL | ATTACGCCAAGCTTGCATGC**CTGCAG**GGCG CACACGTATGGGCAGA | Fw primer Flank1 in pJULΔcg2965 (pK19*mobsacB*, **PstI**) |
| Δcg2965-2 | 95-JL | GAGAACAAAAACCGGTGCGTACCACAATAG AGTCTTAG | Rv primer Flank1 in pJULΔcg2965 (Flank2) |

| Strain, plasmid, or oligo-nucleotide | ID | Relevant characteristics or sequence | Source, reference or purpose |
|---|---|---|---|
| Δcg2965-3 | 96-JL | TGTGGTACGCACCGGTTTTTGTTCTCAGGC GGA | Fw primer Flank2 in pJULΔcg2965 (Flank1) |
| Δcg2965-4 | 97-JL | GAGTGCTTGCGGCAGCGTGAA**GCTAGC**CC ATCGGAAATTCACTGATGTGC | Rv primer Flank2 in pJULΔcg2965 (pK19*mobsacB*, **NheI**) |
| Δcg2746-1 | 98-JL | AACAGCTATGACCATGATTACGCC**AAGCTT** GCGTGGATCCTGACCTGAAG | Fw primer Flank1 in pJULΔcg2746 (pK19*mobsacB*, **HindIII**) |
| Δcg2746-2 | 99-JL | AACCTGGGATTCCAAAATTGCACCTATATAT ATGGTGCAAAAC | Rv primer Flank1 in pJULΔcg2746 (Flank2) |
| Δcg2746-3 | 100-JL | TAGGTGCAATTTTGGAATCCCAGGTTAGCG GGG | Fw primer Flank2 in pJULΔcg2746 (Flank1) |
| Δcg2746-4 | 101-JL | GTGCTTGCGGCAGCGTGAA**GCTAGC**CGTC GTCGTGCTGGATGC | Rv primer Flank2 in pJULΔcg2746 (pK19*mobsacB*, **NheI**) |
| ΔsutR-1 | 107-JL | AACAGCTATGACCATGATTACGCC**AAGCTT** CACAATCATGATCGCAGCGG | Fw primer Flank1 in pJULΔ*sutR* (pK19*mobsacB*, **HindIII**) |
| ΔsutR-2 | 108-JL | TCACGGAGGAATACCTTTTACCCTCTAGAG ACGACTATCAG | Rv primer Flank1 in pJULΔ*sutR* (Flank2) |
| ΔsutR-3 | 109-JL | AGAGGGTAAAAGGTATTCCTCCGTGACTAG GCTAGATGACGGATCC | Fw primer Flank2 in pJULΔ*sutR* (Flank1) |
| ΔsutR-4 | 110-JL | CCTGAGTGCTTGCGGCAGCGTGAA**GCTAG C**GCATGCGGGTGTTTGCGCGG | Rv primer Flank2 in pJULΔ*sutR* (pK19*mobsacB*, **NheI**) |
| Δcg1327-1 | 111-JL | GCATGCCTGCAGGTCGACTCTAGA**GGATCC** GCTCGGCAACTGAGGTGCCC | Fw primer Flank1 in pJULΔcg1327 (pK19*mobsacB*, **BamHI**) |
| Δcg1327-2 | 112-JL | CAAGCGGAAAGTAAAGCCCATGCTACCCAG GATATTTTC | Rv primer Flank1 in pJULΔcg1327 (Flank2) |
| Δcg1327-3 | 113-JL | GTAGCATGGGCTTTACTTTCCGCTTGTTTGA TCTAG | Fw primer Flank2 in pJULΔcg1327 (Flank1) |
| Δcg1327-4 | 114-JL | CCTGAGTGCTTGCGGCAGCGTGAA**GCTAG C**CAGGTCTTCCACGTTTTCATG | Rv primer Flank2 in pJULΔcg1327 (pK19*mobsacB*, **NheI**) |
| Δznr-1 | 115-JL | AACAGCTATGACCATGATTACGCC**AAGCTT** GTCCGCACGGTAACGCTTGTG | Fw primer Flank1 in pJULΔ*znr* (pK19*mobsacB*, **HindIII**) |
| Δznr-2 | 116-JL | GTACTTCGATAGTGGGGAAGTCCTTCCGTC CTTAG | Rv primer Flank1 in pJULΔ*znr* (Flank2) |
| Δznr-3 | 117-JL | GAAGGACTTCCCCACTATCGAAGTACATTTT GTGTC | Fw primer Flank2 in pJULΔ*znr* (Flank1) |
| Δznr-4 | 118-JL | CCTGAGTGCTTGCGGCAGCGTGAA**GCTAG C**CAAGGCTATTTTTCGAAATAG | Rv primer Flank2 in pJULΔ*znr* (pK19*mobsacB*, **NheI**) |

| Strain, plasmid, or oligo-nucleotide | ID | Relevant characteristics or sequence | Source, reference or purpose |
|---|---|---|---|
| Δzur-1 | 119-JL | AACAGCTATGACCATGATTACGCC**AAGCTT** GTCATTTTGCGGTCTTCGCG | Fw primer Flank1 in pJULΔ*zur* (pK19*mobsacB*, **HindIII**) |
| Δzur-2 | 120-JL | ATATGTCCTTGAACGTTGATCCTCCTCAATG ACAC | Rv primer Flank1 in pJULΔ*zur* (Flank2) |
| Δzur-3 | 121-JL | AGGAGGATCAACGTTCAAGGACATATGAAG CTGTCGAAC | Fw primer Flank2 in pJULΔ*zur* (Flank1) |
| Δzur-4 | 122-JL | CCTGAGTGCTTGCGGCAGCGTGAA**GCTAG C**CATCGCCGGAGTCGTCATCA | Rv primer Flank2 in pJULΔ*zur* (pK19*mobsacB*, **NheI**) |
| ΔfarR-1 | 123-JL | AACAGCTATGACCATGATTACGCC**AAGCTT** GATCCTTTGGCTCGAAATCAAAAG | Fw primer Flank1 in pJULΔ*farR* (pK19*mobsacB*, **HindIII**) |
| ΔfarR-2 | 124-JL | AAATGGGTTCACGGGTGTTCATTTTAGCCG ATCTG | Rv primer Flank1 in pJULΔ*farR* (Flank2) |
| ΔfarR-3 | 125-JL | TAAAATGAACACCCGTGAACCCATTTTGGT GGC | Fw primer Flank2 in pJULΔ*farR* (Flank1) |
| ΔfarR-4 | 126-JL | CCTGAGTGCTTGCGGCAGCGTGAA**GCTAG C**CTTCCGCAGGTGGCAGGATC | Rv primer Flank2 in pJULΔ*farR* (pK19*mobsacB*, **NheI**) |
| ΔripA-1 | 127-JL | AACAGCTATGACCATGATTACGCC**AAGCTT** GACCCCTATTTTCCAGGGATC | Fw primer Flank1 in pJULΔ*ripR* (pK19*mobsacB*, **HindIII**) |
| ΔripA-2 | 128-JL | ACCTTTACTACCTATCTCATCCTCACTACAA GCAAATTT | Rv primer Flank1 in pJULΔ*ripR* (Flank2) |
| ΔripA-3 | 129-JL | GTGAGGATGAGATAGGTAGTAAAGGTGTGA AAATAGTTCCTCACG | Fw primer Flank2 in pJULΔ*ripR* (Flank1) |
| ΔripA-4 | 130-JL | CCTGAGTGCTTGCGGCAGCGTGAA**GCTAG C**GTGCCAAGGACTGCCTGGCC | Rv primer Flank2 in pJULΔ*ripR* (pK19*mobsacB*, **NheI**) |
| Δcg2648-1 | 131-JL | AACAGCTATGACCATGATTACGCC**AAGCTT** GTGATCTTTGAACGGGTGTC | Fw primer Flank1 in pJULΔcg2648 (pK19*mobsacB*, **HindIII**) |
| Δcg2648-2 | 132-JL | TTCTTTAATCTCAAAATTTAAAATTCCATAAA TTTAGACAATC | Rv primer Flank1 in pJULΔcg2648 (Flank2) |
| Δcg2648-3 | 133-JL | GAATTTTAAATTTTGAGATTAAAGAAGCAGC TTCTTG | Fw primer Flank2 in pJULΔcg2648 (Flank1) |
| Δcg2648-4 | 134-JL | CCTGAGTGCTTGCGGCAGCGTGAA**GCTAG C**GTAGTGAAATTCTCCGCGCG | Rv primer Flank2 in pJULΔcg2648 (pK19*mobsacB*, **NheI**) |
| ΔiclR-1 | 135-JL | GCATGCCTGCAGGTCGACTCTAGA**GGATCC** GTGTCATAGCCGAAGAGAAG | Fw primer Flank1 in pJULΔ*iclR* (pK19*mobsacB*, **BamHI**) |
| ΔiclR-2 | 136-JL | GTCAATGAATTGCATTTGATCCGTTTTTCTA AAG | Rv primer Flank1 in pJULΔ*iclR* (Flank2) |

| Strain, plasmid, or oligo-nucleotide | ID | Relevant characteristics or sequence | Source, reference or purpose |
|---|---|---|---|
| ΔiclR-3 | 137-JL | AAACGGATCAAATGCAATTCATTGACGTACA AAGTGATG | Fw primer Flank2 in pJULΔ*iclR* (Flank1) |
| ΔiclR-4 | 138-JL | CCTGAGTGCTTGCGGCAGCGTGAA**GCTAG C**CGATTCAGACAGGCGGACGT | Rv primer Flank2 in pJULΔ*iclR* (pK19*mobsacB*, **NheI**) |
| ΔcspA-1 | 139-JL | GCATGCCTGCAGGTCGACTCTAGA**GGATCC** GGTTACTTTTTCGGGGCCTTTTG | Fw primer Flank1 in pJULΔ*cspA* (pK19*mobsacB*, **BamHI**) |
| ΔcspA-2 | 140-JL | TAGCAGTTAGAGCATTTGTACCTTTTCCTAA TCAGGTGATG | Rv primer Flank1 in pJULΔ*cspA* (Flank2) |
| ΔcspA-3 | 141-JL | AAAAGGTACAAATGCTCTAACTGCTAGCTAA AAATTCCGC | Fw primer Flank2 in pJULΔ*cspA* (Flank1) |
| ΔcspA-4 | 142-JL | CGACGTTGTAAAACGACGGCCAGT**GAATTC** GGAAGGCTTGCTCCCACTGC | Rv primer Flank2 in pJULΔ*cspA* (pK19*mobsacB*, **EcoRI**) |
| ΔrbsR-1 | 143-JL | GCATGCCTGCAGGTCGACTCTAGA**GGATCC** GACCTTCACGGGAATTGGAC | Fw primer Flank1 in pJULΔ*rbsR* (pK19*mobsacB*, **BamHI**) |
| ΔrbsR-2 | 144-JL | ATGAAGCGCTTGTCTCCTCACCAACTTTCTG GAAG | Rv primer Flank1 in pJULΔ*rbsR* (Flank2) |
| ΔrbsR-3 | 145-JL | AGTTGGTGAGGAGACAAGCGCTTCATCAGC ATG | Fw primer Flank2 in pJULΔ*rbsR* (Flank1) |
| ΔrbsR-4 | 146-JL | CCTGAGTGCTTGCGGCAGCGTGAA**GCTAG C**CAATTTCACGACCAGTCAACG | Rv primer Flank2 in pJULΔ*rbsR* (pK19*mobsacB*, **NheI**) |
| ΔgenR-1 | 147-JL | AACAGCTATGACCATGATTACGCC**AAGCTT** CCACAGGGTAGGGGAGATG | Fw primer Flank1 in pJULΔ*genR* (pK19*mobsacB*, **HindIII**) |
| ΔgenR-2 | 148-JL | GGAAAGAGTGATTATGGGGGGAATTTTCAG AGC | Rv primer Flank1 in pJULΔ*genR* (Flank2) |
| ΔgenR-3 | 149-JL | AAATTCCCCCCATAATCACTCTTTCCAGATA GCG | Fw primer Flank2 in pJULΔ*genR* (Flank1) |
| ΔgenR-4 | 150-JL | CCTGAGTGCTTGCGGCAGCGTGAA**GCTAG C**GGTCTTACGTGGAACCAAATC | Rv primer Flank2 in pJULΔ*genR* (pK19*mobsacB*, **NheI**) |
| Δcg0150-1 | 151-JL | GCATGCCTGCAGGTCGACTCTAGA**GGATCC** CTCGGACTGCGGGGTGTAC | Fw primer Flank1 in pJULΔcg0150 (pK19*mobsacB*, **BamHI**) |
| Δcg0150-2 | 152-JL | CACAATCGATGAACTCCATAACGAGAACTTA ATCGAGCAAC | Rv primer Flank1 in pJULΔcg0150 (Flank2) |
| Δcg0150-3 | 153-JL | TCTCGTTATGGAGTTCATCGATTGTGAGTGA GCGGTAATAATG | Fw primer Flank2 in pJULΔcg0150 (Flank1) |
| Δcg0150-4 | 154-JL | CCTGAGTGCTTGCGGCAGCGTGAA**GCTAG C**GAAATTGTGCGAGGCCCCCG | Rv primer Flank2 in pJULΔcg0150 (pK19*mobsacB*, **NheI**) |

| Strain, plasmid, or oligo-nucleotide | ID | Relevant characteristics or sequence | Source, reference or purpose |
|---|---|---|---|
| ΔmmpLR-1 | 155-JL | GCATGCCTGCAGGTCGACTCTAGA**GGATCC** GAACAAGACAACCTCTACATCTTCG | Fw primer Flank1 in pJULΔ*mmpLR* (pK19*mobsacB*, **BamHI**) |
| ΔmmpLR-2 | 156-JL | AAGGAAAATGTAGAAATTGTGGCGTGTGAA CCTC | Rv primer Flank1 in pJULΔ*mmpLR* (Flank2) |
| ΔmmpLR-3 | 157-JL | CACGCCACAATTTCTACATTTTCCTTCAGTT CCTCGGTGC | Fw primer Flank2 in pJULΔ*mmpLR* (Flank1) |
| ΔmmpLR-4 | 158-JL | CCTGAGTGCTTGCGGCAGCGTGAA**GCTAG C**CATTGATCGCGGCTCTGGGC | Rv primer Flank2 in pJULΔ*mmpLR* (pK19*mobsacB*, **NheI**) |
| ΔramB1 | 198-JL | CCACGCCGGGCACCTG | Fw primer Δ*ramB* verification |
| ΔramB2 | 199-JL | GGCGCGATAGTGGATTCGTG | Rv primer Δ*ramB* verification |

* oligonucleotides designed by Dr. Bastian Blombach

# 3.2. Culture media and conditions

## 3.2.1. General

Reaction tube and shaking flask cultivations were performed on a rotary shaker at 120 rpm (benchtop shaker AK 85, Infors AG, Bottmingen/Basel, Switzerland) at 37 °C or 30 °C for *E. coli* or *C. glutamicum*, respectively.

As general complex medium 2x yeast extract tryptone (YT) medium (Sambrook and Russell, 2001) (Table S 7, p. 217) was used and supplemented with 18 g $L^{-1}$ agar for passaging on semi-solid media. For special applications, like electrocompetent cells or transformation, BHI (Table S 8, p. 218) or BHIS (Table S 9, p. 218) was applied as enriched complex broth for *C. glutamicum* (cf. 3.5.2, p. 85).

## 3.2.2. Minimal media for cultivation of *C. glutamicum*

*C. glutamicum* was cultivated in standard defined medium **CGXIIs** (**pH 7.4**; Table S 11, p. 220; Table S 12, p. 220), which was modified compared to the originally published CGXII (Table S 10, p. 219) (Eikmanns *et al.*, 1991; Keilhauer *et al.*, 1993). The medium

constitutes per liter 5 g $(NH_4)_2SO_4$, 5 g urea, 21 g 3-(N-morpholino) propane sulphonic acid (MOPS), 1 g $KH_2PO_4$, 1 g $K_2HPO_4$, 0.25 g $MgSO_4 \cdot 7\ H_2O$, 10 mg $CaCl_2$, 10 mg $MnSO_4 \cdot H_2O$, 16.4 mg $FeSO_4 \cdot 7\ H_2O$, 1 mg $ZnSO_4 \cdot 7\ H_2O$, 0.2 mg $CuSO_4 \cdot 5\ H_2O$, 0.02 mg $NiCl_2 \cdot 6\ H_2O$, and 0.2 mg biotin. The chosen pH of the medium is inspired by published results investigating the intracellular pH of *C. glutamicum* (Follmann *et al.*, 2009).

$CGXII_S$ medium was modified to **$CGXII_1$ (no urea, pH 6.5)**, when pyrolysis water (PW) was applied as substrate in shaking flask experiments and to **$CGXII_2$ (no urea, no MOPS, pH 7.4)** for bioreactor cultivations (seed train information can be found in Figure 3.1, p. 83). The supplementation of protocatechuate (PCA; for more details cf. 3.2.3, p. 77) is indicated as subscript in the respective experiment (for example $CGXII_{S+PCA}$ or $CGXII_{2+PCA}$).

### 3.2.3. Carbon sources and supplements

In the conducted experiments, defined as well as complex substrates were added to cultivation media from concentrated aqueous stock solutions (as included in parenthesis): D-glucose (500 g $L^{-1}$ or 100 mM), L-arabinose (100 mM), D-xylose (100 mM), acetol (hydroxyacetone, 50 g $L^{-1}$), potassium acetate (500 g $L^{-1}$), yeast extract (200 g $L^{-1}$). The initial concentrations are indicated in the respective experiments.

Additionally, side streams from two different biorefinery conversion technologies were surveyed as complex substrate for cultivations with *C. glutamicum*. PW and hemicellulose fraction originate in the thermochemical conversion technologies pyrolysis of wheat straw and organosolv treatment of beech wood, respectively. For both substrates a pretreatment procedure is described below (cf. 3.10.1, p. 91). In experiments using pretreated **pyrolysis water (PW)** as carbon source, 3.5 % (v/v) was used as initial concentration for clarified (pH 6.5, centrifugation, filtration) and 0.5 h heat treated (HT) PW (cf. 3.10.1, p. 91 for further explanations). To compare supplementation with the 0.5 h HT PW with respect to various times of heat exposure at 80 °C (n), adapted concentrations c* of were applied by considering the residual volume (V) after heat treatment (equation 3.1).

$$c^{*} = \frac{V_{\mathrm{n\,h}} \cdot 3.5}{V_{0.5\,\mathrm{h}}} \quad \left[\%(\mathrm{v/v})\right] \qquad [3.1]$$

For easier communication, these adapted concentrations will be referred to as rel. 3.5 % (v/v). The **hemicellulose fraction** was given aseptically after pretreatment for aerobic cultivations (cf. 3.10.2, p. 92 for precise details). For anaerobic shaking flasks the clarified hemicellulose fraction was added to the $CGXII_S$ medium before adjusting the pH to 7.4. The entire medium was then sterilized via membrane filters (Rotilabo®-syringe filters, CME Filter 0.45 µm, Carl Roth GmbH + Co. KG, Karlsruhe, Germany).

Experiments investigating the role of reduced glutathione (GSH) during growth with PW used 1 mM supplementation from a freshly prepared 100 mM aqueous stock solution.

Protocatechuate (PCA) was added, where mentioned, to a final concentration of 30 mg $L^{-1}$ (30 g $L^{-1}$ stock solution; for stock preparation appropriate amounts of 2 M NaOH were given).

In aerobic/microaerobic bioreactor experiments mimicking shaking flasks (cf. 3.2.8, p. 81) the urea was added after sterilization from a sterile filtered 500 g $L^{-1}$ aqueous stock solution.

The strain *C. glutamicum* Δ*aceE* Δ*pqo* Δ*ilvE* Δ*ldhA* Δ*mdh* (Blombach *et al.*, 2011) and successor strains *C. glutamicum* Δ*pqo* Δ*ilvE* Δ*ldhA* Δ*mdh*, CArXy and CIsArXy carry a deletion of the *ilvE* gene and exhibit thus an auxotrophy for the branched chain amino acids leucine (Leu), isoleucine (Ile) and valine (Val). To enable cell proliferation, 2 mM of each amino acid was provided in all cultivations using this strain. A combined aqueous 500 mM stock solution was produced by suspending the amino acids in deionized water ($dH_2O$) and adding concentrated HCl for complete solubilization.

For all strains carrying a Δ*aceE* mutation 0.5 % (w/v) potassium acetate was added to the cultivation medium unless HF or PW were given as substrate.

To maintain selection pressure for plasmids, antibiotics were supplemented according to (Table 3.1, p. 66) from stock solutions as described in parenthesis: 50 µg kanamycin $mL^{-1}$ (Kan; 50 mg $mL^{-1}$ in 0.1 M NaOH), 100 µg spectinomycin $mL^{-1}$ (Spec; 100 mg $mL^{-1}$ in $dH_2O$), 6 µg chloramphenicol $mL^{-1}$ (Cm; 6 mg $mL^{-1}$ in 50 % (v/v) ethanol).

All stock solutions were sterilized via membrane filters (Rotilabo®-syringe filters, CME Filter 0.22 µm [0.44 µm for hemicellulose fraction], Carl Roth GmbH + Co. KG, Karlsruhe, Germany) before use. For 30 L scale bioreactor cultivations, the D-glucose stock solution was autoclaved in maximum 1 L volume.

### 3.2.4. Bacterial glycerol stocks

Bacterial strain preservation was accomplished in 30 % (v/v) glycerol stocks. For this purpose, 5 mL 2x YT medium was inoculated from a single colony and incubated overnight (o/n). Then, 700 µl suspension was added to sterile 300 µL glycerol (≥ 98 %, Carl-Roth GmbH, Karlsruhe, Germany), frozen and stored at -70 °C. This working cell bank was used to initiate each presented experiment by streaking bacteria from the chilled glycerol stock on suitable agar plates.

### 3.2.5. Shaking flask cultivations of *C. glutamicum*

Aerobic/microaerobic shaking flask cultivations were performed in 500 mL flasks with four baffles or oxygen limitation further enhanced in flasks without baffles. *C. glutamicum* strains were streaked from a glycerol stock on 2x YT agar plates and incubated for 2-3 days at 30 °C. The bacteria were passaged consecutively (Figure 3.1 A): o/d (5 mL 2x YT, 6-8 h), o/n (50 mL 2x YT, 12-16 h, inoculated with complete o/d), and main culture (50 mL $CGXII_{S\pm PCA}$ or $CGXII_1$). Main cultures were started with a defined biomass concentration by harvesting the appropriate amount of cells from the o/n culture (4,500 rcf for 5-10 min, centrifuge 5804 R, rotor: A-4-44, Eppendorf AG, Hamburg, Germany), discarding the supernatant and resuspending the pellet in a defined volume of 0.9 % (w/v) NaCl solution.

### 3.2.6. Anaerobic shaking flask cultivations of *C. glutamicum*

For anaerobic cultivation 100 mL shaking flasks (without baffles) were sealed with a silicon septum enabling aseptic sampling and preventing gas exchange (Figure 4.8, p. 132; Figure 4.16, p. 149). The consecutive cultivation steps were as follows (Figure 3.1 B): 2x TY agar plate (2-3 days), $o/n_1$ (5 mL 2x TY, 15-16 h), o/d (50 mL 2x YT, 7-8 h, inoculated with complete $o/n_1$), $o/n_2$ (50 mL $CGXII_{S\pm PCA}$, 13-14 h, starting biomass

~ 0.2 g CDW $L^{-1}$), anaerobic culture (50 mL $CGXII_{S\pm PCA}$). For the $o/n_2$ as well as anaerobic culture defined initial cell densities were set as described above (cf. 3.2.5, p. 79).

### 3.2.7. Triple glass reactor system

Defined and parallelized cultivation conditions were realized in a triple glass bioreactor system (250 mL working volume, HWS Labortechnik, Mainz, Germany) with 200 mL $CGXII_2$ minimal medium at ambient pressure. A seed train was developed as follows (Figure 3.1 C): 2x TY agar plate (2-3 days), o/d (5 mL 2x YT, 6-8 h), o/n (50 mL 2x YT, 12-13 h, inoculated with complete o/d), main culture (200 mL $CGXII_2$, starting biomass ~ 0.5 g CDW $L^{-1}$). The dissolved oxygen concentration (DO) and the pH were monitored with standard probes (Mettler-Toledo GmbH, Gießen, Germany). DO probe calibration at 30 °C was conducted by gassing with $N_2$ for 0 % and air for 100 % DO in the cultivation medium. During cultivation the pH was controlled at setpoint 7.4 by controlled addition of 10 % *o*-phosphoric acid and 25 % ammonia solution. Calibration of the pH electrodes was conducted externally in buffer solutions at pH 4.0 and pH 7.0. To counteract foaming, Struktol™ J 647 (Schill+Seilacher GmbH, Hamburg, Germany) was given manually on demand.

For **aerobic intermittent fed-batch** cultivations (cf. 4.3.1, p. 117) the DO level was maintained above 35 % by adapting gassing and agitation (initial conditions: 0.1 vvm [20 mL $min^{-1}$; mass flow controller 0-500 mL $min^{-1}$; Analyt-MTC GmbH, Müllheim, Germany] and 100 rpm, respectively).

In the **two-phase aerobic/microaerobic intermittent fed-batch** fermentation (cf. 4.3.2, p. 120) a constant agitation of 100 rpm was installed throughout the process. In the first aerobic phase a constant gassing of 0.1 vvm was set. At 5 h of cultivation the gas supply was decreased to 0.025 vvm (5 mL $min^{-1}$) to further restrict the oxygen transfer rate (OTR) and establish a microaerobic environment.

In both fed-batch approaches, rel. 3.5 % (v/v) PW and 0.5 g YE $L^{-1}$ were supplemented and identical volumes added for each feeding from the same stock solutions.

### 3.2.8. 30 L bioreactor cultivations

For systemic investigation of the adaptation of *C. glutamicum* to a shift from aerobic via microaerobic to anaerobic conditions a defined cultivation in a 30 L bioreactor (Figure 3.2, Bioengineering AG, Wald, Switzerland) was established. A seed train was conceptualized as follows (Figure 3.1 D): 2x TY agar plate (2-3 days), o/$n_1$ (5 mL 2x YT, 15-16 h), o/d (50 mL 2x YT, 7-8 h, inoculated with complete o/$n_1$), o/$n_2$ (200 mL $CGXII_{S+PCA}$ + 40 g glucose $L^{-1}$, 2 L flask with baffles, starting biomass ~ 0.2 g CDW $L^{-1}$), main culture (10 L $CGXII_{S+PCA}$ or $CGXII_{2+PCA}$ + 60 g glucose $L^{-1}$, 30 L stainless steel bioreactor, starting biomass ~ 0.4 g CDW $L^{-1}$). The DO and the pH were analyzed online via standard probes (Mettler-Toledo GmbH, Gießen, Germany). Calibration was achieved externally at 30 °C for the DO electrode at 0 % ($dH_2O$ + sodium sulfite) and 100 % ($dH_2O$ + air gassing) and pH electrodes in buffer solutions at pH 4.0 and pH 7.0. The cultivation temperature was controlled to 30 °C through the reactor mantle. Excessive foaming was prevented by manually adding Struktol™ J 647 (Schill+Seilacher GmbH, Hamburg, Germany) on demand. Agitation was constant (445 rpm) using a single six blade Rushton turbine and four baffles at the reactor wall. Low aeration rates of 1 L $min^{-1}$ (0.1 vvm; mass flow controller 0-2 L $min^{-1}$ Analyt-MTC GmbH, Müllheim, Germany) were realized through a needle directly inside the cultivation broth, an overpressure was controlled at 0.5 bar and the exhaust gas composition was analyzed for $O_2$ and $CO_2$ content (BlueSens gas sensor GmbH, Herten, Germany).

The **aerobic/microaerobic fermentation** mimicking shaking flask cultivations was conducted in $CGXII_{S+PCA}$ medium being sterilized in the same batch as the shaking flasks. Importantly, in these experiments urea was added after sterilization from a 500 g $L^{-1}$ sterile stock solution. This was necessary, as urea decomposes upon heat exposure to $NH_3$ and isocyanic acid, which in terms can hydrolyze to $NH_3$ and $CO_2$ in dilute aqueous solutions (Meessen *et al.*, 2010). In the process no pH regulation was installed.

The **triple-phase batch fermentation** was for the first 11 h conducted analogously to the aerobic/microaerobic fermentation, but used $CGXII_{2+PCA}$ medium. To initiate anaerobic conditions, the aeration was stopped after 11 h of cultivation, the headspace flushed through a needle with 10 L nitrogen gas ($N_2$) $min^{-1}$ for 15 min. To maintain a pH of 7.4 throughout the cultivation, 25 % ammonia solution was given automatically.

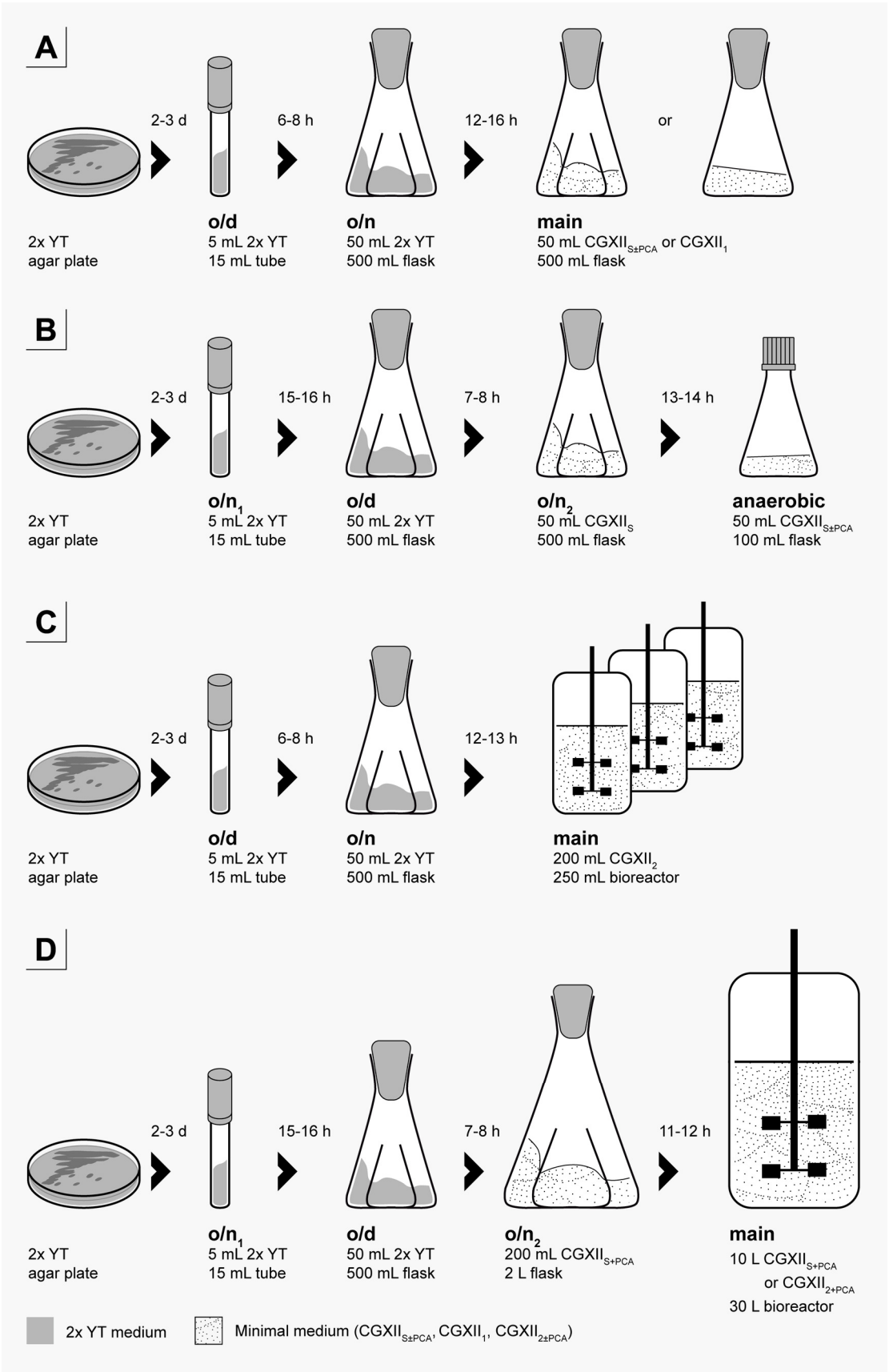
A
2-3 d
6-8 h
12-16 h
or
2x YT
agar plate
o/d
5 mL 2x YT
15 mL tube
o/n
50 mL 2x YT
500 mL flask
main
50 mL CGXII$_{S±PCA}$ or CGXII$_1$
500 mL flask
B
2-3 d
15-16 h
7-8 h
13-14 h
2x YT
agar plate
o/n$_1$
5 mL 2x YT
15 mL tube
o/d
50 mL 2x YT
500 mL flask
o/n$_2$
50 mL CGXII$_S$
500 mL flask
anaerobic
50 mL CGXII$_{S±PCA}$
100 mL flask
C
2-3 d
6-8 h
12-13 h
2x YT
agar plate
o/d
5 mL 2x YT
15 mL tube
o/n
50 mL 2x YT
500 mL flask
main
200 mL CGXII$_2$
250 mL bioreactor
D
2-3 d
15-16 h
7-8 h
11-12 h
2x YT
agar plate
o/n$_1$
5 mL 2x YT
15 mL tube
o/d
50 mL 2x YT
500 mL flask
o/n$_2$
200 mL CGXII$_{S+PCA}$
2 L flask
main
10 L CGXII$_{S+PCA}$
or CGXII$_{2+PCA}$
30 L bioreactor
2x YT medium
Minimal medium (CGXII$_{S±PCA}$, CGXII$_1$, CGXII$_{2±PCA}$)

**Figure 3.1. Seed trains for cultivation of *C. glutamicum***. Full information is given elsewhere as indicated. **A**. Aerobic/microaerobic shaking flask (cf. 3.2.5, p. 79). **B**. Anaerobic shaking flask (cf. 3.2.6, p. 79). **C**. Triple glass reactor system (cf. 3.2.7, p. 80). **D**. 30 L bioreactor (cf. 3.2.8, p. 81). Complex medium 2x YT (grey) and minimal medium variations of the CGXII (dotted; $CGXII_{S\pm PCA}$, $CGXII_1$, $CGXII_{2\pm PCA}$; cf. 3.2.2, p. 76) were used. Carbon sources and supplements were provided as described above (cf. 3.2.3, p. 77) or the respective experiment.

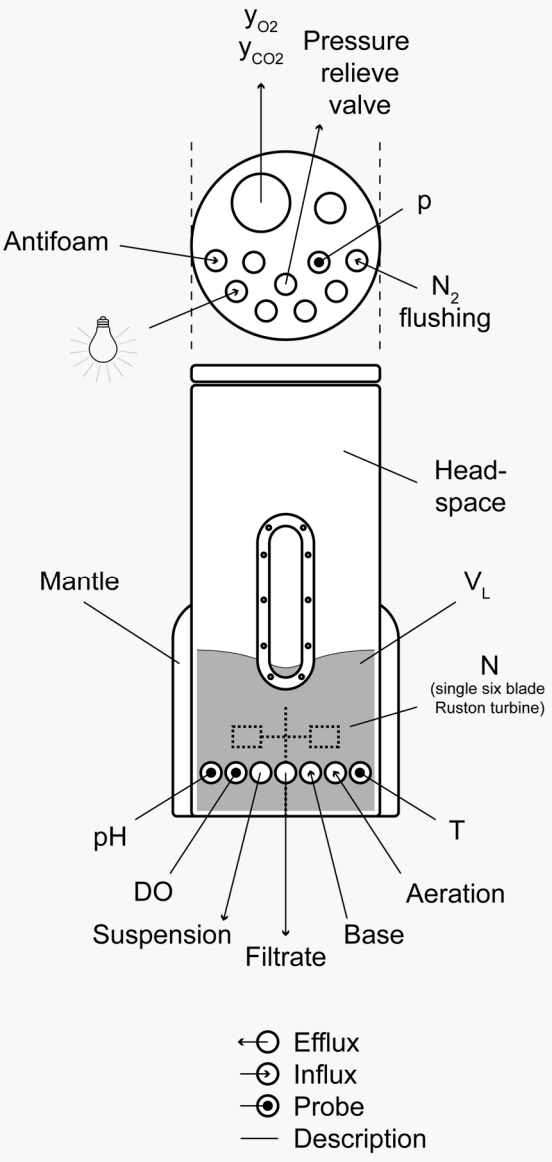


**Figure 3.2. Triple-phase batch fermentation 30 L reactor setup**. 7 slots at the reactor bottom were equipped with: pH probe, DO probe, biosuspension harvest valve, filtrate unit, base influx (25 % ammonia solution, $pH_{setpoint}$ =7.4), aeration [1 L $min^{-1}$ (0.1 vvm), aerobic and microaerobic phase], and a temperature (T) probe. Agitation was achieved with a single six blade Rushton turbine stirrer at 445 rpm (N, rotational speed; dashed line). Temperature was regulated through the reactor mantle. The liquid volume ($V_L$) was 10 L. To initiate anaerobic conditions the aeration was stopped and the headspace flushed with $N_2$ (10 L $min^{-1}$, 15 min). The reactor pressure (p) was controlled at 0.5 bar. The exhaust gas was analyzed in the aerobic and microaerobic phase for oxygen ($y_{O2}$) and carbondioxide ($y_{CO2}$). For safety reasons a pressure relieve valve was installed. Visual foam inspection was possible using a light and on demand antifoam addition realized manually through a syringe and septum.

## 3.3. Standard molecular biology methods

Standard molecular biology methods (for example agarose gel electrophoresis, restriction digests, ligations and others) were conducted according to Sambrook *et al.* (Sambrook and Russell, 2001) or available manufacturers' instructions. After linearization of plasmids with restriction nucleases, alkaline phosphatase treatment (Thermo Fisher Scientific Inc., Waltham, USA) was conducted standardly. Verification of plasmid cloning was achieved by sequencing (GATC Biotech AG, Constance, Germany) covering the entire introduced genetic information.

## 3.4. Plasmid, PCR fragment and chromosomal DNA isolation and purification

Plasmids and PCR fragments were isolated or purified with *E.Z.N.A.® Plasmid Mini Kit I* (Omega Bio-tek, Inc., Norcross, USA) and *NucleoSpin® Gel and PCR Clean-up* (Macherey-Nagel GmbH & Co. KG, Düren, Germany) after respective manufacturers' instructions. Using the *DNeasy Blood & Tissue Kit* (QIAGEN, Hilden, Germany), chromosomal DNA was extracted following the supplied protocol.

## 3.5. Electrocompetent cells and transformation

### 3.5.1. *E. coli*

**Electrocompetent** *E. coli* DH5α were gained as described in literature (Dower *et al.*, 1988). In brief, a 250 mL 2x YT (Table S 7, p. 217) medium culture was inoculated with 500 µL overnight culture (5 mL 2x TY, 12-16 h) and grown in a 1 L flask with baffles to an $OD_{600}$ of 0.3-0.5 (Ultrospec 10 Cell Density Meter, GE Healthcare Europe GmbH, Freiburg, Germany). Cells were harvested by centrifugation at 4,500 rcf for 15-30 min at 4 °C (centrifuge 5804 R, rotor: A-4-44, Eppendorf AG, Hamburg, Germany). Subsequently, bacteria were washed first in ice cold $dH_2O$ and then in ice cold 10 % (v/v) glycerol. Finally, the pellet was resuspended in 0.5 mL ice cold 10 % (v/v) glycerol and

50 µL aliquots shock frozen in liquid $N_2$ and stored at -70 °C.

**Transformation** of *E. coli* DH5α with plasmids or isothermal assembly mixes (cf. 3.7, p. 86) was performed according to Dower *et al.* in electroporation cuvettes (2 mm, 40-400 µL; Radnor, Pennsylvania, USA) with an Eporator® (Eppendorf AG, Hamburg, Germany) using a 2.5 kV pulse (Dower *et al.*, 1988). Regeneration was conducted in 5 mL 2x YT medium at 37 °C for 50 min and bacteria finally spread on a 2x YT agar plate including antibiotics for selection as given in Table 3.1 (p. 66).

### 3.5.2. *C. glutamicum*

*C. glutamicum* was pretreated to yield **electrocompetent** cells according to literature (Tauch *et al.*, 2002). For this purpose, a preculture was inoculated with a single colony from a 2x YT agar plate, incubated for 6 h in 5 mL brain heart infusion (BHI, Table S 8, p. 218) medium and transferred to an overnight culture in 50 mL BHI medium supplemented with 91 g sorbitol $L^{-1}$ (BHIS, Table S 9, p. 218). 5 mL of this preculture were transferred to a 250 mL BHIS main culture (1 L baffled flask) and cultivated to a biomass concentration of approximately 0.56 g CDW $L^{-1}$. The culture was harvested at 4,500 rcf for 15-30 min at 4 °C (centrifuge 5804 R, rotor: A-4-44, Eppendorf AG, Hamburg, Germany), resuspended and washed three times in 100 mL ice cold 10 % (v/v) glycerol. Finally, pellets were resuspended in 1.6 mL ice cold 10 % (v/v) glycerol and 150 µL aliquots shock frozen in liquid $N_2$ and stored at -70 °C.

**Transformation** of *C. glutamicum* with plasmids (for pk19*mobsacB* systems ≥ 1 µg plasmid DNA used) was conducted following published guidelines (Liebl *et al.*, 1989) in electroporation cuvettes (2 mm, 40-400 µL; Radnor, Pennsylvania, USA) with an Eporator® (Eppendorf AG, Hamburg, Germany) using a 2.5 kV pulse. Prior to regeneration in BHIS medium a recommended heat shock for 6 min at 46 °C was performed instantly after electroporation (van der Rest *et al.*, 1999). Incubation was followed at 30 °C for 50 min, before plating complete pellets on BHIS agar plates supplemented with required antibiotics as given in Table 3.1 (p. 66).

## 3.6. Polymerase chain reaction

Polymerase chain reaction (PCR) (Mullis and Faloona, 1987; Saiki *et al.*, 1988) was used to amplify DNA fragments with designed primers in a Biometra TAdvanced thermocycler (Biometra GmbH, Göttingen, Germany). A standard protocol for DNA amplification with Phusion Hot Start II HF DNA Polymerase (Thermo Fisher Scientific Inc., Waltham, USA) is given in the appendix (Table S 19, p. 210). Colony PCR with Taq DNA Polymerase S (Genaxxon BioScience GmbH, Ulm, Germany) was used to verify plasmid inheritance and genetic deletion or integration in *E. coli* and *C. glutamicum*. To prepare the template DNA for this purpose, a single colony was picked, resuspended in 50 µL $dH_2O$ and incubated at 95 °C for 10 min. The suspension was then clarified by centrifugation (≥ 11,000 rcf, ≥ 1 min) and 10 µL of the supernatant applied in the colony PCR (Table S 20, p. 222).

## 3.7. Isothermal assembly

Isothermal assembly of PCR fragments with a plasmid backbone was achieved according to literature (Gibson *et al.*, 2009). The experimental assembly procedure is based on published recommendations (Gibson, 2011). For the isothermal reaction, a 5x Iso reaction buffer (Table S 14, p. 221) and an Iso enzyme-reagent mix (Table S 15, p. 221) was prepared as depicted in the appendix. Single fragments were beforehand produced via PCR and granted ≥ 15 bps homologous overlaps. Fragments and linearized plasmid ratio calculation was inspired by available protocols (Gibson, 2011; NEB, 2015). 5 µL DNA fragment master mix was added to 15 µL of the Iso enzyme-reagent mix and assembly realized in a thermocycler at 50 °C for 60 min. Where fragment sizes varied notably, overlap extension PCR (Horton *et al.*, 1990) was harnessed with given primers to approximate fragment size and thereby also lower total fragment number. After incubation, the assembly batch was diafiltered (MF-Millipore Membrane Filter, 0,025 µm pore size, Merck Chemicals GmbH, Billerica, Massachusetts, USA) for 15 min with $dH_2O$ and subsequently introduced into *E. coli* via electroporation as elucidated above (cf. 3.5.1, p. 84).

## 3.8. Chromosomal deletion and integration of genetic information in *C. glutamicum*

The possibility to manipulate the host's genetic information is a prerequisite for metabolic engineering. In this study, we exploited an established markerless system based on homologous recombination by using the mobilizable and integrative vector pK19*mobsacB* (Schäfer *et al.*, 1994). The vector originates in the vectors pK18 and pK19 that were constructed for *E. coli* (Pridmore, 1987). Schäfer *et al.* combined these vectors with the broad host-range transfer machinery of the plasmid RP4 and a modified *sacB* gene from *B. subtilis* for positive selection (Datta *et al.*, 1971; Selbitschka *et al.*, 1993; Schäfer *et al.*, 1994). In order to enable homologous recombination, flanking regions of ≥ 500 bps outside the genomic section to be deleted or the targeted integration site were amplified via PCR. For integrative purposes the flanks were designed to embrace the genomic information, which is intended for insertion. Cloning of the plasmids was conceived via isothermal assembly (cf. 3.7, p. 86) and harnessed the provided multiple cloning site of pK19*mobsacB*. Briefly, a plasmid was assembled, introduced into *E. coli*, verified by sequencing, purified and introduced into *C. glutamicum* via electroporation (cf. 3.5, p. 84). As pK19*mobsacB* is devoid of a functional origin of replication for *C. glutamicum*, selection on kanamycin is feasible to identify rare double-crossover events that lead to a full chromosomal integration of the plasmid. The constitutively expressed *sacB* gene confers a sucrose sensitive phenotype. Counter selection was thus realized on BHIS agar plates (Table S 9, p. 218), which induced selective pressure to resolve the integrated plasmid, again, by homologous recombination. Mutant strains were finally distinguished from WT strains by colony PCR (cf. 3.6, p. 86).

## 3.9. Plasmid and strain construction

### 3.9.1. *C. glutamicum* engineered for 1,2-PDO production

In Part I (p. 106) of this thesis, *C. glutamicum* was engineered for 1,2-PDO production. The plasmid **pJUL*gldA***, which constitutively expresses the *E. coli* glycerol dehydrogenase *gldA* (ordered locus names: b3945, JW5556; gene accession number:

ECK3937) (Asnis and Brodie, 1953; Tang *et al.*, 1979; Truniger and Boos, 1994) and confers a kanamycin resistance was constructed based on the episomal vector pJC4 (Cordes *et al.*, 1992). The shuttle vector pJC4 originally goes back to pZ1 (Menkel *et al.*, 1989). This hybrid vector was constructed by a fusion of the native *C. glutamicum* plasmid pHM1519 and the *E. coli* plasmid pACYC177 (Chang and Cohen, 1978; Miwa *et al.*, 1984; Rose, 1988). To clone pJUL*gldA*, pJC4 was linearized with the restriction endonucleases XbaI and NotI. Overlapping fragments of the constitutive promoter of the *C. glutamicum* elongation factor EF-TU (cg0587, $P_{tuf}$), the *E. coli* gene *gldA* and the strong terminator of the *E. coli* gene *rrnB* ($T_{rrnB}$) (Brosius *et al.*, 1981; Orosz *et al.*, 1991) were amplified from the particular chromosomal DNA via PCR with the primer pairs P1.1/P2, gldA1/gldA2 and T1/T2 (Table 3.1, p. 66), respectively. During amplification the native GTG start codon of the *C. glutamicum* EF-TU was substituted by the original ATG codon of the *E. coli gldA* gene. Additionally, prior to the start codon the three native nucleotides CAT of $P_{tuf}$ were substituted by ACC. The plasmid was connected by isothermal assembly as described above (cf. 3.7, p. 86) yielding the expression vector pJUL*gldA* (8380 bps). Its integrity was evaluated via colony PCR and verified by sequencing (GATC Biotech AG, Constance, Germany) with the primers gldAseq1-gldAseq4 (Table 3.1, p. 66).

To establish the 1,2-PDO producing strains **PDO1** and **PDO2**, pJUL*gldA* was isolated from *E. coli* and transferred into *C. glutamicum* WT and Δ*pqo* Δ*aceE* Δ*ldhA* Δ*mdh* (Radoš *et al.*, 2015), respectively, as elucidated above (cf. 3.5.2, p. 85). For **PDO2** a verification to comprise pJUL*gldA* is shown in the appendix (Figure S 5, p. 227). The strain PDO2 carries an *aceE* deletion and is thus devoid of a functional pyruvate dehydrogenase complex. For appropriate growth 0.5 % (w/v) potassium acetate was supplemented as discussed in literature (Blombach *et al.*, 2011). This supplementation was not required, where PW was used as substrate for it already contains acetate as major carbon source for growth (cf. 2.5.2, p. 24; Table S 21, p. 239).

### 3.9.2. *C. glutamicum* engineered for isobutanol production based on D-xylose and L-arabinose

*C. glutamicum* was genetically engineered to be capable of isobutanol production from the substrates D-xylose and L-arabinose (cf. Part II, p. 123). Synthetic operons for

pentose metabolization were conceived for chromosomal integration into newly identified *C. glutamicum* landing pads (CgLPs; cf. 4.5, p. 123; Figure 4.5, p. 124, Table 4.3, p. 127) and made use of the discussed pK19*mobsacB* system (cf. 3.8, p. 87). The three consecutive strains, which are discussed in the following, originate in the basic isobutanol producer *C. glutamicum* Δ*aceE* Δ*pqo* Δ*ilvE* Δ*ldhA* Δ*mdh* (Blombach *et al.*, 2011), which requires 0.5 % (w/v) potassium acetate supplementation as discussed above (cf. 3.9.1, p. 87). Furthermore, due to the deletion of the *ilvE* gene this strain exhibits an auxotrophy for the branched chain amino acids leucine (Leu), isoleucine (Ile) and valine (Val), of which 2 mM were henceforth provided for cultivation.

To release this strain of the necessity to supply acetate for adequate cultivation, we restored the *aceE* gene (cg2466) encoding the E1p subunit of the pyruvate dehydrogenase complex (PDHC). This was accomplished by **pJUL*aceE*** (8918 bps), which was constructed by ligation of both SalI restricted pK19*mobsacB* (Schäfer *et al.*, 1994) and an *aceE* PCR fragment (template: chromosomal DNA of *C. glutamicum* WT, primer pair: aceE1/aceE2) using the T4 DNA Ligase (Thermo Fisher Scientific Inc., Waltham, USA). The plasmid was sequenced via the primers pK19seqfw, aceEseq1, aceEseq2 and pK19seqrv (GATC Biotech AG, Konstanz, Germany). The plasmid pJUL*aceE* was then used as described above (cf. 3.8, p. 87) to obtain the *aceE* restored ***C. glutamicum* Δ*pqo* Δ*ilvE* Δ*ldhA* Δ*mdh*** as precursor for further strain construction.

Chromosomal integration of the genetic information enabling pentose metabolization was achieved with the plasmids pJUL*araBAD* and pJUL*xylAB* that were also constructed based on pK19*mobsacB*. Upstream flanks (Flank1) and downstream flanks (Flank2) were designed to locate into the newly identified landing pads CgLP4 and CgLP12 (cf. 4.5, p. 123; Table 4.3, p. 127) for *xylAB* and *araBAD* integration, respectively.

Concerning **pJUL*araBAD***, pK19*mobsacB* was linearized via PaeI/NheI restriction. Fragments for the desired integrative construct Flank1-$P_{tuf}$-*araBAD*-$T_{rrnB}$-Flank2 were amplified via PCR using *C. glutamicum*'s chromosomal DNA as template and primer pairs P1.2/P2 ($P_{tuf}$), ara1/ara2 (Flank1) and ara5/ara6 (Flank2) and pVWEx1-*araBAD* (Schneider *et al.*, 2011) with primers ara3/ara4 (*araBAD*-$T_{rrnB}$) including the strong terminator (Brosius *et al.*, 1981; Orosz *et al.*, 1991). For **pJUL*xylAB*** cloning, the backbone pK19*mobsacB* was linearized by single restriction with NheI. Building blocks of the integrative construct Flank1-$P_{tuf}$-*xylAB*-$T_{rrnB}$-Flank2 were amplified from

*C. glutamicum*'s chromosomal DNA with the primers P1.2/P2 ($P_{tuf}$), xyl1/xyl2 (Flank1) and xyl5/xyl6 (Flank2) and using pEKEx3-*xylA*$_{Xc}$-*xylB*$_{Cg}$ (Meiswinkel *et al.*, 2013) as template with primers xyl3/xyl4 (*xylAB*-$T_{rrnB}$). Connection of fragments and backbone was accomplished by isothermal assembly (cf. 3.7, p. 86). The synthetic operons' integrity was verified by sequencing with primers pK19seqfw and pK19seqrv and xylseq1-xylseq6 for pJUL*xylAB* (10237 bps) and araseq1-araseq8 for pJUL*araBAD* (11230 bps).

The pentose utilizing strain **CArXy** (*C. glutamicum* Δ*pqo* Δ*ilvE* Δ*ldhA* Δ*mdh* CgLP4::($P_{tuf}$-*xylAB*-$T_{rrnB}$) CgLP12::($P_{tuf}$-*araBAD*-$T_{rrnB}$)) was constructed by markerless synthetic operon integration via pJUL*xylAB* and pJUL*araBAD* as mentioned above (cf. 3.8, p. 87).

For isobutanol production the plasmids pJC4*ilvBNCD-pntAB* and pBB1*kivd-adhA* (Blombach *et al.*, 2011) were introduced into CArXy yielding the strain **CIsArXy**.

All strains *C. glutamicum* Δ*pqo* Δ*ilvE* Δ*ldhA* Δ*mdh*, CArXy and CIsArXy were verified via colony PCR, respectively (primer pairs: aceE3/aceE4 [Figure S 6; p. 228]; ara1/P2, araseq3/P1.2, araseq6/ara6, xyl1/P2, xylseq4/xyl6, xylseq3/xylseq5 [Figure S 7, p. 229]; iso1/iso2 and iso3/iso4 [Figure S 8, p. 230]).

### 3.9.3. Deletion of putatively oxygen responsive regulators

Selected transcriptional regulators (cf. 4.12.8, p. 157) deduced from RNA-sequencing of the triple-phase process were deleted form the chromosome of *C. glutamicum* WT and harness the elsewhere described pK19*mobsacB* system (Schäfer *et al.*, 1994) (cf. 3.8, p. 87). The plasmid was linearized by restriction with HindIII/NheI, PstI/NheI, BamHI/NheI or BamHI/EcoRI as given in Table 3.1. Cloning was performed using isothermal assembly as elucidated above (cf. 3.7, p. 86). Deletion plasmids pJULΔcg3303, pJULΔcg2320, pJULΔcg2965, pJULΔcg2746, pJULΔ*sutR*, pJULΔcg1327, pJULΔ*znr*, pJULΔ*zur*, pJULΔ*farR*, pJULΔ*ripA*, pJULΔcg2648, pJULΔ*iclR*, pJULΔ*cspA*, pJULΔ*rbsR*, pJULΔ*genR*, pJULΔcg0150, pJULΔ*mmpLR* harbor a Flank1 and a Flank2 of > 500 bp homology to up- or downstream regions of the targeted regulator. Flank1 and Flank2 were amplified from the *C. glutamicum* WT chromosome with respective primer pairs Δ*-1/Δ*-2 and Δ*-3/Δ*-4 (asterisk stands for

targeted gene; Table 3.1). Cloning was verified by sequencing with the primers pK19seqfw and pK19seqrv.

Markerless deletion of the regulators including the RamB (cg0444) through pK19Δ*ramB* (Gerstmeir *et al.*, 2004) was conducted as mentioned (cf. 3.8, p. 87). Deletion was verified through colony PCR using the outside primer pair Δ*-1/ Δ*-4 or ΔramB1/ ΔramB2. The resulting strains as well as *C. glutamicum ΔoxyR* (cg2109) (Milse *et al.*, 2014) are given in Table 3.1.

## 3.10. Biorefinery side streams applied in this study

In the presented study, the two biorefinery side streams pyrolysis water (PW) and hemicellulose fraction (HF) were assayed as substrate for cultivations with *C. glutamicum*. They originate from thermochemical conversion of wheat straw by fast pyrolysis and beech wood by ethanol/water organosolv processing, respectively. For either of the side streams, a pretreatment procedure was established as described in the following.

### 3.10.1. Pyrolysis water and its pretreatment

The biorefinery side stream PW used in this study arose from fast pyrolysis of wheat straw in the bioliq® plant (KIT, Eggenstein-Leopoldshafen, Germany) (Pfitzer *et al.*, 2016). From this straw liquefaction process, the brownish PW was delivered with a water content of approximately 80 % (w/w) at pH ~ 2.5, which is typical for bio-oils (Bridgwater, 2017). It comprises water soluble organic compounds, hydrophobic lignin micelles as a micro-emulsion and minor suspended char (Fratini *et al.*, 2006; Bridgwater, 2017). A GC-MS analysis was performed by the Johann Heinrich von Thünen-Institut (Braunschweig, Germany) and prompted by Prof. Dr. Nicolaus Dahmen (Institute for Catalysis Research and Technology, Karlsruhe Institute of Technology (KIT), Eggenstein-Leopoldshafen, Germany). A full list of identified substances is given in the appendix (Table S 21, p. 239 pp.). As the products of fast pyrolysis are thermochemically not equilibrated and are instable even at moderate temperatures (Oasmaa *et al.*, 1997; Meier and Faix, 1999), the PW was stored at -21 °C until further use to provide a

comparable substrate in all experiments.

To transform this liquid into a fermentable substrate, a **pretreatment procedure** (Figure 3.3) was established starting with 100 mL initial volume of PW. First, the pH was adjusted to 6.5 with 10 M potassium hydroxide. A phase separation occurred and was accelerated by centrifugation at 4,500 rcf for 30 min (centrifuge 5804 R, rotor: A-4-44, Eppendorf AG, Hamburg, Germany). The hydrophobic upper layer was then removed with a syringe. Remnants thereof and the small solid char pellet were hereafter separated from the aqueous phase by paper filtration enriched with hydrophobic interaction surface (plastic shred). The accordingly treated substrate will henceforth be referred to as **clarified PW**. For removal of volatile growth inhibitors like methanol and to progress thermochemical equilibration under oxygen atmosphere, a heat treatment was conducted at constant stirring in open beakers at 80 °C on heating plates. The temperature was measured within the liquid and adjusted manually. Three different heat exposure times (0.5 h, 1 h and 1.5 h) were systematically compared to clarify the effect of the treatment. The yielded heat treated (HT) substrates will be referred to as **0.5 h, 1 h and 1.5 h HT PW**. Heat treatment in open vessels was accompanied with significant volume losses. The respective volume losses were considered (cf. 3.2.3, p. 77) and relative volumes of PW referred to the 0.5 h treatment (indicated as rel. % (v/v)) were applied for cultivation experiments. Eventually, the PW was sterilized by filtration (Rotilabo®-syringe filter, CME 0.22 µM, Carl Roth GmbH + Co. KG, Karlsruhe, Germany) and stored at -21 °C.

### 3.10.2. Hemicellulose fraction and its pretreatment

The hemicellulose fraction (HF) was delivered from a beech wood ethanol/water organosolv processing after lignin precipitation (without enzymatic hydrolysis and further purification procedures; Dr.-Ing. Susanne Zibek, Fraunhofer Institute for Interfacial Engineering and Biotechnology, Stuttgart, Germany) and as black liquor with high viscosity (Ludwig *et al.*, 2014). For cultivation purposes, a short pretreatment procedure was developed. The desired amount of HF was weighed and thoroughly mixed with 5 mL $dH_2O$. Solids were floated and sedimented in a centrifugal step at 4,500 rcf for 30 min (centrifuge 5804 R, rotor: A-4-44, Eppendorf AG, Hamburg, Germany) and the clarified liquid applied in cultivations as described above (cf. 3.2.3, p. 77).

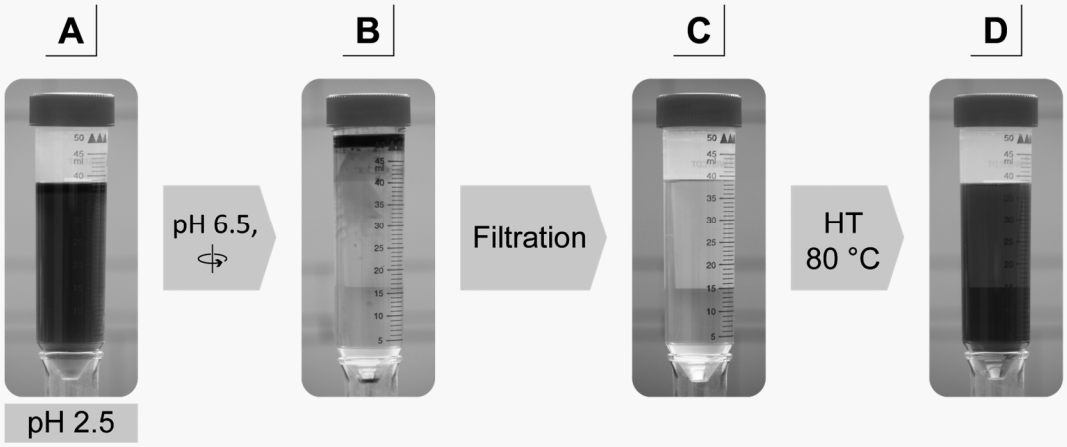


**Figure 3.3. Pyrolysis water (PW) pretreatment**. **A**. Crude PW as stable emulsion at pH 2.5. **B**. Adjustment of the pH to 6.5 and phase separation by centrifugation. **C**. Removal of the hydrophobic top layer and char via syringe and filtration yields the clarified PW. **D**. Systematic exposure to 80 °C in open beakers (0.5 h, 1 h and 1.5 h) yields heat treated (HT) PW. Volume variations seen here are not representative and do not originate in the treatment. Graphic modified from publication (Lange, Müller, *et al.*, 2017).

# 3.11. Lysis of *C. glutamicum*

## 3.11.1. Mechanical

Lysates for enzyme assays with *C. glutamicum* (cf. 3.12.6, p. 97) were produced from aerobic and anaerobic shaking flask cultivations. In general, bacteria were harvested from a cultivation by centrifugation at 4,500 rcf for 10 min (centrifuge 5804 R, rotor: A-4-44, Eppendorf AG, Hamburg, Germany). The pellet of about 50 mg CDW (corresponding to a harvest of 50 mL culture at 0.9 g CDW $L^{-1}$) was then washed once in 0.2 M Tris-HCl buffer (pH 7.4), resuspended in 400 µL lysis buffer (Table S 17, p. 222) and added to ~ 300 µL glass beads. Mechanical cell disruption occurred in a Precellys®24 (Bertin Instruments, Montigny-le-Bretonneux, France) apparatus at 3x 20 s (6,500 rpm) vibration cycles. The cell debris was separated from the soluble extract by centrifugation at 20,000 rcf for 1 min at 4 °C (centrifuge 5804 R, rotor: FA 45-30-11, Eppendorf AG, Hamburg, Germany). Lysate supernatants were kept on ice until further analysis (cf. 3.12.6, p. 97)

### 3.11.2. Chemical

Chemical lysis of *C. glutamicum* was achieved with perchloric acid using a modified procedure (Cserjan-Puschmann *et al.*, 1999; Löffler *et al.*, 2016). For the bacterial harvest process see below (cf. 3.13.1, p. 99). 1 mL of bacterial suspension (2-5 g CDW $L^{-1}$) was added to 0.25 mL lysis buffer (-20 °C, 35 % (v/v) perchloric acid, 80 µM EDTA) and incubated rolling for 15 min at 4 °C. Then 0.25 mL 1 M $K_2HPO_4$ was added and stepwise neutralization promoted to pH 7.0 with 5 M KOH. After centrifugation (20,000 rcf, 5 min, 4 °C; centrifuge 5427 R, rotor: FA 45-30-11, Eppendorf AG, Hamburg, Germany) the pH was verified and the supernatant stored at -70 °C before analysis. Throughout the protocol, volume alterations were noted and used for later recalculations.

## 3.12. Analytical methods

### 3.12.1. Optical density

Bacterial growth was monitored by photometric inspection of turbidity at 600 nm wavelength ($OD_{600}$). For this purpose, a biosuspension sample was taken, diluted in 0.9 % (w/v) NaCl and analyzed in the DR 2800 Portable spectrophotometer (Hach Lange GmbH, Düsseldorf, Germany) or Ultrospec 10 Cell Density Meter (GE Healthcare Europe GmbH, Freiburg, Germany) in the range of 0.1-0.3. A correlation of the turbidity to the cell number was adopted ($OD_{600}$ of 1 correlates with $10^8$ cells).

### 3.12.2. Cell dry weight

$OD_{600}$ was correlated to the cell dry weight (CDW) concentrations after equation 3.2.

$$CDW = \alpha \cdot OD_{600} \quad \left[\frac{g}{L}\right] \qquad [3.2]$$

Analysis of the cell dry weight was achieved with the following procedure. Test tubes were dried at 105 °C for > 1 days, cooled to room temperature (RT) in a desiccator and weighed (centrifuge tubes round bottom DURAN®, 12 mL, Carl-Roth GmbH, Karlsruhe, Germany). 5 mL of a biosuspension aliquot was taken from a bacterial cultivation experiment and harvested in the test tubes at 4,000 rcf for 10 min at 4 °C (centrifuge 5427

R, rotor: F-35-6-30, Eppendorf AG, Hamburg, Germany). The supernatant was discarded and the pellet washed twice in 5 mL $dH_2O$. The pellets were then dried for > 2 days at 105 °C, gravimetrically analyzed and the tubes' differential mass determined.

Representative $CDW/OD_{600}$ correlation coefficients α were determined with *C. glutamicum* WT in $CGXII_{S+PCA}$ or $CGXII_{2+PCA}$ medium and 60 g glucose $L^{-1}$ as sole substrate over a wide range of growth rates (0.02-0.47 $h^{-1}$). 8-level $CDW/OD_{600}$ correlation curves were analyzed and correlation coefficients calculated via linear regression (Figure S 2, p. 224). Two coefficients α in $CGXII_{2+PCA}$ medium of 0.22 g $L^{-1}$ (used for shaking flask experiments; Ultrospec 10 Cell Density Meter, GE Healthcare Europe GmbH, Freiburg, Germany) and 0.30 g $L^{-1}$ (used for bioreactor cultivations; DR 2800 Spectrophotometer, Hach Lange GmbH, Düsseldorf, Germany) and two coefficients α in $CGXII_{S+PCA}$ medium of 0.35 g $L^{-1}$ (used for shaking flask experiments; Pharmacia LKB Ultrospec III UV/Vis spectrophotometer, GE Healthcare Europe GmbH, Freiburg, Germany) and 0.31 g $L^{-1}$ (used for bioreactor cultivations; DR 2800 Spectrophotometer, Hach Lange GmbH, Düsseldorf, Germany) were determined.

### 3.12.3. Nucleic acids

#### 3.12.3.1 DNA

DNA concentrations and purity were measured with a Nano Drop ND-1000 Spectrophotometer (PEQLAB Biotechnologie GmbH, Erlangen, Germany). The cDNA sequencing library for RNA-sequencing was verified with Agilent DNA 7500 Kit using 2100 Bioanalyzer Instruments (Agilent Technologies, Santa Clara, USA).

#### 3.12.3.2 RNA

RNA was analyzed and quantified by DropSense16 Micro-Volume Spectrophotometer [Xpose dscvry] (Unchained Labs [Trinean], Pleasanton, USA). RNA integrity and removal of rRNA was verified by Agilent RNA 6000 Nano Kit and Agilent RNA 6000 Pico Kit using 2100 Bioanalyzer Instruments (Agilent Technologies, Santa Clara, USA), respectively.

### 3.12.4. Protein quantification

Soluble protein concentrations in bacterial lysates of *C. glutamicum* were analyzed after the manufacturer's instructions (*BCA Protein Assay Kit*, Thermo Fisher Scientific Inc., Waltham, USA). The lysates were produced mechanically as described above (cf. 3.11.1, p. 93). Quantification was accomplished by analyzing a 9-level standard calibration curve of diluted albumin (BSA; Figure S 1, p. 223) at 560 nm in a Synergy 2 microplate reader (BioTek Instruments GmbH, Bad Friedrichshall, Germany) using 96-well plates (Greiner Bio-One GmbH, Frickenhausen, Germany).

### 3.12.5. HPLC

#### 3.12.5.1 Sugars, organic acids and alcohols

Metabolite concentrations in the culture supernatant were analyzed from clarified cultivation broth (centrifugation at ≥ 11,000 rcf for ≥ 1 min; Centrifuge MiniSpin®, rotor F-45-12-11, Eppendorf AG, Hamburg, Germany). Concentrations of **D-glucose**, **L-arabinose**, **D-xylose**, **acetate**, **lactate**, **succinate**, **acetol**, **1,2-propanediol** (1,2-PDO) and **isobutanol** were quantified according to literature (Buchholz *et al.*, 2013) using an Agilent 1200 series apparatus (Agilent Technologies, Santa Clara, USA) equipped with a Rezex™ ROA-Organic Acid $H^+$ (8 %) LC column (300 x 7.8 mm, 8 µm) protected by a Carbo-$H^+$ SecurityGuard™ (4 x 3 mm) column (Phenomenex Inc., Aschaffenburg, Germany).

A **sample pretreatment** to precipitate phosphate (Buchholz *et al.*, 2013) was carried out as follows: 45 µl 4 M $NH_3$ and 100 µl 1.2 M $MgSO_4$ were added to 1 ml culture supernatant. After 5 min of incubation, the sample was centrifuged for 5 min at 18,000 rcf and RT (Centrifuge 5417 R, rotor: FA45-30-11, Eppendorf AG, Hamburg, Germany). 500 µL supernatant were then transferred to 500 µL 0.1 M $H_2SO_4$, mixed thoroughly and incubated for 15 min at RT. Eventually, remainder suspended matter was separated by centrifugation at 18,000 rcf and RT for 15 min.

In general, **isocratic chromatography** was realized with 5 mM $H_2SO_4$ as mobile phase and 0.4 mL $min^{-1}$ flow rate for 45 min at 50 °C column temperature. This standard procedure was used to analyze D-glucose, L-arabinose, D-xylose, acetate, lactate, and succinate. To capture the lately eluting isobutanol, the analysis timespan was extended to

52 min. For acetol and 1,2-propanediol quantification the column temperature was lowered to 20 °C and promoted peak separation. The injection sample volume was standardly set to 10 µL and detection achieved with an Agilent 1200 series refractive index detector at 32 °C. Peaks were quantified using 6- or 8-level standard calibrations for each analyte as external reference. Exemplary calibration curves are given in the appendix (Figure S 4, p. 226). Unless samples contained the hemicellulose fraction, L-rhamnose was spiked as internal standard to each sample prior to phosphate precipitation.

#### 3.12.5.2 L-Glutamate

Bacterial lysates produced via the perchloric acid (cf. 3.11.2, p. 94) were analyzed for intracellular L-glutamate concentrations with an Agilent 1200 series apparatus equipped with an Agilent Zorbax Eclipse Plus C18 (250 x 4.6 mm, 5 µm) column protected by an Agilent Zorbax Eclipse Plus C18 (12.5 x 4.6 mm, 5 µm) guard column (Agilent Technologies, Santa Clara, CA, USA) as described previously (Buchholz *et al.*, 2013). Fluorometric detection (FLD (DAD), excitation at 230 nm and emission at 450 nm) was conducted after automatic pre-column derivatization with *o*-phthaldialdehyde (OPA). The protocol was originally developed based on literature (Henderson and Brooks, 2010). The elution buffer consisted of a polar phase (10 mM $Na_2HPO_4$, 10 mM $Na_2B_4O_7$, 0.5 mM $NaN_3$, pH 8.2) and a nonpolar phase (45 % (v/v) methanol, 45 % (v/v) acetonitrile). The injection volume was 36.4 µL (2.5 µL 10 mM $Na_2B_4O_7$, 1 µL sample, 0.5 µL OPA reagent, 0.4 µL Fmoc chloride and 32 µL injection dilution solution). Quantification was achieved using a 7-point calibration curve for the analytes as external standard. To correct variabilities in the analysis, a 200 mM L-ornithine internal standard was implemented.

### 3.12.6. Enzyme assays

Enzymatic activities of the glucose-6-phosphate dehydrogenase (G6P-DH, glucose-6P dehydrogenase) and 6-phosphogluconate dehydrogenase (6PG-DH, 6P-gluconate dehydrogenase), the two key enzymes in the oxidative branch of the pentose phosphate pathway (Figure 3.4), were analyzed in clarified bacterial lysates (cf. 3.11.1, p. 93) by a modified protocol from literature (Moritz *et al.*, 2000). Photometric quantification was

performed at 340 nm wavelength ($\varepsilon = 6{,}3$ (mM cm)$^{-1}$) in acrylic semi-micro cuvettes (Sarstedt AG & Co, Nümbrecht, Germany) with an Ultrospec™ 2100 pro UV/Visible spectrophotometer (GE Healthcare Europe GmbH, Freiburg, Germany) at 30 °C. The reaction batch was composed of 500 µL analysis buffer (Table S 18, p. 222) and 50-100 µL 1:10 diluted extract and was added to 0.95 mL with $dH_2O$. The extinction was followed for 1 min ($S_0$) before the reaction was started by addition of 4 mM glucose-6-phosphate or 1 mM 6-phospho-gluconate (50 µL of 20x aqueous stock solution, stored at -21 °C) for the analysis of G6P-DH or 6PG-DH activity, respectively. An increase of extinction was followed for 5 min ($S_1$). Slopes $S_0$ and $S_1$ were determined by linear regression (equation 3.12, p. 104).

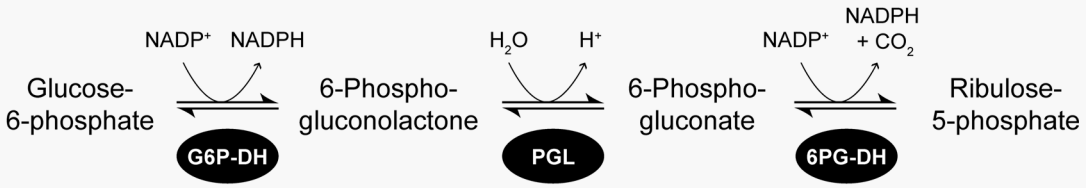


**Figure 3.4. Oxidative branch of the pentose phosphate pathway**. The glucose-6-phosphate dehydrogenase (G6P-DH) is encoded by the genes *zwf* (cg1778) and *opcA* (cg1779), the 6-phosphogluconolactonase (PGL) by *devB* (cg1780) and the 6-phosphogluconate dehydrogenase (6PG-DH) by *gnd* (cg1643). The reaction sequence involves the cofactor $NADP^+$/NADPH.

### 3.12.7. Total organic carbon

The total organic carbon (TOC) content was quantified in this study to analyze crude and pretreated PW. The method was developed previously (Buchholz, Graf, Blombach, *et al.*, 2014) with a total carbon analyzer (Multi N/C 2100s, Analytik Jena, Jena, Germany) and uses a parallelized detection approach of the total inorganic carbon (TIC) and total carbon (TC) to determine the TOC concentration differentially (TOC = TC – TIC). A standard mix of potassium hydrogen phthalate and sodium carbonate was prepared. Standard curves for an 18-level external calibration of the TC (30-3000 C-mg $L^{-1}$) and TIC (15-1500 C-mg $L^{-1}$) are shown in the appendix (Figure S 3, p. 224).

# 3.13. RNA-sequencing

The analysis of the transcriptomic repertoire of organisms has achieved a quantum leap forward since the development of RNA-sequencing (RNA-seq) tools. The technology can capture the entire RNA species of an organism at base pair resolution at any given point in time and thus facilitates for example strand-specific analysis, transcription start site mapping or the detection of alternative splicing events (Wilhelm and Landry, 2009; Ozsolak and Milos, 2011) even at single cell level (Hedlund and Deng, 2017). The analysis of massive RNA-seq datasets demands a robust statistical processing, where the number of biological replicates influences the significance of the experiments (Schurch *et al.*, 2016). Normalization of the sequencing results allows quantitative statements, which have the potential to substitute former microarray analysis (Heller, 2002; Dillies *et al.*, 2013). For *C. glutamicum* whole transcriptome analysis was developed previously (Pfeifer-Sancar *et al.*, 2013).

In this thesis, we harness RNA-seq for the analysis of *C. glutamicum*'s transcriptomic response towards various oxygen concentrations (Part III, p. 138). Whole RNA-sequencing was conducted in collaboration with Prof. Dr. J. Kalinowski and Dr. Tobias Busche at the Center for Biotechnology (CeBiTec) at the University of Bielefeld after established protocols (Pfeifer-Sancar *et al.*, 2013).

## 3.13.1. Sample harvest and processing

The biomass was harvested during the triple-phase process at six selected points in time with various oxygen availabilities and growth rates (cf. 4.11, p. 140). The adapted volume to yield around $2 \cdot 10^9$ cells of cell suspension was directly filled into precooled (-21 °C) and manually graded 1.5 mL and 2 mL cups. These were subsequently subjected to a centrifugation in a precooled rotor (-21 °C) at ≥ 13,000 rcf for 30 s (Centrifuge MiniSpin®, rotor F-45-12-11, Eppendorf AG, Hamburg, Germany). The supernatant was discarded and the cell pellets immediately frozen in liquid $N_2$ and stored at -70 °C.

## 3.13.2. RNA isolation, processing and library preparation

RNA-isolation was conducted from three independent experiments of the triple phase

process and six samples each fermentation after the manufacturer's instructions of *RNeasy Mini Kit* (QIAGEN, Hilden, Germany) and DNA depleted via *RNase-Free DNase Set* (QIAGEN, Hilden, Germany). The absence of residual DNA was demonstrated by PCR with the primer pair P1.2/P2 (data not shown). The RNA concentration was determined as described Figure S 20 A (p. 239). For each sampling point of the triple-phase process (Figure 4.12, p. 143) 5 µg RNA was pooled giving a total of 15 µg RNA. Pooling of material is an often-applied strategy to minimize costs for RNA-seq analysis. RNA integrity was then analyzed as shown in Figure S 20 B (p. 239). The rRNA was degraded of 2 µg pooled RNA sample using Ribo-Zero rRNA Removal Kit (Bacteria) (Illumina, Inc., San Diego, USA) and verified as elucidated in Figure S 20 C (p. 239). Finally, the cDNA library was prepared using a TruSeq Stranded mRNA Library Prep Kit (Illumina, Inc., San Diego, USA).

### 3.13.3. cDNA sequencing, data editing and analysis

Sequencing of the cDNA library was achieved with MiSeq and HiSeq systems (Illumina, Inc., San Diego, USA). Sequencing data were processed with the CeBiTec established pipelines including the provided software package (Wibberg *et al.*, 2016), trimming with the tool *Trimmomatic* V0.33 (Bolger *et al.*, 2014) and read mapping with *Bowtie* V2.2.7 (Langmead and Salzberg, 2012). Visualization and differential gene expression calculations were performed with the software *ReadXplorer* (Hilker *et al.*, 2014), applying RPKM (reads per kilobase) and TPM (transcripts per million) normalization. Differentially transcribed genes were given as m-value ($log_2$TPM, $log_2$-fold change). Further analysis was conducted with the spreadsheet software *Excel* (Microsoft Corporation, Redmond, USA). Differential gene expression analysis of reduced data sets such as the pooled samples in this study, often harnesses the null hypothesis and the assumption that the majority of genes are not differentially transcribed. Dramatic transitions in the triple-phase process (cf. 4.11, p. 140; Figure 4.12, p. 143) ranging from exponential growth under aerobic conditions to non-growth anaerobic conditions, however, were expected to affect transcription of many genes (Gerosa *et al.*, 2013). Therefore, we alternatively defined a significance level based on the graph shown in the appendix (Figure S 22, p. 239) at an empirical $log_2$-fold change of $> 1.50$ and $< -1.50$ (corresponding to a fold-change of 2.80 and 0.40, respectively) and an average

value (a-value[3]) > 1.00 to exclude results that are derived from very few reads.

## 3.14. Calculations

### 3.14.1. Growth rates

Unless stated differently growth rates ($\mu$) in $h^{-1}$ were calculated by linear regression in a semi-logarithmic plot of the biomass concentration ($OD_{600}$ or g CDW $L^{-1}$) over the cultivation time. The exponential growth phase was determined by following a coefficient of determination value (R-squared) maximization strategy.

### 3.14.2. Yields

In general, yields were calculated by linear regression in graphs of the biomass or product versus substrate concentration giving the biomass/substrate yield ($Y_{X/S}$) in g CDW per g substrate or the product/substrate yield ($Y_{P/S}$) in mol or C-mol product per mol or C-mol substrate, respectively. In cultivations using PW as substrate supplemented with yeast extract, the apparent biomass/substrate yield ($Y_{X/S}$*) in g CDW per g acetate or acetol was calculated. The $Y_{X/S}$* in these experiments is not a true value because biomass, besides the major carbon source acetate or acetol, is also formed simultaneously from the complex shares within the medium. In mentioned cases, the yields were calculated differentially over the entire production or consumption period.

### 3.14.3. Uptake and production rates

The biomass specific substrate uptake ($q_S$) was calculated using the correlation given in equation 3.3 within the exponential growth phase. Alternatively, the $q_S$ and the biomass specific product formation rate ($q_P$) were calculated differentially for every hour of the cultivation according to equation 3.4 and 3.5, respectively, with the average biomass ($c_X$) in the time frame ($\Delta t$) and the net consumed substrate ($\Delta c_S$) or formed product ($\Delta c_P$). From these differential values the maximal rates $q_S^{max}$ and $q_P^{max}$ are depicted.

[3] Is the average value of the two $log_2$TPM values that were used for m-value calculation.

$$q_S = \frac{\mu}{Y_{X/S}} \quad \left[\frac{mmol}{g_{CDW} \cdot h}\right] \qquad [3.3]$$

$$q_S = \frac{\Delta c_S}{\frac{c_{X_1} + c_{X_2}}{2} \cdot \Delta t} \quad \left[\frac{mmol}{g_{CDW} \cdot h}\right] \qquad [3.4]$$

$$q_P = \frac{\Delta c_P}{\frac{c_{X_1} + c_{X_2}}{2} \cdot \Delta t} \quad \left[\frac{mmol}{g_{CDW} \cdot h}\right] \qquad [3.5]$$

### 3.14.4. Buffer capacity

The buffer capacity (β) of PW (Figure 4.1, p. 107) was calculated according to equation 3.6 by the differential concentrations of the added titration agent KOH ($c_{KOH}$) and the pH change (ΔpH).

$$\beta = \frac{\Delta c_{KOH}}{\Delta pH} \quad [-] \qquad [3.6]$$

### 3.14.5. Total organic carbon

The TOC given in g carbon $L^{-1}$ (C-g $L^{-1}$) was calculated as published previously after equation 3.7 (Buchholz, Graf, Blombach, *et al.*, 2014). Therein, the directly measured TIC is subtracted from the TC giving the TOC (cf. 3.12.7, p. 98).

$$TOC = TC - TIC \quad \left[\frac{C\text{-}g}{L}\right] \qquad [3.7]$$

### 3.14.6. Carbon balance

A carbon balance compares the amount of consumed substrates with the formed products. If all substrates and products are completely analyzed the balance closes and equation 3.8 is true. Such approaches can evaluate microbial process performance and identify unquantified carbon streams (Buchholz, Graf, Blombach, *et al.*, 2014). The carbon was balanced for the triple-phase fermentations using available analyses of substrate (glucose) and products (biomass, lactate, succinate, acetate, $CO_2$) and

considering the fermentation liquid volume ($V_L$ = 10 L). For substrates and products, the net amount of substance (Δn) in mol was recalculated to C-mol ($\Delta n^C$) after equation 3.9 by multiplication with the number of carbon atoms ($N_C$) within the entity. The net produced amount of substance of $CO_2$ was determined via the exhaust gas analysis and the volumetric $CO_2$ evolution rate ($Q_{CO2}$, C-mol $L^{-1}$ $h^{-1}$) after equation 3.10 and summed after equation 3.11. The net produced biomass concentrations were determined by the correlation factor (α) mentioned above (cf. 3.12.2, p. 94; Figure S 2, p. 224) and recalculated with the published percental carbon content of *C. glutamicum* dry biomass of 51.4 % (Buchholz, Graf, Blombach, *et al.*, 2014). The amount of the applied substrate D-glucose as sole carbon source is 100 % and carbon molar fractions of the products were calculated.

$$\sum \Delta n^C_{Substrates} - \sum \Delta n^C_{Products} \overset{!}{=} 0 \qquad [3.8]$$

$$\Delta n^C_{Glc,Lac,Suc,Ac} = \Delta c \cdot V_L \cdot N_C \quad [C\text{-}mol] \qquad [3.9]$$

$$\Delta n^C_{CO_2}(t_{i+1}) = \left( \frac{Q^{i+1}_{CO_2} + Q^{i}_{CO_2}}{2} \right) \cdot V_L \cdot (t_{i+1} - t_i) \quad [C\text{-}mol] \qquad [3.10]$$

$$\Delta n^C_{CO_2} = \sum_{i=0}^{16} \Delta n^C_{CO_2}(t_{i+1}) \quad [C\text{-}mol] \qquad [3.11]$$

### 3.14.7. Venn diagram

RNA-sequencing data were visualized in a three-circle-overlap in the Venn diagram format (Venn, 1880). For this purpose, the software *Venn Diagram Plotter* V2.0[4] written by Littlefield and Monroe for the Department of Energy (PNNL, Richland, WA) was used.

[4] Online available at *https://omics.pnl.gov/software/venn-diagram-plotter*. With respect to this software we appreciate the original funding by the W.R. Wiley Environmental Molecular Science Laboratory, a national scientific user facility sponsored by the U.S. Department of Energy's Office of Biological and Environmental Research and located at PNNL. PNNL is operated by Battelle Memorial Institute for the U.S. Department of Energy under contract DE-AC05-76RL0 1830.

### 3.14.8. Enzyme activity

The volumetric (A) and specific (a) enzyme activity of the G6P-DH and 6PG-DH (cf. 3.12.6, p. 97) was calculated as follows. Equation 3.12 describes the change of extinction (E) in the given timeframe (t). For the blank slope $S_0$ and the reaction slope $S_1$ in $min^{-1}$ this was solved by linear regression. The volumetric activity was determined with equation 3.13 using the assay volume (V = 1 mL), the cuvette diameter (d = 1 cm), the extinction coefficient ($\varepsilon$ = 6,3 $(mM\ cm)^{-1}$), the overall dilution factor (D) and the slopes $S_0$ and $S_1$. The specific activity was finally calculated after equation 3.14 dividing the volumetric activity by the protein concentration (c) of the bacterial lysate, which was determined as described above (cf. 3.12.4, p. 96)

$$S_n = \left[\frac{dE}{dt}\right]_n \quad \left[\frac{1}{min}\right] \qquad [3.12]$$

$$A = \left(S_1 - S_0\right) \cdot \frac{V}{\varepsilon \cdot d} \cdot D \quad \left[\frac{U}{mL}\right] \qquad [3.13]$$

$$a = \frac{A}{c} \quad \left[\frac{U}{mg}\right] \qquad [3.14]$$

### 3.14.9. Intracellular L-glutamate concentration

To recalculate the analyzed L-glutamate concentrations by HPLC within the triple-phase process from samples ①-⑥ (Figure 4.12, p. 143) to intracellular concentrations, the following considerations were followed. First, we recalculated the analyzed concentration to the utilized biomass within the harvested sample (similar batches used as for RNA-sequencing cf. 3.13.1, p. 99) and from lysis dilution (cf. 3.11.2, p. 94). Second, we harnessed the published cell volume to biomass ratio of 1.95 µL per mg CDW (Krömer *et al.*, 2004).

### 3.14.10. Intracellular RNA content

The intracellular total RNA content (Figure 4.19 A2, p. 163) was calculated from samples ①-⑥ within the triple-phase process (Figure 4.12, p. 143) as part of the RNA-sequencing library preparation (cf. 3.13.2, p. 99). Total isolated RNA was analyzed after

primary purification (*RNeasy Mini Kit*, QIAGEN, Hilden, Germany) using a quantification method as stated above (cf. 3.12.3.2, p. 95). Contemplating dilution effects, biomass concentrations used for lysis, the CDW/$OD_{600}$ correlation (cf. 3.12.2, p. 94) and the assumption that 1 $OD_{600}$ corresponds to $10^8$ cells, we could recalculate the available data to the cellular total RNA content in fg per cell.

# CHAPTER 4: RESULTS AND DISCUSSION

## PART I: VALORIZATION OF PYROLYSIS WATER FOR 1,2-PROPANEDIOL PRODUCTION WITH ENGINEERED *C. GLUTAMICUM*

In this part, the biorefinery-side stream pyrolysis water was used as substrate for cultivations of *C. glutamicum* and for 1,2-PDO production with an engineered strain expressing the *E. coli* glycerol dehydrogenase. Bioprocess optimization facilitated a growth coupled biotransformation in an aerobic/microaerobic two-phase process operating at maximal product yield. Ultimately, the eligibility of microorganisms as flexible catalyst towards so far unexploited streams in biorefinery systems operating with pyrolysis of lignocellulose is demonstrated as proof of concept.

## 4.1. Pyrolysis water pretreatment

During the liquefaction of wheat straw in the bioliq® fast pyrolysis process, pyrolysis water (PW) is formed as side product with proportions up to 25 % (w/w) (Dahmen *et al.*, 2016; Pfitzer *et al.*, 2016). So far, no efficient further utilization of PW was proposed for the bioliq® process – a drawback that we challenged by microbial conversion to value-

added products. PW was analyzed with a GC-MS apparatus performed by the Johann Heinrich von Thünen-Institut (Braunschweig, Germany). A list of identified substances is given in the appendix (Table S 21, p. 239 pp.). The analysis demonstrates the remarkable complexity, which on the one side provides *C. glutamicum* with various potential substrates but on the other side challenges the robustness of this industrial workhorse. In-house analysis quantified the major entities acetate and acetol with concentrations of 0.93 ± 0.02 M (~ 21 % of the TOC of the PW) and 0.50 ± 0.02 M (~ 17 % of the TOC), respectively. PW was delivered as stable micro-emulsion of dispersed hydrophobic lignin micelles as well as suspended solid char. Upon direct usage, these would impede general analytic procedures such as photometric $OD_{600}$ or gravimetric CDW measurement in microbial cultures. A pretreatment procedure was thus developed (3.10.1, p. 91 and Figure 3.3, p. 93) with the aim to clarify PW and retain acetate as major carbon source and acetol as precursor for later 1,2-PDO production with engineered strains. The removal or scavenging of substances like methanol, heterocyclic aromatics or furan derivatives capable of negatively influencing cell growth, viability and later product formation was also intended.

Initially, a titration curve of crude PW was recorded (Figure 4.1) and demonstrated a

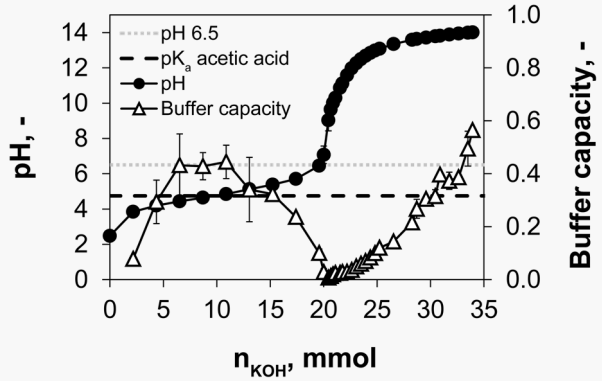


**Figure 4.1. Titration curve of crude pyrolysis water** was recorded by the addition of potassium hydroxide (from a 4.4 M KOH stock solution). The titration curve (black circles) and buffer capacity β (open triangles) are plotted above the added amount of KOH in mmol. Horizontal lines depict the $pK_a$ 4.76 of acetic acid (dashed line, (Serjeant and Dempsey, 1979)) and pH 6.5 (dotted line), which was set for pyrolysis water pretreatment and in the $CGXII_1$ medium for shaking flask cultivations. Error bars show standard deviation (SD) of three independent experiments. Graphic modified from publication (Lange, Müller, *et al.*, 2017).

maximal buffer capacity close to the $pK_a$ (logarithmic acid dissociation constant) of acetic acid. Therefore, acetate is the major buffering entity in PW and predominantly accounts for the low initial pH ~ 2.5. This is in accordance to observations found for bio-oils, where volatile acids were identified as principle cause for 60-70 % of the total acidity (Oasmaa *et al.*, 2010). Upon pH adjustment to 6.5 with potassium hydroxide, a destabilization of the bio-oil micro-emulsion was found presumably due to polarity changes of stabilizing surfactants and a dilution effect (Bridgwater, 2017). The solid and liquid phase were eliminated by centrifugation and filtration, which resulted in a decrease of the TOC by approximately 33 ± 6 % (Figure 4.2). The acetate and acetol concentrations were only slightly reduced by 11 % and 14 %, respectively. During the following heat treatment at 80 °C, volatile substances such as methanol evaporated. A longer heat exposure time (0.5 h, 1 h, 1.5 h) led to a minor decline of acetate (13.3 ± 2.0 %, 11.7 ± 2.2 %, 21.6 ± 2.5 %) but substantial loss of acetol (32.5 ± 4.4 %, 52.2 ± 22.5, 77.7 ± 73.9 %) compared to the initial concentration, respectively (Figure 4.2; Table 4.1; Figure S 9, p. 231). It is known from observations with bio-oils, that the volatile acid content does not change even in long term (24 h) heat treatment at 80 °C but the overall carbonyl content is dramatically reduced (Oasmaa *et al.*, 2010, 2015). This is in accordance to the moderate loss of acetate found during the heat treatment. In general, the products of fast pyrolysis of lignocellulose (bio-oil and aqueous condensates, such as PW) are thermochemically instable even at low temperatures (Oasmaa *et al.*, 1997; Meier and

Faix, 1999). Among the reasons are high oxygen contents, presence of catalysts and the unequilibrated thermochemical state. In contrast to petroleum (Figure 2.3, p. 24; Table S 1, p. 210) with an oxygen content of 0.05-1.5 % (w/w), pyrolysis products such as bio-oil typically contain around 38 % (w/w) (James G. Speight, 1982; Bridgwater, 2017). It is important to consider potassium itself, which was added during pH adjustment, because it is catalytically active and enhances secondary reactions in the PW (Bridgwater, 2017). As consequence, the treatment variability, viscosity and discoloration of PW elevated with prolonged heat exposure time at oxygen excess. The increase in viscosity was most prominent in the 1.5 h heat treated (HT) PW sample and thus restricted further application. Color changes and thickening can be explained by secondary polymerization and Maillard reactions as described for bio-oils. Polymerization, condensation, etherification and esterification reactions can presumably be allocated to the loss of acetol

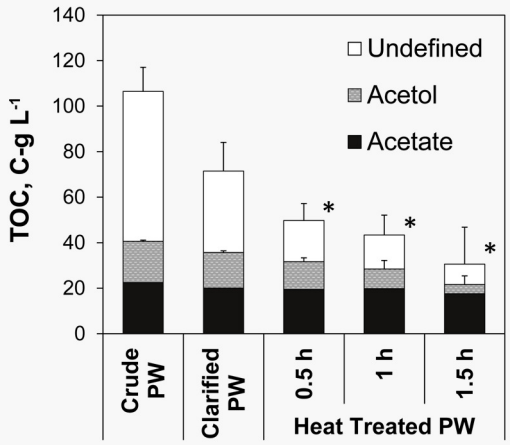


**Figure 4.2. Total organic carbon (TOC) content of pyrolysis water (PW)** as g carbon $L^{-1}$ (C-g $L^{-1}$) in the course of respective pretreatment procedures (from left to right): crude PW; clarified PW (adjustment from pH ~ 2.5 to 6.5, removal of solid and hydrophobic phase); heat treated (HT) PW, 80 °C for 0.5 h, 1 h, and 1.5 h in open vessels. For comparability between the applied procedures, the volume losses during heat treatment were considered and the concentrations of the indicated samples (*) were recalculated with respect to the initial volume (Table 4.1; Figure S 9, p. 231). Error bars show SD of ≥ 4 independent treatments and measurements. Graphic modified from publication (Lange, Müller, *et al.*, 2017).

**Table 4.1. True concentrations of the total organic carbon (TOC), acetate and acetol in pyrolysis water** as either C-g $L^{-1}$ or M. Pretreatment from top to bottom: crude PW; clarified PW (after adjustment from pH ~ 2.5 to 6.5 with 10 mM KOH; solid and hydrophobic phase removal); systematically heat treated (HT) PW, 80 °C for 0.5 h, 1 h, and 1.5 h in open vessels. The undefined amount of organic carbon was determined by the subtraction of the acetate and acetol concentrations from the TOC. The volume loss during heat treatment is not considered here. SD of ≥ 4 independent treatments and measurements. Error for the undefined fraction given relatively to the TOC analysis SD. Table modified from publication (Lange, Müller, *et al.*, 2017).

| Pretreatment | | TOC | Acetate | | Acetol | | Undefined |
|---|---|---|---|---|---|---|---|
| | | C-g $L^{-1}$ | C-g $L^{-1}$ | M | C-g $L^{-1}$ | M | C-g $L^{-1}$ |
| **Crude PW** | | 106 ± 11 | 22 ± 1 | 0.93 ± 0.02 | 18 ± 1 | 0.50 ± 0.02 | 66 ± 7 |
| **Clarified PW** | | 71 ± 13 | 20 ± 1 | 0.83 ± 0.04 | 16 ± 1 | 0.43 ± 0.02 | 36 ± 6 |
| **HT PW** | **0.5 h** | 80 ± 7 | 30 ± 2 | 1.23 ± 0.08 | 18 ± 1 | 0.50 ± 0.02 | 32 ± 3 |
| | **1 h** | 131 ± 27 | 44 ± 11 | 1.84 ± 0.45 | 20 ± 8 | 0.55 ± 0.22 | 67 ± 14 |
| | **1.5 h** | 223 ± 91 | 155 ± 70 | 6.45 ± 2.93 | 24 ± 1 | 0.65 ± 0.02 | 45 ± 18 |

(Diebold, 2000; Oasmaa and Peacocke, 2010; Pfitzer *et al.*, 2016). Performing the heat treatment under oxygen atmosphere progresses thermochemical equilibration of PW and ultimately improves also storing possibilities. In the lab scale pretreatment several consecutive, laborious and energy intensive steps were performed. Such a procedure is not economic in large scale, a problem that could be tackled by adaptation of the fast pyrolysis process itself. The current standard process of the bioliq® plant involves two consecutive condensation steps after fast pyrolysis (Westerhof *et al.*, 2011). Bio-oil is first recovered by cooling the pyrolysis vapors to 80-90 °C and PW in the secondary condensation to ambient temperatures (Dahmen *et al.*, 2016; Pfitzer *et al.*, 2016). The pilot plant, exhibits a high modularity with respect to the condensation processes and allows the implementation of more specific condensation procedures, which in theory could directly yield a fermentable PW fraction. A more specific fractionated condensation could thus prevent extensive pretreatment procedures as developed here.

In summary, we established a pretreatment of the PW including pH adjustment, centrifugation, filtration and heat exposure. The yielded fractions will be assayed for cultivation with *C. glutamicum* in the following section.

# 4.2. Pyrolysis water as substrate for growth

## 4.2.1. The effect of pretreatment and yeast extract supplementation

To integrate fermentation technologies into biorefineries in a meaningful manner, it is important to guarantee fast growth of the bacteria acting as catalyst for product formation. This allows processes with high volumetric productivities. For the first time, we investigated the suitability of PW and pretreated fractions for applicability as substrates for growth of *C. glutamicum* WT. As discussed above, a direct use of PW was not considered due to the inability of standard analytics like turbidity measurements. First experiments using clarified PW with various concentrations revealed, that growth was not significantly promoted unless yeast extract (YE) was supplemented (data not shown). YE was proven to also be essential for heat treated (HT) fractions (Figure 4.3 A, B). In all following cultivations involving PW as substrate, 5 g YE $L^{-1}$ was on this respect supplemented to the medium unless stated differently. Initial screenings revealed that growth in rel. 3.5 % (v/v) HT PW was feasible but highlighted heat treatment as mandatory step.

**Table 4.2. Parameters during shaking flask cultivations of *C. glutamicum* WT using pyrolysis water as substrate**. Growth rate (μ), maximum differential biomass specific substrate uptake rates ($q_S^{max}$) and the apparent biomass substrate yields ($Y_{X/S}$*) in respective shaking flask experiments with 1 h and 1.5 h heat treated (HT) pyrolysis water (PW) containing either 5 g yeast extract (YE) $L^{-1}$ or 1 mM reduced glutathione (GSH) as well as 5 g acetol $L^{-1}$ with 5 g YE $L^{-1}$. Error bars depict the SD of ≥ 3 independent experiments. Table adapted from publication (Lange, Müller, *et al.*, 2017).

| | | 1 h HT PW + YE | 1.5 h HT PW + YE | 1 h HT PW + GSH | Acetol + YE |
|---|---|---|---|---|---|
| μ | $h^{-1}$ | 0.31 ± 0.06 | 0.36 ± 0.04 | 0.18 ± 0.02 | 0.03 ± 0.01 [a] |
| $q_S^{max}$ | $mmol_{acetate}\ g_{CDW}^{-1}\ h^{-1}$ | 10.0 ± 1.2 | 11.1 ± 2.2 | 9.4 ± 0.8 | - |
| | $mmol_{acetol}\ g_{CDW}^{-1}\ h^{-1}$ | 1.3 ± 0.3 | 1.0 ± 0.1 | 1.1 ± 0.2 | 3.6 ± 0.7 |
| $Y_{X/S}$* | $g_{CDW}\ g_{acetate}^{-1}$ | 0.83 ± 0.05 | 0.86 ± 0.08 | 0.44 ± 0.01 | - |
| | $g_{CDW}\ g_{acetol}^{-1}$ | - | - | - | 0.24 ± 0.09 [a] |

[a] calculated for the second growth phase (Figure 4.3 D)

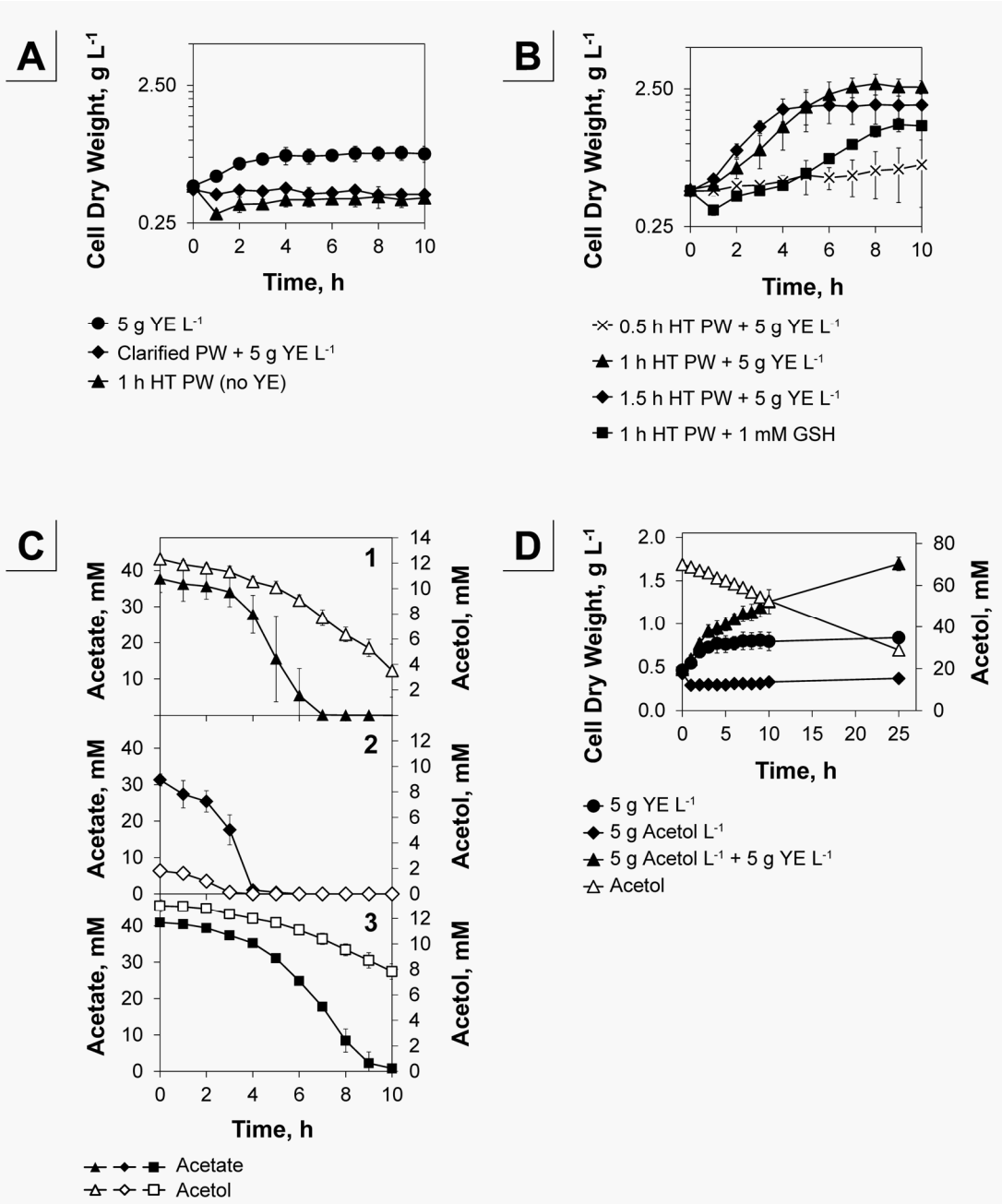


**Figure 4.3. Shaking flask cultivations of *C. glutamicum* WT with pyrolysis water** under various growth conditions in CGXII$_1$ medium (Figure 3.1 A, p. 83). **A**. Reference cultivations with supplementation of 5 g yeast extract (YE) L$^{-1}$ as sole carbon source (circles) as well as experiments with 3.5 % (v/v) and rel. 3.5 % (v/v) pyrolysis water (PW) that was clarified (diamonds) or 1 h heat treated (HT) PW without YE (triangles). **B**. Growth on differently HT PW (0.5 h (crosses), 1 h (triangles), and 1.5 h (diamonds)) as well as 1 h HT PW with 1 mM reduced glutathione (GSH, squares) supplementation. **C**. Course of acetate and acetol concentrations during growth on 1 h HT PW + YE (1), 1.5 h HT PW + YE (2) and 1 h HT PW + GSH (3) corresponding to experiments shown in B. **D**. Investigation of the use of acetol as carbon source. Sole adding of acetol (diamonds) and YE (circles) is shown. The acetol concentration (open triangles) refers to the experiment of acetol and YE supplementation (triangles). Analysis of the culture supernatants was conducted via HPLC (cf. 3.12.5.1, p. 96). Error bars represent the SD of ≥ 3 independent cultivations and measurements. Graphic modified from publication (Lange, Müller, *et al.*, 2017).

An increase of heat treatment at 80 °C from 0.5 h, 1 h to 1.5 h, corroborated cell proliferation with an enhancement of growth rates from 0.03 ± 0.05 $h^{-1}$, 0.31 ± 0.06 $h^{-1}$ to 0.36 ± 0.04 $h^{-1}$, respectively (Figure 4.3 B, Table 4.2). The rates using the latter two substrates are comparable to published cultivations in minimal medium with glucose (0.32 $h^{-1}$ (Buchholz *et al.*, 2013)) and own experiments (Table 4.4, p. 139; Figure 4.10, p. 138) or acetate (0.28 $h^{-1}$ (Wendisch *et al.*, 2000). This highlights the applicability of pretreated pyrolysis water as substrate promoting high growth rates. For 0.5 h HT PW the reproducibility of cultivation was low; where growth was hampered or even absent (Figure 4.3 B). The highest net generated biomass of 2.39 ± 0.37 g $L^{-1}$ was accumulated with the use of 1 h HT PW (reference cultivation on 5 g YE $L^{-1}$ yielded 0.39 ± 0.05 g $L^{-1}$; Figure 4.3 B, Table 4.2). The maximum biomass specific substrate uptake rates ($qs^{max}$) using 1 h HT PW were 10.04 ± 1.25 mmol acetate per g CDW per h and 1.27 ± 0.28 mmol acetol per g CDW per h (Table 4.2). The apparent biomass/acetate yield ($Y^*_{X/S}$) for the 1 h HT PW or 1.5 h HT PW was 0.83 ± 0.05 and 0.86 ± 0.08 g CDW per g acetate (Table 4.2). Compared to the published 0.23 g CDW per g acetate (recalculated from given datac[5]) this indicates an accumulation of biomass from other carbon sources, such as YE or acetol within the PW (Wendisch *et al.*, 2000). For all following cultivations, we used 1 h HT PW as substrate, as it offered robust growth at highest rates, maximal net generated biomass and suitable acetate and acetol availability. Interestingly, we found in experiments using PW (1 h HT PW or 1.5 h HT PW) that *C. glutamicum* is capable of a parallel uptake of acetate and acetol (Figure 4.3 C1, C2). Maximum biomass specific acetate and acetol uptake rates occurred at a ratio of 9 ± 1 to 1 (1 h HT PW) and 12 ± 3 to 1 (1.5 h HT PW) indicating an expected preference for the assimilation of the organic acid (Table 4.2).

In conclusion, a suitable pretreatment procedure of PW was established and promoted proliferation of *C. glutamicum* WT with high rates on the biorefinery side stream. So far, YE, however, remains an obligatory supplement. Growth mainly relies on acetate but *C. glutamicum* was also shown to incorporate acetol into biomass.

[5] Calculated from the published $Y_{X/S}$ = 0.29 $g_{(C\ in\ CDW)}$ per $g_{(C\ in\ acetate)}$ and using the published percental carbon content of *C. glutamicum* dry biomass of 51.4 % (Buchholz, Graf, Blombach, *et al.*, 2014).

### 4.2.2. Acetol as carbon source for *C. glutamicum*

The use of acetol as carbon source was for the first time linked to an acetone metabolization in natural bacterial isolates that may belonged to the group of *Corynebacteriaceae* (Taylor *et al.*, 1980), but remains a yet undescribed behavior for *C. glutamicum* ATCC 13032. To investigate whether *C. glutamicum* can use acetol as sole substrate for growth, experiments with 5 g acetol $L^{-1}$ as sole carbon source were conducted (Figure 4.3 D). The experiments disclosed that growth was only manifested, where YE was provided as parallel supplement and yielded a net biomass of 1.25 ± 0.10 g CDW $L^{-1}$ after 24 h of cultivation. Remarkably, the growth showed a clear biphasic behavior. A primary growth phase with a rate of 0.23 ± 0.02 $h^{-1}$ was succeeded by a growth limited stage at 0.03 ± 0.00 $h^{-1}$. The primary phase duration corresponds well with the growth on YE as sole carbon source ($\mu$ = 0.16 ± 0.03 $h^{-1}$). The beginning of the second growth phase coincides with a cessation of cell division in the YE supplemented reference cultivation (Figure 4.3 A). This indicates, that unexhausted ingredients of the YE are obligatory to maintain growth beyond the primary phase, but cannot account for the increased final biomass concentration. The maximal biomass specific acetol uptake rate was 3.6 ± 0.7 mmol acetol per g CDW per h and thus threefold higher compared to the cultivations using PW as substrate (Table 4.2). At the current standpoint we can hypothesize that acetol metabolization may involve previously described reversible reactions within the methylglyoxal metabolism by channeling carbon into glycolysis to the level of pyruvate (Kalapos, 1999). The reactive aldehyde methylglyoxal was linked to cellular stresses such as free radical generation, reaction with macromolecules, cell death, oxidative stress, arrest of cell division, and others (Cooper, 1984). The hypothesis that acetol is metabolized via methylglyoxal may be corroborated by experiments applying a parallel supply of glucose and acetol (Figure S 10, p. 232). It was shown that after an initial fast growth, cell proliferation was strongly hampered compared to the experiment with glucose as sole carbon source. This may indicate that an intracellular accumulation of acetol-derived toxic metabolites such as methylglyoxal provoke an emerging metabolic inhibition.

For all further experiments, these findings are relevant to be considered, as *C. glutamicum* WT can metabolize and even generate biomass from the substrate acetol, whenever YE is provided.

### 4.2.3. GSH or MSH as potential targets to improve strain robustness

Since YE is an undefined, complex and expensive supplement, investigations of possible substitutions were conducted. It was shown above that biomass accumulation with 1 h HT PW as substrate did not manifest in the absence of YE (Figure 4.3 A, B). Initially, we allocated this effect to a potential intracellular accumulation of methylglyoxal as intermediate of acetol degradation and related toxicity. From literature it is known that the genes *gloA* (glyoxalase I) and *gloB* (glyoxalase II) involve glutathione as cofactor for detoxification of methylglyoxal in *E. coli* (Ferguson *et al.*, 1998; Grabar *et al.*, 2006; O'Young *et al.*, 2007). Therefore, we overexpressed both heterologous genes from *E. coli* under control of the strong promoter ($P_{tuf}$) in a synthetic operon ($P_{tuf}$-*gloAB*-$T_{rrnB}$) on a pJC4-based plasmid (data not shown) and supplemented 1 mM reduced glutathione (GSH, Figure 2.8 A, p. 50). Although the gene expression did not increase overall resistance (data not shown), we found that supplementation of GSH alone could partially substitute YE even in the absence of the glyoxylase system. Indeed, we could promote growth of *C. glutamicum* with parallel consumption of acetate and acetol on 1 h HT PW and 1 mM GSH without YE (Figure 4.3 B, C3). Still, the growth rate was only around 58 % ($0.18 \pm 0.02$ $h^{-1}$) and the net generated biomass 46 % ($1.09 \pm 0.08$ g $L^{-1}$) with respect to the comparable experiment using 1 h HT PW and 5 g YE $L^{-1}$ as supplement. On the other hand, maximum biomass specific substrate uptake rates were within the range of the YE supplemented reference with $9.35 \pm 0.75$ mmol acetate per g CDW per h and $1.13 \pm 0.21$ mmol acetol per g CDW per h (Table 4.2). Nevertheless, the use of acetol as sole carbon source in the presence of GSH was unsuccessful (Figure S 11, p. 232) meaning yet unidentified compounds in the PW or YE substantiate the acetol consumption rates shown above. At the current standpoint, we can speculate that GSH either acts extracellularly or intracellularly. Extracellular action could potentially be explained by cell independent direct reaction of GSH with thiol-reactive electrophiles (e.g. furfural or 5-hydroxymethylfurfural) within the PW (Kim and Hahn, 2013). For intracellular effects, an uptake of GSH by *C. glutamicum* is required. Yet, the bacterium does not naturally produce GSH and relies on the functional analogous agent mycothiol (MSH, Figure 2.8 B, p. 50) and utilization of GSH is not described in literature. A database search (NCBI Resource Coordinators, 2017) for the two GSH synthetizing enzymes γ-glutamylcysteine synthetase (GshA) or glutathione synthetase (GshB) was, as

expected, not positive in the genome of *C. glutamicum*. On the other hand, di-/tripeptide permeases (such as NP_601804 or NP_602246) and a glutathione ABC transporter ATP binding protein (WP_011015118) were identified, which could hypothetically execute GSH uptake. The only described enzyme (γ-glutamyl-transpeptidase, GGT) hydrolyzing the glutamyl-cysteinyl bond in GSH, was also not found. A metabolization therefore is unlikely or involves yet undescribed enzymes (Masip *et al.*, 2006). Interestingly, GSH utilizing enzymes are annotated in the genome of *C. glutamicum*. Among these are for example a putative GSH reductase (accession: CAF20344, with identical sequence to a mycothione reductase (AJE67696)), a glutathione peroxidase (NP_601789) and a glutathione S-transferase (NP_600487). As GSH and MSH utilizing enzymes mostly function analogously, a misleading annotation may also be causative.

Because GSH is an expensive compound, a use for microbial fermentation as supplement is not economic. Therefore, we followed metabolic engineering strategies to produce GSH as well as MSH intracellularly and assay growth on PW in the absence of YE. As low molecular weight thiols interact globally with the host metabolism, a heterologous production of GSH could be an advantage, because native mechanisms in *C. glutamicum* are not or less influenced. On the other hand, no GSH utilizing enzymes are biochemically described in *C. glutamicum*, which speaks in favor of MSH overproduction to exploit the available cellular machinery. For this reason, plasmids were constructed (data not shown), harboring synthetic operons for heterologous expression of *gshAB* from *E. coli* based on an inducible system of pVWEx-1 ($P_{tac}$-*gshAB*-$T_{rrnB}$) and *mshA* (cg0481, mycothiol glycosyl transferase) from *C. glutamicum* as leaderless transcript under control of the constitutive promoter ($P_{dapA\text{-}A16}$) (Vasicová *et al.*, 1999) in the plasmid pJC4 ($P_{dapA\text{-}A16}$-*mshA*-$T_{rrnB}$). Interestingly, construction of *gshAB* expressing plasmids under control of strong $P_{tuf}$ and $P_{dapA\text{-}A16}$ were not successful, which may be due to a intracellular cysteine limitation as described before (Li *et al.*, 1998). Also, *mshA* under control of $P_{tuf}$ could not be cloned highlighting the importance to balance the intracellular levels of low molecular weight thiols. Unfortunately, neither of the manufactured constructs had beneficial effects during cultivations with PW as substrate (data not shown) and the supplementation of YE could not be overcome. Yet, a functional gene expression was not verified and could be target of future research.

In summary, we demonstrated that supplementation of GSH could partially substitute

YE as obligatory supplement during cultivations involving PW. Unfortunately, the metabolic engineering strategies followed here (implementation of GSH dependent detoxification systems (glyoxylase I/II) or production of the low molecular weight thiols GSH and MSH via *gshAB* or *mshA* expression, respectively) could not enhance strain robustness.

## 4.3. 1,2-PDO production with engineered *C. glutamicum*

### 4.3.1. Aerobic 1,2-PDO production with *C. glutamicum* PDO1

We conceived a growth-coupled biotransformation using PW as substrate with acetate as main carbon source for cell proliferation and acetol as direct precursor for 1,2-PDO production. The producer strain *C. glutamicum* PDO1 was constructed harboring the plasmid pJUL*gldA*, which constitutively expresses the *gldA* gene encoding the *E. coli* glycerol dehydrogenase. In **aerobic shaking flask** experiments using 1 h HT PW and 5 g YE $L^{-1}$, a growth rate of 0.23 ± 0.1 $h^{-1}$, a $q_S^{max}$ of 8.8 ± 0.4 mmol acetate per g CDW per h and 1.2 ± 0.1 mmol acetol per g CDW per h was found and 2.6 ± 0.1 mM 1,2-PDO were produced after 6 h of cultivation. After depletion of acetate, the dialcohol was rapidly degraded, whilst the acetol concentration increased *vice versa* (Figure 4.4 A1). This observation is most likely due to a reverse oxidation of 1,2-PDO by the GldA enzyme, which was found previously in *in vitro* assays (Figure 2.9, p. 54) (Tang *et al.*, 1979). A product yield of 0.49 ± 0.01 mol 1,2-PDO per mol acetol indicates, that acetol is in parallel funneled to the central metabolism and used for biomass generation as described for *C. glutamicum* WT above (cf. 4.2.2, p. 114, Figure 4.3 D, p. 112)

To prolong the production phase and enhance the overall titer, we implemented an **aerobic intermittent fed-batch** fermentation with *C. glutamicum* PDO1 (Figure 4.4 A2). 1 h HT PW and YE was fed two times (F1 at 7.3 h, F2 at 10.3 h) after an initial batch phase. This resulted in a final effective concentration up to 8.6 % (v/v) PW. The manual feeding was triggered by a sharp increase of the online DO signal indicating a full consumption of the major carbon source acetate (data not shown). An immediate feeding was necessary to prevent consumption of 1,2-PDO as seen above in shaking flask

cultivations. With increasing PW concentrations, an inhibiting effect was discernible through a stepwise reduction of the growth rate (0.26 ± 0.00, 0.19 ± 0.01, 0.12 ± 0.01 $h^{-1}$) and the apparent biomass substrate yield ($Y_{X/S}$*; 0.72 ± 0.02, 0.67 ± 0.01, 0.59 ± 0.01 g CDW per g acetate) for the batch, F1 and F2 phase, respectively. In accordance, this affected the $q_{acetate}^{max}$ (9.08 ± 0.11, 6.40 ± 0.35, 4.48 ± 0.09 mmol acetate per g CDW per h) and $q_{acetol}^{max}$ (1.36 ± 0.06, 1.23 ± 0.36, 0.37 ± 0.17 mmol acetol per g CDW per h) and the $q_{1,2\text{-}PDO}^{max}$ (0.65 ± 0.20, 0.21 ± 0.04, 0.13 ± 0.01 mmol 1,2-PDO per g CDW per h) in the respective phases. Compared to the shaking flask experiment we could elevate the accumulated biomass to 4.5 ± 0.0 g $L^{-1}$ and the 1,2-PDO titer to 4.7 ± 0.0 mM with an overall differential $Y_{P/S}$ of 0.64 ± 0.03 mol 1,2-PDO per mol acetol after 13 h of cultivation (cf. Figure 4.4 C). The $q_{acetate}^{max}$ surpassed the $q_{acetol}^{max}$ by a ratio of about 6:1, which led to an accumulation of acetol as only 18 % of the total supply was consumed. With respect to the shaking flask experiments, which exhibited ratios of $q_{acetate}^{max}$ to $q_{acetol}^{max}$ with *C. glutamicum* WT of 8:1 and PDO1 of 7:1 (Figure 4.4 D) the bioprocess implementation was beneficial for production.

In summary, aerobic production of 1,2-PDO with *C. glutamicum* PDO1 showed parallel consumption of acetol for biomass formation, product degradation upon acetate depletion and an accumulation of acetol in the fed-batch approach due to a faster $q_{acetate}^{max}$ compared to $q_{acetol}^{max}$. The problem of acetol accumulation was addressed by metabolic and process engineering in the following.

**Figure 4.4. 1,2-PDO production using pyrolysis water** (PW) with *C. glutamicum* PDO1 (**A**; WT + pJUL*gldA*) and *C. glutamicum* PDO2 (**B**; Δ*pqo* Δ*aceE* Δ*ldhA* Δ*mdh* + pJUL*gldA*). Cultivations were performed in shaking flasks (**1**; $CGXII_1$ medium, Figure 3.1 A, p. 83) and bioreactors (**2**; $CGXII_2$ medium, Figure 3.1 C, p. 83) and were supplemented with 1 h HT PW and yeast extract (YE). Depicted are the concentrations of cell dry weight (CDW) in g $L^{-1}$ and acetate, acetol and 1,2-PDO in mM over the process time. PW and YE were fed intermittently after the initial batch phase at indicated points in time in the aerobic fermentation (**A2**; F1, F2) and two-phase aerobic/microaerobic processes (**B2**; F1). A gradually increasing oxygen deprivation is indicated in A2 by a triangle in the feed phase (F1). The product yields ($Y_{P/S}$) are shown in mol 1,2-PDO per mol acetol (**C**) as well as ratios of the maximal acetate and acetol uptake rates (**D**; $q_{acetate}^{max}$, $q_{acetol}^{max}$). Analysis of the culture supernatants was conducted via HPLC (cf. 3.12.5.1, p. 96). Error bars represent SD of triplicate experiments. Graphic modified from publication (Lange, Müller, *et al.*, 2017).

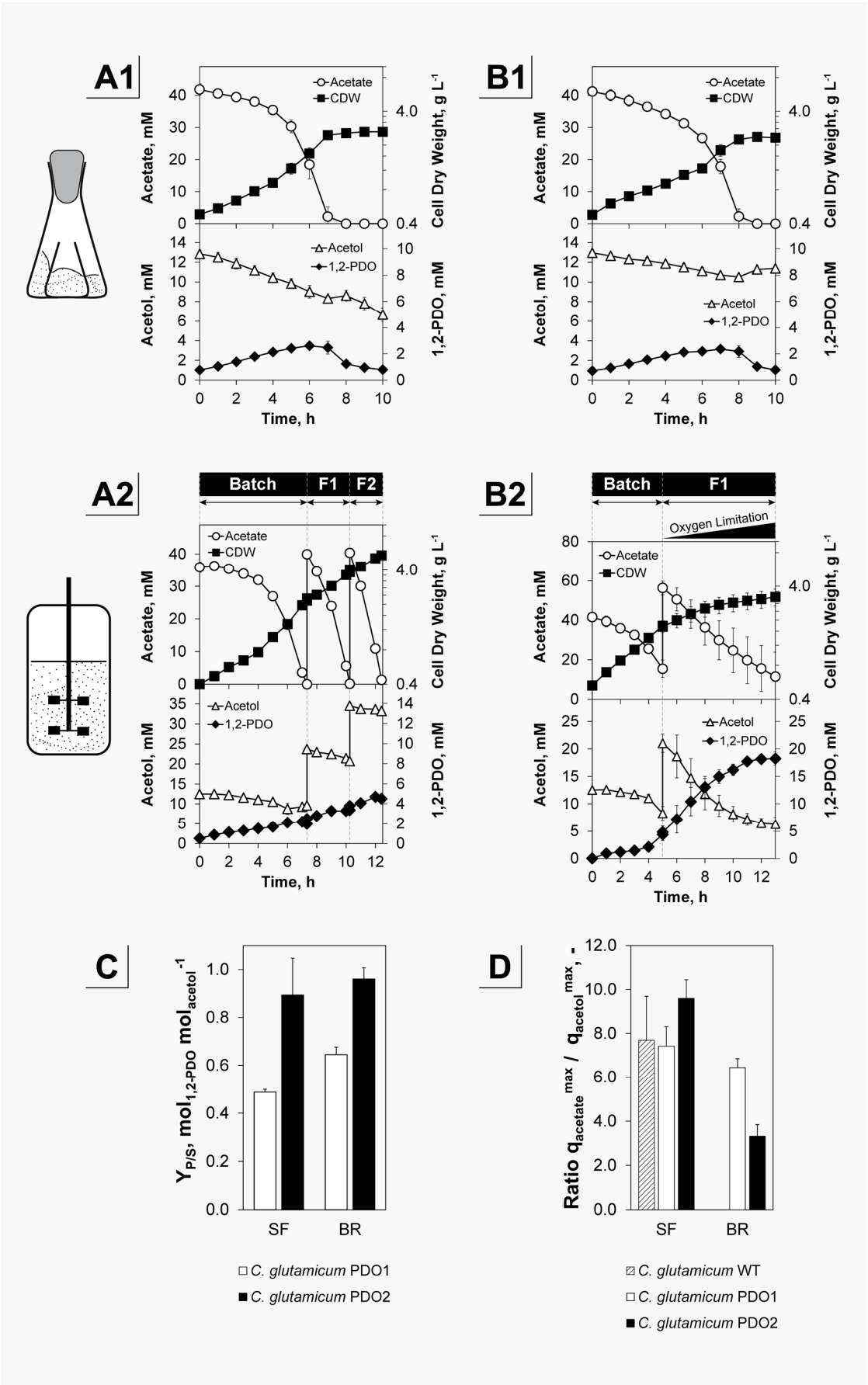
A1
B1
A2
B2
C
D
Acetate
CDW
Acetol
1,2-PDO
Acetate, mM
Cell Dry Weight, g L-1
Acetol, mM
1,2-PDO, mM
Time, h
Batch
F1
F2
Oxygen Limitation
YP/S, molacetol molacetol-1
Ratio qacetatemax / qacetolmax, -
SF
BR
C. glutamicum PDO1
C. glutamicum PDO2
C. glutamicum WT

### 4.3.2. Aerobic and two-phase aerobic/microaerobic 1,2-PDO production with *C. glutamicum* PDO2

An efficient exploitation of PW for growth-coupled production of 1,2-PDO demands a balanced use of acetate and acetol. In an optimal scenario, both consumption rates are identical and depletion of acetate and acetol coincide. As shown in the previous paragraph, in aerobic cultivations with *C. glutamicum* PDO1 this balance was by far not reached. Because the conversion of acetol to 1,2-PDO by the glycerol dehydrogenase involves NADH, a general strategy to improve product formation is the production under oxygen limitation that enhances the cells NADH pool and thus reducing power. For the $NADH/NAD^+$ ratio a drastic increase with decreasing oxygen availability compared to anaerobiosis was shown previously for *C. glutamicum* (Molenaar *et al.*, 2000; Inui, Murakami, *et al.*, 2004) but also for *E. coli* (de Graef *et al.*, 1999). Under oxygen deprived conditions *C. glutamicum* is capable of fermentation and produces lactate, acetate and succinate (Dominguez *et al.*, 1993). To prevent this loss of carbon, we considered *C. glutamicum* Δ*pqo* Δ*aceE* Δ*ldhA* Δ*mdh* (Radoš *et al.*, 2015), which is severely impaired in the capability to secrete these organic acids and equipped it with the plasmid pJUL*gldA*, yielding *C. glutamicum* PDO2. Still, a complete anaerobic scenario is not feasible because growth on acetate relies on oxygen as terminal electron acceptor. The here presented conception involves a microaerobic production stage to limit acetate consumption and thereby enhance NADH availability and product formation.

First, we tested the strain's performance under aerobic conditions in shaking flasks (Figure 4.4 B1). In comparison to the corresponding experiment with *C. glutamicum* PDO1 (Figure 4.4 A1), PDO2 showed a slightly reduced growth rate and $q_{acetate}^{max}$ ($0.23 \pm 0.01$ vs. $0.18 \pm 0.01$ $h^{-1}$, $8.8 \pm 0.4$ vs. $6.2 \pm 0.5$ mmol acetate per g CDW per h) and an about 50 % lowered $q_{acetol}^{max}$ ($1.2 \pm 0.1$ vs. $0.7 \pm 0.0$ mmol acetol per g CDW per h) (Figure 4.4 D, Figure S 12, p. 234). The maximum 1,2-PDO titer was not increased ($2.4 \pm 0.1$ mM) and the $q_{1,2\text{-PDO}}^{max}$ remained similar ($0.6 \pm 0.0$ mmol 1,2-PDO per g CDW per h) to corresponding experiments with *C. glutamicum* PDO1. Surprisingly, the $Y_{P/S}$ was improved by 80 % up to $0.89 \pm 0.15$ mol 1,2-PDO per mol acetol (Figure 4.4 C; Figure S 12, p. 234). This originates in the inability of *C. glutamicum* PDO2 to utilize acetol for biomass formation as seen in the WT (Figure 4.3 D, p. 112). Most likely, this fact can be explained by the deletion of the lactate dehydrogenase, which is under debate

to be involved in the conversion of acetol towards pyruvate (Figure 2.9, p. 54) (Kalapos, 1999). After full consumption of acetate, 1,2-PDO was again rapidly converted to acetol, which this time maintained a constant level, whereas *C. glutamicum* PDO1 continually metabolized acetol in the ongoing experiment (data not shown). Overall, this led to an elevated ratio of the $q_{acetate}^{max}$ to $q_{acetol}^{max}$ up to 10:1 (Figure 4.4 D) because only 20 % of the provided acetol were consumed (48 % with *C. glutamicum* PDO1).

The enhanced yield was a promising prerequisite to develop a two-phase aerobic/microaerobic fermentation process in $CGXII_2$ medium with 1 h HT PW and YE. As mentioned above the oxygen limitation was intended to hamper acetate consumption, elevate NADH availability and thus enhance acetol conversion to 1,2-PDO. During the process an aerobic phase was followed by a feed phase (F1 starting at 5 h), where a reduced aeration rate gradually increased oxygen limitation. This escalated in a steadily reducing growth rate and biomass specific acetate uptake (Figure 4.4 B2). As expected, the fermentation's by-products lactate and succinate were below detection limit (< 0.4 mM). This most likely enhanced NADH availability and the GldA catalyzed reduction of acetol. In the F1 phase the $q_S^{max}$ were 3.6 ± 0.9 mmol acetate per g CDW per h and 2.0 ± 0.3 mmol acetol per g CDW per h, respectively and thus converged to a ratio of 2:1 (Figure 4.4 D). Overall this resulted in a significantly improved consumption of 75 % of the provided acetol. Acetol was efficiently converted to 1,2-PDO close to the theoretical maximum with a $Y_{P/S}$ of 0.96 ± 0.05 mol 1,2-PDO per mol acetol. Considering the overall total organic carbon content of the provided 1 h HT PW within the process, the $Y_{P/S}$ was 0.11 ± 0.03 C-mol 1,2-PDO per C-mol pretreated PW. A final titer of 18.3 ± 1.2 mM 1,2-PDO was reached. In comparison to literature, this process exhibited the highest overall differential volumetric productivity (1.4 ± 0.1 mmol 1,2-PDO $L^{-1}$ $h^{-1}$) for a production of 1,2-PDO with an engineered producer strain (considering the entire processes including the period of biomass formation and production). The process parameters are compared in Table 2.1 (p. 45) to prominent published microbial production processes, and compiled in Figure S 12 (p. 234).

In summary, we engineered *C. glutamicum* for enhanced 1,2-PDO production and disrupted the ability to funnel acetol to the central metabolism. The product yield and titers were thus notably improved. Additionally, an aerobic/microaerobic production scenario proved to be valuable in balancing acetate and acetol uptake rates and ultimately

revealed the highest volumetric 1,2-PDO productivities employing an engineered strain.

## 4.4. Conclusion

This part of the thesis presented the access to a value chain connecting a newly accessed biorefinery side stream derived of pyrolytic decomposition of lignocellulosic biomass with microbial 1,2-PDO production. As an example, the aqueous condensate – pyrolysis water – was shown to be a possible substrate for *C. glutamicum* following a pretreatment procedure. As proof of concept, a 1,2-PDO producer strain was engineered, that uses the main carbon contents (acetate and acetol) of pyrolysis water in a growth-coupled biotransformation. Acetate is therein accepted as major substrate for growth and acetol reduced to 1,2-PDO by a heterologously expressed glycerol dehydrogenase of *E. coli*. *C. glutamicum* WT assimilated both substrates to the central metabolism presumably to the level of pyruvate. This fans out the thinkable product spectrum based on pyrolysis water in future biorefinery strategies with engineered derivatives and novel bioprocesses.

# PART II: HARNESSING NOVEL CHROMOSOMAL INTEGRATION LOCI TO UTILIZE A HEMICELLULOSE FRACTION FOR ISOBUTANOL PRODUCTION WITH ENGINEERED *C. GLUTAMICUM*

This part of the thesis describes the identification of novel chromosomal loci termed CgLPs for integration of genetic information, the broadening of the substrate spectrum of *C. glutamicum* towards the pentoses L-arabinose and D-xylose in the strain CArXy and finally the exemplarily production of isobutanol as biofuel based on the organosolv-derived hemicellulose fraction with CIsArXy.

## 4.5. Identification of CgLPs

Metabolic engineering of bacteria is a strategy to tailor industrial workhorses for an enhancement of substrate uptake, product spectra or other purposes. In contrast to plasmid-based systems the chromosome offers a more stable and robust basis for the introduction of genetic information and spares the necessity to use selection markers like antibiotics. Although the tools for genetic engineering of industrial microbial strains such as *C. glutamicum* are available in abundance (Pátek and Nesvera, 2013; Suzuki and Inui, 2013) and facilitate a fast and exact targeting of genes or synthetic operons to the integration site, the sites themselves represent a current bottleneck. The exploration of suitable loci that provide a general integration platform and minimize effects on the native genetic integrity is a crucial prerequisite to fully exploit bacteria's biotechnological

potential.

In the here presented approach, current knowledge about prophage regions (Kalinowski, 2005), non-essential gene clusters (Unthan, Baumgart, *et al.*, 2014) and transcription units (Pfeifer-Sancar *et al.*, 2013) was gathered in a systematic approach to identify novel integration loci termed ***Corynebacterium glutamicum*** **landing pads (CgLPs)**. The guidelines for the site identification were conceptualized as follows. First, the three prophage regions of *C. glutamicum* [CGP1 (cg1507-cg1524), CGP2 (cg1746-cg1752), and CGP3 (cg1890-cg2071)] were not considered for CgLPs (Kalinowski, 2005). Although they were shown to be non-essential under standard laboratory conditions (Baumgart *et al.*, 2013), their overall function including complex regulatory phenomena, spontaneous excision and induction of the largest prophage region CGP3 is to date not clarified in depth and thus a genetic stability is not guaranteed (Frunzke *et al.*, 2008; Nanda *et al.*, 2014; Pfeifer *et al.*, 2016). Second, we contemplated the non-essential

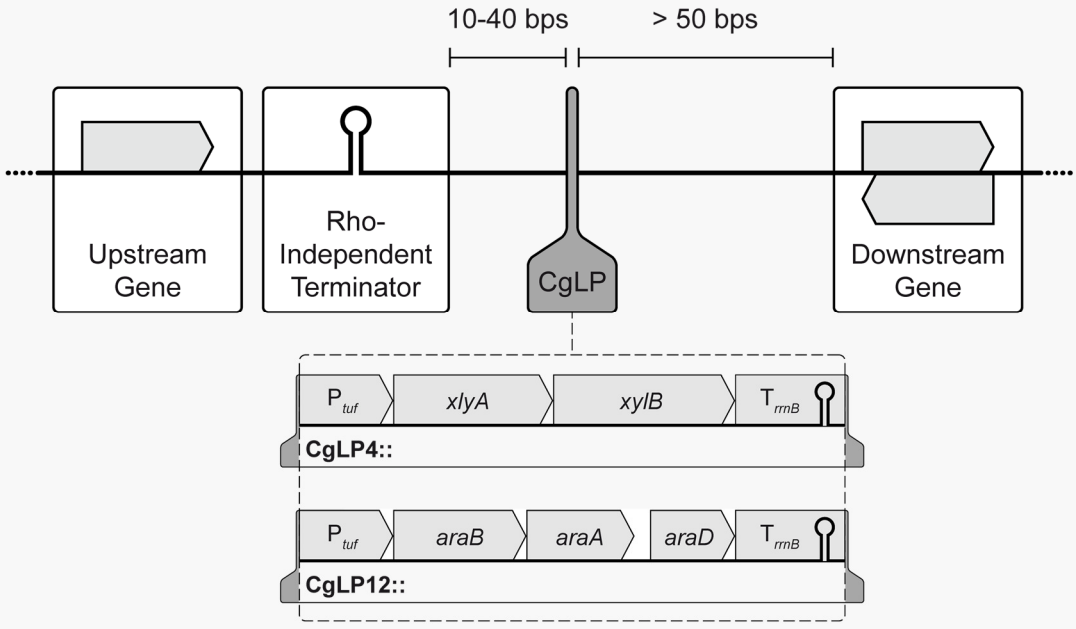


**Figure 4.5. Schematic chromosomal location of *C. glutamicum* landing pads** (CgLPs) for chromosomal integration of genetic information. In the strain CArXy, synthetic operons $P_{tuf}$-*xylAB*-$T_{rrnB}$ and $P_{tuf}$-*araBAD*-$T_{rrnB}$ for D-xylose and L-arabinose metabolization were inserted exemplarily into CgLP4 and CgLP12, respectively. $P_{tuf}$: promoter of the *C. glutamicum* elongation factor EF-TU; $T_{rrnB}$: terminator of the *E. coli rrnB* operon; *xylAB*: encoding XylA (xylose isomerase) of *Xanthomonas campestris* and XylB (xylulokinase) of *C. glutamicum*; *araBAD*: encoding AraB (L-ribulokinase), AraA (L-arabinose isomerase) and AraD (L-ribulose-5-phosphate 4-epimerase) of *E. coli*. Arrows indicate gene direction. Graphic modified from publication (Lange, J., Müller, F., *et al.*, 2018).

chromosomal sections of the published list of deletable regions (Unthan, Baumgart, *et al.*, 2014). These provide ideal regions for the integration of genetic information and restrict the probability of lethal effects that arise from disruption essential genetic structures and obligatory cellular functions. At last these regions were analyzed for suitable CgLPs with respect to knowledge about transcription start sites, operon structures and Rho-

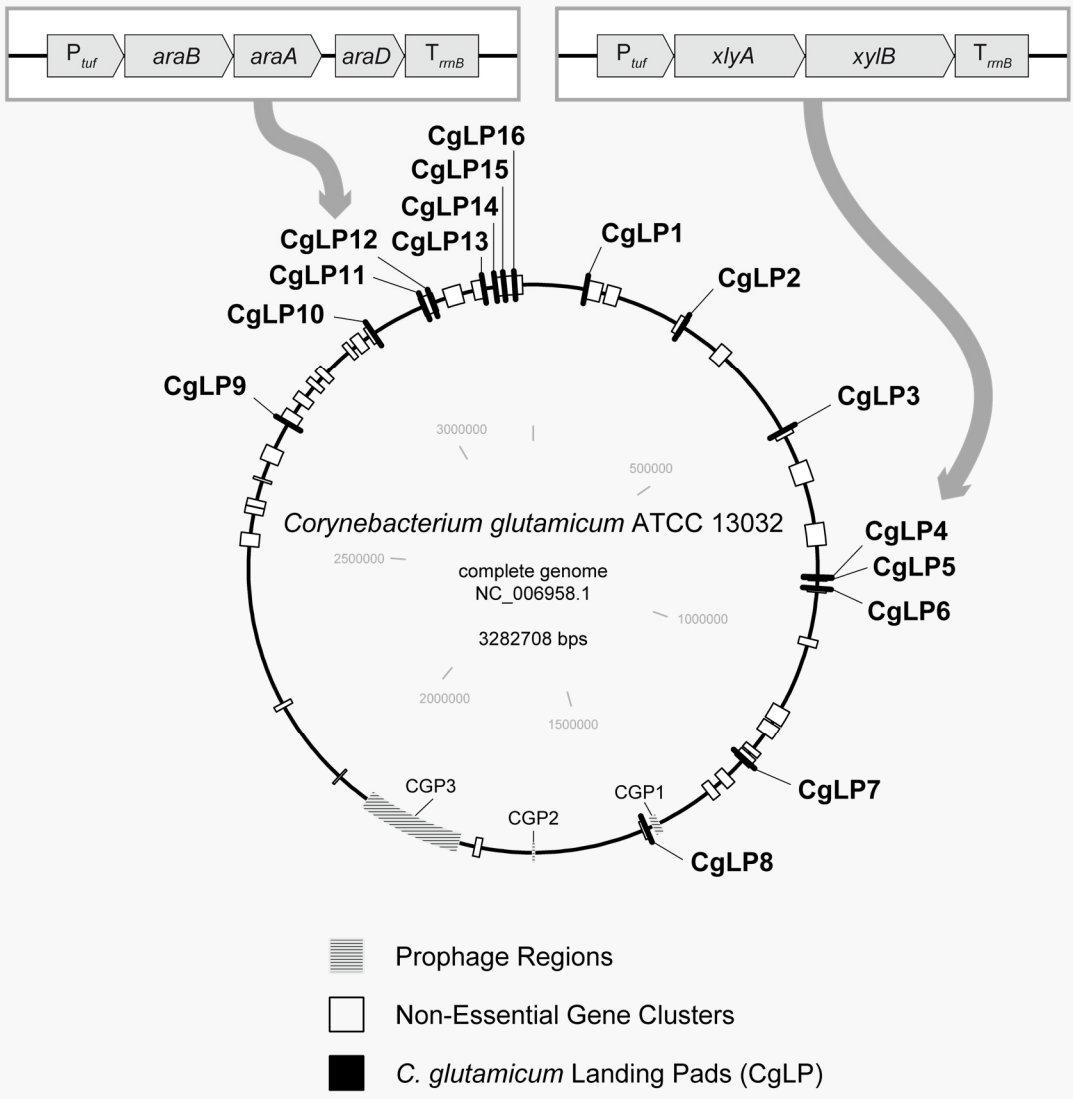


**Figure 4.6. Newly proposed *C. glutamicum* landing pads** (black, CgLPs) located in the genome of *C. glutamicum* ATCC 13032 (NCBI reference sequence NC_006958.1). Exact position of each CgLP is given in Table 4.3. Additionally, prophage regions of *C. glutamicum* (Kalinowski, 2005) [CGP1 (cg1507-cg1524), CGP2 (cg1746-cg1752), and CGP3 (cg1890-cg2071); shaded grey] and non-essential gene clusters (Unthan, Baumgart, *et al.*, 2014) (open box) are depicted. For D-xylose and L-arabinose metabolization the synthetic operons $P_{tuf}$-*xylAB*-$T_{rrnB}$ and $P_{tuf}$-*araBAD*-$T_{rrnB}$ were integrated into the CgLP4 and CgLP12 as indicated, respectively. Graphic modified from publication (Lange, J., Müller, F., *et al.*, 2018).

independent termination sites (Pfeifer-Sancar *et al.*, 2013). Following this strategy, 16 CgLPs were compiled and provide sweet spots for integration of genetic information (Table 4.3; Figure 4.5; Figure 4.6). In theory, these sites pose a minimal influence on the cells native genetic repertoire.

In general, all proposed CgLPs are positioned after a Rho-independent terminator of the upstream gene with a distance of 10-40 bps (Figure 4.5). They are followed by a stop or start codon depending on the direction of the downstream gene at > 50 bps spacing. Terminators of upstream genes outside but directly adjacent to the non-essential gene cluster were included in the search. The two cases of a sense and reverse downstream gene must be considered separately. Where upstream and downstream gene direction are identical, knowledge about promoters and transcription start sites of the downstream genes were considered. For CgLP7 and CgLP15 the promoters of the downstream genes were previously predicted (Pfeifer-Sancar *et al.*, 2013) and the selected integration site do not interfere with transcription initiation. For other sense transcribed downstream genes promoter location is not yet known. With respect to opposing upstream and downstream genes the terminator usage was considered. Occasionally, up- and downstream genes harness the same terminator or overlap with the promoter or open reading frame and were, in this respect, excluded. For other downstream genes, termination remains unknown. As a general prerequisite, integration of synthetic gene constructs should provide a strong termination site. The tightly delimited transcription unit should therefore minimize downstream effects.

**Table 4.3. Compilation of *C. glutamicum* landing pads (CgLPs)** for chromosomal integration of additional genetic information. Highlighted in bold are CgLP4 and CgLP12, which were used in the strain CArXy for integration of synthetic operons for D-xylose and L-arabinose metabolization, respectively. Table modified from publication (Lange, J., Müller, F., *et al.*, 2018)

| *C. glutamicum* Landing Pad | Base position [a] | Adjacence [b] | Spacer [c] | Upstream | | Downstream | | Experimental verification |
|---|---|---|---|---|---|---|---|---|
| | | | | Gene [d] | COG [i] | Gene/operon [e] | COG [i] | |
| CgLP1 | 97220 | ◁ ≀ ∩ ◀ | 20 | cg0121 | G | cg0120 | R | - |
| CgLP2 | 287966 | ▶ ∩ ≀ ◁ | 20 | cg0327 | S | cg0328 | S | - |
| CgLP3 [f] | 558101 | ▶ ∩ ≀ ◁ | 40 | cg0634 (*rplO*) [g] | J | cg0635 | - | - |
| **CgLP4** | **836158** | ▶ ∩ ≀ ▷ | **10** | **cg0901** | **-** | **cg0902** | **-** | ***xylAB*** |
| CgLP5 | 837445 | ▶ ∩ ≀ ▷ | 20 | cg0903 | - | cg0904 | - | - |
| CgLP6 [f] | 857008 | ▶ ∩ ≀ ▷ | 20 | cg0928 [g] | E | *rrnB* | | - |
| CgLP7 | 1205320 | ◁ ≀ ∩ ◀ | 20 | cg1302 | K | cg1301 (*cydA*) | C | - |
| CgLP8 | 1427460 | ▶ ∩ ≀ ▷ | 40 | cg1538 (*coaE*) [g] | H | cg1540 | - | - |
| CgLP9 | 2741407 | ▶ ∩ ≀ ◁ | 40 | cg2880 | E | cg2883 | Q | - |
| CgLP10 [f] | 2971748 | ◁ ≀ ∩ ◀ | 40 | cg3112 (*cysZ*) [g] | R | cg3111 | - | - |
| CgLP11 | 3077633 | ▶ ∩ ≀ ▷ | 10 | cg3212 | S | cg3213 | - | yes [h] |
| **CgLP12** | **3094266** | ▶ ∩ ≀ ▷ | **20** | **cg3227 (*lldD*)** | **C** | **cg3228** | **-** | ***araBAD*** |
| CgLP13 | 3191992 | ▶ ∩ ≀ ▷ | 10 | cg3344 | C | cg3345 | - | yes [h] |
| CgLP14 [f] | 3213531 | ▷ ≀ ∩ ◀ | 10 | cg3365 (*rmpC*) | S | cg3364 (*trpA*) [g] | E | - |
| CgLP15 | 3229705 | ◁ ≀ ∩ ◀ | 10 | cg3385 (*rhcD2*) | C | cg3384 | Q | - |
| CgLP16 | 3248838 | ◁ ≀ ∩ ◀ | 40 | cg3397 | - | cg3396 | O | - |

[a] referring to the *C. glutamicum* ATCC 13032 complete genome NCBI reference sequence: NC_006958.1

[b] ≀ = CgLP; ∩ = Terminator loop; ◀, ▶ = upstream gene; ◁, ▷ = downstream gene; arrowheads indicate gene direction

[c] spacer between the predicted end of terminator site (Pfeifer-Sancar *et al.*, 2013) and the CgLP position

[d] delivers the terminator site

[e] in succession of the CgLP

[f] directly adjacent to the non-essential gene cluster [outside location: CgLP3 (80 bps), CgLP6 (39 bps), CgLP10 (342 bps), CgLP14 (123 bps)]

[g] gene outside (up- or downstream) the non-essential gene cluster (Unthan, Baumgart, *et al.*, 2014); downstream gene is located inside the non-essential gene cluster

[h] were used in our labs and are evidentially feasible (data not shown)

[i] Clusters of Orthologous Groups of proteins (Tatusov *et al.*, 2000). For each protein the major COG category is given for *C. glutamicum* (Meyer *et al.*, 2003). INFORMATION STORAGE AND PROCESSING: J = Translation, ribosomal structure and biogenesis; A = RNA processing and modification; K = Transcription; L = Replication, recombination and repair; B = Chromatin structure and dynamics. CELLULAR PROCESSES AND SIGNALING: D = Cell cycle control, cell division, chromosome partitioning; Y = Nuclear structure; V = Defense mechanisms; T = Signal transduction mechanisms; M = Cell wall / membrane / envelope biogenesis; N = Cell motility; Z = Cytoskeleton; W = Extracellular structures; U = Intracellular trafficking, secretion, and vesicular transport; O = Posttranslational modification, protein turnover, chaperones. METABOLISM: C = Energy production and conversion; G = Carbohydrate transport and metabolism; E = Amino acid transport and metabolism; F = Nucleotide transport and metabolism; H = Coenzyme transport and metabolism; I = Lipid transport and metabolism; P = Inorganic ion transport and metabolism; Q = Secondary metabolites biosynthesis, transport and catabolism. POORLY CHARACTERIZED: R = General function prediction only; S = Function unknown. No Category: -

In the presented study, two of the novel integration loci CgLP4 and CgLP12 were exemplarily used to engineer *C. glutamicum* for D-xylose and L-arabinose metabolization, respectively (Figure 4.5; Table 4.3). Two additional landing pads (CgLP11, CgLP13) were harnessed in our labs and proved functionality (data not shown). None of the engineered strains exhibited distinguishable abnormality of the native phenotype under standard laboratory conditions by such penetrations. This demonstrates the suitability of the newly proposed landing pads as methodological platform for future metabolic engineering of *C. glutamicum*.

## 4.6. L-Arabinose and D-xylose metabolization in CArXy

An efficient valorization of renewable resources such as wood demands meaningful applications for hemicelluloses besides more established utilization of cellulose and lignin. Therefore, we intended to equip *C. glutamicum* with genetic information for the metabolization of the pentoses L-arabinose and D-xylose – major compounds of hemicellulose – harnessing the novel CgLPs. As basic strain *C. glutamicum* Δ*aceE* Δ*pqo* Δ*ilvE* Δ*ldhA* Δ*mdh* was chosen, which was originally cloned as platform for anaerobic isobutanol production development (Blombach *et al.*, 2011). The strain carries deletions of the E1p subunit of the pyruvate dehydrogenase complex (PDHC; encoded by *aceE*), the pyruvate:quinone oxidoreductase (Pqo), transaminase B (IlvE), the lactate dehydrogenase (LdhA), and the malate dehydrogenase (Mdh). The necessity to supplement acetate to cultivations with PDHC-deficient strains (Blombach, Arndt, *et al.*, 2009) was circumvented by restoration of the *aceE* gene via pJUL*aceE* giving *C. glutamicum* Δ*pqo* Δ*ilvE* Δ*ldhA* Δ*mdh* (cf. 3.9.2, p. 88). For pentose metabolization, two synthetic operons were created introducing XylA (xylose isomerase, *Xanthomonas campestris*) and XylB (xylulokinase, *C. glutamicum*) and AraB (L-ribulokinase), AraA (L-arabinose isomerase) and AraD (L-ribulose-5-phosphate 4-epimerase) of *E. coli* into CgLP4 and CgLP12, respectively (Figure 4.5, Figure 4.9). The obtained the strain CArXy (*C. glutamicum* Δ*pqo* Δ*ilvE* Δ*ldhA* Δ*mdh* CgLP12::($P_{tuf}$-*araBAD*-$T_{rrnB}$)

CgLP4::($P_{tuf}$-*xylAB*-$T_{rrnB}$)) was first cultivated in minimal medium on D-glucose, L-arabinose and D-xylose to verify functionality of the pathways (Figure 4.7 A). On D-glucose the growth rate reached 0.39 ± 0.03 $h^{-1}$ with a biomass substrate yield ($Y_{X/S}$) of 0.52 ± 0.02 g CDW per g D-glucose and a biomass specific substrate uptake rate ($q_S$) of 4.18 ± 0.16 mmol D-glucose per g CDW per h. The parameters are highly comparable to published WT data (Buchholz, Graf, Freund, *et al.*, 2014) and thus confirm that gene integration into CgLP4 and CgLP12 did not negatively influence the strains vitality under these conditions. Also, the wild typical growth phenotype confirms the functional restoration of the E1p subunit of the PDHC via pJUL*aceE*. CArXy proliferated on L-arabinose and D-xylose with growth rates of 0.16 ± 0.01 $h^{-1}$ and 0.18 ± 0.02 $h^{-1}$, respectively (Figure 4.7 B, C). This verifies a functional expression of the *araBAD* and *xylAB* genes. The growth rate on D-xylose with pEKEx3-*xylAB* was published as 0.20 ± 0.01 $h^{-1}$ with 100 mM substrate (Meiswinkel *et al.*, 2013), which is comparable to the here presented strain with chromosomal gene integration. Unfortunately, uptake rates of the pentoses were rather low as only 14 ± 4 % of L-arabinose and 78 ± 7 % of D-xylose were metabolized in the overall experiment. Poor uptake can be explained with a relatively high Monod constant for L-arabinose of 120 mM that was published for the pVWEx1-*araBAD* plasmid system (Schneider *et al.*, 2011). This issue could be mitigated before by providing an L-arabinose transporter protein AraE from *C. glutamicum* ATCC 31831, which was shown to benefit L-arabinose but also D-xylose uptake (Sasaki *et al.*, 2009). As expected from literature data (Kawaguchi *et al.*, 2008; Radek *et al.*, 2014) the combined supplementation of 25 mM D-glucose, L-arabinose and D-xylose exhibited a clear preference for the hexose (Figure 4.7 D). Similarly, engineered strains show contradicting results in literature concerning sequential consumption behavior under aerobic conditions. Whereas some studies could not find a preference for glucose over the pentoses (Kawaguchi *et al.*, 2009; Gopinath *et al.*, 2011; Radek *et al.*, 2016), a clear sequential consumption is seen in most studies (Kawaguchi *et al.*, 2006, 2008, Sasaki *et al.*, 2009, 2010; Kim *et al.*, 2010; Buschke *et al.*, 2011; Kang *et al.*, 2014; Radek *et al.*, 2014; Wang *et al.*, 2014). It is known that the *Weimberg* pathway, which was established in *C. glutamicum* previously, is an attractive alternative to prevent diauxic growth behaviors on D-glucose and D-xylose (Radek *et al.*, 2014, 2016). Interestingly, the transporter AraE could also eradicate a sugar uptake preference; an effect that was most

prominent under oxygen deprived conditions (Sasaki *et al.*, 2009). Compared to the experiments using D-glucose as sole carbon source the overall net generated biomass could be doubled. A full consumption of D-xylose and 80 % of L-arabinose were achieved in the given timespan (Figure 4.7 D).

In summary, we could demonstrate that CArXy functionally expresses genes for L-arabinose and D-xylose metabolization by the synthetic operons, which were integrated into two of the novel CgLPs. This genetic tailoring did not negatively influence the bacterium's viability and it was capable of biomass formation with preferential consumption of D-glucose before L-arabinose and D-xylose.

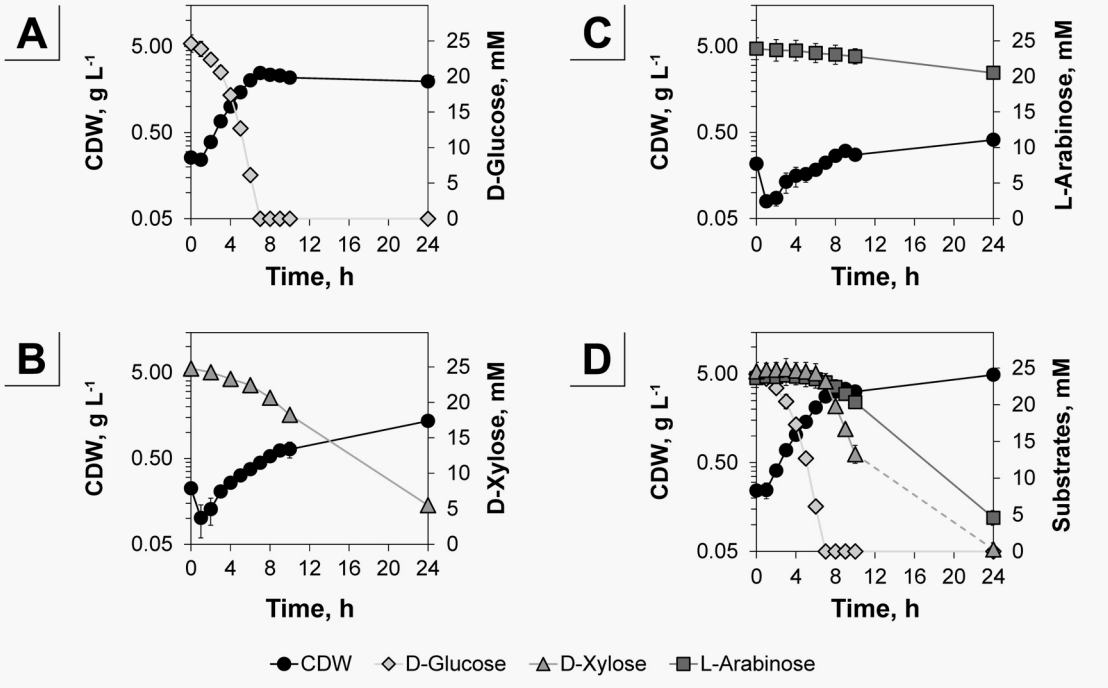


**Figure 4.7. Shaking flask cultivations of the strain CArXy in defined medium** (Figure 3.1 A, p. 83). CArXy (*C. glutamicum* Δ*pqo* Δ*ilvE* Δ*ldhA* Δ*mdh* CgLP4::($P_{tuf}$-*xylAB*-$T_{rrnB}$) CgLP12::($P_{tuf}$-*araBAD*-$T_{rrnB}$)) was grown in $CGXII_S$ (+ 2 mM Val, Leu and Ile) with either combined or single supplementation of 25 mM D-glucose, D-xylose and L-arabinose. Bacterial growth (cell dry weight, CDW) and substrate consumption is depicted over time. Analysis of the culture supernatants was conducted via HPLC (cf. 3.12.5.1, p. 96). Error bars represent the SD of three independent experiments. Graphic modified from publication (Lange, J., Müller, F., *et al.*, 2018).

# 4.7. Aerobic growth on the hemicellulose fraction

In the previous paragraph the performance of CArXy was tested in minimal medium supplemented with single or mixed sugars as substrate. Here, this strain was cultivated on various concentrations of hemicellulose fraction (HF; Figure 4.8 A, B), which originates in beech wood organosolv processing (cf. 2.5.3, p. 28). The substance comprises sugars (monomers such as D-xylose, L-arabinose or D-glucose and oligomeric forms), weak acids (mainly acetate), furan derivatives, phenolic residues and other extractives (Zhao *et al.*, 2009). A short pretreatment procedure of the renewable side stream is described above (cf. 3.10.2, p. 92). Initial experiments revealed that growth was not sustained directly (Figure S 13, p. 234) and only manifested after supplementation of 5 g YE $L^{-1}$, analogously to previous findings with pyrolysis water (cf. 4.2.1, p. 111; Figure 4.3 A, p. 112). The growth rates with sole 5 g YE $L^{-1}$ (control experiment) and supplementation of 9.7 g HF $L^{-1}$, 19.3 g HF $L^{-1}$ and 38.7 g HF $L^{-1}$ were $0.14 \pm 0.03$, $0.34 \pm 0.02$, $0.33 \pm 0.01$ and $0.17 \pm 0.02$ $h^{-1}$ and corresponding maximal net generated biomasses of $0.29 \pm 0.06$, $1.02 \pm 0.15$, $1.50 \pm 0.11$ and $2.19 \pm 0.41$ g CDW $L^{-1}$, respectively. Surprisingly, we found under aerobic conditions a consumption carbon sources with preference of acetate over the L-arabinose and D-xylose (Figure 4.8 B; Figure S 14, p. 235). An arrest of the exponential growth phase coincided with the depletion of acetate. Biomass accumulation thus mainly relied on the organic acid and not the pentoses for the given time frame. Still, L-arabinose and D-xylose were slowly metabolized in the ongoing experiment. The growth rates in the exponential phase were comparable to 0.28 $h^{-1}$, which was previously published for *C. glutamicum* in minimal medium cultivations with acetate as sole carbon source (Wendisch *et al.*, 2000).

The shown experiments represent the first example for the utilization of beech wood organosolv processing derived hemicellulose fraction with *C. glutamicum*. The previously demonstrated high resistance towards typical lignocellulose derived inhibitors (Sakai *et al.*, 2007) was beneficial for proliferation and demonstrates the strain's robustness.

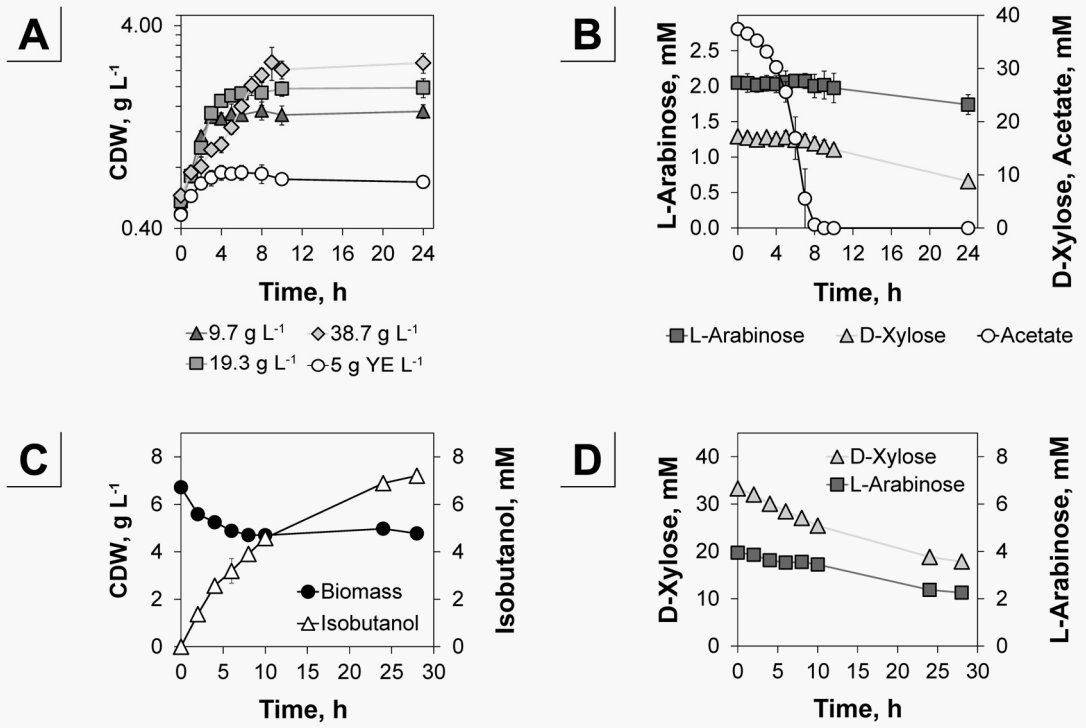


**Figure 4.8. Cultivation and isobutanol production using the hemicellulose fraction**. Aerobic cultivation (A, B) of the strain **CArXy** (*C. glutamicum* Δ*pqo* Δ*ilvE* Δ*ldhA* Δ*mdh* CgLP4::($P_{tuf}$-*xylAB*-$T_{rrnB}$) CgLP12::($P_{tuf}$-*araBAD*-$T_{rrnB}$)) and anaerobic isobutanol production (C, D) with **CIsArXy** (CArXy harboring pJC4*ilvBNCD-pntAB* and pBB1*kivd-adhA*). **A**. CArXy was cultivated in $CGXII_S$ (+ 2 mM Val, Leu and Ile) minimal medium supplemented with 5 g YE $L^{-1}$ as reference (open circles) and variable concentrations of the hemicellulose fraction (HF) [9.7 g HF $L^{-1}$ (triangles), 19.3 g HF $L^{-1}$ (squares) and 38.7 g HF $L^{-1}$ (diamonds)] + 5 g YE $L^{-1}$ (Figure 3.1 A, p. 83). **B**. Consumption of acetate (circles), D-xylose (triangles) and L-arabinose (squares) is depicted for the respective experiment using 38.7 g HF $L^{-1}$ (A). **C**. Two-stage isobutanol production (anaerobic stage shown) was realized with the strain CIsArXy using 77.3 g HF $L^{-1}$ + 5 g YE $L^{-1}$ ($CGXII_S$ + 2 mM Val, Leu and Ile + 50 µg Kan $mL^{-1}$ + 6 µg Cm $mL^{-1}$), Figure 3.1 B, p. 83). **D**. Metabolization of D-xylose and L-arabinose during the incubation is shown. The delineation of acetate throughout the experiment is depicted in Figure S 16 (p. 237). Analysis of the culture supernatants was conducted via HPLC (cf. 3.12.5.1, p. 96). Error bars represent SD of three independent experiments. Graphic modified from publication (Lange, J., Müller, F., *et al.*, 2018).

## 4.8. Two-stage isobutanol production

So far, we could verify that CArXy can proliferate under aerobic conditions on L-arabinose and D-xylose in defined medium as well as on the complex substrate hemicellulose fraction. To close the chain from substrate to product, we intended to produce the exemplary biofuel isobutanol based on HF. Therefore, we created the strain

CIsArXy (CArXy harboring the plasmids pJC4*ilvBNCD-pntAB* and pBB1*kivd-adhA*) according to previous studies (Figure 4.9) (Blombach *et al.*, 2011). The implemented isobutanol synthesis pathway (cf. 2.8.2, p. 47) harnesses the native L-valine biosynthesis but branches at the level of 2-ketoisovalerate by introduction of the enzyme KIVD (2-ketoacid decarboxylase from *Lactococcus lactis*) catalyzing the synthesis of isobutyraldehyde. Subsequently, AdhA (alcohol dehydrogenase from *C. glutamicum*) forms the product isobutanol in a single reductive step, which can diffuse through the cell envelope. Typical processes for fermentative production of low energy demanding products such as acids and alcohols are frequently performed under anaerobic conditions (Lange, Takors, *et al.*, 2017). As *C. glutamicum* is unable to proliferate significantly under oxygen deprivation in standard conditions (Michel *et al.*, 2015), growth arrested zero-growth approaches with high cell densities are commonly applied (Lange, Takors, *et al.*, 2017). This inherits the additional advantage that non-growing bacteria exhibit an enhanced resistance towards cellular stress stimuli and lignocellulose-derived inhibitors (e.g. Sakai *et al.*, 2007). The conceived process of this study is a typical example for a lab-scale two-stage approach (Lange, Takors, *et al.*, 2017), where an aerobic stage is implemented to enable biomass formation under maximal growth conditions, which is followed by an anaerobic production stage at high cell densities under growth arrest (Figure 4.8; Figure S 15, p. 236; Figure 3.1 B, p. 83). Most advanced production conditions were identified using 77.3 g HF $L^{-1}$ with densely packed cells at 6.72 ± 0.14 g CDW $L^{-1}$ initial biomass concentration (Figure S 15, p. 236). It has been described that engineered *C. glutamicum* is capable of growth and organic acid production using L-arabinose (Kawaguchi *et al.*, 2008) and D-xylose as substrate (Kawaguchi *et al.*, 2006) under oxygen deprivation. In both studies a preference of glucose towards the respective pentose was seen under aerobic conditions. Later, this issue could be overcome by the introduction of the L-arabinose transporter protein AraE as discussed above (Sasaki *et al.*, 2009, 2010). In an adaptive mutant of *C. glutamicum* R this sequential uptake was not seen (Sasaki *et al.*, 2008). We found in the here presented experiment, a parallel metabolization of L-arabinose and D-xylose under strict anaerobic conditions (Figure 4.8 D). As expected, a production of lactate and succinate did not occur (< 0.4 mM) due to the strain's genetic background (Blombach *et al.*, 2011). Acetate was not consumed nor produced due to the oxygen limitation (Figure S 16, p. 237). Of the

total supply, 1.7 ± 0.0 mM (43 ± 1 %) and 15.5 ± 0.6 mM (46 ± 1 %) of L-arabinose and D-xylose were metabolized, respectively. After 28 h of production a maximum titer of 7.2 ± 0.2 mM isobutanol was analyzed with a carbon molar $Y_{P/S}$ of 0.31 ± 0.02 C-mol isobutanol C-mol substrate (L-arabinose + D-xylose)$^{-1}$ with respect to the pentoses. Most prominent examples of isobutanol production in literature reached 0.51 C-mol C-mol$^{-1}$ (equals 0.77 mol mol$^{-1}$) (Blombach *et al.*, 2011) and 0.52 C-mol C-mol$^{-1}$ (equals 0.78 mol mol$^{-1}$) (Yamamoto *et al.*, 2013) in engineered *C. glutamicum* or 0.57 C-mol C-mol$^{-1}$ (equals 0.85 mol mol$^{-1}$) (Atsumi *et al.*, 2008) in engineered *E. coli*. The mentioned studies are impressive examples of metabolic engineering, where the $Y_{P/S}$ could be approximated close to the anaerobic theoretical maximum of 0.66 C-mol C-mol$^{-1}$ (equals 1.00 mol mol$^{-1}$) (Bastian *et al.*, 2011). A summary of the yields of prominent producers in comparison to in this study achieved yield is given in Table 2.2 (p. 48). Isobutanol production based on L-arabinose and D-xylose within the difficult-to-access HF has not been demonstrated before. Therefore, these proof of concept experiments represent a promising example, in particular considering the $Y_{P/S}$, for the valorization of HF within a novel value chain. Under anaerobic production conditions CIsArXy could not metabolize acetate, which is a major compound of the HF. As a future perspective, a dual-phase process is therefore reasonable, where an aerobic growth phase allowing the formation of biomass on mainly acetate is directly followed by an anaerobic isobutanol production phase on the remaining pentoses (Blombach *et al.*, 2011; Lange, Takors, *et al.*, 2017).

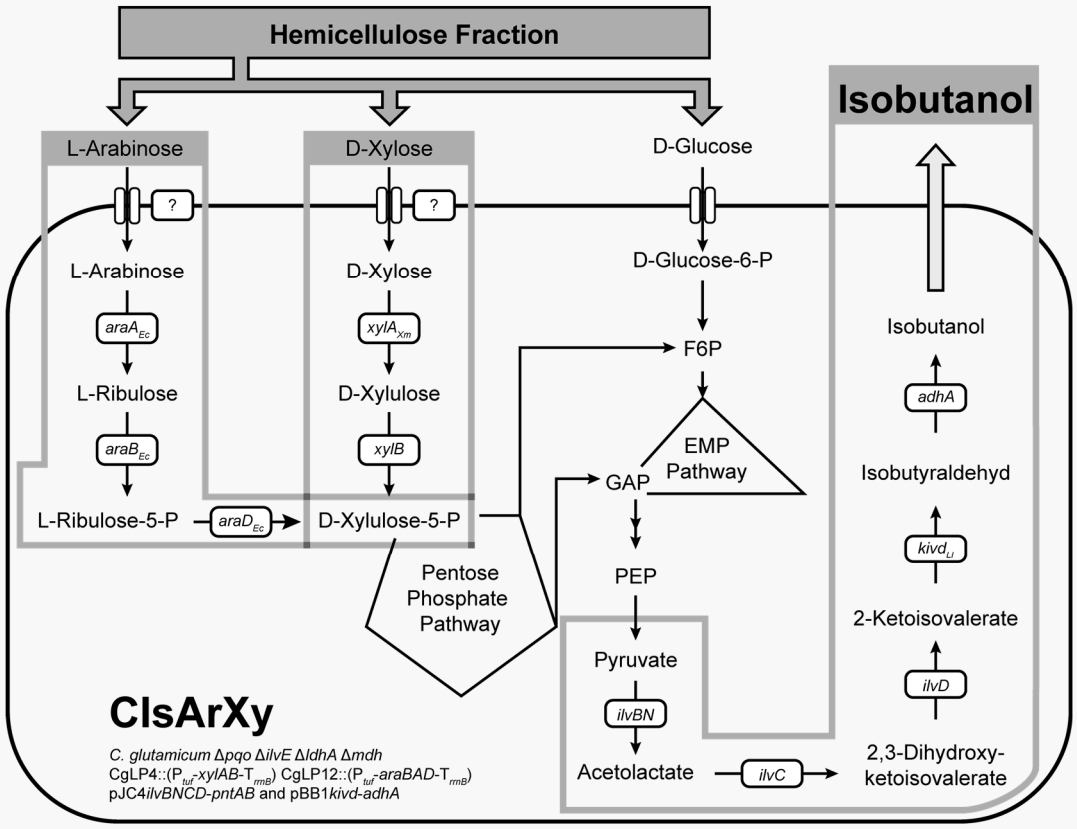


**Figure 4.9. Metabolic pathway engineering for Isobutanol production based on pentoses in ClsArXy**. The strain provides heterologous pathways for L-arabinose and D-xylose metabolization via the genetically introduced synthetic operons $P_{tuf}$-*araBAD*-$T_{rrnB}$ and $P_{tuf}$-*xylAB*-$T_{rrnB}$ in the CgLP4 and CgLP12, respectively. The genes encode as follows: *araB* (L-ribulokinase), *araA* (L-arabinose isomerase) and *araD* (L-ribulose-5-phosphate 4-epimerase) of *E. coli* ($_{Ec}$); *xylA* (xylose isomerase) of *Xanthomonas campestris* ($_{Xm}$) and *xylB* (xylulokinase) of *C. glutamicum* (Schneider *et al.*, 2011; Meiswinkel *et al.*, 2013). Uptake systems are not clarified but may involve the D-glucose PTS system or other low affinity transporters . Additionally, for anaerobic isobutanol production ClsArXy harbors two plasmids pJC4*ilvBNCD-pntAB* and pBB1*kivd-adhA* expressing genes with respective proteins in parenthesis: *kivd* (2-ketoacid decarboxylase) of *Lactococcus lactis* ($_{LI}$); *adhA* (alcohol dehydrogenase), *ilvBN* (acetohydroxyacid synthase), *ilvC* (acetohydroxyacid isomeroreductase), *ilvD* (dihydroxyacid dehydratase) of *C. glutamicum* and *pntAB* (membrane bound transhydrogenase) of *E. coli*. F6P, fructose-6-phosphate; GAP, glyceraldehyde-3-phosphate; PEP, phosphoenol pyruvate; EMP, Embden-Meyerhof-Parnas pathway.

## 4.9. Conclusion

In the presented study, a systematic approach for the identification of novel

loci – termed *C. glutamicum* landing pads (CgLPs) – is described, that provide a sound basis for the chromosomal integration of genetic information. These loci could in future be exploited by the *C. glutamicum* community for metabolic engineering. The general systematic approach for identification of the loci could be even projected to other organisms. As a proof of concept, two of the proposed CgLPs were harnessed for the integration of synthetic operons that enable a metabolization of L-arabinose and D-xylose in the engineered strain CArXy. This strain was used for cultivation on a hemicellulose fraction, a yet unexploited biorefinery side stream, which arises from beech wood organosolv processing. Due to the complex nature of the hemicellulose fraction a direct application for example in chemical synthesis is not feasible and would demand laborious and expensive purification steps. Here, we present a straightforward valorization of the substrate by industrial biotechnology. It was demonstrated that the cell proliferation was promoted in minimal medium supplemented with yeast extract and without effortful pretreatment of the hemicellulose fraction. Encouraged by these experiments, a two-stage production scenario was conceived, where the CArXy-derivative isobutanol producer strain CIsArXy, was first grown aerobically on glucose and a subsequent production stage realized with hemicellulose fraction as substrate under anaerobic conditions. For the first time, we could facilitate isobutanol production based on pentoses in *C. glutamicum*. The carbon molar product yields were in the range of prominent literature examples using glucose as sole carbon source.

Overall, the work demonstrates the suitability to microbially convert complex side streams to valuable products. Such scenarios could in future be integrated into biorefinery approaches and drive their overall efficiency and profitability.

# PART III: SYSTEMIC DECIPHERMENT OF *C. GLUTAMICUM*'S RESPONSE TO SELF-ENFORCING OXYGEN DEPRIVATION

In the last part of the *results and discussion* section, the systemic investigation of *C. glutamicum*'s adaptation to a gradual shift from aerobiosis to anaerobiosis, highlights microaerobiosis as distinct transition point with remarkable physiology. This statement was corroborated with RNA-sequencing, metabolite and enzyme activity analysis. The essence of this part was published (Lange, J., Münch, E., *et al.*, 2018).

# 4.10. Reference aerobic/microaerobic cultivations

Blombach *et al.* observed that the shaking flask environment, in two-stage isobutanol production scenarios, had a beneficial effect on the product yields and production performance compared to rapid transition to anaerobiosis in dual-phase fermentations (Blombach *et al.*, 2011). Based on this original observation, we intended to conceive a defined bioprocess delineating a gradual transition from aerobiosis via microaerobiosis to anaerobiosis. As a first developing step we compared microaerobic 30 L batch fermentations to shaking flask cultivations. For a detailed description of the cultivation

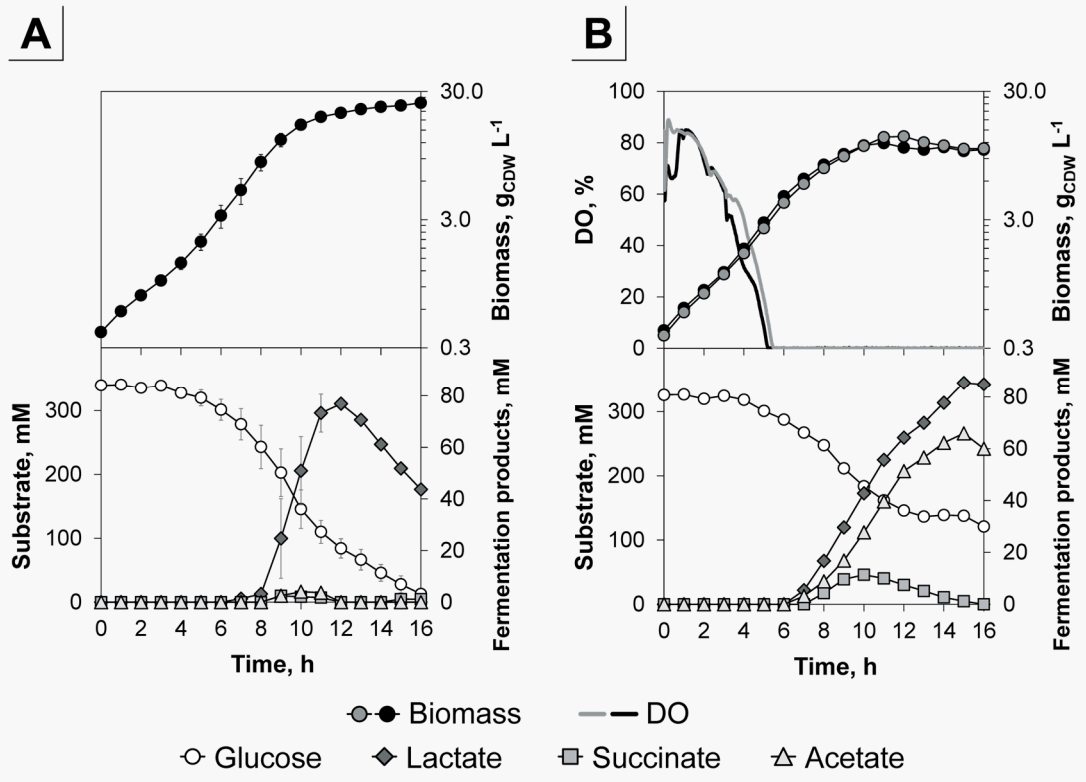


**Figure 4.10. Reference aerobic/microaerobic cultivations** of *C. glutamicum* WT. Cultivations were performed in $CGXII_{S+PCA}$ + 60 g glucose $L^{-1}$. **A**. The experiment was conducted with 50 mL medium in baffled 500 mL shaking flasks following the same seed train as bioreactor cultivations (Figure 3.1 D, p. 83). **B**. 30 L bioreactor cultivation in 10 L minimal medium with constant agitation (445 rpm) and gassing (0.1 vvm). Two representative experiments are shown, one of which (grey) was analyzed via HPLC as depicted. The pH was not controlled (Figure S 17 A, B, p. 237). Analysis of the culture supernatants was conducted for the substrate (glucose) and the fermentation products (lactate, succinate, acetate) via HPLC (cf. 3.12.5.1, p. 96). Error bars in A represent the SD of five independent experiments. The figure A was analogously published (Lange, J., Münch, E., *et al.*, 2018).

**Table 4.4. Comparison of aerobic/microaerobic shaking flask and bioreactor cultivations** of *C. glutamicum* WT. Cultivations were performed in $CGXII_{S+PCA}$ + 60 g glucose $L^{-1}$ as substrate. SD given for shaking flasks calculated from five independent experiments. Average values of two independent cultivations are given for the bioreactor. Analysis of lactate, succinate and acetate conducted for only one bioreactor cultivation.

| | | | Shaking flask | Bioreactor |
|---|---|---|---|---|
| Max. concentrations | Biomass | g $L^{-1}$ | 24.5 ± 0.8 | 12.5 |
| | Lactate | mM | 76.9 ± 0.9 | 85.6 |
| | Succinate | mM | 2.4 ± 0.0 | 11.4 |
| | Acetate | mM | 4.1 ± 0.6 | 65.9 |
| | μ | $h^{-1}$ | 0.39 ± 0.01 | 0.38 |
| | $Y_{X/S}$ | $g_{CDW}$ $g_{Glc}^{-1}$ | 0.42 ± 0.01 | 0.42 |
| DO = 0 % | Time | h | - | 5.4 |
| Initiation of lactate production | Time | h | 7 ± 0 | 7 |
| | Biomass | g $L^{-1}$ | 5.1 ± 1.2 | 6.0 |

conditions see paragraphs 3.2.8 (p. 81) and 3.2.5 (p. 79), respectively. The experiments serve as reference to the later developed triple-phase process (cf. 4.11, p. 140) and give answers to how comparable the two systems are with respect to oxygen supply. Shaking flask reference cultivations were conducted in the identical seed train as bioreactor experiments (Figure 3.1 D, p. 83). Similarities of both systems can be found in the exponential phase for example in the average growth rates or biomass yields of 0.39 ± 0.01 and 0.38 $h^{-1}$ or 0.42 ± 0.01 and 0.42 g CDW per g glucose for shaking flasks and bioreactor experiments, respectively. A high initial glucose concentration of 60 g $L^{-1}$ provoked an oxygen limitation in the progression of the experiment due to the accumulating biomass. For the shaking flask as well as the bioreactor experiment we found an initiation of lactate production as major fermentation product in accordance to literature (Dominguez *et al.*, 1993) at 7 h of cultivation (Figure 4.10 A, B; Table 4.4). In shaking flasks, lactate concentration peaked earlier with 76.9 ± 0.9 mM and was successively consumed, whereas in the bioreactor a later maximum of 85.6 mM was found but consumption did not progress. While succinate and acetate were analyzed at low levels in shaking flasks, significant amounts were formed in the bioreactor with maximum titers of 11.4 mM and 65.9 mM, respectively (Table 4.4). Interestingly, the reduction of the DO to 0 % did not coincide with the occurrence of fermentation products. This highlights that this online signal does not adequately describe the initiation of

microaerobiosis. The fermentative phenotype is a response to the limiting terminal electron acceptor oxygen in the respiratory chain. To maximize energy conservation *C. glutamicum* can trigger fermentative pathways in parallel to respiration and scavenges NADH not being oxidizable via the respiratory chain. Contemplating this physiological background, we define microaerobic conditions by the first occurrence of lactate in the culture supernatant. A full consumption of glucose was achieved in shaking flasks but not in the bioreactor. Apart from the oxygen limitation, glucose consumption and biomass formation decrease in the bioreactor presumably because of the low pH value, which did not re-increase by acid metabolization in contrast to the shaking flask experiment (Figure S 17, p. 237).

In summary, these observations indicate a stronger oxygen limitation in the bioreactor compared to shaking flasks in the progressing experiment. Concerning the development of the triple-phase experiment, we verified that initial conditions are highly comparable to shaking flask phenomena.

## 4.11. The triple-phase batch fermentation

The aerobic/microaerobic reference cultivation served as basis for the developed triple-phase process. Here, aerobic, microaerobic and anaerobic phases were installed as successive transition (Figure 4.12). The initiation of strict anaerobic conditions was realized by a stop of aeration and flushing of the headspace with $N_2$ as shown in Figure S 18 (p. 238). In the aerobic, microaerobic and anaerobic phase a stepwise reduction of the growth rate[6] (see also Figure 4.19 A1, p. 163) from $0.40 \pm 0.01$, $0.21 \pm 0.00$ to $0.09 \pm 0.01$ $h^{-1}$ and the biomass/substrate yield ($Y_{X/S}$) of $0.52 \pm 0.04$, $0.29 \pm 0.02$ and $0.16 \pm 0.01$ g CDW per g glucose was found, respectively. It is known from previous work that growth under anaerobic conditions is marginally supported in the absence of nitrate as terminal electron acceptor (Nishimura *et al.*, 2007; Michel *et al.*, 2015). As found above (cf. 4.10, p. 138), the DO of 0 % does not per se indicate the initiation of microaerobiosis on a physiological basis. The microaerobic phase was again defined by

[6] As the growth behavior in the microaerobic and anaerobic phase is not exponential, the average differential rate is given until full consumption of glucose.

**Table 4.5. Secondary parameters characterizing the triple-phase process**. Errors represent the SD of four independent experiments.

| Phase | μ, $h^{-1}$ | $Y_{X/S}$, mol $mol^{-1}$ | $Y_{P/S}$, mol $mol^{-1}$ | | |
|---|---|---|---|---|---|
| | | | Lactate | Succinate | Acetate |
| **aerobic** [a] | 0.40 ± 0.01 | 0.52 ± 0.04 | 0.03 ± 0.01 | 0.00 ± 0.00 | 0.00 ± 0.00 |
| **microaerobic** [a] | 0.21 ± 0.00 [b] | 0.29 ± 0.02 | 0.49 ± 0.03 | 0.22 ± 0.02 | 0.31 ± 0.01 |
| **anaerobic** [a] | 0.09 ± 0.01 [b] | 0.16 ± 0.01 | 1.39 ± 0.05 | 0.37 ± 0.01 | 0.13 ± 0.02 |

[a] physiological and technic states: aerobiosis (0-6 h), microaerobiosis (6-11 h), anaerobiosis (11-16 h)

[b] given as average differential rate

the first occurrence of fermentative side products after 6 h of cultivation. Although oxygen deprivation steadily tightens within the microaerobic phase, a rather constant product/substrate yield ($Y_{P/S}$) of the fermentation products with 0.49 ± 0.03, 0.22 ± 0.02 or 0.31 ± 0.01 mol lactate, succinate or acetate per mol glucose was found, respectively (Figure 4.12). The successive anaerobic phase is clearly distinguishable from microaerobiosis by a change in the respective $Y_{P/S}$ to 1.39 ± 0.05, 0.37 ± 0.01 or 0.13 ± 0.02 mol lactate, succinate or acetate per mol glucose. A preference for the production of acetate over succinate under microaerobiosis enabling further generation of one ATP and *vice versa* behavior under anaerobiosis was described previously (Shinfuku *et al.*, 2009; Kaboré *et al.*, 2016). Given values are summarized in Table 4.5 and an additional graphic of the differential biomass specific substrate uptake and product formation rates given in the appendix (Figure S 19, p. 239). For the fermentative metabolism with the products lactate, succinate and acetate a totalized $Y_{P/S}$ was calculated for the respective microaerobic and anaerobic phase with 1.02 ± 0.07 and 1.90 ± 0.08 mol fermentation products per mol glucose. In the anaerobic phase this is close to the maximum theoretical yield of 2 mol per mol (Yamamoto *et al.*, 2011). A carbon balance (Figure 4.11) was calculated comparing the entirely analyzed products (biomass, lactate, succinate, acetate and $CO_2$) with respect to the supplied carbon source (glucose). It was resolved that under aerobic and microaerobic cultivation conditions $CO_2$ is saturated in the medium accordingly to published studies (Buchholz, Graf, Blombach, *et al.*, 2014) and subsequently consumed again in the anaerobic phase for succinate production. It is with this consideration that the carbon balance fully closes over the entire cultivation period

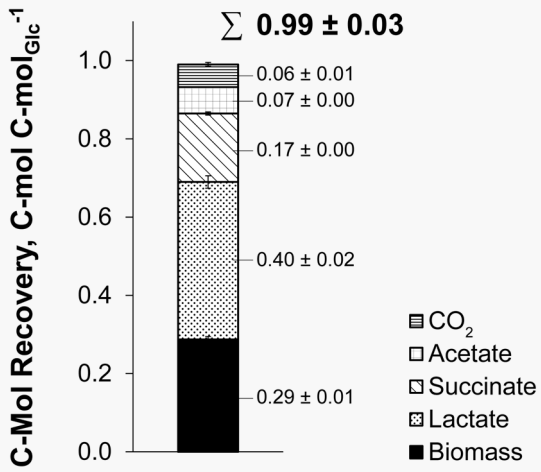


**Figure 4.11. Carbon balance of the triple-phase process**. Analyzed products (biomass, lactate, succinate, acetate and $CO_2$) were balanced with respect to the sole substrate (glucose) over the entire cultivation period of 0-16 h (Figure 4.12, p. 143). Error bars represent the SD of four independent experiments. Graphic was analogously published (Lange, J., Münch, E., *et al.*, 2018).

to 0.99 ± 0.03 C-mol per C-mol glucose and no significant carbon is lost during aerated phases.

In summary, the triple phase process shows distinct physiological characteristics in the aerobic, microaerobic and anaerobic phase. Thus, it represents an ideal platform for further investigations using RNA-sequencing analysis to investigate the global transcriptional response.

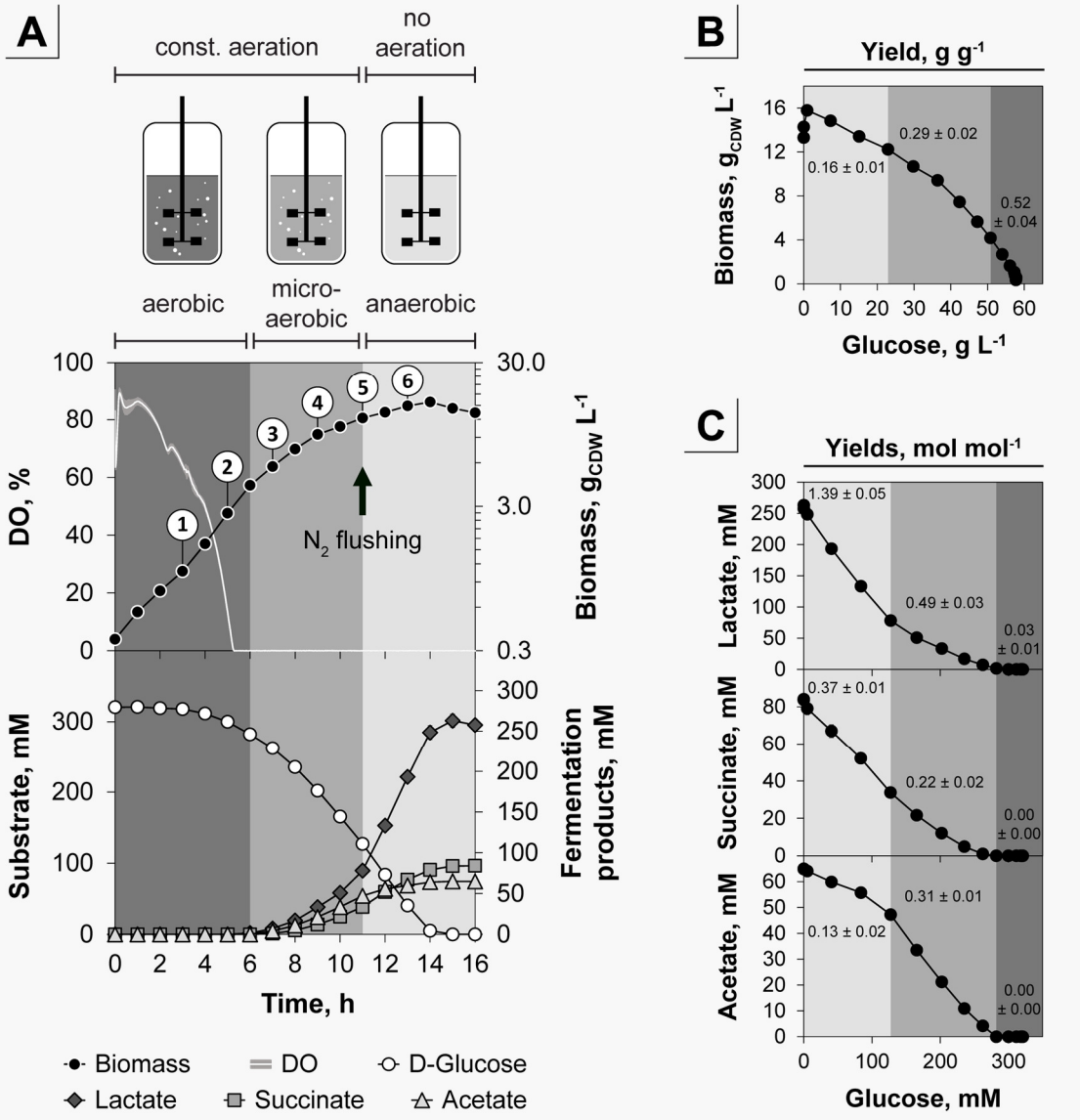


**Figure 4.12. The triple-phase process**. *C. glutamicum* WT was cultivated after the established seed train (Figure 3.1 D, p. 83) in $CGXII_{2+PCA}$ + 60 g glucose $L^{-1}$. **A**. The 30 L bioreactor cultivation in 10 L minimal medium was realized with constant agitation (445 rpm) throughout the entire process and a gassing of 0.1 vvm within the aerobic (dark grey) and microaerobic (grey) phase. The anaerobic (light grey) phase was initiated by a stop of aeration and gassing of the headspace with $N_2$ (Figure S 18, p. 238). Sampling for RNA-sequencing analysis is indicated with circled numbers (①, ②, ③, ④, ⑤, ⑥). The pH was regulated to 7.4 by the addition of 25 % ammonium hydroxide solution (Figure S 17 C, p. 237). The biomass/substrate yield ($Y_{X/S}$, **B**) and the product/substrate yields ($Y_{P/S}$, **C**) are stated and were calculated for each phase by linear regression. Analysis of the culture supernatants was conducted for the substrate (glucose) and the fermentation products (lactate, succinate, acetate) via HPLC (cf. 3.12.5.1, p. 96). Error bars and shaded area of the DO represent the SD of four independent experiments. Graphic was analogously published (Lange, J., Münch, E., *et al.*, 2018).

# 4.12. RNA-sequencing analysis

## 4.12.1. General considerations

At six distinct points in time (Figure 4.12, p. 143), samples for RNA-sequencing analysis were taken during the triple-phase process under aerobic (①, ②), microaerobic (③, ④, ⑤) and anaerobic conditions (⑥). The experimental design allows for the first time a gradual investigation of *C. glutamicum*'s response to a progressing oxygen limitation. For all interpretation of the transcriptome data it is important to consider that during the triple-phase bioprocess oxygen availability and growth rate reduction go hand in hand. It is thus expected that transcriptional activity is globally reduced as seen for

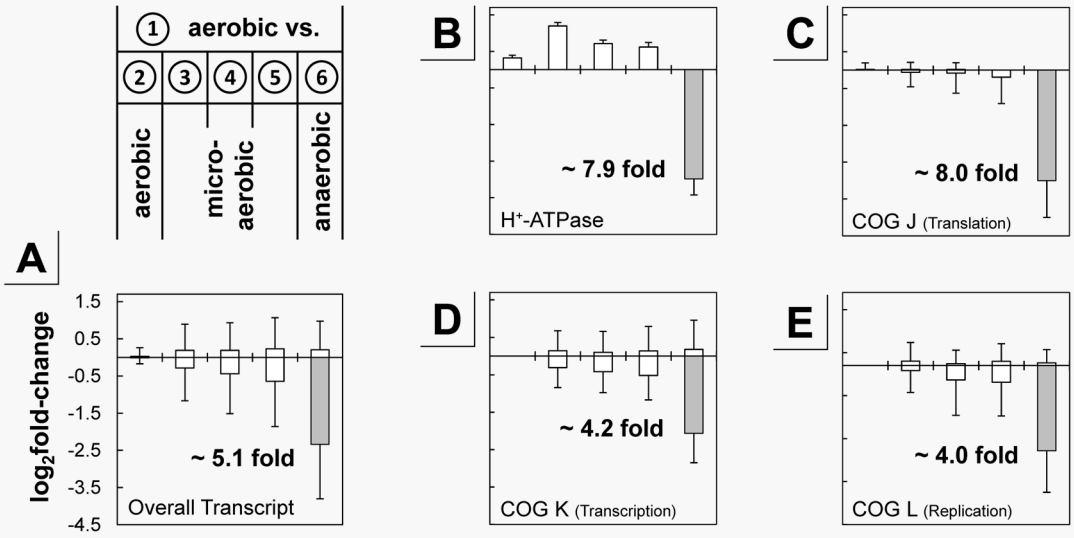


**Figure 4.13. Average transcriptional response of *C. glutamicum*** to altering oxygen concentrations. **A**. The entire differentially expressed genes (201 up- and 1234 down-regulated) were averaged based on $log_2$-fold changes. **B**. Average of the eight structural genes of the $H^+$-ATPase transcribed in the *atpBEFHAGDC* operon. **C**. Of the overall COG J (translation, 133 genes) 90 genes were significantly changed in expression. **D**. The COG K (transcription, 161 genes) showed 54 genes with altered transcription. **E**. The COG L (replication, 54 genes) showed 54 genes with altered transcription. Column graphs represent $log_2$-fold changes reduced expression (grey). Open columns are values outside the significance constraints (m-value > 1.50, < -1.50 and a-value > 1.00). From left to right aerobiosis (②), microaerobiosis (③, ④, ⑤) and anaerobiosis (⑥) versus the aerobic reference (①; Figure 4.12, p. 143). Average values were calculated for up- and downregulated genes separately using the entire (B) or only significant (A, C, D, E) $log_2$-fold changes. Given numbers represent the approximate average fold-change under anaerobiosis (⑥) compared to aerobiosis (①). Error bars show SD between all included $log_2$-fold changes within the category.

example in yeast (Regenberg *et al.*, 2006) or in *E. coli* (Gerosa *et al.*, 2013).

After RNA isolation, the integrity was analyzed and showed 16S/23S RNA ratios from 1.5-1.7 and an RNA integrity number (RIN) > 8. Both indicators confirm a highly suitable RNA quality with low degradation during sampling and processing. Overall the RNA-sequencing yielded a total of 28,720,937 reads as assignable and unique mapping events and which subsequently were used for $\log_2$ transcripts per million ($\log_2$TPM) value calculation. Raw $\log_2$TPM values were analyzed by Pearson correlation (Figure S 21, p. 239) and indicate a logical progression of the transcriptomic response matching sample ID and enforcement of oxygen deprivation. The strict aerobic state of sample ① served as reference for all following analysis. Differential gene expression analysis was defined to be significant based on the graph shown in the appendix (Figure S 22, p. 239) within the following constraints: $\log_2$-fold change of > 1.50 and < -1.50 (corresponding to a fold-change of 2.80 and 0.40, respectively) and an average value (a-value) > 1.00 to exclude results that are derived from very few reads. In Figure 4.14 A, a summary of differentially transcribed genes within the respective phases is shown. Over the entire cultivation time 1421 genes were differentially expressed compared to the aerobic reference state, representing a dramatic change of around 50 % of the 3002 known protein coding genes (Kalinowski *et al.*, 2003). Of this share, only 201 genes were enhanced in expression, whereas 1234 were downregulated, which is in accordance to our initial consideration. The average differential $\log_2$-fold change of these genes is depicted in Figure 4.13 A, shows a change of -2.34 ± 1.46 (~ 5.1-fold down) under anaerobiosis and manifests the reduction of the transcriptional household as dominant response to limiting oxygen. A clustering visualized in the Venn diagram (Figure 4.14 B) clearly indicates that each phase has, besides overlapping features, also unique transcriptional responses. This observation confirms the phenotypic distinction discussed above (cf. 4.11, p. 140) at genetic level.

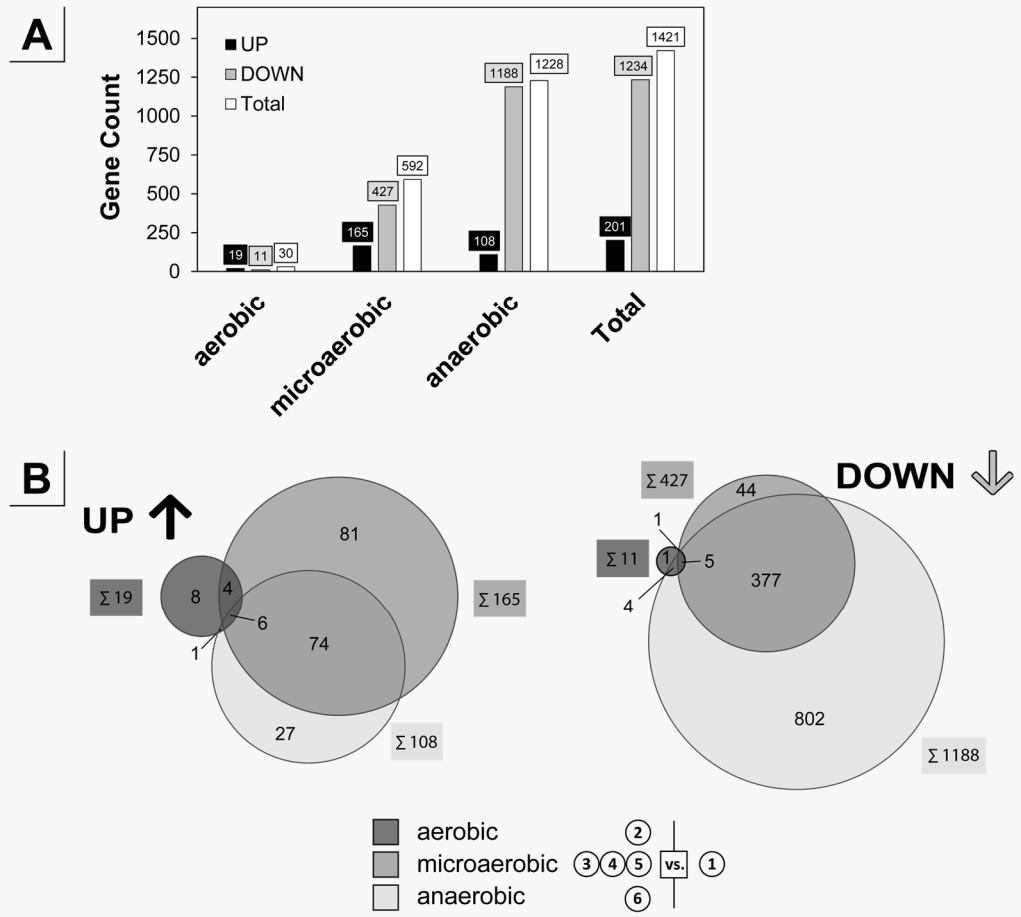


**Figure 4.14. Overall transcriptional change during the triple-phase process**. RNA-sequencing analysis was conducted with an m-value (> 1.50, < -1.50) and a-value (> 1.00) cutoff and the aerobic state ① serving as reference. **A**. Differentially expressed genes were counted within the aerobic (②), microaerobic (③, ④, ⑤) and anaerobic (⑥) phase and summed over the total process timeframe. For the microaerobic phase (samples ③, ④, ⑤) an average value was calculated and allocated to up- or downregulation. **B**. Venn diagram with a three-circle-overlap separated into up- and downregulated genes within the three major process phases. Totally altered genes are given in boxes besides the circle of the respective phase. Graphic was analogously published (Lange, J., Münch, E., *et al.*, 2018).

## 4.12.2. Central metabolism

Previous work with *C. glutamicum* describing transcriptional changes at a direct shift from aerobiosis to anaerobiosis showed dramatic reorganization of glycolysis and the TCA (Inui *et al.*, 2007; Yamamoto *et al.*, 2011). We could confirm the transcriptional enhancement of glycolysis and the reductive branch of the TCA as well as the inactivation of the oxidative branch of the TCA. Moreover, we broaden the current knowledge by further specifying the response in early reacting genes under microaerobiosis

(upregulated e.g. *ldhA*, *mdh*, *pck*, …; downregulated e.g. *adhA*, *ald*, *sucCD*, *malE*, …) and late responses upon strict anaerobiosis (e.g. *sdhABCD*, *gdh*, *gltA*, …). The oxidative branch of the TCA and the glyoxylate shunt is strongly mitigated, because of a transcriptional repression of the *sucCD* genes (max. 45-fold down) and *aceA* (max. 38-fold down) and *aceB* (max. 45-fold down). It is surprising that the cluster *sdhABCD* encoding succinate dehydrogenase is reduced in transcription upon anaerobiosis by up to 5-fold, even though succinate is produced during fermentation. Inui *et al.* observed similar findings (Inui *et al.*, 2007). Under aerobic conditions the electrons of succinate oxidation are directly transferred via the SDH complex (*sdhABCD*; succinate dehydrogenase) to the menaquinone pool (cf. Figure 2.6, p. 39). Therefore, the succinate dehydrogenases represent the only direct connection between the TCA and the respiratory chain (Knapp *et al.*, 2015). It may be this link to the respiratory chain that causes a repression of *sdhABCD* expression through an unknown mechanism. Other genes of the respiratory chain, e.g. of the cytochrome $bc_1$-$aa_3$-oxidase, are similarly affected (cf. 4.12.5, p. 151). A feedback of the quinone pool has also been described for example in *E. coli*, where elevated menaquinone levels activated the ArcB/ArcA transcriptional regulation system and thus the fermentative metabolism (Portnoy *et al.*, 2010).

**Figure 4.15. Transcriptional response of the central metabolism** to a shift from aerobiosis via microaerobiosis to anaerobiosis including glycolysis, TCA, glyoxylate shunt, oxidative pentose phosphate pathway and selected amino acid biosynthesis pathways. Column graphs represent $log_2$-fold changes of enhanced (black) and reduced (grey) expression. Values outside the significance constraints (m-value > 1.50, < -1.50 and a-value > 1.00) are also shown (white). From left to right aerobiosis (②), microaerobiosis (③, ④, ⑤) and anaerobiosis (⑥) versus the aerobic reference (①; Figure 4.12, p. 143). Scaling of these graphs is variable and allows only qualitative comparisons. A quantitative comparison between different genes is therefore not legitimate. Selected enzymes of interest are ahown and encoded by the given genes in italic: *aceA* (isocitrate lyase), *aceB* (malate synthase), *adhA* (alcohol dehydrogenase), *aspT* (aspartate aminotransferase), *alaT* (alanine aminotransferase), *ald* (acetaldehyde dehydrogenase), *fbp* (fructose-1,6-bisphosphatase), *fda* (fructose-bisphosphate aldolase), *fum* (fumarate hydratase), *gapA* (glyceraldehyde-3-phosphate dehydrogenase), *gdh* (glutamate dehydrogenase), *gltA* (citrate synthase), *glyA* (serine hydroxymethyltransferase), *ilvBN* (acetohydroxy acid synthase), *ilvC* (acetohydroxyacid isomeroreductase), *ldhA* (L-lactate dehydrogenase), *leuA* (2-Isopropylmalate synthase), *leuB* (3-isopropylmalate dehydrogenase), *leuCD* (3-isopropylmalate dehydratase), *malE* (malic enzyme), *mdh* (malate dehydrogenase), *pck* (phosphoenolpyruvate carboxykinase), *pfk* (6-phosphofructokinase), *pgk* (3-phosphoglycerate kinase), *ppc* (phosphoenolpyruvate carboxylase), *pyc* (pyruvate carboxylase), *sdhABCD* (succinate dehydrogenase), *serA* (phosphoglycerate dehydrogenase), *serB* (phosphoserine phosphatase), *sucCD* (succinyl-CoA synthetase), *tpi* (triosephosphate isomerase), *zwf* (subunit of the glucose-6P dehydrogenase). Graphic represents extended version to literature (Eikmanns and Blombach, 2014) and was analogously published (Lange, J., Münch, E., *et al.*, 2018).

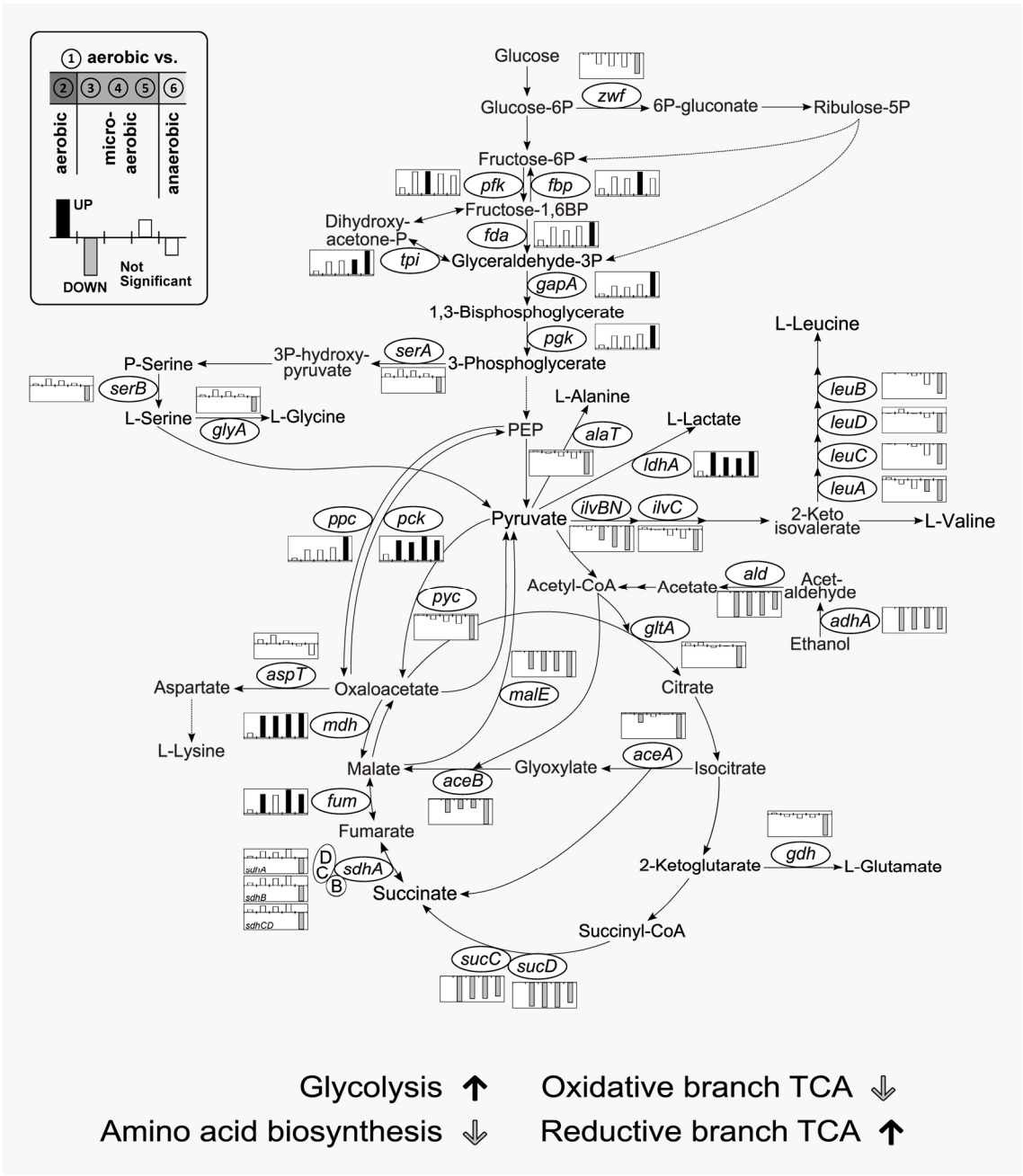
① aerobic vs.
② ③ ④ ⑤ ⑥
aerobic
micro-aerobic
anaerobic
UP
DOWN
Not Significant
Glucose
zwf
Glucose-6P
6P-gluconate
Ribulose-5P
Fructose-6P
pfk
fbp
Fructose-1,6BP
Dihydroxy-acetone-P
fda
tpi
Glyceraldehyde-3P
gapA
1,3-Bisphosphoglycerate
pgk
3-Phosphoglycerate
serA
3P-hydroxy-pyruvate
P-Serine
serB
L-Serine
glyA
L-Glycine
L-Alanine
alaT
PEP
L-Lactate
ldhA
L-Leucine
leuB
leuD
leuC
leuA
2-Keto isovalerate
L-Valine
ppc
pck
Pyruvate
ilvBN
ilvC
Acetyl-CoA
Acetate
ald
Acet-aldehyde
adhA
Ethanol
pyc
gltA
Citrate
aspT
Aspartate
Oxaloacetate
malE
mdh
L-Lysine
Malate
Glyoxylate
aceA
Isocitrate
aceB
fum
Fumarate
sdhA
sdhB
sdhCD
D
C
B
Succinate
2-Ketoglutarate
gdh
L-Glutamate
Succinyl-CoA
sucC
sucD
Glycolysis ↑
Oxidative branch TCA ⇩
Amino acid biosynthesis ⇩
Reductive branch TCA ↑

### 4.12.3. Pentose phosphate pathway

It is known that during growth on glucose the carbon flux in *C. glutamicum* is directed to the pentose phosphate pathway (PPP) with around 69 % under aerobic but only 5 % under anaerobic conditions (Bartek *et al.*, 2011; Radoš *et al.*, 2014). Radoš *et al.* speculated that the PPP is controlled based on the demand of NADPH. The key enzymes of the oxidative branch of the PPP (Figure 3.4, p. 98) are the glucose-6P dehydrogenase (G6P-DH), encoded by the genes *zwf* (cg1778) and *opcA* (cg1779), and the 6P-gluconate dehydrogenase (6PG-DH), encoded by *gnd* (cg1643). We could not detect meaningful transcriptional changes of these enzymes, where only *zwf* with a fold change of 0.33 was mildly reduced in expression towards anaerobiosis. The PPP shutdown must as consequence be predominantly regulated on another control layer such as metabolic governance or posttranslational modification. To clarify a potential post translational modification, specific activities of the G6P-DH and 6PG-DH under exponential growth

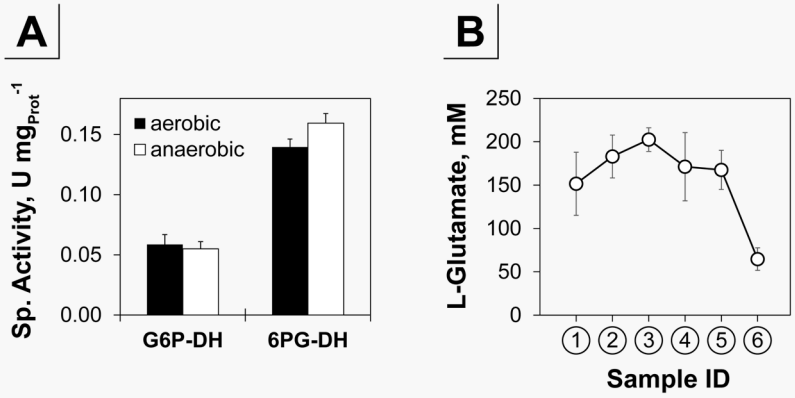


**Figure 4.16. Specific activity of the G6P-DH and 6PG-DH and intracellular L-glutamate concentration**. **A**. The specific activity in U per mg total protein of the glucose-6P dehydrogenase (G6P-DH), encoded by the genes *zwf* (cg1778) and *opcA* (cg1779), and the 6P-gluconate dehydrogenase (6PG-DH), encoded by *gnd* (cg1643), is shown (for reaction sequence see Figure 3.4, p. 98). *C. glutamicum* WT was cultured in CGXII$_{S+PCA}$ + 20 g glucose $L^{-1}$ until mid-exponential phase in an aerobic (starting biomass ~ 0.3 g CDW $L^{-1}$) and anaerobic shaking flasks (starting biomass ~ 3.7 g CDW $L^{-1}$). Anaerobic flasks were flushed with $N_2$ for 10 min before inoculation through a syringe. After 4 h of cultivation cells were harvested (3.11.1, p. 93) and protein and enzymatic analysis was conducted as described above (3.12.4, p. 96; 3.12.6, p. 97). **B**. Intracellular L-glutamate analysis in samples taken during the triple-phase process [aerobic (①, ②), microaerobic (③, ④, ⑤), anaerobic conditions (⑥); Figure 4.12, p. 143]. Lysis (cf. 3.11.2, p. 94) and HPLC analysis (cf. 3.12.5.2, p. 97) conducted as described elsewhere. Error bars represent SD of three (A) or four (B) independent experiments. Graphic was analogously published (Lange, J., Münch, E., *et al.*, 2018).

and aerobic or non-growth and anaerobic conditions were measured (shaking flasks according to Figure 3.1 B, p. 83[7]). Figure 4.16 A highlights that activities are not substantially changed. Enzyme activity control by modification at the protein level to reduce the PPP flux is thus not harnessed by *C. glutamicum*. We speculate that a general reduction of biosynthesis, as also discussed below exemplarily for amino acids (cf. 4.12.4, p. 150), may enhance intracellular NADPH levels. This increased availability could then inhibit the G6P-DH and the 6PG-DH by a feedback mechanism as shown previously, with published inhibitory constants for both enzymes is around 25 μM (Moritz *et al.*, 2000).

### 4.12.4. Amino acid biosynthesis

Expression of genes encoding amino acid synthesis pathways (for example L-glutamate, L-serine, L-glycine, L-alanine and branched chain amino acids) decreased under anaerobic conditions (Figure 4.15). Remarkably, an important branch point between the TCA and the L-aspartate family of amino acid biosynthesis pathways was not affected on transcriptional level. The key enzyme AspT (aspartate amino transferase) was not altered significantly at the transcriptional level (Figure 4.15). The regulation must thus be coordinated by an alternative mechanism. The major donor in amino transferase reactions in *C. glutamicum* is L-glutamate (Marienhagen *et al.*, 2005). The analysis of intracellular L-glutamate (cf. 3.13.1, p. 99) revealed a rather constant level of 167 ± 30 mM under aerobic (average of ①, ②) and 180 ± 22 mM under microaerobic (average of ③, ④, ⑤) conditions. Subsequently, under anaerobiosis (⑥), the concentration dropped by about 70 % to 65 ± 13 mM compared to aerobiosis (Figure 4.16 B). The analyzed concentrations are within the range of published data e.g. for *C. glutamicum* (Gutmann *et al.*, 1992) or *E. coli* (Bennett *et al.*, 2009). We speculate that a shutdown of L-glutamate production by around 4-fold transcriptional reduction *gdh* expression, may be sufficient to mitigate amino acid production of the L-aspartate family due to a low precursor supply.

[7] For aerobic cultivation, the main culture was realized in shaking flasks with baffles instead of the anaerobic flask.

### 4.12.5. Respiratory chain and energy metabolism

*C. glutamicum* possesses the two oxygen dependent terminal cytochrome oxidases: the **cytochrome *bc*$_1$-*aa*$_3$ supercomplex** and the **cytochrome *bd* oxidase** with low and high oxygen affinity, respectively (Kusumoto *et al.*, 2000; Niebisch, 2002; Bott and Niebisch, 2003). The transcriptional response is depicted in Figure 4.17 with respect to the operon structures and protein location within the membrane. We could confirm both known observations that the cytochrome *bc*$_1$-*aa*$_3$ supercomplex and cytochrome *bd* oxidase are mostly transcribed under aerobic and oxygen limited conditions, respectively (Bott and Niebisch, 2003; Kabus *et al.*, 2007; Koch-Koerfges *et al.*, 2013). The induction of the cytochrome *bd* oxidase under microaerobic conditions was shown also in other organisms such as *Mycobacterium smegmatis* (Kana *et al.*, 2001). For the first time, a gradually oxygen dependent expression profile was recorded in *C. glutamicum*. The study resolves transcriptional activation with max. average $\log_2$-fold change of the cytochrome *bc*$_1$-*aa*$_3$ supercomplex of 1.53 ± 0.04 (~ 2.9-fold up) under early microaerobic conditions and of the cytochrome *bd* oxidase of 3.75 ± 0.16 (~ 13.5-fold up) at later microaerobic and anaerobic states. At strict anaerobic stages the cytochrome *bc*$_1$-*aa*$_3$ supercomplex is downregulated by a max. average $\log_2$-fold change of -1.95 ± 0.54 (~ 3.9-fold down). Interestingly, the two genes *ctaA* and *ctaB* encode newly proposed putative heme *o* and *a* synthases (Toyoda and Inui, 2016b), which may contribute to cytochrome oxidase assembly and show similar transcriptional patterns as the cytochrome *bd* oxidase genes. Both genes are transcribed in monocistronic (sub-)operons (Pfeifer-Sancar *et al.*, 2013). Presumably, these two operons and the *cydABCD* operon are activated by similar regulatory mechanisms responding to the microaerobic environment, where their transcription is guided by the sigma factor $\sigma^C$ (Toyoda and Inui, 2016b). In the study of Toyoda and Inui, an overexpression of $\sigma^C$ could indeed enhance expression of the *cydABCD*, *ctaA* and *ctaB* genes and thereby reduced transcription of *ctaE-qcrCAB*. As shown below in our observation, however, $\sigma^C$ was not altered in transcription significantly over the entire cultivation time (cf. 4.12.7, p. 155). Transcriptional regulation of the cytochrome *bc*$_1$-*aa*$_3$ supercomplex genes rely on the GlxR, RamB and HrrA that are global, master and putative two component regulators, respectively (Schröder and Tauch, 2010; Pauling *et al.*, 2012). Remarkably, regulation of the cytochrome *bd* oxidase involves the bacterial redox sensor OxyR (Green and Paget, 2004; Teramoto *et al.*, 2013;

Milse *et al.*, 2014), which is discussed below (cf. 4.12.6, p. 154). An example for a regulator that senses the redox state of NADH/$NAD^+$ pool is Rex from *Streptomyces coelicolor* (Green and Paget, 2004). An increase of the NADH/$NAD^+$ ratio under microaerobiosis indeed led to an induction of the Rex regulon including the *cydABCD* operon (Green and Paget, 2004). Similar regulators, however, are not known in *C. glutamicum*. Although in other organisms such as *E. coli* (Lindqvist *et al.*, 2000) the cytochrome *bd* oxidase was shown to exhibit a peroxidase function, it has not been experimentally demonstrated for *C. glutamicum* (Milse *et al.*, 2014). The physiological role of OxyR-mediated regulation might thus not be fully understood.

We found a continuously reduced expression of the type II **NADH dehydrogenase** encoded by *ndh* (cg1656) reaching a max. $log_2$-fold change of -2.83 (~ 7.1-fold down) under anaerobic conditions. Physiologically, this membrane-bound enzyme transfers electrons from NADH to the menaquinone pool without pumping protons (Molenaar *et al.*, 2000). As menaquinol cannot be reoxidized at the lack of oxygen, electrons from NADH must be transferred to intracellular metabolites. A reduced expression is thus in concordance to our general observations.

Energy conservation in the fermentative metabolism is achieved by substrate level phosphorylation. It is thus not surprising that upon an enhancement of oxygen deprivation the entire operon of the **$H^+$-ATPase** is reduced in transcription. In the triple phase process, a downregulation of the entire *atpBEFHAGDC* operon under strict anaerobic conditions with an average $log_2$-fold change of -2.99 ± 0.44 (~ 7.9-fold down) was observed (Figure 4.13 B, p. 144). Similar observations have been found previously (Inui *et al.*, 2007; Neuweger *et al.*, 2009).

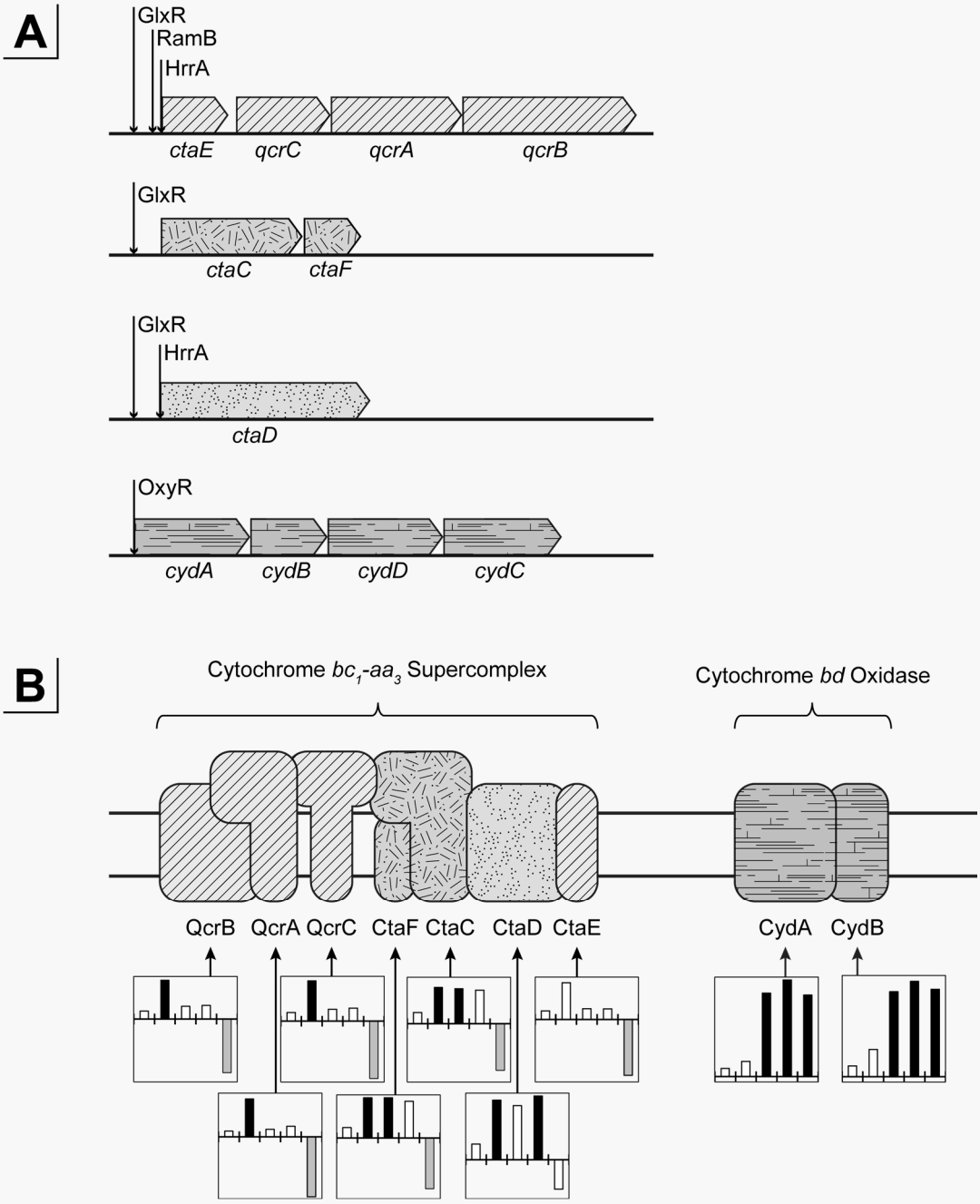


**Figure 4.17. Transcriptional response of the cytochrome *bc₁-aa₃* and cytochrome *bd* oxidase** to altering oxygen availabilities. **A**. Genetic organization and operon structures. Binding of the transcriptional regulators GlxR, RamB, HcrA and OxyR is indicated. **B**. Schematic organization of the cytochrome oxidases in the cytoplasmic membrane. Column graphs represent $log_2$-fold changes of enhanced (black) and reduced (grey) expression. Open columns are values outside the significance constraints (m-value > 1.50, < -1.50 and a-value > 1.00). From left to right aerobiosis (②), microaerobiosis (③, ④, ⑤) and anaerobiosis (⑥) versus the aerobic reference (①; Figure 4.12, p. 143). Scaling of the graphs is variable and allows only qualitative comparisons. A quantitative comparison between different genes is therefore not legitimate. Shading links genes to proteins. Graphic A and B based on the online tool *CoryneRegNet* and Bott and Niebisch, respectively (Bott and Niebisch, 2005; Pauling *et al.*, 2012). The figure was analogously published (Lange, J., Münch, E., *et al.*, 2018).

**Table 4.6. Relative differential expression of genes within the transcription machinery**. Column graphs represent $log_2$-fold changes of enhanced (black) and reduced (grey) expression. Open columns are values outside the significance constraints (m-value > 1.50, < -1.50 and a-value > 1.00). From left to right aerobiosis (②), microaerobiosis (③, ④, ⑤) and anaerobiosis (⑥) versus the aerobic reference (①;Figure 4.12, p. 143). Scaling of these graphs is variable and allows only qualitative comparisons. A quantitative comparison between different genes is therefore not legitimate.

| Gene ID | Name | Description | Rel. diff. expression |
|---|---|---|---|
| cg0655 | *rpoA* | DNA-directed RNA polymerase, α subunit | 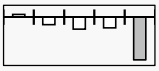 |
| cg1809 | - | DNA-directed RNA polymerase, ω subunit | 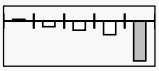 |
| cg1354 | *rho* | Transcription termination factor Rho | 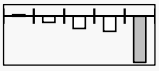 |
| cg1316 | - | DNA/RNA helicase, SNF2 family | 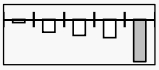 |
| cg1824 | *nusB* | Transcription termination factor | 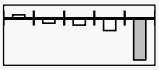 |
| cg1843 | - | Superfamily II DNA/RNA helicase, SNF2 family | 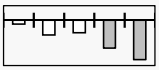 |
| cg1963 | - | Putative DNA/RNA helicase, superfamily II | 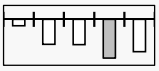 |
| cg2178 | *nusA* | Putative transcriptional termination/antitermination factor | 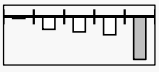 |
| cg2241 | *tex* | Transcriptional accessory protein | 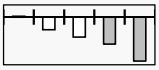 |

## 4.12.6. Translation, transcription and replication

Our initial considerations were in accordance to the observation that the major transcriptional trend towards anaerobic conditions is a reduction of transcriptional activity. Around 41 % of the entire protein coding genes were on reduced in expression by a globally averaged $log_2$-fold change of $-2.34 \pm 1.46$ (~ 5.1-fold down) under anaerobic conditions. We are convinced that such global rearrangements can be traced back to the basic cellular functions such as transcription, translation and replication, which were analyzed here according to clusters of orthologous genes (COG) (Tatusov *et al.*, 2000; Meyer *et al.*, 2003). Indeed, about 80 % (66 of 81) of all structural ribosomal genes (selected based on Martín *et al.* and extended with CoryneRegNet (Martín *et al.*,

2003; Pauling *et al.*, 2012)) were reduced in expression upon anaerobiosis. This also affects the majority of the translation COG J class, where 90 of 133 genes are on average less transcribed with a $log_2$-fold change is -2.99 ± 1.00 (~ 7.9-fold down) under oxygen deprivation (Figure 4.13 C, p. 144). For the transcription COG K class 30 % of the genes (54 of 161) were analogously altered in transcription ($log_2$-fold change -2.07 ± 0.78; ~ 4.2-fold down; Figure 4.13 D, p. 144). Most interestingly, also structural genes of the α- and ω-subunit of the RNA-polymerase (*rpoA* and cg1809) along with essential accessory proteins of the transcription process show a decreased transcription in particular under anaerobiosis (Table 4.6). As the general trend in the triple-phase process is a growth arrest towards anaerobiosis, we additionally examined the COG L class of replication associated genes. Indeed, we found that around 40 % of the genes (54 of 135) were downregulated by -1.99 ± 0.96 (~ 4.0-fold down; Figure 4.13 E, p. 144). Among the genes are also the structural genes of the DNA polymerase III (*dnaE1*, *dnaE2*, cg2576, …), which is consistent with the observation of a reduced growth rate over time (Figure 4.19 A1, p. 163).

In summary, a decline of the fundamental mechanisms translation, transcription and replication are in our opinion an elegant strategy to generally reduce the metabolic and cellular activity including replication.

### 4.12.7. Sigma factors

RNA-polymerase requires specialized factors – the sigma factors (σ-factors) – to recognize promoters of specific cellular functions as holoenzyme (Feklístov *et al.*, 2014). *C. glutamicum* possesses seven described σ-factors as listed in Table 4.7. It is known that they play a key role to respond to global changes such as environmental stresses, growth arrest an others (Gourse *et al.*, 2006; Landini *et al.*, 2014). Two σ-factors namely, $\sigma^B$ and $\sigma^D$, were previously connected to the response of *C. glutamicum* to oxygen deprivation (Ehira *et al.*, 2008; Ikeda *et al.*, 2009). In a Δ*sigB* mutant, Ehira *et al.* found a reduced expression of genes involved in glucose metabolism. The factor $\sigma^B$ is also active as alternative vegetative σ-factor not only under oxygen deprivation and stationary conditions but also under aerobic exponential growth. In accordance, we found a gradual increase of transcription until significant levels are reached under anaerobiosis with $log_2$-fold change of 2.10 (~ 4.3-fold up). By a mutagenized cell library of

**Table 4.7. Relative differential expression of sigma factors**. Description based on literature (Schröder and Tauch, 2010; Toyoda and Inui, 2016b). Column graphs represent $log_2$-fold changes of enhanced (black) and reduced (grey) expression. Open columns are values outside the significance constraints (m-value > 1.50, < -1.50 and a-value > 1.00). From left to right aerobiosis (②), microaerobiosis (③, ④, ⑤) and anaerobiosis (⑥) versus the aerobic reference (①; Figure 4.12, p. 143). Scaling of these graphs is variable and allows only qualitative comparisons. A quantitative comparison between different genes is therefore not legitimate. Table was analogously published (Lange, J., Münch, E., *et al.*, 2018).

| Gene ID | Name | Description | Rel. diff. expression |
|---|---|---|---|
| cg2092 | *sigA* | Primary (housekeeping) sigma factor | 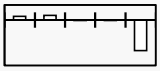 |
| cg2102 | *sigB* | Nonessential primary-like sigma factor involved in gene expression during the transition phase, under oxygen deprivation and during environmental stress responses | 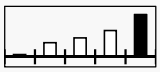 |
| cg0309 | *sigC* | Regulates expression of a branched quinol oxidation pathway | 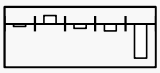 |
| cg0696 | *sigD* | ECF sigma factor probably involved in the adaptation to microaerobic environments | 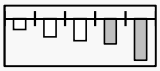 |
| cg1271 | *sigE* | ECF sigma factor involved in responses to cells surface stresses |  |
| cg0876 | *sigH* | ECF sigma factor controlling the heat and oxidative stress response | 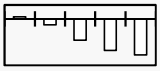 |
| cg3420 | *sigM* | ECF sigma factor controlling the expression of disulfide stress-related genes | 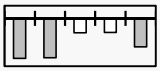 |

*C. glutamicum* R, Ikeda *et al.* identified strains, which were handicapped in proliferating under microaerobic conditions. Among other genes, the $\sigma^D$ was shown to partially compensate hampered growth phenotypes by plasmid-based complementation. In the triple-phase process the gene *sigD* was reduced in transcription with a max. $log_2$-fold change of -2.55 (~ 5.9-fold down). Both significant alterations of the factors $\sigma^B$ and $\sigma^D$ could support the bacterium's adaptation towards a facing lack of oxygen but also stationary phase. However, such a modulation of σ-factor transcription itself must underlie a tightly coordinated regulation, which remains to be unraveled. Other σ-factors do not show significant or interpretable alteration of transcription.

### 4.12.8. Transcriptional regulators

#### 4.12.8.1 Expression profile

In the chapters above, an abundance of transcriptional modulations of the central metabolism, the PPP, amino acid biosynthesis, the respiratory and energy metabolism, translation, transcription, replication and σ-factors were discussed. Many of the transcriptional profiles showed a coordinated response towards the progression of oxygen scarcity. This fact allows a hypothesis that the process, besides global changes, also relies on specific regulation on transcriptional level. It is known that the expression of transcriptional regulators themselves can change to manifest their regulatory purpose. In *E.coli*, for example, it was demonstrated that key regulators involved in the adaptation to alternating oxygen availabilities Fnr and ArcBA show a significantly changed transcriptional level at variation of oxygen supply (Partridge *et al.*, 2007; Ederer *et al.*, 2014). For example *arcA* expression was experimentally verified to increase about 4-fold towards anaerobiosis (Compan and Touati, 1994). Conceiving the working hypothesis that in *C. glutamicum* a similar behavior may be prevalent with oxygen responsive regulators, we screened known 159 genes encoding encoding DNA-binding transcription regulators, response regulators of two-component systems and sigma factor subunits of RNA polymerase (Schröder and Tauch, 2010) for differential expression. 34 regulators were found with reduced or enhanced transcription. From these we selected 18 candidates with a significant response in more than one of the conditions of aerobiosis, microaerobiosis or anaerobiosis (Table 4.8). A brief information about each regulator and putative regulator is given in the appendix (cf. A3.19, p. 239).

Although the transcriptional redox-sensor **OxyR** (cg2109, LysR family) was not differentially expressed in a significant manner throughout the triple-phase process, it is known for its capability to sense the intracellular redox potential. So far, this is only described towards oxidative stress such as $H_2O_2$ exposure (Teramoto *et al.*, 2013; Milse *et al.*, 2014). The investigations showed that deletion of OxyR could enhance the resistance towards $H_2O_2$ as seen also in *C. glutamicum* R (Teramoto *et al.*, 2013) or *C. diphtheriae* (Kim and Holmes, 2012). The corynebacterial observations contrast with *E. coli* and suggest alternative mechanisms (Milse *et al.*, 2014). The expression of the cytochrome *bd* oxidase as described above (cf. 4.12.5, p. 151) is regulated by OxyR as

only known direct regulatory mechanism and was increased in expression upon OxyR disruption (Milse *et al.*, 2014). We speculate that it is in theory possible that this regulator could sense both oxidative stress and oxygen deprivation through the intracellular redox potential (Zheng *et al.*, 1998) and coordinate for example the expression of the highly oxygen affine cytochrome oxidase in response to microaerobic conditions.

In summary, an abundance of differentially expressed transcriptional regulators were identified. Although, many of the regulators were studied previously, a potential link to oxygen deprivation was not explored. Furthermore, we included the known redox sensor OxyR as it regulates the expression of the cytochrome *bd* oxidase. Alternative regulatory systems homologous to other organisms such as Rex (Green and Paget, 2004), Fnr (Jordan *et al.*, 1997; Khoroshilova *et al.*, 1997), ArcBA (Bekker *et al.*, 2010) or DevS/DevR (Mayuri *et al.*, 2002; O'Toole *et al.*, 2003; Sousa *et al.*, 2007) could not be identified in *C. glutamicum*. All stated regulators and putative regulators were in the following deleted in *C. glutamicum* (cf. 3.9.3, p. 90).

**Table 4.8. Relative differential expression of putatively oxygen responsive regulators**. Description based on literature (Schröder and Tauch, 2010; Toyoda and Inui, 2016b). Column graphs represent $log_2$-fold changes of enhanced (black) and reduced (grey) expression. Open columns are values outside the significance constraints (m-value > 1.50, < -1.50 and a-value > 1.00). From left to right aerobiosis (②), microaerobiosis (③, ④, ⑤) and anaerobiosis (⑥) versus the aerobic reference (①; Figure 4.12, p. 143). Scaling of these graphs is variable and allows only qualitative comparisons. A quantitative comparison between different genes is therefore not legitimate. Table was analogously published (Lange, J., Münch, E., *et al.*, 2018).

| No. | Gene ID | Name | Description | Rel. diff. expression |
|---|---|---|---|---|
| 1 | cg0993 | *sutR* | Bacterial regulatory protein |  |
| 2 | cg3303 | - | Putative transcriptional regulator, PadR-family | 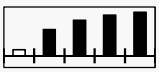 |
| 3 | cg1327 | - | Putative transcriptional regulator, Crp-family | 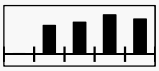 |
| 4 | cg2500 | *znr* | Putative transcriptional regulator, ArsR-family | 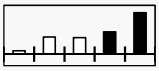 |
| 5 | cg2502 | *zur* | Putative transcriptional regulator, Fur-family |  |
| 6 | cg3202 | *farR* | Transcriptional regulator, GntR-family | 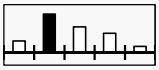 |
| 7 | cg1120 | *ripA* | Repressor of iron protein genes | 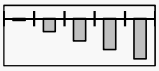 |
| 8 | cg2965 | - | Putative transcriptional regulator, AraC-family | 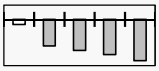 |
| 9 | cg0444 | *ramB* | Master regulator of carbon metabolism | 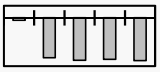 |
| 10 | cg2320 | - | Putative transcriptional regulator, ArsR-family | 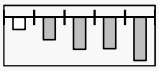 |
| 11 | cg2746 | - | Putative sugar diacid utilization regulator | 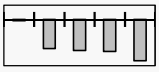 |
| 12 | cg2648 | - | Putative transcriptional regulator, ArsR-family | 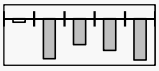 |
| 13 | cg3388 | *iclR* | Activator of putative hydroxyquinol pathway genes | 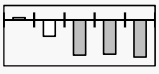 |
| 14 | cg0215 | *cspA* | Cold-shock protein A | 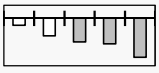 |
| 15 | cg1410 | *rbsR* | Repressor of ribose uptake and uridine utilization genes | 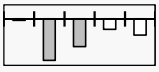 |
| 16 | cg3352 | *genR* | Transcriptional activator of gentisate catabolism | 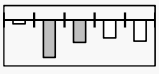 |
| 17 | cg0150 | - | Putative transcriptional regulatory protein, Fic/Doc family | 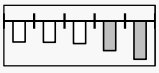 |
| 18 | cg1053 | *mmpLR* | Putative transcriptional regulator, TetR-family | 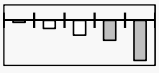 |
| 19 | cg2109 | *oxyR* | Hydrogen peroxide sensing regulator | 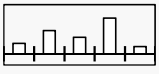 |

### 4.12.8.2 Deletion of putatively oxygen responsive regulators

The entire ORFs of the above stated regulators were deleted by homologous recombination harnessing the pK19*mobsacB* system (cf. 3.9.3, p. 90). Each single mutant was cultivated in shaking flasks without baffles that allow an enforced restriction of oxygen supply. Upon deletion of mandatory regulators that coordinate the strong transcriptional answer to oxygen scarcity, we expected to observe a specifically hampered growth phenotype. Similar findings were published for *C. glutamicum* upon deletion of the cytochrome *bd* oxidase in shaking flask experiments (Kabus *et al.*, 2007). As reference we cultivated *C. glutamicum* WT in shaking flasks with and without baffles

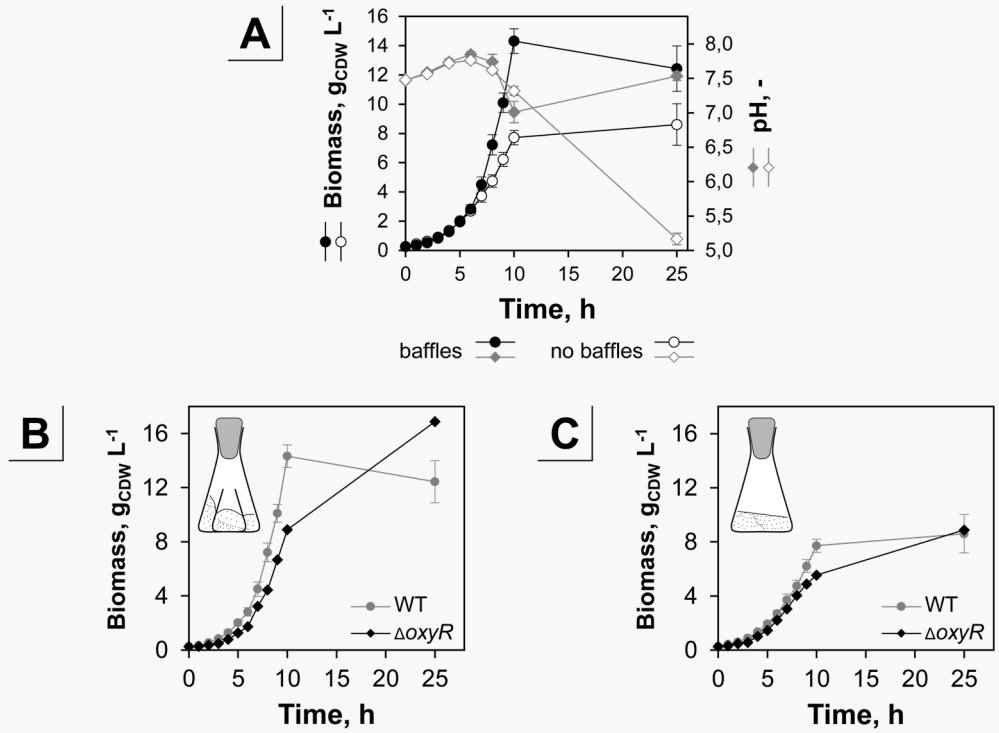


**Figure 4.18. Cultivation of *C. glutamicum* WT and Δ*oxyR* under progressing oxygen limitation** in shaking flasks with baffles or without baffles in $CGXII_{S+PCA}$ + 40 g glucose $L^{-1}$ as sole carbon source. **A**. WT cultivation in baffled (filled symbols) and unbaffled (open symbols) shaking flasks. The biomass concentration (circles) and pH value (diamonds) were analyzed. **B, C**. Cultivation of *C. glutamicum* Δ*oxyR* in shaking flasks with baffles (B) and without baffles (C). In both graphs the WT cultivation is shown in grey (circles) as reference. Error bars show SD of four independent cultivations of the *C. glutamicum* WT strain. For *C. glutamicum* Δ*oxyR* (black, diamonds) the average of two highly comparable independent cultivations is depicted. Graphic was analogously published (Lange, J., Münch, E., *et al.*, 2018).

(Figure 4.18 A). Within the first 6 h of cultivation no remarkable difference in proliferation was found with growth rates of 0.41 ± 0.01 $h^{-1}$ or 0.38 ± 0.01$^{-1}$, respectively. In the ongoing experiment, however, oxygen supply becomes critical in the flask without baffles. Over the entire cultivation respective growth rates were 0.41 ± 0.01 $h^{-1}$ or 0.34 ± 0.01$^{-1}$ for the baffled and unbaffled flasks. Growth significantly ceases in flasks without baffles and results in an enhanced fermentative phenotype allowing less energy conservation. This can be verified by considering the pH value (Figure 4.18 A), which after a primary rise decreases continually in the unbaffled shaking flasks to a minimal value of 5.2 ± 0.1 but has a sigmoidal course in baffled flasks. An initial increase of pH values can be explained by cleavage of the medium-contained urea into carbon dioxide and ammonium through the high urease activity (Burkovski, 2005). Metabolization of the fermentation products lactate, succinate and acetate is possible for *C. glutamicum* under aerobic conditions with quinone dependent lactate and succinate dehydrogenase and the acetate kinase/phosphotransacetylase pathway, respectively (Bott and Niebisch, 2003; Gerstmeir *et al.*, 2003). At critical oxygen concentrations this aerobic degradation machinery is not functional and causes a low stagnating pH at the minimally tolerated pH (Jakob *et al.*, 2007). Based on these observations all strains carrying a deletion of the putatively oxygen sensitive regulators were cultivated in flasks without baffles. Besides the *C. glutamicum* Δ*ramB* and Δ*oxyR* no further regulator showed a remarkable growth phenotype (Figure 4.18 B, C; Figure S 23 , p. 239). *C. glutamicum* Δ*ramB* was generally reduced in proliferation ($\mu$ = 0.29 $h^{-1}$) as known from previous studies (Gerstmeir *et al.*, 2004). This effect, however, could not be allocated to the oxygen deprivation. *C. glutamicum* Δ*oxyR*, was slightly reduced in growth in baffled and unbaffled flasks (Figure 4.18 B, C). Interestingly, a clear hampering of growth can be seen in the flasks without baffles in comparison to the WT starting at 8 h of cultivation. Although previous studies connected the OxyR-mediated regulation to hydrogen peroxide stress (Teramoto *et al.*, 2013; Milse *et al.*, 2014), we postulate that the regulator may also be involved in the adaptation to reduced oxidative conditions – meaning microaerobiosis.

Taken together, the deletion of transcriptionally altered regulators in the triple-phase process could not succeed to unravel an undescribed regulator coordinating *C. glutamicum*'s adaptation towards anaerobiosis. However, knowledge-based search revealed the regulator OxyR, which regulates also the expression of the cytochrome *bd*

oxidase, as potential player in the regulatory regime towards microaerobic conditions.

### 4.12.9. Total RNA concentration

It is known that the growth rate influences the global expression profile (Gerosa *et al.*, 2013) and cellular components such as DNA, total RNA or cell weight (Bremer and Dennis, 2008). For each sampling point (①-⑥) in the triple-phase process, we could determine the total RNA concentration per cell (Figure 4.19 A2). It is important to consider that up to 99 % of total RNA in *C. glutamicum* is rRNA (Pfeifer-Sancar *et al.*, 2013). The following investigations therefore primarily mirror rRNA. As all samples were drawn at different growth rates (Figure 4.19 A1), we could calculate a clear linear correlation[8] (Figure 4.19 B). Projecting this correlation curve to growth arrest ($\mu = 0\ h^{-1}$) may allow the formulation of a minimal total cellular RNA concentration of 8.8 ± 0.7 fg per cell. Most interestingly, we contemplated data from Bremer *et al.* showing an exponential correlation at growth rates of *E. coli*. Interestingly, the extrapolated minimal total RNA concentration of 10.8 fg per cell is very related to our findings (own calculations).

In summary, such considerations give a better understanding of the cells minimal repertoire of RNA species being necessary to fulfil a functional maintenance metabolism. In our example, we connect the reduction of total RNA concentration to the overall shutdown of translation, transcription and replication as discussed above (cf. 4.12.6, p. 154).

[8] The first sampling point (①) was excluded from correlation. This may be justified as in early growth stages an intracellular equilibration may not be given yet.

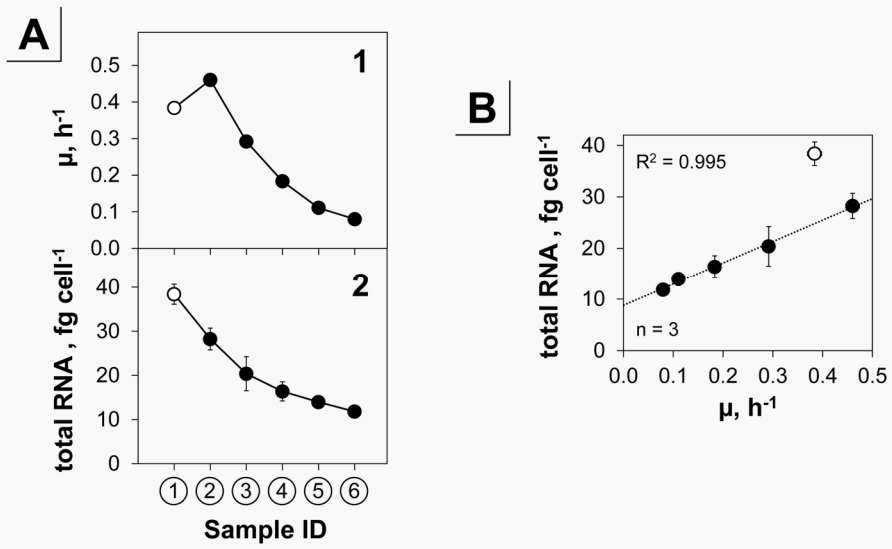


**Figure 4.19. Correlation of total RNA content and growth rate** within the triple-phase process. **A**. The growth rate (μ, **1**) and the total RNA per cell (**2**) is depicted from left to right for the process phases: aerobiosis (①, ②), microaerobiosis (③, ④, ⑤), and anaerobiosis (⑥; Figure 4.12, p. 143). **B**. Direct correlation of the total RNA content and the growth rate. Linear regression was calculated neglecting the first sampling point (①, open circle). The coefficient of determination ($R^2$) is given. Growth rates were calculated including three points in time ($t_{n-1}$, $t_n$, $t_{n+1}$) via linear regression in a semilogarithmic plot of the biomass. Raw RNA concentration derived from RNA-purification (cf. 3.13.2, p. 99) was recalculated using published cell volume of 1.95 μL per mg CDW (Krömer *et al.*, 2004). Error bars represent SD of a triplicate experiment. Graphic was analogously published (Lange, J., Münch, E., *et al.*, 2018).

## 4.13. Conclusion and hypothetical model

In Part III of this thesis, we described an experimental setup, which is suited for a controlled study of *C. glutamicum*'s passage from strict aerobic via microaerobic to anaerobic conditions. The approach enabled a systemic study integrating drastic physiological, metabolic and transcriptional adaptation events to postulate a hypothetical mechanistic model (Figure 4.20). It is important to highlight that through our approach we could closely link specific metabolic states to the cellular transcriptional level at single gene resolution. In the triple-phase process all three phases, with respect to the oxygen availability, were clearly distinguishable considering process parameters and cell physiology. Previously microaerobiosis was a scarcely defined interim state between

aerobic and anaerobic conditions. For *C. glutamicum*, we provide a physiological definition of microaerobiosis as unique condition, where aerobic respiration and fermentation occur in parallel. We linked the initiation of microaerobiosis to a first occurrence of fermentation products and clearly highlight a metabolic switch at scarcity of oxygen. In our model under microaerobiosis (Figure 4.20, top), yet unknown signals or receptors transmit the limiting oxygen concentrations to enhance the transcription of the cytochrome *bd* oxidase and initiate fermentation via glycolysis and the reductive branch of the TCA. Transcriptional changes may be influenced by the two σ-factors ($\sigma^B$, $\sigma^D$), that mirror a logical increase and decrease of transcription of *sigB* and *sigC*, respectively. Most dramatic changes were found at the entrance to strict anaerobiosis. There, almost 50 % of the entire protein coding sequences of *C. glutamicum* were significantly reduced in expression. We could narrow down the poorly described regulation of a shutdown of the pentose phosphate pathway under anaerobiosis by excluding transcriptional mitigation and post translational modification of key enzymes. We postulate that a reduction of biosynthesis, as exemplarily explored for L-glutamate, could harness metabolic governance as possible inhibitory mechanism. We found that intracellular L-glutamate concentrations reduced dramatically towards anaerobiosis. Due to the reduction of this major amino group donor in aminotransferase reactions, we propose an increase of intracellular NADPH levels, which could inhibit the glucose-6-phosphate dehydrogenase of the pentose phosphate pathway and ultimately prevent a branching metabolism. We postulate that drastic transcriptomic reduction found towards anaerobiosis underlies a mitigation of transcription, translation and replication as basic cellular functions. Key structural genes of both fundamental mechanisms were transcriptionally hampered and could thus contribute to an impairment of the entire metabolism. We could quantify such a reduction by analyzing the total intracellular RNA content, which correlated linearly with a reducing growth rate to a hypothetical minimal level of $8.8 \pm 0.7$ fg per cell at growth arrest. Although, key regulatory players coordinating the general trend of shutdown were not identified through intensive deletion studies (18 transcriptionally altered regulators), an influence of the redox-sensor OxyR was found in microaerobic cultivations. The presented laborious search for a transcriptional regulator in charge of the transcriptome adaptations towards anaerobiosis did not generate a clear novel factor. Since decades, many different groups investigated

aerobic and anaerobic processes with *C. glutamicum* but also failed to give explicit results despite the progressing development of analytical methods. It is therefore important to consider, that *C. glutamicum* may harnesses other mechanisms to coordinate such a response and the classical idea of a transcriptional regulation system may not be applicable to this bacterium. It is known that for example under anaerobic conditions the $NADH/NAD^+$ ratio is inversely proportional to the glucose consumption rate (Tsuge *et al.*, 2015) and thus influences the glycolytic activity under anaerobiosis. An explanation is the inhibition of the key glycolytic enzyme glyceraldehyde-3-phosphate dehydrogenase by NADH (Hasegawa *et al.*, 2012). Also, a feedback of the respiratory chain, either mediated by the quinone pool, general cellular energy shortage or heme associated processes may be thinkable. The quinone pool is directly linked to the central metabolism for example through the succinate dehydrogenase or redox carriers $[NAD(P)H/NAD(P)^+]$ and we could confirm that heme synthases are affected by scarcity of oxygen in *C. glutamicum*. Hemes as oxygen sensing molecules are known for example also in *S. cerevisiae* (Grahl and Cramer, 2010). Such metabolic regulation could represent an alternative or addition to the classical model based on transcriptional reactions. More likely the regulation may be a complex interplay as drafted in Figure 4.20 of tightly interlocked systems.

Overall, we generated genetic targets for strain improvement and gathered data as sound basis for future investigations. Ultimately, the accumulated knowledge could contribute to a better understanding of dual-phase production scenario deficiencies and may be projected to other organisms such as pathogenic bacteria facing similar shifts in oxygen availabilities upon ingestion.

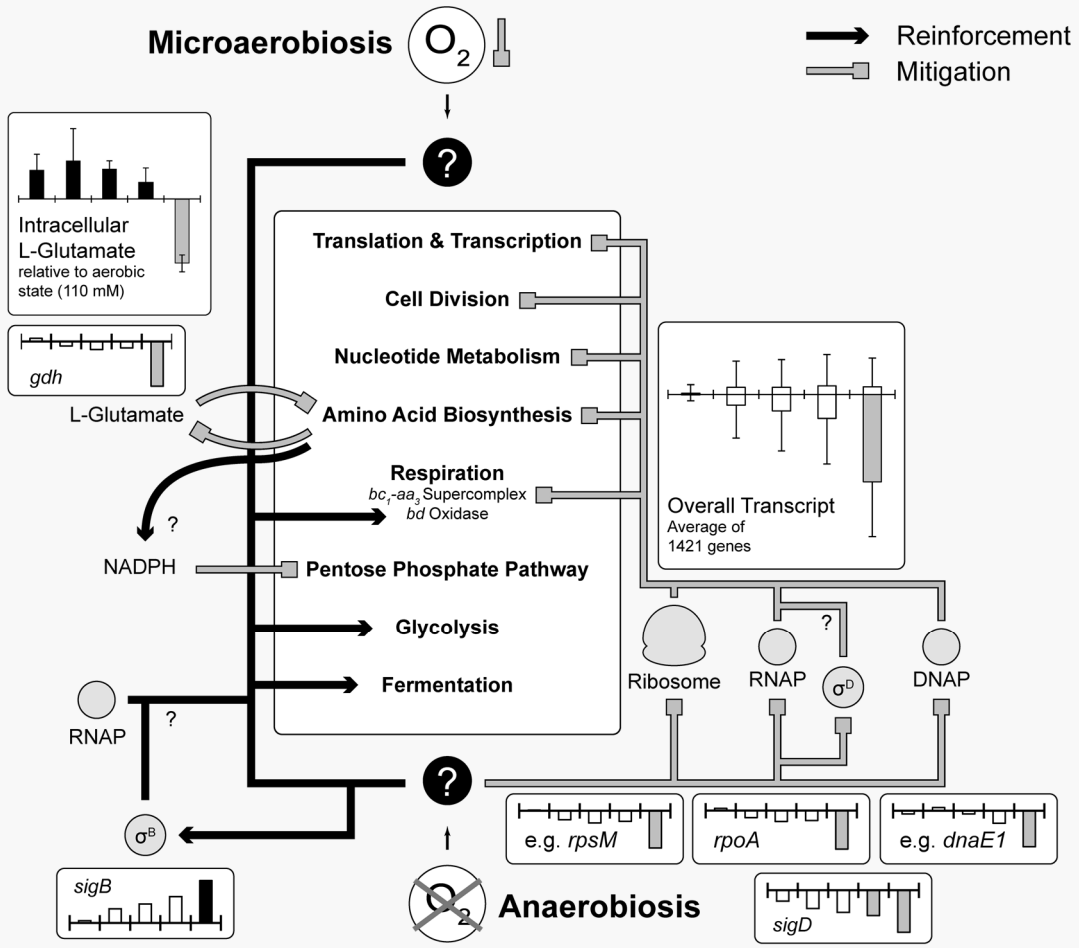


**Figure 4.20. Hypothetical model of *C. glutamicum*'s response to micro- and anaerobiosis** including unknown regulatory mechanisms, metabolites or cellular signals (?). Top: Under oxygen limitation in microaerobic conditions the major response is an enhancement of the cytochrome *bd* oxidase, glycolysis and fermentation. Bottom: Under the absence of oxygen as terminal electron acceptor in anaerobic conditions an enhancement of the σ-factor $\sigma^B$ (*sigB*) could redirect the RNA polymerase (RNAP), which may also be initiated under microaerobiosis. Reduced transcription of the ribosomal protein genes (e.g. *rpsM*), the RNAP (*rpoA*) and the DNA polymerase (DNAP; *dnaE1* encoding DNA polymerase III, alpha subunit) are major contributors for a general reduction of cellular activity. This may be supported by reducing levels of $\sigma^D$ (*sigD*). A reduction of biosynthesis (L-glutamate dehydrogenase encoded by *gdh*; intracellular concentration) could reduce amino acid synthesis due to a mitigated availability of L-glutamate in transaminase reactions. This may elevate NADPH concentrations, which could ultimately inhibit the pentose phosphate pathway. Reinforcement and mitigation is visualized by arrowheads and squares, respectively. Column graphs (with exception of intracellular L-glutamate titers) represent $\log_2$-fold changes of enhanced (black) and reduced (grey) expression. Open columns are values outside the significance constraints (m-value > 1.50, < -1.50 and a-value > 1.00). From left to right aerobiosis (②), microaerobiosis (③, ④, ⑤) and anaerobiosis (⑥) versus the aerobic reference (①; Figure 4.12, p. 143). Scaling of these graphs is variable and allows only qualitative comparisons. A quantitative comparison between different genes is therefore not legitimate. Intracellular L-glutamate pools are depicted relatively to aerobic intracellular titers analogously to differential expression column graphs. Error bars represent SD. Graphic was analogously published (Lange, J., Münch, E., *et al.*, 2018).

# CHAPTER 5: OPEN QUESTIONS AND FUTURE DIRECTIVES

To conclude the thesis, this chapter poses open questions that arose in Part I, Part II and Part III and gives selected future research perspectives.

Both directly bioeconomy-related sections (Part I and Part II) could implement the production of a bulk chemical and biofuel based on so far unexploited biorefinery side streams. Both studies using pyrolysis water for 1,2-propanediol and hemicellulose fraction for isobutanol production encountered the necessity to provide yeast extract as supplement and a decreasing growth and productivity at enhanced concentrations of the renewable substrate. A partial substitution of yeast extract by external supply of glutathione was presented in **Part I** and enabled growth of *C. glutamicum* on pyrolysis water. This surprising observation needs clarification with respect to: external effects such as direct chemical reaction of glutathione with inhibitory components within pyrolysis water, uptake of glutathione by *C. glutamicum*, metabolization of glutathione, and intracellular action of glutathione. Alternatively, to avoid costly supplements for cultivation and purification of the substrates of typical inhibitors such as furans, 5-hydroxymethyl, furfural or aromats, metabolic engineering could forge producer strains with defense mechanisms. We identified low molecular weight thiols such as glutathione, (non-native) and mycothiol (native) as potential molecules to enhance strain robustness and confirmed proposals from literature. First providing of enhanced pathways for biochemical synthesis of both low molecular weight thiols failed to improve cultivation of *C. glutamicum*. Yet, an investigation of intracellular concentrations of glutathione or mycothiol or whether the synthetic gene expression yielded functional enzymes was not

performed. Both missing analyses may clarify, why an improvement by metabolic engineering was not achieved. Biosynthetical supply of glutathione or mycothiol can be regarded as a future perspective to substitute the use of expensive supplements such as yeast extract and offer more defined cultivation conditions. In fact, the here proposed strategy may not be limited to cultivations with pyrolysis water but could be a global strategy to enhance the robustness of *C. glutamicum* to lignocellulosic substrates or decimate general product inhibition in bioprocesses. Another surprising but unclarified finding in Part I was that *C. glutamicum* channels acetol to the central metabolism and promotes growth. Although metabolization is presumably accomplished to the level of pyruvate, the exact mechanism remains speculative. To use acetol within pyrolysis water also for other products apart from the presented direct biotransformation, the understanding and enhancement of the consumption route is a crucial future directive. In **Part II** of this thesis, we presented novel gene loci for integration of genetic information into the chromosome. So far, we could only demonstrate that 4 out of 16 are evidentially feasible. It will be necessary to verify the suitability of the remaining 12 loci for a future acceptance within the *Corynebacterium community* and to allow a projection of the approach to other organisms. We harnessed two of the loci to construct the strains CArXy and CIsArXy, whose overall consumption of pentoses found in the hemicellulose fraction was unfortunately rather low. A bottleneck is the capability of pentose uptake and the sequential metabolization of acetate, L-arabinose and D-xylose. Future studies should thus provide a suitable transporter such as the known L-arabinose transporter protein (AraE). Second, alternatives to the implemented isomerase pathway such as the *Weimberg* pathway for D-xylose consumption could overcome sequential uptake issues. In **Part III** we intended to shed light into the vague knowledge about *C. glutamicum*'s adaptation from aerobiosis towards anaerobiosis with a focus on the so far poorly defined microaerobic intermediate state. Physiological considerations and RNA-sequencing could clearly define this metabolic state. Yet, we could not solve the overall regulatory puzzle. Although, metabolic governance, sigma factors and general reduction of translational, transcriptional and replicational activity were identified as key mechanisms, a novel regulator transmitting the signal of oxygen deprivation could not be characterized. Our initial consideration that such a regulator may also change transcription itself was not found to be true. We postulated that the redox-sensor OxyR may play a role in regulation

of the cytochrome *bd* oxidase also under oxygen limiting conditions. This novel function needs further investigation and corroboration to manifest a dual-regulatory role under oxidative stress and oxygen scarcity. Alternatively, novel regulators could be identified by fishing with promoters of early (microaerobic phase) or lately (anaerobic phase) responding genes such as the lactate dehydrogenase or L-glutamate dehydrogenase, respectively. This could engender regulators coordinating transcriptomic rearrangements. At the end of the day, it may not be transcriptional regulation as the first and most prominent strategy to adapt towards oxygen starvation. We discussed that metabolic governance through redox carriers such as the quinone pool or NAD(P)H/NAD(P)$^+$ species, heme synthesis or the general energy metabolism may provoke and coordinate the physiological response. It is my opinion that the hierarchical and general shutdown of translation and transcription towards anaerobiosis is an underlying measure majorly contributing to an arrest of cellular activity. Key structural elements of the RNA polymerase and ribosomes must be specifically targeted by unknown mechanisms. Such a basic function may be projected to other organisms and provide knowledge to the very fundamentals of life.

Finally, the entirety of this thesis contributes to the acceptance of microbial conversion technologies in biorefinery strategies, which are so far dominated by chemistry, physics and engineering, to valorize yet unexploited or wasted carbon streams. Additionally, the improved systemic understanding of *C. glutamicum*‘s adaptation towards oxygen scarcity unraveled a novel understanding of microaerobiosis as important physiologically preparative interphase. The approach also generated dogmatic future directions to investigate the connection of oxygen deprivation and growth rate with fundamental cellular mechanisms such as transcription and translation.

# REFERENCES


1. Abe, S., Takayama, K.-I., and Kinoshita, S. (1967) Taxonomical studies on glutamic acid-producing bacteria. *J. Gen. Appl. Microbiol.* **13**: 279–301.
2. Aderem, A. (2005) Systems biology: its practice and challenges. *Cell* **121**: 511–513.
3. Ajinomoto Co., I. (2016) FY2015 Market and other information. https://www.ajinomoto.com/en/ir/event/presentation/main/09/teaserItems1/00/linkList/02/link/FY15_Data_E.pdf.
4. Albenberg, L., Esipova, T. V, Judge, C.P., Bittinger, K., Chen, J., Laughlin, A., *et al.* (2014) Correlation between intraluminal oxygen gradient and radial partitioning of intestinal microbiota. *Gastroenterology* **147**: 1055–1063.
5. Alfenore, S., Cameleyre, X., Benbadis, L., Bideaux, C., Uribelarrea, J.-L., Goma, G., *et al.* (2004) Aeration strategy: a need for very high ethanol performance in *Saccharomyces cerevisiae* fed-batch process. *Appl. Microbiol. Biotechnol.* **63**: 537–542.
6. Almeida, J.R.M., Bertilsson, M., Gorwa-Grauslund, M.F., Gorsich, S., and Lidén, G. (2009) Metabolic effects of furaldehydes and impacts on biotechnological processes. *Appl. Microbiol. Biotechnol.* **82**: 625–638.
7. Alper, H. and Stephanopoulos, G. (2009) Engineering for biofuels: exploiting innate microbial capacity or importing biosynthetic potential? *Nat. Rev. Microbiol.* **7**: 715–723.
8. Altaras, N.E. and Cameron, D.C. (2000) Enhanced production of (R)-1,2-propanediol by metabolically engineered *Escherichia coli*. *Biotechnol. Prog.* **16**: 940–946.
9. Alvira, P., Tomás-Pejó, E., Ballesteros, M., and Negro, M.J. (2010) Pretreatment technologies for an efficient bioethanol production process based on enzymatic hydrolysis: a review. *Bioresour. Technol.* **101**: 4851–4861.
10. Aristidou, A. and Penttilä, M. (2000) Metabolic engineering applications to renewable resource utilization. *Curr. Opin. Biotechnol.* **11**: 187–198.
11. Arndt, A. and Eikmanns, B.J. (2008) Regulation of carbon metabolism in *Corynebacterium glutamicum*. In, Burkovski,A. (ed), *Corynebacteria: Genomics and Molecular Biology*. Caister Academic Press, Norfolk, United Kingdom, pp. 155–182.

12. Arnold, S., Moss, K., Henkel, M., and Hausmann, R. (2017) Biotechnological perspectives of pyrolysis oil for a bio-based economy. *Trends Biotechnol.* **35**: 925–936.

13. Ask, M., Mapelli, V., Höck, H., Olsson, L., and Bettiga, M. (2013) Engineering glutathione biosynthesis of *Saccharomyces cerevisiae* increases robustness to inhibitors in pretreated lignocellulosic materials. *Microb. Cell Fact.* **12**: 87.

14. Asnis, R.E. and Brodie, A.F. (1953) A glycerol dehydrogenase from *Escherichia coli*. *J. Biol. Chem.* **203**: 153–159.

15. Atsumi, S., Hanai, T., and Liao, J.C. (2008) Non-fermentative pathways for synthesis of branched-chain higher alcohols as biofuels. *Nature* **451**: 86–89.

16. Atsumi, S., Higashide, W., and Liao, J.C. (2009) Direct photosynthetic recycling of carbon dioxide to isobutyraldehyde. *Nat. Biotechnol.* **27**: 1177–1180.

17. Auchter, M., Cramer, A., Hüser, A., Rückert, C., Emer, D., Schwarz, P., *et al.* (2011) RamA and RamB are global transcriptional regulators in *Corynebacterium glutamicum* and control genes for enzymes of the central metabolism. *J. Biotechnol.* **154**: 126–139.

18. Balat, M. (2011) Production of bioethanol from lignocellulosic materials via the biochemical pathway: a review. *Energy Convers. Manag.* **52**: 858–875.

19. Baltz, R.H., Davies, J.E., and Demain, A.L. (1999) Manual of industrial microbiology and biotechnology 2nd ed. ASM Press, Washington, DC.

20. Barbier, G.G., Ladd, J.L., Campbell, E.R., and Campbell, W.H. (2012) Genetic modification of *Pichia pastoris* for production of propylene glycol from glycerol. *Int. J. Genet. Eng.* **1**: 6–13.

21. Barksdale, L. (1970) *Corynebacterium diphtheriae* and its relatives. *Bacteriol. Rev.* **34**: 378–422.

22. Barreiro, C., Nakunst, D., Hüser, A.T., de Paz, H.D., Kalinowski, J., and Martín, J.F. (2009) Microarray studies reveal a "differential response" to moderate or severe heat shock of the HrcA- and HspR-dependent systems in *Corynebacterium glutamicum*. *Microbiology* **155**: 359–372.

23. Bartek, T., Blombach, B., Lang, S., Eikmanns, B.J., Wiechert, W., Oldiges, M., *et al.* (2011) Comparative $^{13}C$ metabolic flux analysis of pyruvate dehydrogenase complex-deficient, L-valine-producing *Corynebacterium glutamicum*. *Appl. Environ. Microbiol.* **77**: 6644–6652.

24. Barzantny, H., Schröder, J., Strotmeier, J., Fredrich, E., Brune, I., and Tauch, A. (2012) The transcriptional regulatory network of *Corynebacterium jeikeium* K411 and its interaction with metabolic routes contributing to human body odor formation. *J. Biotechnol.* **159**: 235–248.

25. Bastian, S., Liu, X., Meyerowitz, J.T., Snow, C.D., Chen, M.M.Y., and Arnold, F.H. (2011) Engineered ketol-acid reductoisomerase and alcohol dehydrogenase enable anaerobic 2-methylpropan-1-ol production at theoretical yield in *Escherichia coli*. *Metab. Eng.* **13**: 345–352.

26. Baumgart, M., Unthan, S., Rückert, C., Sivalingam, J., Grünberger, A., Kalinowski, J., *et al.* (2013) Construction of a prophage-free variant of *Corynebacterium*

*glutamicum* ATCC 13032 for use as a platform strain for basic research and industrial biotechnology. *Appl. Environ. Microbiol.* **79**: 6006–6015.

27. Becker, J. and Wittmann, C. (2015) Advanced biotechnology: metabolically engineered cells for the bio-based production of chemicals and fuels, materials, and health-care products. *Angew. Chemie Int. Ed.* 3328–3350.

28. Becker, J. and Wittmann, C. (2012) Bio-based production of chemicals, materials and fuels – *Corynebacterium glutamicum* as versatile cell factory. *Curr. Opin. Biotechnol.* **23**: 631–640.

29. Becker, J., Zelder, O., Häfner, S., Schröder, H., and Wittmann, C. (2011) From zero to hero – Design-based systems metabolic engineering of *Corynebacterium glutamicum* for L-lysine production. *Metab. Eng.* **13**: 159–168.

30. de Beer, D., Stoodley, P., Roe, F., and Lewandowski, Z. (1994) Effects of biofilm structures on oxygen distribution and mass transport. *Biotechnol. Bioeng.* **43**: 1131–1138.

31. Bekker, M., Alexeeva, S., Laan, W., Sawers, G., Teixeira de Mattos, J., and Hellingwerf, K. (2010) The ArcBA two-component system of *Escherichia coli* is regulated by the redox state of both the ubiquinone and the menaquinone pool. *J. Bacteriol.* **192**: 746–754.

32. Bekker, M., de Vries, S., Ter Beek, A., Hellingwerf, K.J., and de Mattos, M.J.T. (2009) Respiration of *Escherichia coli* can be fully uncoupled via the nonelectrogenic terminal cytochrome *bd*-II oxidase. *J. Bacteriol.* **191**: 5510–5517.

33. Bennett, B.D., Kimball, E.H., Gao, M., Osterhout, R., Van Dien, S.J., and Rabinowitz, J.D. (2009) Absolute metabolite concentrations and implied enzyme active site occupancy in *Escherichia coli*. *Nat. Chem. Biol.* **5**: 593–599.

34. Bennett, G.N. and San, K.Y. (2001) Microbial formation, biotechnological production and applications of 1,2-propanediol. *Appl. Microbiol. Biotechnol.* **55**: 1–9.

35. Berríos-Rivera, S.J., Bennett, G.N., and San, K.-Y. (2002) The effect of increasing NADH availability on the redistribution of metabolic fluxes in *Escherichia coli* chemostat cultures. *Metab. Eng.* **4**: 230–237.

36. Bibikov, S.I., Biran, R., Rudd, K.E., and Parkinson, J.S. (1997) A signal transducer for aerotaxis in *Escherichia coli*. *J. Bacteriol.* **179**: 4075–4079.

37. BioBoost (2015) Biomass based energy intermediates boosting biofuel production – executive summary Ganderkesee. http://www.bioboost.eu/home.php

38. Biswas, R., Yamaoka, M., Nakayama, H., Kondo, T., Yoshida, K., Bisaria, V.S., and Kondo, A. (2012) Enhanced production of 2,3-butanediol by engineered *Bacillus subtilis*. *Appl. Microbiol. Biotechnol.* **94**: 651–658.

39. Blombach, B., Arndt, A., Auchter, M., and Eikmanns, B.J. (2009) L-valine production during growth of pyruvate dehydrogenase complex-deficient *Corynebacterium glutamicum* in the presence of ethanol or by inactivation of the transcriptional regulator SugR. *Appl. Environ. Microbiol.* **75**: 1197–1200.

40. Blombach, B. and Eikmanns, B.J. (2011) Current knowledge on isobutanol production with *Escherichia coli*, *Bacillus subtilis* and *Corynebacterium glutamicum*.

*Bioeng. Bugs* **2**: 346–350.

41. Blombach, B., Hans, S., Bathe, B., and Eikmanns, B.J. (2009) Acetohydroxyacid synthase, a novel target for improvement of L-lysine production by *Corynebacterium glutamicum*. *Appl. Environ. Microbiol.* **75**: 419–427.

42. Blombach, B., Riester, T., Wieschalka, S., Ziert, C., Youn, J.-W., Wendisch, V.F., and Eikmanns, B.J. (2011) *Corynebacterium glutamicum* tailored for efficient isobutanol production. *Appl. Environ. Microbiol.* **77**: 3300–3310.

43. Blombach, B. and Seibold, G.M. (2010) Carbohydrate metabolism in *Corynebacterium glutamicum* and applications for the metabolic engineering of L-lysine production strains. *Appl. Microbiol. Biotechnol.* **86**: 1313–1322.

44. Bolger, A.M., Lohse, M., and Usadel, B. (2014) Trimmomatic: a flexible trimmer for Illumina sequence data. *Bioinformatics* **30**: 2114–2120.

45. Borisov, V.B., Forte, E., Siletsky, S.A., Arese, M., Davletshin, A.I., Sarti, P., and Giuffrè, A. (2015) Cytochrome *bd* protects bacteria against oxidative and nitrosative stress: A potential target for next-generation antimicrobial agents. *Biochem.* **80**: 565–575.

46. Borisov, V.B., Gennis, R.B., Hemp, J., and Verkhovsky, M.I. (2011) The cytochrome *bd* respiratory oxygen reductases. *Biochim. Biophys. Acta - Bioenerg.* **1807**: 1398–1413.

47. Borisov, V.B. and Verkhovsky, M.I. (2015) Oxygen as acceptor. *EcoSal Plus* **6**.

48. Bott, M. (2007) Offering surprises: TCA cycle regulation in *Corynebacterium glutamicum*. *Trends Microbiol.* **15**: 417–425.

49. Bott, M. and Eikmanns, B.J. (2013) TCA cycle and glyoxylate shunt of *Corynebacterium glutamicum*. In, Yukawa,H. and Inui,M. (eds), *Corynebacterium glutamicum: biology and biotechnology*. Springer, Berlin, Heidelberg, pp. 281–313.

50. Bott, M. and Niebisch, A. (2005) Respiratory energy metabolism. In, Eggeling,L. and Bott,M. (eds), *Handbook of Corynebacterium glutamicum*. CRC Press, Boca Raton, FL, USA, pp. 305–332.

51. Bott, M. and Niebisch, A. (2003) The respiratory chain of *Corynebacterium glutamicum*. *J. Biotechnol.* **104**: 129–153.

52. Boucher, M.., Chaala, A., Pakdel, H., and Roy, C. (2000) Bio-oils obtained by vacuum pyrolysis of softwood bark as a liquid fuel for gas turbines. Part II: Stability and ageing of bio-oil and its blends with methanol and a pyrolytic aqueous phase. *Biomass and Bioenergy* **19**: 351–361.

53. Boucher, M.., Chaala, A., and Roy, C. (2000) Bio-oils obtained by vacuum pyrolysis of softwood bark as a liquid fuel for gas turbines. Part I: Properties of bio-oil and its blends with methanol and a pyrolytic aqueous phase. *Biomass and Bioenergy* **19**: 337–350.

54. Bozell, J.J. and Petersen, G.R. (2010) Technology development for the production of biobased products from biorefinery carbohydrates – the US Department of Energy's "Top 10" revisited. *Green Chem.* **12**: 539.

55. BP p.l.c. (2017) BP statistical review of world energy 2017, 66th edition.

56. Brat, D. and Boles, E. (2013) Isobutanol production from D-xylose by recombinant *Saccharomyces cerevisiae*. *FEMS Yeast Res.* **13**: 241–244.

57. Bremer, H. and Dennis, P.P. (2008) Modulation of chemical composition and other parameters of the cell at different exponential growth rates. *EcoSal Plus* **3**.

58. Bridgwater, A. (2000) Fast pyrolysis processes for biomass. *Renew. Sustain. Energy Rev.* **4**: 1–73.

59. Bridgwater, A. V. (2012) Upgrading biomass fast pyrolysis liquids. *Environ. Prog. Sustain. Energy* **31**: 261–268.

60. Bridgwater, A.V. (2017) Biomass conversion technologies: fast pyrolysis liquids from biomass: quality and upgrading. In, Rabaçal,M., Ferreira,A.F., Silva,C.A.M., and Costa,M. (eds), *Biorefineries – targeting energy, high value products and waste valorisation*. Springer International Publishing, Cham, pp. 55–98.

61. Brinkrolf, K., Brune, I., and Tauch, A. (2006) Transcriptional regulation of catabolic pathways for aromatic compounds in *Corynebacterium glutamicum*. *Genet. Mol. Res.* **5**: 773–789.

62. Brinkrolf, K., Ploger, S., Solle, S., Brune, I., Nentwich, S.S., Huser, A.T., *et al.* (2008) The LacI/GalR family transcriptional regulator UriR negatively controls uridine utilization of *Corynebacterium glutamicum* by binding to catabolite-responsive element (*cre*)-like sequences. *Microbiology* **154**: 1068–1081.

63. Brinkrolf, K., Schröder, J., Pühler, A., and Tauch, A. (2010) The transcriptional regulatory repertoire of Corynebacterium glutamicum: reconstruction of the network controlling pathways involved in lysine and glutamate production. *J. Biotechnol.* **149**: 173–182.

64. Brockmann-Gretza, O. and Kalinowski, J. (2006) Global gene expression during stringent response in *Corynebacterium glutamicum* in presence and absence of the *rel* gene encoding (p)ppGpp synthase. *BMC Genomics* **7**: 230.

65. Brosius, J., Dull, T.J., Sleeter, D.D., and Noller, H.F. (1981) Gene organization and primary structure of a ribosomal RNA operon from *Escherichia coli*. *J. Mol. Biol.* **148**: 107–127.

66. Brosse, N., Hussin, M.H., and Rahim, A.A. (2017) Organosolv processes. *Adv. Biochem. Eng. Biotechnol.* 1–24.

67. Brosse, N., Mohamad Ibrahim, M.N., and Abdul Rahim, A. (2011) Biomass to bioethanol: initiatives of the future for lignin. *ISRN Mater. Sci.* **2011**: 1–10.

68. Brune, I., Brinkrolf, K., Kalinowski, J., Pühler, A., and Tauch, A. (2005) The individual and common repertoire of DNA-binding transcriptional regulators of *Corynebacterium glutamicum*, *Corynebacterium efficiens*, *Corynebacterium diphtheriae* and *Corynebacterium jeikeium* deduced from the complete genome . *BMC Genomics* **6**: 86.

69. Buchholz, J., Graf, M., Blombach, B., and Takors, R. (2014) Improving the carbon balance of fermentations by total carbon analyses. *Biochem. Eng. J.* **90**: 162–169.

70. Buchholz, J., Graf, M., Freund, A., Busche, T., Kalinowski, J., Blombach, B., and Takors, R. (2014) $CO_2/HCO_3^-$ perturbations of simulated large scale gradients in a scale-down device cause fast transcriptional responses in *Corynebacterium*

*glutamicum*. *Appl. Microbiol. Biotechnol.* **98**: 8563–8572.

71. Buchholz, J., Schwentner, A., Brunnenkan, B., Gabris, C., Grimm, S., Gerstmeir, R., *et al.* (2013) Platform engineering of *Corynebacterium glutamicum* with reduced pyruvate dehydrogenase complex activity for improved production of L-lysine, L-valine, and 2-ketoisovalerate. *Appl. Environ. Microbiol.* **79**: 5566–5575.

72. Bundesministerium für Bildung und Forschung (BMBF) (2010) Nationale Forschungsstrategie Bioökonomie 2030: unser Weg zu einer bio-basierten Wirtschaft, Bonn. *https://www.bmbf.de/pub/Nationale_Forschungsstrategie_Biooekonomie_2030.pdf*

73. Bunn, H.F. and Poyton, R.O. (1996) Oxygen sensing and molecular adaptation to hypoxia. *Physiol Rev* **76**: 839–885.

74. Burkovski, A. (2015) *Corynebacterium glutamicum*: from systems biology to biotechnological applications 1st ed. Caister Academic Press, Norfolk, UK.

75. Burkovski, A. (2005) Nitrogen metabolism and its regulation. In, Eggeling,L. and Bott,M. (eds), *Handbook of Corynebacterium glutamicum*. CRC Press, Boca Raton, FL, USA, pp. 333–349.

76. Buschke, N., Becker, J., Schäfer, R., Kiefer, P., Biedendieck, R., and Wittmann, C. (2013) Systems metabolic engineering of xylose-utilizing *Corynebacterium glutamicum* for production of 1,5-diaminopentane. *Biotechnol. J.* **8**: 557–570.

77. Buschke, N., Schröder, H., and Wittmann, C. (2011) Metabolic engineering of *Corynebacterium glutamicum* for production of 1,5-diaminopentane from hemicellulose. *Biotechnol. J.* **6**: 306–317.

78. Bylund, F., Collet, E., Enfors, S.-O., and Larsson, G. (1998) Substrate gradient formation in the large-scale bioreactor lowers cell yield and increases by-product formation. *Bioprocess Eng.* **18**: 171.

79. Cameron, D.C., Altaras, N.E., Hoffman, M.L., and Shaw, A.J. (1998) Metabolic engineering of propanediol pathways. *Biotechnol. Prog.* **14**: 116–125.

80. Cameron, D.C. and Cooney, C.L. (1986) A novel fermentation: the production of R(-)-1,2-propanediol and acetol by *Clostridium thermosaccharolyticum*. *Nat. Biotechnol.* **4**: 651–654.

81. Chang, A.C. and Cohen, S.N. (1978) Construction and characterization of amplifiable multicopy DNA cloning vehicles derived from the P15A cryptic miniplasmid. *J. Bacteriol.* **134**: 1141–1156.

82. Chen, C.-T. and Liao, J.C. (2016) Frontiers in microbial 1-butanol and isobutanol production. *FEMS Microbiol. Lett.* **363**: fnw020.

83. Chen, D., Cen, K., Jing, X., Gao, J., Li, C., and Ma, Z. (2017) An approach for upgrading biomass and pyrolysis product quality using a combination of aqueous phase bio-oil washing and torrefaction pretreatment. *Bioresour. Technol.* **233**: 150–158.

84. Chen, H. (2014) Biotechnology of lignocellulose: theory and practice. Springer Netherlands, Dordrecht.

85. Chen, T., Zhu, N., and Xia, H. (2014) Aerobic production of succinate from arabinose

by metabolically engineered *Corynebacterium glutamicum*. *Bioresour. Technol.* **151**: 411–414.

86. Chen, X., Xiu, Z., Wang, J., Zhang, D., and Xu, P. (2003) Stoichiometric analysis and experimental investigation of glycerol bioconversion to 1,3-propanediol by *Klebsiella pneumoniae* under microaerobic conditions. *Enzyme Microb. Technol.* **33**: 386–394.

87. Chen, Z., Huang, J., Wu, Y., Wu, W., Zhang, Y., and Liu, D. (2017) Metabolic engineering of *Corynebacterium glutamicum* for the production of 3-hydroxypropionic acid from glucose and xylose. *Metab. Eng.* **39**: 151–158.

88. Chen, Z. and Liu, D. (2016) Toward glycerol biorefinery: metabolic engineering for the production of biofuels and chemicals from glycerol. *Biotechnol. Biofuels* **9**: 205.

89. Cherubini, F. (2010) The biorefinery concept: using biomass instead of oil for producing energy and chemicals. *Energy Convers. Manag.* **51**: 1412–1421.

90. Cherubini, F. and Ulgiati, S. (2010) Crop residues as raw materials for biorefinery systems – A LCA case study. *Appl. Energy* **87**: 47–57.

91. Clark, D.P. (1989) The fermentation pathways of *Escherichia coli*. *FEMS Microbiol. Lett.* **63**: 223–234.

92. Clomburg, J.M. and Gonzalez, R. (2011) Metabolic engineering of *Escherichia coli* for the production of 1,2-propanediol from glycerol. *Biotechnol. Bioeng.* **108**: 867–879.

93. Compan, I. and Touati, D. (1994) Anaerobic activation of arcA transcription in *Escherichia coli*: roles of Fnr and ArcA. *Mol. Microbiol.* **11**: 955–964.

94. Cooper, R.A. (1984) Metabolism of methylglyoxal in microorganisms. *Ann. Rev. Microbiol* **38**: 49–68.

95. Cordes, C., Möckel, B., Eggeling, L., and Sahm, H. (1992) Cloning, organization and functional analysis of *ilvA*, *ilvB* and *ilvC* genes from *Corynebacterium glutamicum*. *Gene* **112**: 113–116.

96. Crestini, C., Melone, F., Sette, M., and Saladino, R. (2011) Milled wood lignin: a linear oligomer. *Biomacromolecules* **12**: 3928–3935.

97. Cserjan-Puschmann, M., Kramer, W., Duerrschmid, E., Striedner, G., and Bayer, K. (1999) Metabolic approaches for the optimisation of recombinant fermentation processes. *Appl. Microbiol. Biotechnol.* **53**: 43–50.

98. Dahmen, N., Abeln, J., Eberhard, M., Kolb, T., Leibold, H., Sauer, J., *et al.* (2016) The bioliq process for producing synthetic transportation fuels. *Wiley Interdiscip. Rev. Energy Environ.* **6**: e236.

99. Dahmen, N., Dinjus, E., Kolb, T., Arnold, U., Leibold, H., and Stahl, R. (2012) State of the art of the bioliq® process for synthetic biofuels production. *Environ. Prog. Sustain. Energy* **31**: 176–181.

100. Dahmen, N., Henrich, E., Dinjus, E., and Weirich, F. (2012) The bioliq® bioslurry gasification process for the production of biosynfuels, organic chemicals, and energy. *Energy. Sustain. Soc.* **2**: 3.

101. Dasari, M.A., Kiatsimkul, P.P., Sutterlin, W.R., and Suppes, G.J. (2005) Low-pressure hydrogenolysis of glycerol to propylene glycol. *Appl. Catal. A Gen.* **281**:

225–231.

102. Datta, N., Hedges, R.W., Shaw, E.J., Sykes, R.B., and Richmond, M.H. (1971) Properties of an R factor from *Pseudomonas aeruginosa*. *J. Bacteriol.* **108**: 1244–1249.

103. Demirbas, A. (2007) The influence of temperature on the yields of compounds existing in bio-oils obtained from biomass samples via pyrolysis. *Fuel Process. Technol.* **88**: 591–597.

104. Desai, S.H., Rabinovitch-Deere, C.A., Fan, Z., and Atsumi, S. (2015) Isobutanol production from cellobionic acid in *Escherichia coli*. *Microb. Cell Fact.* **14**: 52.

105. Desai, S.H., Rabinovitch-Deere, C.A., Tashiro, Y., and Atsumi, S. (2014) Isobutanol production from cellobiose in *Escherichia coli*. *Appl. Microbiol. Biotechnol.* **98**: 3727–3736.

106. Deutscher, J. (2008) The mechanisms of carbon catabolite repression in bacteria. *Curr. Opin. Microbiol.* **11**: 87–93.

107. Dhar, K.S., Wendisch, V.F., and Nampoothiri, K.M. (2016) Engineering of *Corynebacterium glutamicum* for xylitol production from lignocellulosic pentose sugars. *J. Biotechnol.* **230**: 63–71.

108. Dhyani, V. and Bhaskar, T. (2017) A comprehensive review on the pyrolysis of lignocellulosic biomass. *Renew. Energy*. In press. https://doi.org/10.1016/j.renene.2017.

109. Dick, T., Lee, B.H., and Murugasu-Oei, B. (1998) Oxygen depletion induced dormancy in *Mycobacterium smegmatis*. *FEMS Microbiol. Lett.* **163**: 159–164.

110. Diebold, J. (2000) A review of the chemical and physical mechanisms of the storage stability of fast pyrolysis bio-oils. National Renewable Energy Laboratory, Golden, CO (US).

111. Dien, B.S., Cotta, M.A., and Jeffries, T.W. (2003) Bacteria engineered for fuel ethanol production: current status. *Appl. Microbiol. Biotechnol.* **63**: 258–266.

112. Dillies, M.-A., Rau, A., Aubert, J., Hennequet-Antier, C., Jeanmougin, M., Servant, N., *et al.* (2013) A comprehensive evaluation of normalization methods for Illumina high-throughput RNA sequencing data analysis. *Brief. Bioinform.* **14**: 671–683.

113. Directorate-General for Research and Innovation (European Commission) (2012) Innovating for sustainable growth: a bioeconomy for europe, Brussels. DOI: 10.2777/6462.

114. Dominguez, H., Nezondet, C., Lindley, N.D., and Cocaign, M. (1993) Modified carbon flux during oxygen limited growth of *Corynebacterium glutamicum* and the consequences for amino acid overproduction. *Biotechnol. Lett.* **15**: 449–454.

115. Donnelly, M.I., Millard, C.S., Clark, D.P., Chen, M.J., and Rathke, J.W. (1998) A novel fermentation pathway in an *Escherichia coli* mutant producing succinic acid, acetic acid, and ethanol. *Appl. Biochem. Biotechnol.* **70–72**: 187–198.

116. Doran, P.M. (1995) Bioprocess engineering principles Academic Press Ltd., London.

117. Dower, W.J., Miller, J.F., and Ragsdale, C.W. (1988) High efficiency transformation of *E. coli* by high voltage electroporation. *Nucleic Acids Res.* **16**: 6127–6145.

118. Duff, S.J.B. and Murray, W.D. (1996) Bioconversion of forest products industry waste cellulosics to fuel ethanol: A review. *Bioresour. Technol.* **55**: 1–33.

119. Van Dyk, J.S. and Pletschke, B.I. (2012) A review of lignocellulose bioconversion using enzymatic hydrolysis and synergistic cooperation between enzymes – factors affecting enzymes, conversion and synergy. *Biotechnol. Adv.* **30**: 1458–1480.

120. Ederer, M., Steinsiek, S., Stagge, S., Rolfe, M.D., Ter Beek, A., Knies, D., *et al.* (2014) A mathematical model of metabolism and regulation provides a systems-level view of how *Escherichia coli* responds to oxygen. *Front. Microbiol.* **5**: 124.

121. Eggeling, L. and Reyes, O. (2005) Experiments. In, Eggeling,L. and Bott,M. (eds), *Handbook of Corynebacterium glutamicum*. CRC Press, Boca Raton, FL, USA, pp. 421–422.

122. Ehira, S., Ogino, H., Teramoto, H., Inui, M., and Yukawa, H. (2009) Regulation of quinone oxidoreductase by the redox-sensing transcriptional regulator QorR in *Corynebacterium glutamicum*. *J. Biol. Chem.* **284**: 16736–16742.

123. Ehira, S., Shirai, T., Teramoto, H., Inui, M., and Yukawa, H. (2008) Group 2 sigma factor SigB of *Corynebacterium glutamicum* positively regulates glucose metabolism under conditions of oxygen deprivation. *Appl. Environ. Microbiol.* **74**: 5146–5152.

124. Ehira, S., Teramoto, H., Inui, M., and Yukawa, H. (2009) Regulation of *Corynebacterium glutamicum* heat shock response by the extracytoplasmic-function sigma factor SigH and transcriptional regulators HspR and HrcA. *J. Bacteriol.* **191**: 2964–2972.

125. Eikmanns, B.J. (2005) Central metabolism: tricarboxylic acid cycle and anaplerotic reactions. In, Eggeling,L. and Bott,M. (eds), *Handbook of Corynebacterium glutamicum*. CRC Press, Boca Raton, FL, USA, pp. 241–276.

126. Eikmanns, B.J. and Blombach, B. (2014) The pyruvate dehydrogenase complex of *Corynebacterium glutamicum*: an attractive target for metabolic engineering. *J. Biotechnol.* **192 Pt B**: 339–345.

127. Eikmanns, B.J., Metzger, M., Reinscheid, D., Kircher, M., and Sahm, H. (1991) Amplification of three threonine biosynthesis genes in *Corynebacterium glutamicum* and its influence on carbon flux in different strains. *Appl. Microbiol. Biotechnol.* **34**: 617–622.

128. El-Chichakli, B., von Braun, J., Lang, C., Barben, D., and Philp, J. (2016) Policy: Five cornerstones of a global bioeconomy. *Nature* **535**: 221–223.

129. European Commission (2007) Communication from the Commission to the Council and the European Parliament – renewable energy road map – renewable energies in the 21st century: building a more sustainable future, Brussels. http://eur-lex.europa.eu/legal-content/EN/TXT/?uri=celex:52006DC0848

130. European Commission (2010) Europe 2020: a European strategy for smart, sustainable and inclusive growth, Brussels. http://ec.europa.eu/eu2020/pdf/COMPLET%20EN%20BARROSO%20%20%20007%20-%20Europe%202020%20-%20EN%20version.pdf

131. Fahey, R.C. (2013) Glutathione analogs in prokaryotes. *Biochim. Biophys. Acta - Gen. Subj.* **1830**: 3182–3198.

132. Fantini, M. (2017) Biomass availability, potential and characteristics. In, Rabaçal,M., Ferreira,A.F., Silva,C.A.M., and Costa,M. (eds), *Biorefineries – targeting energy, high value products and waste valorisation*. Springer International Publishing, Cham, pp. 21–54.

133. Fatih Demirbas, M. (2009) Biorefineries for biofuel upgrading: a critical review. *Appl. Energy* **86**: S151–S161.

134. Fei, F., Mendonca, M.L., McCarry, B.E., Bowdish, D.M.E., and Surette, M.G. (2016) Metabolic and transcriptomic profiling of *Streptococcus intermedius* during aerobic and anaerobic growth. *Metabolomics* **12**: 46.

135. Feklístov, A., Sharon, B.D., Darst, S.A., and Gross, C.A. (2014) Bacterial sigma factors: A historical, structural, and genomic perspective. *Annu. Rev. Microbiol.* **68**: 357–376.

136. Feng, J., Che, Y., Milse, J., Yin, Y.-J., Liu, L., Rückert, C., *et al.* (2006) The gene ncgl2918 encodes a novel maleylpyruvate isomerase that needs mycothiol as cofactor and links mycothiol biosynthesis and gentisate assimilation in *Corynebacterium glutamicum*. *J. Biol. Chem.* **281**: 10778–10785.

137. Ferguson, G.P., Tötemeyer, S., MacLean, M.J., and Booth, I.R. (1998) Methylglyoxal production in bacteria: suicide or survival? *Arch. Microbiol.* **170**: 209–218.

138. Ferreira, A.F. (2017) Biorefinery concept. In, Rabaçal,M., Ferreira,A.F., Silva,C.A.M., and Costa,M. (eds), *Biorefineries – targeting energy, high value products and waste valorisation*. Springer International Publishing, Cham, pp. 1–20.

139. Fischer, E. and Sauer, U. (2003) Metabolic flux profiling of *Escherichia coli* mutants in central carbon metabolism using GC-MS. *Eur. J. Biochem.* **270**: 880–891.

140. Flach, B., Lieberz, S., Rondon, M., Williams, B., and Wilson, C. (2016) EU-28 biofuels annual 2016 (NL6021), USDA Foreign Agricultural Service. https://gain.fas.usda.gov/Recent%20GAIN%20Publications/Biofuels%20Annual_The%20Hague_EU-28_6-29-2016.pdf

141. Floudas, D., Binder, M., Riley, R., Barry, K., Blanchette, R. a, Henrissat, B., *et al.* (2012) The paleozoic origin of enzymatic lignin decomposition reconstructed from 31 fungal genomes. *Science* **336**: 1715–1719.

142. Follmann, M., Ochrombel, I., Krämer, R., Trötschel, C., Poetsch, A., Rückert, C., *et al.* (2009) Functional genomics of pH homeostasis in *Corynebacterium glutamicum* revealed novel links between pH response, oxidative stress, iron homeostasis and methionine synthesis. *BMC Genomics* **10**: 621.

143. Forsberg, K.J., Patel, S., Witt, E., Wang, B., Ellison, T.D., and Dantas, G. (2015) Identification of genes conferring tolerance to lignocellulose-derived inhibitors by functional selections in soil metagenomes. *Appl. Environ. Microbiol.* **82**: 528–537.

144. Fratini, E., Bonini, M., Oasmaa, A., Solantausta, Y., Teixeira, J., and Baglioni, P. (2006) SANS analysis of the microstructural evolution during the aging of pyrolysis oils from biomass. *Langmuir* **22**: 306–312.

145. Freudl, R. (2017) Beyond amino acids: use of the *Corynebacterium glutamicum* cell factory for the secretion of heterologous proteins. *J. Biotechnol.* **258**: 101–109.

146. Freudl, R. (2015) *Corynebacterium glutamicum* as a platform organism for the

secretory production of heterologous proteins. In, Burkovski,A. (ed), *Corynebacterium glutamicum: from systems biology to biotechnological applications*. Caister Academic Press, Norfolk, UK, pp. 161–178.

147. Frunzke, J. and Bott, M. (2008) Regulation of iron homeostasis in *Corynebacterium glutamicum*. In, Burkovski,A. (ed), *Corynebacteria: Genomics and Molecular Biology*. Caister Academic Press, Norfolk, United Kingdom.

148. Frunzke, J., Bramkamp, M., Schweitzer, J.-E., and Bott, M. (2008) Population heterogeneity in *Corynebacterium glutamicum* ATCC 13032 caused by prophage CGP3. *J. Bacteriol.* **190**: 5111–5119.

149. Fuchs, S., Pané-Farré, J., Kohler, C., Hecker, M., and Engelmann, S. (2007) Anaerobic gene expression in *Staphylococcus aureus*. *J. Bacteriol.* **189**: 4275–4289.

150. Fuchs, T.M., Eisenreich, W., Heesemann, J., and Goebel, W. (2012) Metabolic adaptation of human pathogenic and related nonpathogenic bacteria to extra- and intracellular habitats. *FEMS Microbiol. Rev.* **36**: 435–462.

151. Gaigalat, L., Schlüter, J.-P., Hartmann, M., Mormann, S., Tauch, A., Pühler, A., and Kalinowski, J. (2007) The DeoR-type transcriptional regulator SugR acts as a repressor for genes encoding the phosphoenolpyruvate:sugar phosphotransferase system (PTS) in *Corynebacterium glutamicum*. *BMC Mol. Biol.* **8**: 104.

152. Galinier, A. and Deutscher, J. (2017) Sophisticated regulation of transcriptional factors by the bacterial phosphoenolpyruvate: sugar phosphotransferase system. *J. Mol. Biol.* **429**: 773–789.

153. Gancedo, J.M. (1998) Yeast carbon catabolite repression. *Microbiol. Mol. Biol. Rev.* **62**: 334–361.

154. Geddes, C.C., Mullinnix, M.T., Nieves, I.U., Peterson, J.J., Hoffman, R.W., York, S.W., *et al.* (2011) Simplified process for ethanol production from sugarcane bagasse using hydrolysate-resistant *Escherichia coli* strain MM160. *Bioresour. Technol.* **102**: 2702–2711.

155. Georgellis, D., Kwon, O., and Lin, E.C. (2001) Quinones as the redox signal for the *arc* two-component system of bacteria. *Science* **292**: 2314–2316.

156. Gerosa, L., Kochanowski, K., Heinemann, M., and Sauer, U. (2013) Dissecting specific and global transcriptional regulation of bacterial gene expression. *Mol. Syst. Biol.* **9**: 658.

157. Gerstmeir, R., Cramer, A., Dangel, P., Schaffer, S., and Eikmanns, B.J. (2004) RamB, a novel transcriptional regulator of genes involved in acetate metabolism of *Corynebacterium glutamicum*. *J. Bacteriol.* **186**: 2798–2809.

158. Gerstmeir, R., Wendisch, V.F., Schnicke, S., Ruan, H., Farwick, M., Reinscheid, D., and Eikmanns, B.J. (2003) Acetate metabolism and its regulation in *Corynebacterium glutamicum*. *J. Biotechnol.* **104**: 99–122.

159. Gibson, D.G. (2011) Enzymatic assembly of overlapping DNA fragments. *Methods Enzymol.* **498**: 349–361.

160. Gibson, D.G., Young, L., Chuang, R.-Y., Venter, J.C., Hutchison, C.A., and Smith, H.O. (2009) Enzymatic assembly of DNA molecules up to several hundred kilobases. *Nat. Methods* **6**: 343–345.

161. Gírio, F.M., Fonseca, C., Carvalheiro, F., Duarte, L.C., Marques, S., and Bogel-Łukasik, R. (2010) Hemicelluloses for fuel ethanol: a review. *Bioresour. Technol.* **101**: 4775–4800.

162. Gnansounou, E. and Dauriat, A. (2010) Techno-economic analysis of lignocellulosic ethanol: a review. *Bioresour. Technol.* **101**: 4980–4991.

163. Goncharuk, V. V., Bagrii, V.A., Mel'nik, L.A., Chebotareva, R.D., and Bashtan, S.Y. (2010) The use of redox potential in water treatment processes. *J. Water Chem. Technol.* **32**: 1–9.

164. Gopinath, V., Meiswinkel, T.M., Wendisch, V.F., and Nampoothiri, K.M. (2011) Amino acid production from rice straw and wheat bran hydrolysates by recombinant pentose-utilizing *Corynebacterium glutamicum*. *Appl. Microbiol. Biotechnol.* **92**: 985–996.

165. Gopinath, V., Murali, A., Dhar, K.S., and Nampoothiri, K.M. (2012) *Corynebacterium glutamicum* as a potent biocatalyst for the bioconversion of pentose sugars to value-added products. *Appl. Microbiol. Biotechnol.* **93**: 95–106.

166. Görke, B. and Stülke, J. (2008) Carbon catabolite repression in bacteria: many ways to make the most out of nutrients. *Nat. Rev. Microbiol.* **6**: 613–624.

167. Gosink, K.K., Burón-Barral, M. del C., and Parkinson, J.S. (2006) Signaling interactions between the aerotaxis transducer Aer and heterologous chemoreceptors in *Escherichia coli*. *J. Bacteriol.* **188**: 3487–3493.

168. Gourse, R.L., Ross, W., and Rutherford, S.T. (2006) General pathway for turning on promoters transcribed by RNA polymerases containing alternative sigma factors. *J. Bacteriol.* **188**: 4589–4591.

169. Grabar, T.B., Zhou, S., Shanmugam, K.T., Yomano, L.P., and Ingram, L.O. (2006) Methylglyoxal bypass identified as source of chiral contamination in L(+) and D(-)-lactate fermentations by recombinant *Escherichia coli*. *Biotechnol. Lett.* **28**: 1527–1535.

170. de Graef, M.R., Alexeeva, S., Snoep, J.L., and Teixeira de Mattos, M.J. (1999) The steady-state internal redox state (NADH/NAD) reflects the external redox state and is correlated with catabolic adaptation in *Escherichia coli*. *J. Bacteriol.* **181**: 2351–2357.

171. Grahl, N. and Cramer, R.A. (2010) Regulation of hypoxia adaptation: an overlooked virulence attribute of pathogenic fungi? *Med. Mycol.* **48**: 1–15.

172. Grant, A.W., Steel, G., Waugh, H., and Ellis, E.M. (2003) A novel aldo-keto reductase from *Escherichia coli* can increase resistance to methylglyoxal toxicity. *FEMS Microbiol. Lett.* **218**: 93–99.

173. Green, J. and Paget, M.S. (2004) Bacterial redox sensors. *Nat. Rev. Microbiol.* **2**: 954–966.

174. Grünberger, A., van Ooyen, J., Paczia, N., Rohe, P., Schiendzielorz, G., Eggeling, L., *et al.* (2012) Beyond growth rate 0.6: *Corynebacterium glutamicum* cultivated in highly diluted environments. *Biotechnol. Bioeng.* **110**: 220–228.

175. Gu, J., Zhou, J., Zhang, Z., Kim, C.H., Jiang, B., Shi, J., and Hao, J. (2017) Isobutanol and 2-ketoisovalerate production by *Klebsiella pneumoniae* via a native pathway.

*Metab. Eng.* **43**: 71–84.

176. Gucho, E.M., Shahzad, K., Bramer, E.A., Akhtar, N.A., and Brem, G. (2015) Experimental study on dry torrefaction of beech wood and miscanthus. *Energies* **8**: 3903–3923.

177. Gunsalus, R.P. and Park, S.-J. (1994) Aerobic-anaerobic gene regulation in *Escherichia coli*: control by the ArcAB and Fnr regulons. *Res. Microbiol.* **145**: 437–450.

178. Gutmann, M., Hoischen, C., and Krämer, R. (1992) Carrier-mediated glutamate secretion by *Corynebacterium glutamicum* under biotin limitation. *Biochim. Biophys. Acta* **1112**: 115–123.

179. Hahn-Hägerdal, B., Galbe, M., Gorwa-Grauslund, M., Lidén, G., and Zacchi, G. (2006) Bio-ethanol – the fuel of tomorrow from the residues of today. *Trends Biotechnol.* **24**: 549–556.

180. Hanahan, D. (1983) Studies on transformation of *Escherichia coli* with plasmids. *J. Mol. Biol.* **166**: 557–580.

181. Hansen, A.S.L., Lennen, R.M., Sonnenschein, N., and Herrgård, M.J. (2017) Systems biology solutions for biochemical production challenges. *Curr. Opin. Biotechnol.* **45**: 85–91.

182. Hänssler, E., Müller, T., Jessberger, N., Völzke, A., Plassmeier, J., Kalinowski, J., *et al.* (2007) FarR, a putative regulator of amino acid metabolism in *Corynebacterium glutamicum*. *Appl. Microbiol. Biotechnol.* **76**: 625–632.

183. Hasegawa, S., Suda, M., Uematsu, K., Natsuma, Y., Hiraga, K., Jojima, T., *et al.* (2013) Engineering of *Corynebacterium glutamicum* for high-yield L-valine production under oxygen deprivation conditions. *Appl. Environ. Microbiol.* **79**: 1250–1257.

184. Hasegawa, S., Uematsu, K., Natsuma, Y., Suda, M., Hiraga, K., Jojima, T., *et al.* (2012) Improvement of the redox balance increases L-valine production by *Corynebacterium glutamicum* under oxygen deprivation conditions. *Appl. Environ. Microbiol.* **78**: 865–875.

185. Hasona, A., Kim, Y., Healy, F.G., Ingram, L.O., and Shanmugam, K.T. (2004) Pyruvate formate lyase and acetate kinase are essential for anaerobic growth of *Escherichia coli* on xylose. *J. Bacteriol.* **186**: 7593–7600.

186. Hatti-Kaul, R., Törnvall, U., Gustafsson, L., and Börjesson, P. (2007) Industrial biotechnology for the production of bio-based chemicals – a cradle-to-grave perspective. *Trends Biotechnol.* **25**: 119–124.

187. Hedlund, E. and Deng, Q. (2017) Single-cell RNA sequencing: Technical advancements and biological applications. *Mol. Aspects Med.* **59**: 36–46.

188. Heider, S.A.E. and Wendisch, V.F. (2015) Engineering microbial cell factories: metabolic engineering of *Corynebacterium glutamicum* with a focus on non-natural products. *Biotechnol. J.* **10**: 1170–1184.

189. Heller, M.J. (2002) DNA microarray technology: devices, systems, and applications. *Annu. Rev. Biomed. Eng.* **4**: 129–153.

190. Henderson, J. and Brooks, A. (2010) Improved amino acid methods using Agilent ZORBAX Eclipse Plus C18 columns for a variety of Agilent LC instrumentation and separation goals [5990-4547EN], Wilmington.
http: //www.chem.agilent.com/Library/applications/5990-4547EN.pdf.

191. Henrich, E., Dahmen, N., Dinjus, E., and Sauer, J. (2015) The role of biomass in a future world without fossil fuels. *Chemie Ing. Tech.* **87**: 1667–1685.

192. Henrich, E., Dahmen, N., Weirich, F., Reimert, R., and Kornmayer, C. (2016) Fast pyrolysis of lignocellulosics in a twin screw mixer reactor. *Fuel Process. Technol.* **143**: 151–161.

193. Hewitt, L.F. (1950) Oxidation-reduction potentials in bacteriology and biochemistry 6th ed. Baltimore, Williams and Wilkins, Edinburgh.

194. Heyer, A., Gätgens, C., Hentschel, E., Kalinowski, J., Bott, M., and Frunzke, J. (2012) The two-component system ChrSA is crucial for haem tolerance and interferes with HrrSA in haem-dependent gene regulation in *Corynebacterium glutamicum*. *Microbiology* **158**: 3020–3031.

195. Higashide, W., Li, Y., Yang, Y., and Liao, J.C. (2011) Metabolic engineering of *Clostridium cellulolyticum* for production of isobutanol from cellulose. *Appl. Environ. Microbiol.* **77**: 2727–2733.

196. Hilker, R., Stadermann, K.B., Doppmeier, D., Kalinowski, J., Stoye, J., Straube, J., *et al.* (2014) ReadXplorer – visualization and analysis of mapped sequences. *Bioinformatics* **30**: 2247–2254.

197. Himmel, M.E., Ding, S.-Y., Johnson, D.K., Adney, W.S., Nimlos, M.R., Brady, J.W., and Foust, T.D. (2007) Biomass recalcitrance: engineering plants and enzymes for biofuels production. *Science.* **315**: 804–807.

198. Holladay, J.E., White, J.F., Bozell, J.J., and Johnson, D. (2007) Top value added chemicals from biomass volume II – results of screening for potential candidates from biorefinery lignin, Pacific Northwest National Lab (PNNL).
https://www.pnnl.gov/main/publications/external/technical_reports/PNNL-16983.pdf.

199. Hong, S.H. and Lee, S.Y. (2000) Metabolic flux distribution in a metabolically engineered *Escherichia coli* strain producing succinic acid. *J. Microbiol. Biotechnol.* **10**: 496–501.

200. Hopper, D.J. and Cooper, R.A. (1971) The regulation of *Escherichia coli* methylglyoxal synthase; a new control site in glycolysis? *FEBS Lett.* **13**: 213–216.

201. Horton, R.M., Cai, Z.L., Ho, S.N., and Pease, L.R. (1990) Gene splicing by overlap extension: tailor-made genes using the polymerase chain reaction. *Biotechniques* **8**: 528–535.

202. Huang, M., Peabody, G., and Kao, K.C. (2016) Tolerance of microbial biocatalysts to feedstocks, products, and environmental conditions. In, Van Dien,S. (ed), *Metabolic engineering for bioprocess commercialization*. Springer International Publishing, Cham, pp. 73–100.

203. Ideker, T., Galitski, T., and Hood, L. (2001) A new approach to decoding life: systems biology. *Annu. Rev. Genomics Hum. Genet.* **2**: 343–372.

204. Ikeda, M., Baba, M., Tsukamoto, N., Komatsu, T., Mitsuhashi, S., and Takeno, S. (2009) Elucidation of genes relevant to the microaerobic growth of *Corynebacterium glutamicum*. *Biosci. Biotechnol. Biochem.* **73**: 2806–2808.

205. Ikeda, M. and Nakagawa, S. (2003) The *Corynebacterium glutamicum* genome: features and impacts on biotechnological processes. *Appl. Microbiol. Biotechnol.* **62**: 99–109.

206. Ingledew, W.J. and Poole, R.K. (1984) The respiratory chains of *Escherichia coli*. *Microbiol. Rev.* **48**: 222–271.

207. Inoue, Y., Ikemoto, S., Kitamura, K., and Kimura, A. (1992) Occurrence of a NADH-dependent methylglyoxal reducing system: conversion of methylglyoxal to acetol by aldehyde reductase from *Hansenula mrakii*. *J. Ferment. Bioeng.* **74**: 46–48.

208. Inui, M., Kawaguchi, H., Murakami, S., Vertès, A.A., and Yukawa, H. (2004) Metabolic engineering of *Corynebacterium glutamicum* for fuel ethanol production under oxygen-deprivation conditions. *J. Mol. Microbiol. Biotechnol.* **8**: 243–254.

209. Inui, M., Murakami, S., Okino, S., Kawaguchi, H., Vertès, A.A., and Yukawa, H. (2004) Metabolic analysis of *Corynebacterium glutamicum* during lactate and succinate productions under oxygen deprivation conditions. *J. Mol. Microbiol. Biotechnol.* **7**: 182–196.

210. Inui, M., Suda, M., Okino, S., Nonaka, H., Puskas, L.G., Vertes, A.A., and Yukawa, H. (2007) Transcriptional profiling of *Corynebacterium glutamicum* metabolism during organic acid production under oxygen deprivation conditions. *Microbiology* **153**: 2491–2504.

211. Ishii, J., Yoshimura, K., Hasunuma, T., and Kondo, A. (2013) Reduction of furan derivatives by overexpressing NADH-dependent Adh1 improves ethanol fermentation using xylose as sole carbon source with *Saccharomyces cerevisiae* harboring XR–XDH pathway. *Appl. Microbiol. Biotechnol.* **97**: 2597–2607.

212. Isikgor, F.H. and Becer, C.R. (2015) Lignocellulosic biomass: a sustainable platform for the production of bio-based chemicals and polymers. *Polym. Chem.* **6**: 4497–4559.

213. Jacobs, A. and Dahlman, O. (2001) Characterization of the molar masses of hemicelluloses from wood and pulps employing size exclusion chromatography and matrix-assisted laser desorption ionization time-of-flight mass spectrometry. *Biomacromolecules* **2**: 894–905.

214. Vander Jagt, D.L. (1993) Glyoxalase II: molecular characteristics, kinetics and mechanism. *Biochem. Soc. Trans.* **21**: 522–527.

215. Jakob, K., Satorhelyi, P., Lange, C., Wendisch, V.F., Silakowski, B., Scherer, S., and Neuhaus, K. (2007) Gene expression analysis of *Corynebacterium glutamicum* subjected to long-term lactic acid adaptation. *J. Bacteriol.* **189**: 5582–5590.

216. James G. Speight (1982) The chemistry and technology of petroleum 4th ed. CRC Press, Taylor and Francis Group, LLC, Boca Raton, FL, USA.

217. Jarboe, L.R., Wen, Z., Choi, D., and Brown, R.C. (2011) Hybrid thermochemical processing: fermentation of pyrolysis-derived bio-oil. *Appl. Microbiol. Biotechnol.* **91**: 1519–1523.

218. Jenkins, D.E., Schultz, J.E., and Matin, A. (1988) Starvation-induced cross protection

against heat or $H_2O_2$ challenge in *Escherichia coli*. *J. Bacteriol.* **170**: 3910–3914.

219. Jiang, M., Liu, S.-W., Ma, J.-F., Chen, K.-Q., Yu, L., Yue, F.-F., *et al.* (2010) Effect of growth phase feeding strategies on succinate production by metabolically engineered *Escherichia coli*. *Appl. Environ. Microbiol.* **76**: 1298–1300.

220. Jo, S., Yoon, J., Lee, S.-M., Um, Y., Han, S.O., and Woo, H.M. (2017) Modular pathway engineering of *Corynebacterium glutamicum* to improve xylose utilization and succinate production. *J. Biotechnol.* **258**: 69–78.

221. Johnson, D.T. and Taconi, K.A. (2007) The glycerin glut: options for the value-added conversion of crude glycerol resulting from biodiesel production. *Environ. Prog.* **26**: 338–348.

222. Jojima, T., Fujii, M., Mori, E., Inui, M., and Yukawa, H. (2010) Engineering of sugar metabolism of *Corynebacterium glutamicum* for production of amino acid L-alanine under oxygen deprivation. *Appl. Microbiol. Biotechnol.* **87**: 159–165.

223. Jojima, T., Inui, M., and Yukawa, H. (2013) Biorefinery applications of *Corynebacterium glutamicum*. In, Yukawa,H. and Inui,M. (eds), *Corynebacterium glutamicum: biology and biotechnology*. Springer, Berlin, Heidelberg, pp. 149–172.

224. Jojima, T., Inui, M., and Yukawa, H. (2015) Biotechnological application of *Corynebacterium glutamicum* under oxygen deprivation. In, Burkovski,A. (ed), *Corynebacterium glutamicum: from systems biology to biotechnological applications*. Caister Academic Press, Norfolk, UK, pp. 151–160.

225. Jojima, T., Noburyu, R., Sasaki, M., Tajima, T., Suda, M., Yukawa, H., and Inui, M. (2015) Metabolic engineering for improved production of ethanol by *Corynebacterium glutamicum*. *Appl. Microbiol. Biotechnol.* **99**: 1165–1172.

226. Joliff, G., Mathieu, L., Hahn, V., Bayan, N., Duchiron, F., Renaud, M., *et al.* (1992) Cloning and nucleotide sequence of the *csp1* gene encoding PS1, one of the two major secreted proteins of *Corynebacterium glutamicum*: the deduced N-terminal region of PS1 is similar to the *Mycobacterium* antigen 85 complex. *Mol. Microbiol.* **6**: 2349–2362.

227. de Jong, E. and Jungmeier, G. (2015) Biorefinery concepts in comparison to petrochemical refineries. In, *Industrial biorefineries & white biotechnology*. Elsevier, pp. 3–33.

228. Jönsson, L.J., Alriksson, B., Nilvebrant, N.-O., Sousa, F. de, Gorton, L., Jönsson, L., *et al.* (2013) Bioconversion of lignocellulose: inhibitors and detoxification. *Biotechnol. Biofuels* **6**: 16.

229. Jönsson, L.J., Palmqvist, E., Nilvebrant, N.-O., and Hahn-Hägerdal, B. (1998) Detoxification of wood hydrolysates with laccase and peroxidase from the white-rot fungus *Trametes versicolor*. *Appl. Microbiol. Biotechnol.* **49**: 691–697.

230. Jordan, P.A., Thomson, A.J., Ralph, E.T., Guest, J.R., and Green, J. (1997) FNR is a direct oxygen sensor having a biphasic response curve. *FEBS Lett.* **416**: 349–352.

231. Jothivasan, V.K. and Hamilton, C.J. (2008) Mycothiol: synthesis, biosynthesis and biological functions of the major low molecular weight thiol in actinomycetes. *Nat. Prod. Rep.* **25**: 1091.

232. Ju, L.-K., Chen, F., and Xia, Q. (2005) Monitoring microaerobic denitrification of

*Pseudomonas aeruginosa* by online NAD(P)H fluorescence. *J. Ind. Microbiol. Biotechnol.* **32**: 622–628.

233. Jung, J.-Y., Yun, H.S., Lee, J., and Oh, M.-K. (2011) Production of 1,2-propanediol from glycerol in *Saccharomyces cerevisiae*. *J. Microbiol. Biotechnol.* **21**: 846–853.

234. Kaboré, A.-K., Olmos, E., Fick, M., Blanchard, F., Guedon, E., and Delaunay, S. (2016) Aerobiosis–anaerobiosis transition has a significant impact on organic acid production by *Corynebacterium glutamicum*. *Process Biochem.* **52**: 10–21.

235. Kabus, A., Niebisch, A., and Bott, M. (2007) Role of cytochrome *bd* oxidase from *Corynebacterium glutamicum* in growth and lysine production. *Appl. Environ. Microbiol.* **73**: 861–868.

236. Kalapos, M.P. (1999) Methylglyoxal in living organisms: chemistry, biochemistry, toxicology and biological implications. *Toxicol. Lett.* **110**: 145–175.

237. Kalinowski, J. (2005) The genomes of amino acid-producing *Corynebacteria*. In, Eggeling,L. and Bott,M. (eds), *Handbook of Corynebacterium glutamicum*. CRC Press, Boca Raton, FL, USA, pp. 37–56.

238. Kalinowski, J., Bathe, B., Bartels, D., Bischoff, N., Bott, M., Burkovski, A., *et al.* (2003) The complete *Corynebacterium glutamicum* ATCC 13032 genome sequence and its impact on the production of L-aspartate-derived amino acids and vitamins. *J. Biotechnol.* **104**: 5–25.

239. Kallscheuer, N., Vogt, M., Kappelmann, J., Krumbach, K., Noack, S., Bott, M., and Marienhagen, J. (2015) Identification of the phd gene cluster responsible for phenylpropanoid utilization in *Corynebacterium glutamicum*. *Appl. Microbiol. Biotechnol.* **100**: 1871–1881.

240. Kallscheuer, N., Vogt, M., Stenzel, A., Gätgens, J., Bott, M., and Marienhagen, J. (2016) Construction of a *Corynebacterium glutamicum* platform strain for the production of stilbenes and (2S)-flavanones. *Metab. Eng.* **38**: 47–55.

241. Kamm, B. (2015) Microorganisms in biorefineries Springer Berlin Heidelberg, Berlin, Heidelberg.

242. Kana, B.D., Weinstein, E.A., Avarbock, D., Dawes, S.S., Rubin, H., and Mizrahi, V. (2001) Characterization of the *cydAB*-encoded cytochrome *bd* oxidase from *Mycobacterium smegmatis*. *J. Bacteriol.* **183**: 7076–7086.

243. Kang, M.-K., Lee, J., Um, Y., Lee, T.S., Bott, M., Park, S.J., and Woo, H.M. (2014) Synthetic biology platform of CoryneBrick vectors for gene expression in *Corynebacterium glutamicum* and its application to xylose utilization. *Appl. Microbiol. Biotechnol.* **98**: 5991–6002.

244. Kang, Y., Weber, K.D., Qiu, Y., Kiley, P.J., and Blattner, F.R. (2005) Genome-wide expression analysis indicates that FNR of *Escherichia coli* K-12 regulates a large number of genes of unknown function. *J. Bacteriol.* **187**: 1135–1160.

245. Kato, O., Youn, J.-W., Stansen, K.C., Matsui, D., Oikawa, T., and Wendisch, V.F. (2010) Quinone-dependent D-lactate dehydrogenase Dld (Cg1027) is essential for growth of *Corynebacterium glutamicum* on D-lactate. *BMC Microbiol.* **10**: 321.

246. Kawaguchi, H., Sasaki, M., Vertès, A.A., Inui, M., and Yukawa, H. (2008) Engineering of an L-arabinose metabolic pathway in *Corynebacterium glutamicum*.

*Appl. Microbiol. Biotechnol.* **77**: 1053–1062.

247. Kawaguchi, H., Sasaki, M., Vertès, A.A., Inui, M., and Yukawa, H. (2009) Identification and functional analysis of the gene cluster for L-arabinose utilization in *Corynebacterium glutamicum*. *Appl. Environ. Microbiol.* **75**: 3419–3429.

248. Kawaguchi, H., Vertès, A.A., Okino, S., Inui, M., and Yukawa, H. (2006) Engineering of a xylose metabolic pathway in *Corynebacterium glutamicum*. *Appl. Environ. Microbiol.* **72**: 3418–3428.

249. Keilhauer, C., Eggeling, L., and Sahm, H. (1993) Isoleucine synthesis in *Corynebacterium glutamicum*: molecular analysis of the *ilvB-ilvN-ilvC* operon. *J. Bacteriol.* **175**: 5595–5603.

250. Khoroshilova, N., Popescu, C., Münck, E., Beinert, H., and Kiley, P.J. (1997) Iron-sulfur cluster disassembly in the FNR protein of *Escherichia coli* by $O_2$: [4Fe-4S] to [2Fe-2S] conversion with loss of biological activity. *Proc. Natl. Acad. Sci. U. S. A.* **94**: 6087–6092.

251. Kikuchi, Y., Date, M., Yokoyama, K., Umezawa, Y., and Matsui, H. (2003) Secretion of active-form *Streptoverticillium mobaraense* transglutaminase by *Corynebacterium glutamicum*: processing of the pro-transglutaminase by a cosecreted subtilisin-like protease from *Streptomyces albogriseolus*. *Appl. Environ. Microbiol.* **69**: 358–366.

252. Kim, D. and Hahn, J.-S. (2013) Roles of the Yap1 transcription factor and antioxidants in *Saccharomyces cerevisiae*'s tolerance to furfural and 5-hydroxymethylfurfural, which function as thiol-reactive electrophiles generating oxidative stress. *Appl. Environ. Microbiol.* **79**: 5069–5077.

253. Kim, J.-S. and Holmes, R.K. (2012) Characterization of OxyR as a negative transcriptional regulator that represses catalase production in *Corynebacterium diphtheriae*. *PLoS One* **7**: e31709.

254. Kim, S.-H., Yun, J.-Y., Kim, S.-G., Seo, J.-H., and Park, J.-B. (2010) Production of xylitol from D-xylose and glucose with recombinant *Corynebacterium glutamicum*. *Enzyme Microb. Technol.* **46**: 366–371.

255. Kim, W.-S., Park, S.-D., Lee, S.-M., Kim, Y., Kim, P., and Lee, H.-S. (2007) Expression analysis of the *csp*-like genes from *Corynebacterium glutamicum* encoding homologs of the *Escherichia coli* major cold-shock protein *cspA*. *J. Microbiol. Biotechnol.* **17**: 1353–1360.

256. Kinoshita, S., Nakayama, K., and Akita, S. (1958) Taxonomical study of glutamic acid accumulating bacteria, *Micrococcus glutamicus* nov. sp. *Bull. Agric. Chem. Soc. Japan* **22**: 176–185.

257. Kinoshita, S., Udaka, S., and Shimono, M. (1957) Studies on the amino acid fermentation: I. Production of L-glutamic acid by various microorganisms. *J. Gen. Appl. Microbiol.* **3**: 193–205.

258. Kirk, T.K. and Farrell, R.L. (1987) Enzymatic "combustion": the microbial degradation of lignin. *Annu. Rev. Microbiol.* **41**: 465–501.

259. Kirubakaran, V., Sivaramakrishnan, V., Nalini, R., Sekar, T., Premalatha, M., and Subramanian, P. (2009) A review on gasification of biomass. *Renew. Sustain. Energy Rev.* **13**: 179–186.

260. Kitano, H. (2002) Systems biology: a brief overview. *Science.* **295**: 1662–1664.

261. Kjeldsen, K.R. and Nielsen, J. (2009) In silico genome-scale reconstruction and validation of the *Corynebacterium glutamicum* metabolic network. *Biotechnol. Bioeng.* **102**: 583–597.

262. Kleinert, T.N. (1971) Organosolv pulping and recovery. *US Pat. 3,585,104* 1–6.

263. Klinke, H.B., Thomsen, A.B., and Ahring, B.K. (2004) Inhibition of ethanol-producing yeast and bacteria by degradation products produced during pre-treatment of biomass. *Appl. Microbiol. Biotechnol.* **66**: 10–26.

264. Knapp, G.S., Lyubetskaya, A., Peterson, M.W., Gomes, A.L.C., Ma, Z., Galagan, J.E., and McDonough, K.A. (2015) Role of intragenic binding of cAMP responsive protein (CRP) in regulation of the succinate dehydrogenase genes Rv0249c-Rv0247c in TB complex mycobacteria. *Nucleic Acids Res.* **43**: 5377–5393.

265. Koch-Koerfges, A., Pfelzer, N., Platzen, L., Oldiges, M., and Bott, M. (2013) Conversion of *Corynebacterium glutamicum* from an aerobic respiring to an aerobic fermenting bacterium by inactivation of the respiratory chain. *Biochim. Biophys. Acta* **1827**: 699–708.

266. Kohl, T.A. and Tauch, A. (2009) The GlxR regulon of the amino acid producer *Corynebacterium glutamicum*: detection of the corynebacterial core regulon and integration into the transcriptional regulatory network model. *J. Biotechnol.* **143**: 239–246.

267. Krispin, O. and Allmansberger, R. (1998) The *Bacillus subtilis* AraE protein displays a broad substrate specificity for several different sugars. *J. Bacteriol.* **180**: 3250–3252.

268. Krömer, J.O., Sorgenfrei, O., Klopprogge, K., Heinzle, E., and Wittmann, C. (2004) In-depth profiling of lysine-producing *Corynebacterium glutamicum* by combined analysis of the transcriptome, metabolome, and fluxome. *J. Bacteriol.* **186**: 1769–1784.

269. Küberl, A., Fränzel, B., Eggeling, L., Polen, T., Wolters, D.A., and Bott, M. (2014) Pupylated proteins in *Corynebacterium glutamicum* revealed by MudPIT analysis. *Proteomics* **14**: 1531–1542.

270. Kuge, T., Teramoto, H., and Inui, M. (2015) AraR, an L-arabinose-responsive transcriptional regulator in *Corynebacterium glutamicum* ATCC 31831, exerts different degrees of repression depending on the location of its binding sites within the three target promoter regions. *J. Bacteriol.* **197**: 3788–3796.

271. Kumar, A., Jones, D.D., and Hanna, M.A. (2009) Thermochemical biomass gasification: a review of the current status of the technology. *Energies* **2**: 556–581.

272. Kumar, P., Barrett, D.M., Delwiche, M.J., and Stroeve, P. (2009) Methods for pretreatment of lignocellulosic biomass for efficient hydrolysis and biofuel production. *Ind. Eng. Chem. Res.* **48**: 3713–3729.

273. Kusumoto, K., Sakiyama, M., Sakamoto, J., Noguchi, S., and Sone, N. (2000) Menaquinol oxidase activity and primary structure of cytochrome *bd* from the amino-acid fermenting bacterium *Corynebacterium glutamicum*. *Arch. Microbiol.* **173**: 390–397.

274. Van Laer, K., Hamilton, C.J., and Messens, J. (2013) Low-molecular-weight thiols in thiol-disulfide exchange. *Antioxid. Redox Signal.* **18**: 1642–1653.

275. Landini, P., Egli, T., Wolf, J., and Lacour, S. (2014) sigmaS, a major player in the response to environmental stresses in *Escherichia coli*: role, regulation and mechanisms of promoter recognition. *Environ. Microbiol. Rep.* **6**: 1–13.

276. Lange, J., Müller, F., Bernecker, K., Dahmen, N., Takors, R., and Blombach, B. (2017) Valorization of pyrolysis water: a biorefinery side stream, for 1,2-propanediol production with engineered *Corynebacterium glutamicum*. *Biotechnol. Biofuels* **10**: 277.

277. Lange, J., Müller, F., Takors, R., and Blombach, B. (2018) Harnessing novel chromosomal integration loci to utilize an organosolv-derived hemicellulose fraction for isobutanol production with engineered *Corynebacterium glutamicum*. *Microb. Biotechnol.* **11**: 257–263.

278. Lange, J., Münch, E., Müller, J., Busche, T., Kalinowski, J., Takors, R., and Blombach, B. (2018) Deciphering the adaptation of *Corynebacterium glutamicum* in transition from aerobiosis via microaerobiosis to anaerobiosis. *Genes*. **9**: 297.

279. Lange, J., Takors, R., and Blombach, B. (2017) Zero-growth bioprocesses – a challenge for microbial production strains and bioprocess engineering. *Eng. Life Sci.* **17**: 27–35.

280. Langmead, B. and Salzberg, S.L. (2012) Fast gapped-read alignment with Bowtie 2. *Nat. Methods* **9**: 357–359.

281. Lara, A.R., Galindo, E., Ramírez, O.T., and Palomares, L.A. (2006) Living with heterogeneities in bioreactors: understanding the effects of environmental gradients on cells. *Mol. Biotechnol.* **34**: 355–382.

282. Lara, A.R., Leal, L., Flores, N., Gosset, G., Bolívar, F., and Ramírez, O.T. (2006) Transcriptional and metabolic response of recombinant Escherichia coli to spatial dissolved oxygen tension gradients simulated in a scale – down system. *Biotechnol. Bioeng.* **93**: 372–385.

283. Lee, J., Saddler, J.N., Um, Y., and Woo, H.M. (2016) Adaptive evolution and metabolic engineering of a cellobiose- and xylose- negative *Corynebacterium glutamicum* that co-utilizes cellobiose and xylose. *Microb. Cell Fact.* **15**: 20.

284. Lee, L.G. and Whitesides, G.M. (1986) Preparation of optically active 1,2-diols and α-hydroxy ketones using glycerol dehydrogenase as catalyst. Limits to enzyme-catalyzed synthesis due to noncompetitive and mixed inhibition by product. *J. Org. Chem.* **51**: 25–36.

285. Lee, S.Y. and Kim, H.U. (2015) Systems strategies for developing industrial microbial strains. *Nat. Biotechnol.* **33**: 1061–1072.

286. Lee, W.-H., Seo, S.-O., Bae, Y.-H., Nan, H., Jin, Y.-S., and Seo, J.-H. (2012) Isobutanol production in engineered *Saccharomyces cerevisiae* by overexpression of 2-ketoisovalerate decarboxylase and valine biosynthetic enzymes. *Bioprocess Biosyst. Eng.* **35**: 1467–1475.

287. Leible, L., Kälber, S., Kappler, G., Lange, S., Nieke, E., Proplesch, P., *et al.* (2007) Kraftstoff, Strom und Wärme aus Stroh und Waldrestholz - eine Systemanalytische

Untersuchung (FZKA-7170), Karlsruhe.
https://publikationen.bibliothek.kit.edu/270068790.

288. Lemoine, A., Maya Martínez-Iturralde, N., Spann, R., Neubauer, P., and Junne, S. (2015) Response of *Corynebacterium glutamicum* exposed to oscillating cultivation conditions in a two- and a novel three-compartment scale-down bioreactor. *Biotechnol. Bioeng.* **112**: 1220–1231.

289. Leßmeier, L. and Wendisch, V.F. (2015) Identification of two mutations increasing the methanol tolerance of *Corynebacterium glutamicum*. *BMC Microbiol.* **15**: 216.

290. Leßmeier, L., Zahoor, A., Lindner, S.N., and Wendisch, V.F. (2015) Metabolic engineering of *Corynebacterium glutamicum* for alternative carbon source utilization. In, Burkovski,A. (ed), *Corynebacterium glutamicum: from systems biology to biotechnological applications*. Caister Academic Press, Norfolk, UK, pp. 57–70.

291. Li, H. and Liao, J.C. (2013) Engineering a cyanobacterium as the catalyst for the photosynthetic conversion of $CO_2$ to 1,2-propanediol. *Microb. Cell Fact.* **12**: 4.

292. Li, H., Opgenorth, P.H., Wernick, D.G., Rogers, S., Wu, T.-Y., Higashide, W., *et al.* (2012) Integrated electromicrobial conversion of $CO_2$ to higher alcohols. *Science.* **335**: 1596.

293. Li, S., Huang, D., Li, Y., Wen, J., and Jia, X. (2012) Rational improvement of the engineered isobutanol-producing *Bacillus subtilis* by elementary mode analysis. *Microb. Cell Fact.* **11**: 101.

294. Li, Y., Chen, J., Mao, Y., Lun, S., and Koo, Y. (1998) Effect of additives and fed-batch culture strategies on the production of glutathione by recombinant *Escherichia coli*. *Process Biochem.* **33**: 709–714.

295. Li, Y., Hugenholtz, J., Abee, T., and Molenaar, D. (2003) Glutathione protects *Lactococcus lactis* against oxidative stress. *Appl. Environ. Microbiol.* **69**: 5739–5745.

296. Li, Y., Hugenholtz, J., Sybesma, W., Abee, T., and Molenaar, D. (2004) Using *Lactococcus lactis* for glutathione overproduction. *Appl. Microbiol. Biotechnol.* **67**: 83–90.

297. Li, Y., Li, M., Zhang, X., Yang, P., Liang, Q., and Qi, Q. (2013) A novel whole-phase succinate fermentation strategy with high volumetric productivity in engineered *Escherichia coli*. *Bioresour. Technol.* **149**: 333–340.

298. Li, Y., Wei, G., and Chen, J. (2004) Glutathione: a review on biotechnological production. *Appl. Microbiol. Biotechnol.* **66**: 233–242.

299. Lian, J., Garcia-Perez, M., Coates, R., Wu, H., and Chen, S. (2012) Yeast fermentation of carboxylic acids obtained from pyrolytic aqueous phases for lipid production. *Bioresour. Technol.* **118**: 177–186.

300. Liao, J.C., Mi, L., Pontrelli, S., and Luo, S. (2016) Fuelling the future: microbial engineering for the production of sustainable biofuels. *Nat. Rev. Microbiol.* **14**: 288–304.

301. Liebl, W. (2005) *Corynebacterium* taxonomy. In, Eggeling,L. and Bott,M. (eds), *Handbook of Corynebacterium glutamicum*. CRC Press, Boca Raton, FL, USA, pp. 9–34.

302. Liebl, W., Bayerl, A., Schein, B., Stillner, U., and Schleifer, K.H. (1989) High efficiency electroporation of intact *Corynebacterium glutamicum* cells. *FEMS Microbiol. Lett.* **53**: 299–303.

303. Limberg, M.H., Joachim, M., Klein, B., Wiechert, W., and Oldiges, M. (2017) pH fluctuations imperil the robustness of *C. glutamicum* to short term oxygen limitation. *J. Biotechnol.* **259**: 248–260.

304. Limberg, M.H., Schulte, J., Aryani, T., Mahr, R., Baumgart, M., Bott, M., *et al.* (2017) Metabolic profile of 1,5-diaminopentane producing *Corynebacterium glutamicum* under scale-down conditions: blueprint for robustness to bioreactor inhomogeneities. *Biotechnol. Bioeng.* **114**: 560–575.

305. Lin, P.P., Mi, L., Morioka, A.H., Yoshino, K.M., Konishi, S., Xu, S.C., *et al.* (2015) Consolidated bioprocessing of cellulose to isobutanol using *Clostridium thermocellum*. *Metab. Eng.* **31**: 44–52.

306. Lin, P.P., Rabe, K.S., Takasumi, J.L., Kadisch, M., Arnold, F.H., and Liao, J.C. (2014) Isobutanol production at elevated temperatures in thermophilic *Geobacillus thermoglucosidasius*. *Metab. Eng.* **24**: 1–8.

307. Lindqvist, A., Membrillo-Hernández, J., Poole, R.K., and Cook, G.M. (2000) Roles of respiratory oxidases in protecting *Escherichia coli* K12 from oxidative stress. *Antonie Van Leeuwenhoek* **78**: 23–31.

308. Litsanov, B., Brocker, M., and Bott, M. (2012) Toward homosuccinate fermentation: metabolic engineering of *Corynebacterium glutamicum* for anaerobic production of succinate from glucose and formate. *Appl. Environ. Microbiol.* **78**: 3325–3337.

309. Liu, H., Liang, S., Jiang, T., Han, B., and Zhou, Y. (2012) Hydrogenolysis of glycerol to 1,2-propanediol over Ru-Cu bimetals supported on different supports. *CLEAN - Soil, Air, Water* **40**: 318–324.

310. Liu, W.-J., Jiang, H., and Yu, H.-Q. (2015) Thermochemical conversion of lignin to functional materials: a review and future directions. *Green Chem.* **17**: 4888–4907.

311. Liu, Y.-B., Chen, C., Chaudhry, M.T., Si, M.-R., Zhang, L., Wang, Y., and Shen, X.-H. (2014) Enhancing *Corynebacterium glutamicum* robustness by over-expressing a gene, *mshA*, for mycothiol glycosyltransferase. *Biotechnol. Lett.* **36**: 1453–1459.

312. Liu, Y.-B., Long, M.-X., Yin, Y.-J., Si, M.-R., Zhang, L., Lu, Z.-Q., *et al.* (2013) Physiological roles of mycothiol in detoxification and tolerance to multiple poisonous chemicals in *Corynebacterium glutamicum*. *Arch. Microbiol.* **195**: 419–429.

313. Liu, Z.L. and Moon, J. (2009) A novel NADPH-dependent aldehyde reductase gene from *Saccharomyces cerevisiae* NRRL Y-12632 involved in the detoxification of aldehyde inhibitors derived from lignocellulosic biomass conversion. *Gene* **446**: 1–10.

314. Löffler, M., Simen, J.D., Jäger, G., Schäferhoff, K., Freund, A., and Takors, R. (2016) Engineering *E. coli* for large-scale production – strategies considering ATP expenses and transcriptional responses. *Metab. Eng.* **38**: 73–85.

315. Loi, V. Van, Rossius, M., and Antelmann, H. (2015) Redox regulation by reversible protein S-thiolation in bacteria. *Front. Microbiol.* **6**: 187.

316. López-Bellido, L., Wery, J., and López-Bellido, R.J. (2014) Energy crops: prospects

in the context of sustainable agriculture. *Eur. J. Agron.* **60**: 1–12.

317. Ludwig, D., Michael, B., Hirth, T., Rupp, S., and Zibek, S. (2014) High solids enzymatic hydrolysis of pretreated lignocellulosic materials with a powerful stirrer concept. *Appl. Biochem. Biotechnol.* **172**: 1699–1713.

318. Luo, Z., Wang, S., and Guo, X. (2012) Selective pyrolysis of Organosolv lignin over zeolites with product analysis by TG-FTIR. *J. Anal. Appl. Pyrolysis* **95**: 112–117.

319. MacLean, M.J., Ness, L.S., Ferguson, G.P., and Booth, I.R. (1998) The role of glyoxalase I in the detoxification of methylglyoxal and in the activation of the KefB $K^+$ efflux system in *Escherichia coli*. *Mol. Microbiol.* **27**: 563–571.

320. Maiorella, B.L., Blanch, H.W., and Wilke, C.R. (1984) Feed component inhibition in ethanolic fermentation by *Saccharomyces cerevisiae*. *Biotechnol. Bioeng.* **26**: 1155–1166.

321. Marienhagen, J., Kennerknecht, N., Sahm, H., and Eggeling, L. (2005) Functional analysis of all aminotransferase proteins inferred from the genome sequence of *Corynebacterium glutamicum*. *J. Bacteriol.* **187**: 7639–7646.

322. Martín, J.F., Barreiro, C., González-Lavado, E., and Barriuso, M. (2003) Ribosomal RNA and ribosomal proteins in *Corynebacteria*. *J. Biotechnol.* **104**: 41–53.

323. Martínez, I., Bennett, G.N., and San, K.-Y. (2010) Metabolic impact of the level of aeration during cell growth on anaerobic succinate production by an engineered *Escherichia coli* strain. *Metab. Eng.* **12**: 499–509.

324. Masip, L., Veeravalli, K., and Georgiou, G. (2006) The many faces of glutathione in bacteria. *Antioxidants Redox Signal.* **8**: 753–762.

325. Matsuda, F., Ishii, J., Kondo, T., Ida, K., Tezuka, H., Kondo, A., *et al.* (2013) Increased isobutanol production in *Saccharomyces cerevisiae* by eliminating competing pathways and resolving cofactor imbalance. *Microb. Cell Factories 2013 121* **72**: 1136–1143.

326. Matsushita, K. (2013) Respiratory chain and energy metabolism of *Corynebacterium glutamicum*. In, Yukawa,H. and Inui,M. (eds), *Corynebacterium glutamicum: biology and biotechnology*. Springer, Berlin, Heidelberg, pp. 315–334.

327. Mayuri, Bagchi, G., Das, T.K., and Tyagi, J.S. (2002) Molecular analysis of the dormancy response in *Mycobacterium smegmatis*: expression analysis of genes encoding the DevR-DevS two-component system, Rv3134c and chaperone α-crystallin homologues. *FEMS Microbiol. Lett.* **211**: 231–237.

328. McKendry, P. (2002a) Energy production from biomass (part 1): overview of biomass. *Bioresour. Technol.* **83**: 37–46.

329. McKendry, P. (2002b) Energy production from biomass (part 2): conversion technologies. *Bioresour. Technol.* **83**: 47–54.

330. Meessen, J.H., Meessen, and H., J. (2010) Urea. In, *Ullmann's Encyclopedia of Industrial Chemistry*. Wiley-VCH Verlag GmbH & Co. KGaA, Weinheim, Germany.

331. Meier, D. (2017) Pyrolysis oil biorefinery. Springer Berlin Heidelberg, Berlin, Heidelberg, pp. 1–37.

332. Meier, D. and Faix, O. (1999) State of the art of applied fast pyrolysis of

lignocellulosic materials – a review. *Bioresour. Technol.* **68**: 71–77.

333. Meiswinkel, T.M., Gopinath, V., Lindner, S.N., Nampoothiri, K.M., and Wendisch, V.F. (2013) Accelerated pentose utilization by *Corynebacterium glutamicum* for accelerated production of lysine, glutamate, ornithine and putrescine. *Microb. Biotechnol.* **6**: 131–140.

334. Menkel, E., Thierbach, G., Eggeling, L., and Sahm, H. (1989) Influence of increased aspartate availability on lysine formation by a recombinant strain of *Corynebacterium glutamicum* and utilization of fumarate. *Appl. Environ. Microbiol.* **55**: 684–688.

335. Meyer, F., Goesmann, A., McHardy, A.C., Bartels, D., Bekel, T., Clausen, J., *et al.* (2003) GenDB – an open source genome annotation system for prokaryote genomes. *Nucleic Acids Res.* **31**: 2187–2195.

336. Michel, A., Koch-Koerfges, A., Krumbach, K., Brocker, M., and Bott, M. (2015) Anaerobic growth of *Corynebacterium glutamicum* by mixed-acid fermentation. *Appl. Environ. Microbiol.* In press. DOI: 10.1128/AEM.02413-15

337. Miller, E.N., Jarboe, L.R., Yomano, L.P., York, S.W., Shanmugam, K.T., and Ingram, L.O. (2009) Silencing of NADPH-dependent oxidoreductase genes (*yqhD* and *dkgA*) in furfural-resistant ethanologenic *Escherichia coli*. *Appl. Environ. Microbiol.* **75**: 4315–4323.

338. Miller, E.N., Turner, P.C., Jarboe, L.R., and Ingram, L.O. (2010) Genetic changes that increase 5-hydroxymethyl furfural resistance in ethanol-producing *Escherichia coli* LY180. *Biotechnol. Lett.* **32**: 661–667.

339. Mills, E. (2015) The bioeconomy - a primer. TNI and Hands on the Land.

340. Mills, T.Y., Sandoval, N.R., and Gill, R.T. (2009) Cellulosic hydrolysate toxicity and tolerance mechanisms in *Escherichia coli*. *Biotechnol. Biofuels* **2**: 26.

341. Milse, J., Petri, K., Rückert, C., and Kalinowski, J. (2014) Transcriptional response of *Corynebacterium glutamicum* ATCC 13032 to hydrogen peroxide stress and characterization of the OxyR regulon. *J. Biotechnol.* **190**: 40–54.

342. Ministry of Science Research and the Arts (MWK) of Baden-Württemberg (2013) Bioökonomie im System aufstellen - Konzept für eine Baden-Württembergische Forschungsstrategie “Bioökonomie”, Stuttgart. https://www.baden-wuerttemberg.de/de/service/publikation/did/biooekonomie-im-system-aufstellen/.

343. Minty, J.J., Singer, M.E., Scholz, S.A., Bae, C.-H., Ahn, J.-H., Foster, C.E., *et al.* (2013) Design and characterization of synthetic fungal-bacterial consortia for direct production of isobutanol from cellulosic biomass. *Proc. Natl. Acad. Sci. U. S. A.* **110**: 14592–14597.

344. Miwa, K., Matsui, H., Terabe, M., Nakamori, S., Sano, K., and Momose, H. (1984) Cryptic plasmids in glutamic acid-producing bacteria. *Agric. Biol. Chem.* **48**: 2901–2903.

345. Mohr, A. and Raman, S. (2013) Lessons from first generation biofuels and implications for the sustainability appraisal of second generation biofuels. *Energy Policy* **63**: 114–122.

346. Möker, N., Brocker, M., Schaffer, S., Krämer, R., Morbach, S., and Bott, M. (2004)

Deletion of the genes encoding the MtrA-MtrB two-component system of *Corynebacterium glutamicum* has a strong influence on cell morphology, antibiotics susceptibility and expression of genes involved in osmoprotection. *Mol. Microbiol.* **54**: 420–438.

347. Molenaar, D., van der Rest, M.E., Drysch, A., and Yücel, R. (2000) Functions of the membrane-associated and cytoplasmic malate dehydrogenases in the citric acid cycle of *Corynebacterium glutamicum*. *J. Bacteriol.* **182**: 6884–6891.

348. Möller, R., Toonen, M.A.J., Beilen, J.B., Salentijn, E.M.J., and Clayton, D. (2007) Crop platforms for cell wall biorefining: lignocellulose feedstocks CPL Press, Newbury, Berks, UK.

349. Moritz, B., Striegel, K., De Graaf, A.A., and Sahm, H. (2000) Kinetic properties of the glucose-6-phosphate and 6-phosphogluconate dehydrogenases from *Corynebacterium glutamicum* and their application for predicting pentose phosphate pathway flux in vivo. *Eur. J. Biochem.* **267**: 3442–3452.

350. Mullis, K.B. and Faloona, F.A. (1987) Specific synthesis of DNA *in vitro* via a polymerase-catalyzed chain reaction. *Methods Enzymol.* **155**: 335–350.

351. Murata, K. and Kimura, A. (1982) Cloning of a gene responsible for the biosynthesis of glutathione in *Escherichia coli* B. *Appl. Environ. Microbiol.* **44**: 1444–1448.

352. Nakano, K., Katsu, R., Tada, K., and Matsumura, M. (2000) Production of highly concentrated xylitol by *Candida magnoliae* under a microaerobic condition maintained by simple fuzzy control. *J. Biosci. Bioeng.* **89**: 372–376.

353. Nanda, A.M., Heyer, A., Krämer, C., Grünberger, A., Kohlheyer, D., and Frunzke, J. (2014) Analysis of SOS-induced spontaneous prophage induction in *Corynebacterium glutamicum* at the single-cell level. *J. Bacteriol.* **196**: 180–188.

354. Narayanan, V., Schelin, J., Gorwa-Grauslund, M., van Niel, E.W., and Carlquist, M. (2017) Increased lignocellulosic inhibitor tolerance of *Saccharomyces cerevisiae* cell populations in early stationary phase. *Biotechnol. Biofuels* **10**: 114.

355. NCBI Resource Coordinators (2017) Database resources of the National Center for Biotechnology Information. *Nucleic Acids Res.* **45**: D12–D17.

356. NEB (2015) Gibson Assembly® Protocol (E5510). http://international.neb.com/protocols/2012/12/1.

357. Nentwich, S.S., Brinkrolf, K., Gaigalat, L., Huser, A.T., Rey, D.A., Mohrbach, T., *et al.* (2009) Characterization of the LacI-type transcriptional repressor RbsR controlling ribose transport in *Corynebacterium glutamicum* ATCC 13032. *Microbiology* **155**: 150–164.

358. Neuweger, H., Persicke, M., Albaum, S.P., Bekel, T., Dondrup, M., Hüser, A.T., *et al.* (2009) Visualizing post genomics data-sets on customized pathway maps by ProMeTra-aeration-dependent gene expression and metabolism of *Corynebacterium glutamicum* as an example. *BMC Syst. Biol.* **3**: 82.

359. Newton, G.L., Arnold, K., Price, M.S., Sherrill, C., Delcardayre, S.B., Aharonowitz, Y., *et al.* (1996) Distribution of thiols in microorganisms: mycothiol is a major thiol in most *Actinomycetes*. *J. Bacteriol.* **178**: 1990–1995.

360. Newton, G.L., Buchmeier, N., and Fahey, R.C. (2008) Biosynthesis and functions of

mycothiol, the unique protective thiol of *Actinobacteria*. *Microbiol. Mol. Biol. Rev.* **72**: 471–494.

361. Newton, G.L. and Fahey, R.C. (2002) Mycothiol biochemistry. *Arch. Microbiol.* **178**: 388–394.

362. Newton, G.L., Fahey, R.C., Cohen, G., and Aharonowitz, Y. (1993) Low-molecular-weight thiols in *Streptomycetes* and their potential role as antioxidants. *J. Bacteriol.* **175**: 2734–2742.

363. Niebisch, A. (2002) Purification of a cytochrome $bc_1$-$aa_3$ supercomplex with quinol oxidase Activity from *Corynebacterium glutamicum*. *J. Biol. Chem.* **278**: 4339–4346.

364. Nielsen, J. (2017) Systems biology of metabolism. *Annu. Rev. Biochem.* **86**: 245–275.

365. Nielsen, J., Larsson, C., van Maris, A., and Pronk, J. (2013) Metabolic engineering of yeast for production of fuels and chemicals. *Curr. Opin. Biotechnol.* **24**: 398–404.

366. Niimi, S., Suzuki, N., Inui, M., and Yukawa, H. (2011) Metabolic engineering of 1,2-propanediol pathways in *Corynebacterium glutamicum*. *Appl. Microbiol. Biotechnol.* **90**: 1721–1729.

367. Nishimura, T., Vertès, A.A., Shinoda, Y., Inui, M., and Yukawa, H. (2007) Anaerobic growth of *Corynebacterium glutamicum* using nitrate as a terminal electron acceptor. *Appl. Microbiol. Biotechnol.* **75**: 889–897.

368. Nissen, T.L., Schulze, U., Nielsen, J., and Villadsen, J. (1997) Flux distributions in anaerobic, glucose-limited continuous cultures of *Saccharomyces cerevisiae*. *Microbiology* **143**: 203–218.

369. Niu, W. and Guo, J. (2015) Stereospecific microbial conversion of lactic acid into 1,2-propanediol. *ACS Synth. Biol.* **4**: 378–382.

370. O'Toole, R., Smeulders, M.J., Blokpoel, M.C., Kay, E.J., Lougheed, K., and Williams, H.D. (2003) A two-component regulator of universal stress protein expression and adaptation to oxygen starvation in *Mycobacterium smegmatis*. *J. Bacteriol.* **185**: 1543–1554.

371. O'Young, J., Sukdeo, N., and Honek, J.F. (2007) *Escherichia coli* glyoxalase II is a binuclear zinc-dependent metalloenzyme. *Arch. Biochem. Biophys.* **459**: 20–26.

372. Oasmaa, A., Elliott, D.C., and Korhonen, J. (2010) Acidity of biomass fast pyrolysis bio-oils. *Energy & Fuels* **24**: 6548–6554.

373. Oasmaa, A., Leppawaki, E., Koponen, P., Levander, J., and Topola, E. (1997) Physical characterisation of biomass-based pyrolysis liquids. Applications of standard fuel oil analyses. *VTT Publ.* http://www.vtt.fi/inf/pdf/publications/1997/P306.

374. Oasmaa, A. and Peacocke, C. (2010) Properties and fuel use of biomass-derived fast pyrolysis liquids. A guide. *Vtt Publ.* **731**: 79 p. + app. 46 p.

375. Oasmaa, A., Sundqvist, T., Kuoppala, E., Garcia-Perez, M., Solantausta, Y., Lindfors, C., and Paasikallio, V. (2015) Controlling the phase stability of biomass fast pyrolysis bio-oils. *Energy & Fuels* **29**: 4373–4381.

376. Octave, S. and Thomas, D. (2009) Biorefinery: Toward an industrial metabolism. *Biochimie* **91**: 659–664.

377. OECD-FAO (2016) Agricultural outlook 2016-2025. OECD Publishing, Paris. www.fao.org/3/a-i5778e.pdf

378. Okino, S., Inui, M., and Yukawa, H. (2005) Production of organic acids by *Corynebacterium glutamicum* under oxygen deprivation. *Appl. Microbiol. Biotechnol.* **68**: 475–480.

379. Okino, S., Noburyu, R., Suda, M., Jojima, T., Inui, M., and Yukawa, H. (2008) An efficient succinic acid production process in a metabolically engineered *Corynebacterium glutamicum* strain. *Appl. Microbiol. Biotechnol.* **81**: 459–464.

380. Okino, S., Suda, M., Fujikura, K., Inui, M., and Yukawa, H. (2008) Production of D-lactic acid by *Corynebacterium glutamicum* under oxygen deprivation. *Appl. Microbiol. Biotechnol.* **78**: 449–454.

381. Oktyabrsky, O.N. and Smirnova, G. V. (1989) Dynamics of redox potential in bacterial cultures growing on media containing different sources of carbon, energy and nitrogen. *Acta Biotechnol.* **9**: 203–209.

382. Olsson, L. and Hahn-Hägerdal, B. (1996) Fermentation of lignocellulosic hydrolysates for ethanol production. *Enzyme Microb. Technol.* **18**: 312–331.

383. Oosterhuis, N.M. and Kossen, N.W. (1984) Dissolved oxygen concentration profiles in a production-scale bioreactor. *Biotechnol. Bioeng.* **26**: 546–550.

384. OPEC (2017) Monthly oil market report (May 2017), Vienna. http://www.opec.org/opec_web/static_files_project/media/downloads/publications/OPEC MOMR May 2017.pdf.

385. Orosz, A., Boros, I., and Venetianer, P. (1991) Analysis of the complex transcription termination region of the *Escherichia coli rrnB* gene. *Eur. J. Biochem.* **201**: 653–659.

386. Oude Elferink, S.J., Krooneman, J., Gottschal, J.C., Spoelstra, S.F., Faber, F., and Driehuis, F. (2001) Anaerobic conversion of lactic acid to acetic acid and 1,2-propanediol by *Lactobacillus buchneri*. *Appl. Environ. Microbiol.* **67**: 125–132.

387. Ozsolak, F. and Milos, P.M. (2011) RNA sequencing: advances, challenges and opportunities. *Nat. Rev. Genet.* **12**: 87–98.

388. Palmqvist, E. and Hahn-Hägerdal, B. (2000a) Fermentation of lignocellulosic hydrolysates I: inhibition and detoxification. *Bioresour. Technol.* **74**: 17–24.

389. Palmqvist, E. and Hahn-Hägerdal, B. (2000b) Fermentation of lignocellulosic hydrolysates II: inhibitors and mechanisms of inhibition. *Bioresour. Technol.* **74**: 25–33.

390. Partridge, J.D., Sanguinetti, G., Dibden, D.P., Roberts, R.E., Poole, R.K., and Green, J. (2007) Transition of *Escherichia coli* from aerobic to micro-aerobic conditions involves fast and slow reacting regulatory components. *J. Biol. Chem.* **282**: 11230–11237.

391. Pátek, M. and Nesvera, J. (2013) Promoters and plasmid vectors of *Corynebacterium glutamicum*. In, Yukawa,H. and Inui,M. (eds), *Corynebacterium glutamicum: biology and biotechnology*. Springer, Berlin, Heidelberg, pp. 51–88.

392. Patschkowski, T., Bates, D.M., and Kiley, P.J. (2000) Mechanisms for sensing and responding to oxygen deprivation. In, Storz,G. and Hengge-Aronis,R. (eds), *Bacterial*

*stress responses*. ASM Press, Washington, D.C., pp. 61–78.

393. Pauling, J., Röttger, R., Tauch, A., Azevedo, V., and Baumbach, J. (2012) CoryneRegNet 6.0 – Updated database content, new analysis methods and novel features focusing on community demands. *Nucleic Acids Res.* **40**: D610–D614.

394. Petersson, A., Almeida, J.R.M., Modig, T., Karhumaa, K., Hahn-Hägerdal, B., Gorwa-Grauslund, M.F., and Lidén, G. (2006) A 5-hydroxymethyl furfural reducing enzyme encoded by the *Saccharomyces cerevisiae* ADH6 gene conveys HMF tolerance. *Yeast* **23**: 455–464.

395. Pfeifer-Sancar, K., Mentz, A., Rückert, C., and Kalinowski, J. (2013) Comprehensive analysis of the *Corynebacterium glutamicum* transcriptome using an improved RNAseq technique. *BMC Genomics* **14**: 888.

396. Pfeifer, E., Hünnefeld, M., Popa, O., Polen, T., Kohlheyer, D., Baumgart, M., and Frunzke, J. (2016) Silencing of cryptic prophages in *Corynebacterium glutamicum*. *Nucleic Acids Res.* **44**: gkw692.

397. Pfitzer, C., Dahmen, N., Tröger, N., Weirich, F., Sauer, J., Günther, A., and Müller-Hagedorn, M. (2016) Fast pyrolysis of wheat straw in the bioliq pilot plant. *Energy & Fuels* **30**: 8047–8054.

398. Poole, R.K. and Cook, G.M. (2000) Redundancy of aerobic respiratory chains in bacteria? Routes, reasons and regulation. *Adv. Microb. Physiol.* **43**: 165–224.

399. Portnoy, V.A., Scott, D.A., Lewis, N.E., Tarasova, Y., Osterman, A.L., and Palsson, B.Ø. (2010) Deletion of genes encoding cytochrome oxidases and quinol monooxygenase blocks the aerobic-anaerobic shift in *Escherichia coli* K-12 MG1655. *Appl. Environ. Microbiol.* **76**: 6529–6540.

400. Postma, P.W., Lengeler, J.W., and Jacobson, G.R. (1993) Phosphoenolpyruvate:carbohydrate phosphotransferase systems of bacteria. *Microbiol. Rev.* **57**: 543–594.

401. Potzkei, J., Kunze, M., Drepper, T., Gensch, T., Jaeger, K.-E., and Buechs, J. (2012) Real-time determination of intracellular oxygen in bacteria using a genetically encoded FRET-based biosensor. *BMC Biol.* **10**: 28.

402. Pridmore, R.D. (1987) New and versatile cloning vectors with kanamycin-resistance marker. *Gene* **56**: 309–312.

403. Rabaçal, M., Ferreira, A.F., Silva, C.A.M., and Costa, M. (2017) Biorefineries – targeting energy, high value products and waste valorisation 1st ed. Rabaçal,M., Ferreira,A.F., Silva,C.A.M., and Costa,M. (eds) Springer International Publishing, Cham.

404. Radek, A., Krumbach, K., Gätgens, J., Wendisch, V., Wiechert, W., Bott, M., *et al.* (2014) Engineering of *Corynebacterium glutamicum* for minimized carbon loss during utilization of D-xylose containing substrates. *J. Biotechnol.* **192**: 156–160.

405. Radek, A., Müller, M.-F., Gätgens, J., Eggeling, L., Krumbach, K., Marienhagen, J., and Noack, S. (2016) Formation of xylitol and xylitol-5-phosphate and its impact on growth of D-xylose-utilizing *Corynebacterium glutamicum* strains. *J. Biotechnol.* **231**: 160–166.

406. Radek, A., Tenhaef, N., Müller, M.F., Brüsseler, C., Wiechert, W., Marienhagen, J.,

*et al.* (2017) Miniaturized and automated adaptive laboratory evolution: Evolving *Corynebacterium glutamicum* towards an improved D-xylose utilization. *Bioresour. Technol.* **245**, **Part**: 1377–1385.

407. Radoš, D., Carvalho, A.L., Wieschalka, S., Neves, A.R., Blombach, B., Eikmanns, B.J., and Santos, H. (2015) Engineering *Corynebacterium glutamicum* for the production of 2,3-butanediol. *Microb. Cell Fact.* **14**: 1–14.

408. Radoš, D., Turner, D.L., Fonseca, L.L., Carvalho, A.L., Blombach, B., Eikmanns, B.J., *et al.* (2014) Carbon flux analysis by $^{13}C$ nuclear magnetic resonance to determine the effect of $CO_2$ on anaerobic succinate production by *Corynebacterium glutamicum*. *Appl. Environ. Microbiol.* **80**: 3015–3024.

409. Ragauskas, A.J., Beckham, G.T., Biddy, M.J., Chandra, R., Chen, F., Davis, M.F., *et al.* (2014) Lignin valorization: improving lignin processing in the biorefinery. *Science.* **344**: 1246843.

410. Rajendran, K. and Taherzadeh, M.J. (2014) Pretreatment of lignocellulosic materials. In, Bisaria,V.S. and Kondo,A. (eds), *Bioprocessing of Renewable Resources to Commodity Bioproducts*. John Wiley & Sons, Inc., Hoboken, New Jersy, pp. 43–75.

411. Rawat, M. and Av-Gay, Y. (2007) Mycothiol-dependent proteins in actinomycetes. *FEMS Microbiol. Rev.* **31**: 278–292.

412. Regenberg, B., Grotkjær, T., Winther, O., Fausbøll, A., Åkesson, M., Bro, C., *et al.* (2006) Growth-rate regulated genes have profound impact on interpretation of transcriptome profiling in *Saccharomyces cerevisiae*. *Genome Biol.* **7**: R107.

413. Renewable Fuels Association (2016) Industry statistics: world fuel ethanol production. http://www.ethanolrfa.org/resources/industry/sta.

414. van der Rest, M.E., Lange, C., and Molenaar, D. (1999) A heat shock following electroporation induces highly efficient transformation of *Corynebacterium glutamicum* with xenogeneic plasmid DNA. *Appl. Microbiol. Biotechnol.* **52**: 541–545.

415. Rose, R.E. (1988) The nucleotide sequence of pACYC177. *Nucleic Acids Res.* **16**: 356.

416. Roy, P. and Dias, G. (2017) Prospects for pyrolysis technologies in the bioenergy sector: a review. *Renew. Sustain. Energy Rev.* **77**: 59–69.

417. Rubin, E.M. (2008) Genomics of cellulosic biofuels. *Nature* **454**: 841–845.

418. Rumbold, K., van Buijsen, H.J.J., Gray, V.M., van Groenestijn, J.W., Overkamp, K.M., Slomp, R.S., *et al.* (2010) Microbial renewable feedstock utilization: a substrate-oriented approach. *Bioeng. Bugs* **1**: 359–366.

419. Sabra, W., Groeger, C., and Zeng, A.-P. (2016) Microbial cell factories for diol production. *Adv. Biochem. Eng. Biotechnol.* **155**: 165–197.

420. Saiki, R.K., Gelfand, D.H., Stoffel, S., Scharf, S.J., Higuchi, R., Horn, G.T., *et al.* (1988) Primer-directed enzymatic amplification of DNA with a thermostable DNA polymerase. *Science* **239**: 487–491.

421. Sakai, S., Tsuchida, Y., Nakamoto, H., Okino, S., Ichihashi, O., Kawaguchi, H., *et al.* (2007) Effect of lignocellulose-derived inhibitors on growth of and ethanol

production by growth-arrested *Corynebacterium glutamicum* R. *Appl. Environ. Microbiol.* **73**: 2349–2353.

422. Sambrook, J. and Russell, D.W. (2001) Molecular cloning: a laboratory manual 3rd ed. Cold Spring Harbor Laboratory Press, Cold Spring Harbor, NY, USA.

423. Sánchez, A.M., Bennett, G.N., and San, K.-Y. (2006) Batch culture characterization and metabolic flux analysis of succinate-producing *Escherichia coli* strains. *Metab. Eng.* **8**: 209–226.

424. Sánchez, O.J. and Cardona, C.A. (2008) Trends in biotechnological production of fuel ethanol from different feedstocks. *Bioresour. Technol.* **99**: 5270–5295.

425. Sanderson, K. (2006) US biofuels: a field in ferment. *Nature* **444**: 673–676.

426. Sandoval-Basurto, E.A., Gosset, G., Bolívar, F., and Ramírez, O.T. (2005) Culture of *Escherichia coli* under dissolved oxygen gradients simulated in a two-compartment scale-down system: metabolic response and production of recombinant protein. *Biotechnol. Bioeng.* **89**: 453–463.

427. Sannigrahi, P., Pu, Y., and Ragauskas, A. (2010) Cellulosic biorefineries – unleashing lignin opportunities. *Curr. Opin. Environ. Sustain.* **2**: 383–393.

428. Sasaki, M., Jojima, T., Inui, M., and Yukawa, H. (2008) Simultaneous utilization of D-cellobiose, D-glucose, and D-xylose by recombinant *Corynebacterium glutamicum* under oxygen-deprived conditions. *Appl. Microbiol. Biotechnol.* **81**: 691–699.

429. Sasaki, M., Jojima, T., Inui, M., and Yukawa, H. (2010) Xylitol production by recombinant *Corynebacterium glutamicum* under oxygen deprivation. *Appl. Microbiol. Biotechnol.* **86**: 1057–1066.

430. Sasaki, M., Jojima, T., Kawaguchi, H., Inui, M., and Yukawa, H. (2009) Engineering of pentose transport in *Corynebacterium glutamicum* to improve simultaneous utilization of mixed sugars. *Appl. Microbiol. Biotechnol.* **85**: 105–115.

431. Sauer, M., Steiger, M., Mattanovich, D., and Marx, H. (2014) Biorefineries-concepts for sustainability. In, Bisaria,V.S. and Kondō,A. (eds), *Bioprocessing of renewable resources to commodity bioproducts*. John Wiley & Sons, Inc., Hoboken, NJ, USA, pp. 3–27.

432. Sauer, U. and Eikmanns, B.J. (2005) The PEP-pyruvate-oxaloacetate node as the switch point for carbon flux distribution in bacteria. *FEMS Microbiol. Rev.* **29**: 765–794.

433. Sauer, U., Lasko, D.R., Fiaux, J., Hochuli, M., Glaser, R., Szyperski, T., *et al.* (1999) Metabolic flux ratio analysis of genetic and environmental modulations of *Escherichia coli* central carbon metabolism. *J. Bacteriol.* **181**: 6679–6688.

434. Sawers, G. (1999) The aerobic/anaerobic interface. *Curr. Opin. Microbiol.* **2**: 181–187.

435. Saxena, R.K., Anand, P., Saran, S., Isar, J., and Agarwal, L. (2010) Microbial production and applications of 1,2-propanediol. *Indian J. Microbiol.* **50**: 2–11.

436. Schäfer, A., Tauch, A., Jäger, W., Kalinowski, J., Thierbach, G., and Pühler, A. (1994) Small mobilizable multi-purpose cloning vectors derived from the *Escherichia coli* plasmids pK18 and pK19: selection of defined deletions in the chromosome of

*Corynebacterium glutamicum*. *Gene* **145**: 69–73.

437. Schneider, J., Niermann, K., and Wendisch, V.F. (2011) Production of the amino acids L-glutamate, L-lysine, L-ornithine and L-arginine from arabinose by recombinant *Corynebacterium glutamicum*. *J. Biotechnol.* **154**: 191–198.

438. Schneider, J., Peters-Wendisch, P., Stansen, K.C., Götker, S., Maximow, S., Krämer, R., and Wendisch, V.F. (2012) Characterization of the biotin uptake system encoded by the biotin-inducible *bioYMN* operon of *Corynebacterium glutamicum*. *BMC Microbiol.* **12**: 6.

439. Schreiner, M.E., Fiur, D., Holátko, J., Pátek, M., and Eikmanns, B.J. (2005) E1 enzyme of the pyruvate dehydrogenase complex in *Corynebacterium glutamicum*: molecular analysis of the gene and phylogenetic aspects. *J. Bacteriol.* **187**: 6005–6018.

440. Schröder, J., Jochmann, N., Rodionov, D.A., and Tauch, A. (2010) The Zur regulon of *Corynebacterium glutamicum* ATCC 13032. *BMC Genomics* **11**: 12.

441. Schröder, J. and Tauch, A. (2010) Transcriptional regulation of gene expression in *Corynebacterium glutamicum*: the role of global, master and local regulators in the modular and hierarchical gene regulatory network. *FEMS Microbiol. Rev.* **34**: 685–737.

442. Schurch, N.J., Schofield, P., Gierliński, M., Cole, C., Sherstnev, A., Singh, V., *et al.* (2016) How many biological replicates are needed in an RNA-seq experiment and which differential expression tool should you use? *RNA* **22**: 839–51.

443. Selbitschka, W., Niemann, S., and Pühler, A. (1993) Construction of gene replacement vectors for Gram$^-$ bacteria using a genetically modified *sacRB* gene as a positve selection marker. *Appl. Microbiol. Biotechnol.* **38**: 615–618.

444. Serjeant, E.P. and Dempsey, B. (1979) Ionisation constants of organic acids in aqueous solution Pergamon Press, Oxford, New York.

445. Shah, A. and Eikmanns, B.J. (2016) Transcriptional Regulation of the β-Type Carbonic Anhydrase Gene bca by RamA in *Corynebacterium glutamicum*. *PLoS One* **11**: e0154382.

446. Shanmugam, S.R., Adhikari, S., and Shakya, R. (2017) Nutrient removal and energy production from aqueous phase of bio-oil generated via hydrothermal liquefaction of algae. *Bioresour. Technol.* **230**: 43–48.

447. Shen, X.-H., Jiang, C.-Y., Huang, Y., Liu, Z.-P., and Liu, S.-J. (2005) Functional identification of novel genes involved in the glutathione-independent gentisate pathway in *Corynebacterium glutamicum*. *Appl. Environ. Microbiol.* **71**: 3442–3452.

448. Shen, X.-H., Zhou, N.-Y., and Liu, S.-J. (2012) Degradation and assimilation of aromatic compounds by Corynebacterium glutamicum: another potential for applications for this bacterium? *Appl. Microbiol. Biotechnol.* **95**: 77–89.

449. Shi, X., Chen, Y., Ren, H., Liu, D., Zhao, T., Zhao, N., and Ying, H. (2014) Economically enhanced succinic acid fermentation from cassava bagasse hydrolysate using Corynebacterium glutamicum immobilized in porous polyurethane filler. *Bioresour. Technol.* **174C**: 190–197.

450. Shinfuku, Y., Sorpitiporn, N., Sono, M., Furusawa, C., Hirasawa, T., and Shimizu, H.

(2009) Development and experimental verification of a genome-scale metabolic model for *Corynebacterium glutamicum*. *Microb. Cell Fact.* **8**: 43.

451. Shuler, M.L. and Kargi, F. (1992) Bioprocess engineering: basic concepts. P T R Prentice Hall, Englewood Cliffs, New Jersey.

452. Siebert, D. and Wendisch, V.F. (2015) Metabolic pathway engineering for production of 1,2-propanediol and 1-propanol by *Corynebacterium glutamicum*. *Biotechnol. Biofuels* **8**: 91.

453. Silva, C.A.M., Prunescu, R.M., Gernaey, K. V., Sin, G., and Diaz-Chavez, R.A. (2017) Biorefinery sustainability analysis. In, *Biorefineries – targeting energy, high value products and waste valorisation*. Springer, Cham, Cham, pp. 161–200.

454. Silver, W.L., Lugo, A.E., and Keller, M. (1999) Soil oxygen availability and biogeochemistry along rainfall and topographic gradients in upland wet tropical forest soils. *Biogeochemistry* **44**: 301–328.

455. Singh, A., Cher Soh, K., Hatzimanikatis, V., and Gill, R.T. (2011) Manipulating redox and ATP balancing for improved production of succinate in *E. coli*. *Metab. Eng.* **13**: 76–81.

456. Smith, G.M., Lee, S.A., Reilly, K.C., Eiteman, M.A., and Altman, E. (2006) Fed-batch two-phase production of alanine by a metabolically engineered *Escherichia coli*. *Biotechnol. Lett.* **28**: 1695–1700.

457. Smith, K.M., Cho, K.-M., and Liao, J.C. (2010) Engineering *Corynebacterium glutamicum* for isobutanol production. *Appl. Microbiol. Biotechnol.* **87**: 1045–1055.

458. Sondreal, E.A., Benson, S.A., Hurley, J.P., Mann, M.D., Pavlish, J.H., Swanson, M.L., *et al.* (2001) Review of advances in combustion technology and biomass cofiring. *Fuel Process. Technol.* **71**: 7–38.

459. Song, H.-S., Jeon, J.-M., Kim, H.-J., Bhatia, S.K., Sathiyanarayanan, G., Kim, J., *et al.* (2017) Increase in furfural tolerance by combinatorial overexpression of NAD salvage pathway enzymes in engineered isobutanol-producing E. coli. *Bioresour. Technol.* **245**, **Part**: 1430–1435.

460. Sonmez, M., Ince, H.Y., Yalcin, O., Ajdžanović, V., Spasojević, I., Meiselman, H.J., and Baskurt, O.K. (2013) The effect of alcohols on red blood cell mechanical properties and membrane fluidity depends on their molecular size. *PLoS One* **8**: e76579.

461. Sousa, A.M. and Pereira, M.O. (2014) *Pseudomonas aeruginosa* diversification during infection development in cystic fibrosis lungs – a review. *Pathog. (Basel, Switzerland)* **3**: 680–703.

462. Sousa, E.H.S., Tuckerman, J.R., Gonzalez, G., and Gilles-Gonzalez, M.-A. (2007) DosT and DevS are oxygen-switched kinases in *Mycobacterium tuberculosis*. *Protein Sci.* **16**: 1708–1719.

463. Starck, J., Källenius, G., Marklund, B.-I., Andersson, D.I., and Akerlund, T. (2004) Comparative proteome analysis of *Mycobacterium tuberculosis* grown under aerobic and anaerobic conditions. *Microbiology* **150**: 3821–3829.

464. Steels, E.L., Learmonth, R.P., and Watson, K. (1994) Stress tolerance and membrane lipid unsaturation in *Saccharomyces cerevisiae* grown aerobically or anaerobically.

*Microbiology* **140**: 569–576.

465. Stephanopoulos, G. (1999) Metabolic fluxes and metabolic engineering. *Metab. Eng.* **1**: 1–11.

466. Stickel, J.J., Elander, R.T., McMillan, J.D., and Brunecky, R. (2014) Enzymatic hydrolysis of lignocellulosic biomass. In, Bisaria,V.S. and Kondo,A. (eds), *Bioprocessing of renewable resources to commodity bioproducts*. John Wiley & Sons, Inc., Hoboken, New Jersy.

467. Subedi, K.P., Choi, D., Kim, I., Min, B., and Park, C. (2011) Hsp31 of *Escherichia coli* K-12 is glyoxalase III. *Mol. Microbiol.* **81**: 926–936.

468. Subedi, K.P., Kim, I., Kim, J., Min, B., and Park, C. (2008) Role of GldA in dihydroxyacetone and methylglyoxal metabolism of *Escherichia coli* K12. *FEMS Microbiol. Lett.* **279**: 180–187.

469. Sun, Y. and Cheng, J. (2002) Hydrolysis of lignocellulosic materials for ethanol production: a review. *Bioresour. Technol.* **83**: 1–11.

470. Sun, Y., Guo, W., Wang, F., Peng, F., Yang, Y., Dai, X., *et al.* (2016) Transcriptome and multivariable data analysis of *Corynebacterium glutamicum* under different dissolved oxygen conditions in bioreactors. *PLoS One* **11**: e0167156.

471. Suppes, G.J., Sutterlin, W.R., and Dasari, M. (2005) Method of producing lower alcohols from glycerol. *US Pat. 2005/0244312 A1* 1–19.

472. Suzuki, N. and Inui, M. (2013) Genome engineering of *Corynebacterium glutamicum*. In, Yukawa,H. and Inui,M. (eds), *Corynebacterium glutamicum: biology and biotechnology*. Springer, Berlin, Heidelberg, pp. 89–105.

473. Szyperski, T. (1995) Biosynthetically directed fractional $^{13}$C-labeling of proteinogenic amino acids. An efficient analytical tool to investigate intermediary metabolism. *Eur. J. Biochem.* **232**: 433–448.

474. Takors, R., Bathe, B., Rieping, M., Hans, S., Kelle, R., and Huthmacher, K. (2007) Systems biology for industrial strains and fermentation processes – example: amino acids. *J. Biotechnol.* **129**: 181–190.

475. Tang, C.T., Ruch, F.E., and Lin, C.C. (1979) Purification and properties of a nicotinamide adenine dinucleotide-linked dehydrogenase that serves an *Escherichia coli* mutant for glycerol catabolism. *J. Bacteriol.* **140**: 182–187.

476. Taniguchi, H. (2016) Exploring the potential of sigma factors for strain development in *Corynebacterium glutamicum*. https://pub.uni-bielefeld.de/publication/2903682

477. Taniguchi, H. and Wendisch, V.F. (2015) Exploring the role of sigma factor gene expression on production by *Corynebacterium glutamicum*: sigma factor H and FMN as example. *Front. Microbiol.* **6**: 740.

478. Tatusov, R.L., Galperin, M.Y., Natale, D.A., and Koonin, E. V (2000) The COG database: a tool for genome-scale analysis of protein functions and evolution. *Nucleic Acids Res.* **28**: 33–36.

479. Tauch, A. (2008) Genomics of industrially and medically relevant Corynebacteria. In, Burkovski,A. (ed), *Corynebacteria: Genomics and Molecular Biology*. Caister Academic Press, Norfolk, United Kingdom, pp. 7–32.

480. Tauch, A., Kirchner, O., Löffler, B., Götker, S., Pühler, A., and Kalinowski, J. (2002) Efficient electrotransformation of *Corynebacterium diphtheriae* with a mini-replicon derived from the *Corynebacterium glutamicum* plasmid pGA1. *Curr. Microbiol.* **45**: 362–367.

481. Taylor, D.G., Trudgill, P.W., Cripps, R.E., and Harris, P.R. (1980) The microbial metabolism of acetone. *Microbiology* **118**: 159–170.

482. Teramoto, H., Inui, M., and Yukawa, H. (2012) *Corynebacterium glutamicum* Zur acts as a zinc-sensing transcriptional repressor of both zinc-inducible and zinc-repressible genes involved in zinc homeostasis. *FEBS J.* **279**: 4385–4397.

483. Teramoto, H., Inui, M., and Yukawa, H. (2013) OxyR acts as a transcriptional repressor of hydrogen peroxide-inducible antioxidant genes in *Corynebacterium glutamicum* R. *FEBS J.* **280**: 3298–3312.

484. The Bioeconomy Council (2015) Communiqué of the global bioeconomy summit - making bioeconomy work for sustainable development. http://gbs2015.com/fileadmin/gbs2015/Downloads/Communique_final.pdf.

485. The European Parliament and The Council of the European Union (2009) Directive 2009/28/EC on the promotion of the use of energy from renewable sources. *Off. J. Eur. Union*. http://eur-lex.europa.eu/legal-content/EN/ALL/?uri=celex%3A32009L0028.

486. The General Assembly (2015) Transforming our world: the 2030 agenda for sustainable development (A/RES/70/1). https://undocs.org/A/RES/70/1.

487. Theobald, A., Arcella, D., Carere, A., Croera, C., Engel, K.-H., Gott, D., *et al.* (2012) Safety assessment of smoke flavouring primary products by the European Food Safety Authority. *Trends Food Sci. Technol.* **27**: 97–108.

488. Tolbert, A., Akinosho, H., Khunsupat, R., Naskar, A.K., and Ragauskas, A.J. (2014) Characterization and analysis of the molecular weight of lignin for biorefining studies. *Biofuels, Bioprod. Biorefining* **8**: 836–856.

489. Tolla, D.A. and Savageau, M.A. (2010) Regulation of aerobic-to-anaerobic transitions by the FNR cycle in *Escherichia coli*. *J. Mol. Biol.* **397**: 893–905.

490. Toyoda, K. and Inui, M. (2016a) Regulons of global transcription factors in *Corynebacterium glutamicum*. *Appl. Microbiol. Biotechnol.* **100**: 45–60.

491. Toyoda, K. and Inui, M. (2016b) The extracytoplasmic function σ factor $\sigma^C$ regulates expression of a branched quinol oxidation pathway in *Corynebacterium glutamicum*. *Mol. Microbiol.* **100**: 486–509.

492. Tran, Q.H. and Unden, G. (1998) Changes in the proton potential and the cellular energetics of *Escherichia coli* during growth by aerobic and anaerobic respiration or by fermentation. *Eur. J. Biochem.* **251**: 538–543.

493. Tröger, N., Richter, D., and Stahl, R. (2013) Effect of feedstock composition on product yields and energy recovery rates of fast pyrolysis products from different straw types. *J. Anal. Appl. Pyrolysis* **100**: 158–165.

494. Truniger, V. and Boos, W. (1994) Mapping and cloning of *gldA*, the structural gene of the *Escherichia coli* glycerol dehydrogenase. *J. Bacteriol.* **176**: 1796–1800.

495. Trunk, K., Benkert, B., Quäck, N., Münch, R., Scheer, M., Garbe, J., *et al.* (2010) Anaerobic adaptation in *Pseudomonas aeruginosa*: definition of the Anr and Dnr regulons. *Environ. Microbiol.* **12**: 1719–1733.

496. Tschan, M.J.-L., Brulé, E., Haquette, P., and Thomas, C.M. (2012) Synthesis of biodegradable polymers from renewable resources. *Polym. Chem.* **3**: 836–851.

497. Tsuge, Y., Hori, Y., Kudou, M., Ishii, J., Hasunuma, T., and Kondo, A. (2014) Detoxification of furfural in *Corynebacterium glutamicum* under aerobic and anaerobic conditions. *Appl. Microbiol. Biotechnol.* **98**: 8675–8683.

498. Tsuge, Y., Uematsu, K., Yamamoto, S., Suda, M., Yukawa, H., and Inui, M. (2015) Glucose consumption rate critically depends on redox state in *Corynebacterium glutamicum* under oxygen deprivation. *Appl. Microbiol. Biotechnol.* **99**: 5573–5582.

499. Uhde, A. (2014) Kontrolle des Aminozuckerstoffwechsels in *Corynebacterium glutamicum*. kups.ub.uni-koeln.de/5498/

500. Unden, G., Becker, S., Bongaerts, J., Schirawski, J., and Six, S. (1994) Oxygen regulated gene expression in facultatively anaerobic bacteria. *Antonie Van Leeuwenhoek* **66**: 3–22.

501. Unden, G. and Bongaerts, J. (1997) Alternative respiratory pathways of *Escherichia coli*: energetics and transcriptional regulation in response to electron acceptors. *Biochim. Biophys. Acta* **1320**: 217–234.

502. Unthan, S., Baumgart, M., Radek, A., Herbst, M., Siebert, D., Brühl, N., *et al.* (2014) Chassis organism from *Corynebacterium glutamicum* – a top-down approach to identify and delete irrelevant gene clusters. *Biotechnol. J.* **10**: 290–301.

503. Unthan, S., Grünberger, A., van Ooyen, J., Gätgens, J., Heinrich, J., Paczia, N., *et al.* (2014) Beyond growth rate 0.6: What drives *Corynebacterium glutamicum* to higher growth rates in defined medium. *Biotechnol. Bioeng.* **111**: 359–371.

504. Valdivia, M., Galan, J.L., Laffarga, J., and Ramos, J.-L. (2016) Biofuels 2020: biorefineries based on lignocellulosic materials. *Microb. Biotechnol.* **9**: 585–594.

505. Valentine, J., Clifton-Brown, J., Hastings, A., Robson, P., Allison, G., and Smith, P. (2012) Food vs. fuel: the use of land for lignocellulosic "next generation" energy crops that minimize competition with primary food production. *GCB Bioenergy* **4**: 1–19.

506. Varadarajan, S. and Miller, D.J. (1999) Catalytic upgrading of fermentation-derived organic acids. *Biotechnol. Prog.* **15**: 845–854.

507. Varma, A. and Palsson, B.O. (1994) Stoichiometric flux balance models quantitatively predict growth and metabolic by-product secretion in wild-type *Escherichia coli* W3110. *Appl. Environ. Microbiol.* **60**: 3724–3731.

508. Varman, A.M., Xiao, Y., Pakrasi, H.B., and Tang, Y.J. (2013) Metabolic engineering of *Synechocystis* sp. strain PCC 6803 for isobutanol production. *Appl. Environ. Microbiol.* **79**: 908–914.

509. Vasicová, P., Pátek, M., Nešvera, J., Sahm, H., and Eikmanns, B. (1999) Analysis of the *Corynebacterium glutamicum dapA* promoter. *J. Bacteriol.* **181**: 6188–6191.

510. Vemuri, G.N., Eiteman, M.A., and Altman, E. (2002a) Effects of growth mode and

pyruvate carboxylase on succinic acid production by metabolically engineered strains of *Escherichia coli*. *Appl. Environ. Microbiol.* **68**: 1715–1727.

511. Vemuri, G.N., Eiteman, M.A., and Altman, E. (2002b) Succinate production in dual-phase *Escherichia coli* fermentations depends on the time of transition from aerobic to anaerobic conditions. *J. Ind. Microbiol. Biotechnol.* **28**: 325–332.

512. Venderbosch, R. and Prins, W. (2010) Fast pyrolysis technology development. *Biofuels, Bioprod. Biorefining* **4**: 178–208.

513. Venn, J. (1880) I. On the diagrammatic and mechanical representation of propositions and reasonings. *Philos. Mag. Ser. 5* **10**: 1–18.

514. Vertès, A.A. (2013) Protein secretion systems of *Corynebacterium glutamicum*. In, Yukawa,H. and Inui,M. (eds), *Corynebacterium glutamicum: biology and biotechnology*. Springer, Berlin, Heidelberg, pp. 351–389.

515. Vidal, M. (2009) A unifying view of 21st century systems biology. *FEBS Lett.* **583**: 3891–3894.

516. Villadsen, J., Nielsen, J., and Lidén, G. (2011) Bioreaction engineering principles 3rd ed. Springer Science+Business Media, LCC, New York, Dordrecht, Heidelberg, London.

517. Vispute, T.P. and Huber, G.W. (2009) Production of hydrogen, alkanes and polyols by aqueous phase processing of wood-derived pyrolysis oils. *Green Chem.* **11**: 1433.

518. Wall, D., Delaney, J.M., Fayet, O., Lipinska, B., Yamamoto, T., and Georgopoulos, C. (1992) *arc*-dependent thermal regulation and extragenic suppression of the *Escherichia coli* cytochrome *d* operon. *J. Bacteriol.* **174**: 6554–6562.

519. Wang, C., Cai, H., Zhou, Z., Zhang, K., Chen, Z., Chen, Y., *et al.* (2014) Investigation of *ptsG* gene in response to xylose utilization in *Corynebacterium glutamicum*. *J. Ind. Microbiol. Biotechnol.* **41**: 1249–1258.

520. Wang, C., Thygesen, A., Liu, Y., Li, Q., Yang, M., Dang, D., *et al.* (2013) Bio-oil based biorefinery strategy for the production of succinic acid. *Biotechnol. Biofuels* **6**: 74.

521. Wang, C., Zhang, H., Cai, H., Zhou, Z., Chen, Y., Chen, Y., and Ouyang, P. (2014) Succinic acid production from corn cob hydrolysates by genetically engineered *Corynebacterium glutamicum*. *Appl. Biochem. Biotechnol.* **172**: 340–350.

522. Wang, D., Li, Q., Mao, Y., Xing, J., and Su, Z. (2010) High-level succinic acid production and yield by lactose-induced expression of phosphoenolpyruvate carboxylase in *ptsG* mutant *Escherichia coli*. *Appl. Microbiol. Biotechnol.* **87**: 2025–2035.

523. Wang, J., Zhu, J., Bennett, G.N., and San, K.-Y. (2011) Succinate production from different carbon sources under anaerobic conditions by metabolic engineered *Escherichia coli* strains. *Metab. Eng.* **13**: 328–335.

524. Wayne, L.G. and Hayes, L.G. (1996) An *in vitro* model for sequential study of shiftdown of *Mycobacterium tuberculosis* through two stages of nonreplicating persistence. *Infect. Immun.* **64**: 2062–2069.

525. Wayne, L.G. and Lin, K.Y. (1982) Glyoxylate metabolism and adaptation of

*Mycobacterium tuberculosis* to survival under anaerobic conditions. *Infect. Immun.* **37**: 1042–1049.

526. Wendisch, V.F., Bott, M., Kalinowski, J., Oldiges, M., and Wiechert, W. (2006) Emerging *Corynebacterium glutamicum* systems biology. *J. Biotechnol.* **124**: 74–92.

527. Wendisch, V.F., Brito, L.F., Gil Lopez, M., Hennig, G., Pfeifenschneider, J., Sgobba, E., and Veldmann, K.H. (2016) The flexible feedstock concept in industrial biotechnology: metabolic engineering of *Escherichia coli*, *Corynebacterium glutamicum*, *Pseudomonas*, *Bacillus* and yeast strains for access to alternative carbon sources. *J. Biotechnol.* **234**: 139–157.

528. Wendisch, V.F., de Graaf, A.A., Sahm, H., and Eikmanns, B.J. (2000) Quantitative determination of metabolic fluxes during coutilization of two carbon sources: comparative analyses with *Corynebacterium glutamicum* during growth on acetate and/or glucose. *J. Bacteriol.* **182**: 3088–3096.

529. Wennerhold, J., Krug, A., and Bott, M. (2005) The AraC-type regulator RipA represses aconitase and other iron proteins from *Corynebacterium* under iron limitation and is itself repressed by DtxR. *J. Biol. Chem.* **280**: 40500–40508.

530. Werpy, T. and Petersen, G. (2004) Top value added chemicals from biomass volume I – results of screening for potential candidates from sugars and synthesis gas energy efficiency and renewable energy, Springfield, VA.

531. Westerhof, R.J.M., Brilman, D.W.F., Garcia-Perez, M., Wang, Z., Oudenhoven, S.R.G., van Swaaij, W.P.M., and Kersten, S.R.A. (2011) Fractional condensation of biomass pyrolysis vapors. *Energy & Fuels* **25**: 1817–1829.

532. Weusthuis, R.A., Lamot, I., van der Oost, J., and Sanders, J.P.M. (2011) Microbial production of bulk chemicals: development of anaerobic processes. *Trends Biotechnol.* **29**: 153–158.

533. Wibberg, D., Andersson, L., Tzelepis, G., Rupp, O., Blom, J., Jelonek, L., *et al.* (2016) Genome analysis of the sugar beet pathogen *Rhizoctonia solani* AG2-2IIIB revealed high numbers in secreted proteins and cell wall degrading enzymes. *BMC Genomics 2016 171* **17**: 245.

534. Wieschalka, S., Blombach, B., Bott, M., and Eikmanns, B.J. (2013) Bio-based production of organic acids with *Corynebacterium glutamicum*. *Microb. Biotechnol.* **6**: 87–102.

535. Wieschalka, S., Blombach, B., and Eikmanns, B.J. (2012) Engineering *Corynebacterium glutamicum* for the production of pyruvate. *Appl. Microbiol. Biotechnol.* **94**: 449–459.

536. de Wild, P.J., Huijgen, W.J.J., and Heeres, H.J. (2012) Pyrolysis of wheat straw-derived organosolv lignin. *J. Anal. Appl. Pyrolysis* **93**: 95–103.

537. Wilhelm, B.T. and Landry, J.-R. (2009) RNA-Seq – quantitative measurement of expression through massively parallel RNA-sequencing. *Methods* **48**: 249–257.

538. Williams, A., Pourkashanian, M., and Jones, J.M. (2001) Combustion of pulverised coal and biomass. *Prog. Energy Combust. Sci.* **27**: 587–610.

539. Williamson, M.P. (2005) Systems biology: will it work? *Biochem. Soc. Trans.* **33**: 503–506.

540. Wimpenny, J.W. and Firth, A. (1972) Levels of nicotinamide adenine dinucleotide and reduced nicotinamide adenine dinucleotide in facultative bacteria and the effect of oxygen. *J. Bacteriol.* **111**: 24–32.

541. Wishner, K.F., Gowing, M.M., and Gelfmana, C. (1998) Mesozooplankton biomass in the upper 1000 m in the Arabian Sea: overall seasonal and geographic patterns, and relationship to oxygen gradients. *Deep Sea Res. Part II Top. Stud. Oceanogr.* **45**: 2405–2432.

542. Woo, H.M. and Park, J.-B. (2014) Recent progress in development of synthetic biology platforms and metabolic engineering of *Corynebacterium glutamicum*. *J. Biotechnol.* **180**: 43–51.

543. Wu, H., Li, Z.-M., Zhou, L., and Ye, Q. (2007) Improved succinic acid production in the anaerobic culture of an *Escherichia coli pflB ldhA* double mutant as a result of enhanced anaplerotic activities in the preceding aerobic culture. *Appl. Environ. Microbiol.* **73**: 7837–7843.

544. Wu, H., Li, Z., Zhou, L., Xie, J., and Ye, Q. (2009) Enhanced anaerobic succinic acid production by *Escherichia coli* NZN111 aerobically grown on gluconeogenic carbon sources. *Enzyme Microb. Technol.* **44**: 165–169.

545. Xu, H., Zhou, Z., Wang, C., Chen, Z., and Cai, H. (2016) Enhanced succinic acid production in *Corynebacterium glutamicum* with increasing the available NADH supply and glucose consumption rate by decreasing $H^+$-ATPase activity. *Biotechnol. Lett.* **38**: 1181–1186.

546. Xu, R., Ferrante, L., Briens, C., and Berruti, F. (2011) Bio-oil production by flash pyrolysis of sugarcane residues and post treatments of the aqueous phase. *J. Anal. Appl. Pyrolysis* **91**: 263–272.

547. Xu, R., Ferrante, L., Briens, C., and Berruti, F. (2009) Flash pyrolysis of grape residues into biofuel in a bubbling fluid bed. *J. Anal. Appl. Pyrolysis* **86**: 58–65.

548. Yamamoto, S., Gunji, W., Suzuki, H., Toda, H., Suda, M., Jojima, T., *et al.* (2012) Overexpression of genes encoding glycolytic enzymes in *Corynebacterium glutamicum* enhances glucose metabolism and alanine production under oxygen deprivation conditions. *Appl. Environ. Microbiol.* **78**: 4447–4457.

549. Yamamoto, S., Sakai, M., Inui, M., and Yukawa, H. (2011) Diversity of metabolic shift in response to oxygen deprivation in *Corynebacterium glutamicum* and its close relatives. *Appl. Microbiol. Biotechnol.* **90**: 1051–1061.

550. Yamamoto, S., Suda, M., Niimi, S., Inui, M., and Yukawa, H. (2013) Strain optimization for efficient isobutanol production using *Corynebacterium glutamicum* under oxygen deprivation. *Biotechnol. Bioeng.* **110**: 2938–2948.

551. Yamauchi, Y., Hirasawa, T., Nishii, M., Furusawa, C., and Shimizu, H. (2014) Enhanced acetic acid and succinic acid production under microaerobic conditions by *Corynebacterium glutamicum* harboring *Escherichia coli* transhydrogenase gene *pntAB*. *J. Gen. Appl. Microbiol.* **60**: 112–118.

552. Yang, J. and Yang, S. (2017) Comparative analysis of *Corynebacterium glutamicum* genomes: a new perspective for the industrial production of amino acids. *BMC Genomics* **18**: 940.

553. Yokota, A. and Lindley, N.D. (2005) Central metabolism: sugar uptake and conversion. In, Eggeling,L. and Bott,M. (eds), *Handbook of Corynebacterium glutamicum*. CRC Press, Boca Raton, FL, USA, pp. 215–240.

554. Yukawa, H., Omumasaba, C.A., Nonaka, H., Kos, P., Okai, N., Suzuki, N., *et al.* (2007) Comparative analysis of the *Corynebacterium glutamicum* group and complete genome sequence of strain R. *Microbiology* **153**: 1042–1058.

555. Zahoor, A., Lindner, S.N., and Wendisch, V.F. (2012) Metabolic engineering of *Corynebacterium glutamicum* aimed at alternative carbon sources and new products. *Comput. Struct. Biotechnol. J.* **3**: e201210004.

556. Zaldivar, J., Nielsen, J., and Olsson, L. (2001) Fuel ethanol production from lignocellulose: a challenge for metabolic engineering and process integration. *Appl. Microbiol. Biotechnol.* **56**: 17–34.

557. Zeng, A.-P. and Sabra, W. (2011) Microbial production of diols as platform chemicals: recent progresses. *Curr. Opin. Biotechnol.* **22**: 749–757.

558. Zhang, Y., Cai, J., Shang, X., Wang, B., Liu, S., Chai, X., *et al.* (2017) A new genome-scale metabolic model of *Corynebacterium glutamicum* and its application. *Biotechnol. Biofuels* **10**: 169.

559. Zhao, X., Cheng, K., and Liu, D. (2009) Organosolv pretreatment of lignocellulosic biomass for enzymatic hydrolysis. *Appl. Microbiol. Biotechnol.* **82**: 815–827.

560. Zhao, X., Li, S., Wu, R., and Liu, D. (2017) Organosolv fractionating pre-treatment of lignocellulosic biomass for efficient enzymatic saccharification: chemistry, kinetics, and substrate structures. *Biofuels, Bioprod. Biorefining* **11**: 567–590.

561. Zheng, M., Aslund, F., and Storz, G. (1998) Activation of the OxyR transcription factor by reversible disulfide bond formation. *Science* **279**: 1718–1721.

562. Zhou, C.-H.C., Beltramini, J.N., Fan, Y.-X., and Lu, G.Q.M. (2008) Chemoselective catalytic conversion of glycerol as a biorenewable source to valuable commodity chemicals. *Chem. Soc. Rev.* **37**: 527–549.

563. Zhou, L., Wang, A., Li, C., Zheng, M., and Zhang, T. (2012) Selective production of 1,2-propylene glycol from Jerusalem artichoke tuber using Ni-$W_2C$/AC catalysts. *ChemSusChem* **5**: 932–938.

564. Zhu, J., Thakker, C., San, K.-Y., and Bennett, G. (2011) Effect of culture operating conditions on succinate production in a multiphase fed-batch bioreactor using an engineered *Escherichia coli* strain. *Appl. Microbiol. Biotechnol.* **92**: 499–508.

565. Zibek, S., Rupp, S., Hirth, T., Amann, M., Ludwig, D., and Hirth, T. (2010) Laccase-katalysierte Detoxifizierung von löslichen Ligninabbauprodukten in vorbehandelten Lignocellulose-Hydrolysaten. *Chemie Ing. Tech.* **82**: 1183–1189.

# CURRICULUM VITAE

**PERSONAL INFORMATION**

| | |
|---|---|
| Name: | Julian Lange |
| Academic Degree: | Diploma-Biologist (technically orientated), Dipl.-Biol. (t. o.) |
| Date of Birth, Birthplace: | 17.05.1988, Aalen, Germany |

**ACADEMIC CAREER**

| | |
|---|---|
| 2018 | Intended final qualification: Dr. rer. nat. |
| Since 08/2014 | **Ph.D. Student** (as part of the BBW-ForWerts graduate program)<br>Molecular Biotechnology, Institute of Biochemical Engineering (IBVT), University of Stuttgart |
| 10/2007 - 08/2013 | **Degree Course "Technical Biology"**<br>Faculty Energy-, Process- and Bio-Engineering, University of Stuttgart, Germany<br>Overall Grade: A (with distinction)<br>Diploma Thesis: Institute of Industrial Genetics, University of Stuttgart<br>Major Exam: Microbiology, physiology of the brain<br>Minor Exams: Technical biochemistry, biochemical engineering<br>Research Project: Laboratory of Structural Microbiology, Rockefeller University, New York |
| 09/1998 - 07/2007 | **Hariolf Gymnasium**, Ellwangen, Germany |

**EMPLOYMENT AND WORK EXPERIENCE**

| | |
|---|---|
| Since 11/2017 | **Process Engineer:** Aseptic Filling, Rentschler Biopharma SE, Laupheim |
| 08/2014 - 10/2017 | **Research Associate:** Molecular Biotechnology, IBVT, University of Stuttgart |
| 09/2015 | **Cooperative Research Stay:** Center for Biotechnology, University of Bielefeld |
| 02/2014 - 04/2014 | **Research Associate:** Molecular Biotechnology, IBVT, University of Stuttgart |
| 10/2013 - 01/2014 | **Research Associate:** Institute of Industrial Genetics, University of Stuttgart |
| 10/2012 - 08/2013 | **Diploma Thesis:** Institute of Industrial Genetics, University of Stuttgart |
| 07/2012 - 09/2012 | **Internship:** R&D, evoxx technologies GmbH (former evocatal GmbH), Monheim am Rhein |
| 03/2011 - 08/2011 | **Research Project:** Rockefeller University, New York, USA |
| 12/2010 - 02/2011 | **Student Research Associate:** Institute of Microbiology, University of Stuttgart |

**PUBLICATIONS (PEER-REVIEWED JOURNALS)**

| | |
|---|---|
| 06/2018 | **Lange, J.** *et al.* (2018) Deciphering the adaptation of *Corynebacterium glutamicum* in transition from aerobiosis via microaerobiosis to anaerobiosis. *Genes*. **9**: 297. |
| 01/2018 | **Lange, J.** *et al.* (2018) Harnessing novel chromosomal integration loci to utilize an organosolv-derived hemicellulose fraction for isobutanol production with engineered *Corynebacterium glutamicum*. *Microb. Biotechnol.* **11**: 257–63. |
| 11/2017 | **Lange, J.** *et al.* (2017) Valorization of pyrolysis water: a biorefinery side stream, for 1,2-propanediol production with engineered *Corynebacterium glutamicum*. *Biotechnol. Biofuels* **10**: 277. |
| 09/2017 | Hoffart, E., Grenz, S., **Lange, J**., *et al.* (2017) High substrate uptake rates empower *Vibrio natriegens* as production host for industrial biotechnology. *Appl. Environ. Microbiol.* AEM.01614-17. |
| 01/2017 | **Lange J**, *et al.* 2017. Zero-growth bioprocesses: A challenge for microbial production strains and bioprocess engineering. *Eng. Life Sci.* **17**:27-35. |
| 12/2014 | Morabbi Heravi K., **Lange J.**, *et al.* (2014) Transcriptional regulation of the vanillate utilization genes (*vanABK* operon) of *Corynebacterium glutamicum* by VanR, a PadR-like repressor. *J. Bacteriol.* **197**:959-72. |

# APPENDIX

# A1. Supplementary background

## A1.1. Elemental analysis of bioresources

**Table S 1. Elemental analysis of crude and pretreated biomasses and in comparison to petroleum**. Representative values from literature are given and depicted as % (w/w). Data are visualized in Figure 2.3 (p. 24).

| Material | Ultimate elemental analysis in % (w/w) | | | | Reference |
|---|---|---|---|---|---|
| | C | H | O [a] | N | |
| **Petroleum** | 83.0-87.0 [b] | 10.0-14.0 [b] | 0.05-1.5 [b] | 0.10-2.0 [b] | (James G. Speight, 1982) |
| **Wheat straw** | 47.3 | 5.5 | 45.3 | 0.9 | (Fantini, 2017) |
| **Beech wood** | 47.8 | 6.3 | 45.1 | 0.4 | (Gucho *et al.*, 2015) |
| **Bio-oil (typical)** | 56 | 6 | 38 | 0-0.1 | (Bridgwater, 2017) |
| **Bio-oil (wheat straw)** | 49.0 | 5.9 | 44.5 | 0.7 | (Tröger *et al.*, 2013) |
| **Organosolv (beech wood lignin)** | 62.6 | 6.0 | 31.2 | 0.2 | (Luo *et al.*, 2012) |

[a] calculated differentially

[b] for Figure 2.3 the average values are visualized

# A2. Supplementary methods

## A2.1. Devices and materials

**Table S 2. Devices and materials**.

| Product | Company | Purpose | Cat. No. |
|---|---|---|---|
| 2100 Bioanalyzer Instruments | Agilent Technologies | For RNA and DNA analysis by capillary electrophoresis | |

| Product | Company | Purpose | Cat. No. |
|---|---|---|---|
| Agilent 1200 Series | Agilent Technologies | HPLC apparatus (sugar, acid, alcohol and amino acid quantification) | |
| BCP-CO2 | BlueSens gas sensor GmbH | Exhaust gas $CO_2$ analysis | |
| BCP-O2 | BlueSens gas sensor GmbH | Exhaust gas $O_2$ analysis | BCP-02 |
| benchtop shaker AK 85 | Infors AG | Rotary incubation of bacterial cultures | |
| Centrifuge 5417 R, rotor: FA45-30-11 | Eppendorf AG | Tabletop centrifuge for 1.5 mL and 2 mL tubes | |
| Centrifuge 5427 R, rotor: FA-45-30-11 or F-35-6-30 | Eppendorf AG | Tabletop centrifuge for centrifugation of 1.5 mL, 2 mL, 15 mL and 50 mL reaction tubes and DURAN® Centrifuge Tubes Round Bottom | 5409000012 |
| Centrifuge 5804 R, rotor: A-4-44 or FA 45-30-11 | Eppendorf AG | Tabletop centrifuge for centrifugation of 1.5 mL, 2 mL, 15 mL and 50 mL reaction tubes | 5805000327 |
| Centrifuge MiniSpin®, rotor F-45-12-11 | Eppendorf AG | Tabletop centrifuge for centrifugation of 0.2 µL, 1.5 mL and 2 mL reaction tubes | 5452000018 |
| Centrifuge Tubes Round Bottom (DURAN® 50x 12 ml) | Carl-Roth GmbH | CDW determination | C102.1 |
| DR 2800 Portable spectrophotometer | Hach Lange GmbH | $OD_{600}$ analysis | |
| DropSense16 - Micro-Volume Spectrophotometer [Xpose dscvry] | Unchained Labs [Trinean] | RNA quantification | |
| Electroporation cuvettes, 2 mm, 40-400 µL | VWR International GmbH | For transformation of strains with plasmids | 732-1136 |
| Eporator® | Eppendorf AG | Device for electroporation | 4309000019 |
| High performance ZORBAX guard fittings kit | Agilent Technologies | HPLC hardware kit (amino acid quantification) | 820999-901 |
| InLab® Easy | Mettler-Toledo GmbH | pH electrode | 51343010 |
| InPro® 3100/255 Pt100 | Mettler-Toledo GmbH | pH probe bioreactors | 52000661 |
| InPro® 6800 Series $O_2$ Sensors | Mettler-Toledo GmbH | DO probe | 52200968 |
| Mass flow controller, 0-2 l/min | Analyt-MTC GmbH | Mass flow controller for gassing during 30 L cultivations | GFC 171S |
| Mass flow controller, 0-500 ml/min | Analyt-MTC GmbH | Mass flow controller for gassing during triple glass reactor cultivations | GFC 171S |
| MF-Millipore Membrane Filter, mixed cellulose esters, hydrophile, 0,025 µm pore size, 13 mm | Merck Chemicals GmbH | Diafiltration | VSWP01300 |
| Microplate, 96 well, PS | Greiner Bio-One GmbH | Plates for protein analytics | 655101 |
| Multi N/C 2100s | Analytik Jena AG | TOC analysis | |

| Product | Company | Purpose | Cat. No. |
|---|---|---|---|
| Nano Drop ND-1000 Spectrophotometer | PEQLAB Biotechnologie GmbH | Quantification of purified DNA | |
| PARAFILM® M | Carl-Roth GmbH | Plastic shred for pyrolysis water purification | H666.1 |
| Pharmacia LKB Ultrospec III UV/Vis spectrophotometer | GE Healthcare Europe GmbH | $OD_{600}$ analysis | |
| Precellys®24 | Bertin Instruments | Mechanical cell lysis | |
| Refractive Index Detector (RID) Detector (Serial CN60557304) | Agilent Technologies | HPLC detector (sugar, acid and alcohol quantification) | |
| Rezex™ ROA-Organic Acid H+ (8%) | Phenomenex Inc. | HPLC column (sugar, acid and alcohol quantification) | 00H-0138-K0 |
| Rotilabo®-syringe filters, CME, 0.22 µm | Carl-Roth GmbH | Filters for stock solution sterilization | KH54.1 |
| Rotilabo®-syringe filters, CME, 0.45 µm | Carl-Roth GmbH | Filters for stock solution sterilization | KH55.1 |
| S20 - SevenEasy™ pH | Mettler-Toledo GmbH | pH meter interface | 51302803 |
| SecurityGuard™ Guard Cartridge Kit | Phenomenex Inc. | HPLC equipment (sugar, acid and alcohol quantification) | KJ0-4282 |
| SecurityGuard™ Standard Carbo-$H^+$ | Phenomenex Inc. | HPLC guard column (sugar, acid and alcohol quantification) | AJ0-4490 |
| Semi-micro cuvette, acrylic | Sarstedt AG & Co | Photometric analysis of enzyme activities | 67.740 |
| Semi-micro cuvette, PS | Sarstedt AG & Co | Photometric analysis of $OD_{600}$ | 67.742 |
| Silicon plate, 6 mm, transparent | Industriebedarf Castan GmbH | Cut septi for anaerobic shaking flasks | CASIL501T-6MM |
| Synergy 2 Multi-Mode Reader | BioTek Instruments GmbH | Protein analytics at 560 nm | |
| TAdvanced thermocycler | Biometra GmbH | Thermocycler for standard and colony PCR and isothermal assembly | |
| Ultrospec 10 Cell Density Meter (Amersham Biosciences) | GE Healthcare Europe GmbH | $OD_{600}$ analysis | |
| Ultrospec™ 2100 pro UV/Visible spectrophotometer | GE Healthcare Europe GmbH | Photometric enzyme activity analysis | |
| UV Transilluminator 312 nm | INTAS Science Imaging Instruments GmbH | UV screen to cut out bands in agarose gels prior to gel elution | |
| Zorbax Eclipse Plus C18 | Agilent Technologies | HPLC column (amino acid quantification) | 959990-902 |
| ZORBAX Eclipse Plus C18 | Agilent Technologies | HPLC guard column (amino acid quantification) | 820950-936 |

## A2.2. Kits

**Table S 3. Commercial kits**.

| Product | Company | Purpose | Cat. No. |
|---|---|---|---|
| Agilent DNA 7500 Kit | Agilent Technologies | Sequencing library verification | 5067-1506 |
| Agilent RNA 6000 Nano Kit | Agilent Technologies | RNA integrity analysis | 5067-1511 |
| Agilent RNA 6000 Pico Kit | Agilent Technologies | rRNA depletion verification | 5067-1513 |
| DNeasy Blood & Tissue Kit | QIAGEN | Chromosomal DNA Isolation from *E. coli* and *C. glutamicum* | 69504 |
| E.Z.N.A.® Plasmid Mini Kit I | Omega Bio-Tek, Inc. | Plasmid isolation from *E. coli* | D6942-02 |
| NucleoSpin® Gel and PCR Clean-up | Macherey-Nagel GmbH & Co. KG | PCR clean-up and purification of plasmids or PCR fragments from agarose gels | 740.609.250 |
| Pierce™ BCA Protein Assay Kit | Thermo Fisher Scientific Inc. | Protein quantification | 23227 |
| Ribo-Zero rRNA Removal Kit (Bacteria) | Illumina, Inc. | rRNA removal Kit | MRZMB126 |
| RNeasy Mini Kit | QIAGEN | RNA isolation | 74106 |
| TruSeq Stranded mRNA Library Prep Kit | Illumina, Inc. | cDNA library preparation | RS-122-2101 |

## A2.3. Chemicals

**Table S 4. Chemicals**.

| Product | Company | Cat. No. |
|---|---|---|
| Acetic acid ROTIPURAN®, 100 % | Carl-Roth GmbH | 3738.2 |
| Acetol, hydroxyacetone, 95 % | Alfa Aesar, Thermo Fisher Scientific | L15008 |
| Acetonitrile | VWR International GmbH | 83639 320 |
| Ammonia solution, $NH_3 + H_2O$, ≥ 25 % | Carl-Roth GmbH | 5460.4 |
| Ammonium sulphate, $(NH_4)_2SO_4$, ≥ 99 % | Carl-Roth GmbH | 9218.5 |
| Arabinose, L-(+)-, ≥ 99 % | Carl-Roth GmbH | 5118.2 |
| Bacto™ Brain Heart Infusion | Becton, Dickinson and Company | 237500 |
| Biotin, D(+)-, ≥ 98.5 % | Carl-Roth GmbH | 3822.1 |
| Boric acid | Merck Chemicals GmbH | 1.00165.0500 |
| Bromophenol blue sodium salt | Sigma-Aldrich Co. LLC. | B8026 |
| Buffer solution, pH 4,00 ± 0,02 (20 °C) | Carl-Roth GmbH | A517.1 |
| Buffer solution, pH 7,00 ± 0,02 (20 °C) | Carl-Roth GmbH | P713.1 |

| Product | Company | Cat. No. |
|---|---|---|
| Buffer solution, pH 9,00 ± 0,02 (20 °C) | Carl-Roth GmbH | P714.3 |
| Calcium chloride, $CaCl_2$, (discontinued; similar product #1023791000) | Merck Chemicals GmbH | 2389 |
| Chloramphenicol, ≥ 99 % | Sigma-Aldrich Co. LLC. | 23275 |
| Copper(II) sulfate pentahydrate, $CuSO_4 \cdot 5\ H_2O$, ≥ 99 % | Sigma-Aldrich Co. LLC. | 61240 |
| DMSO (dimethyl sulfoxide), 100 % | Thermo Fisher Scientific Inc. | F-515 |
| Ethylenediamine tetraacetic acid (EDTA) disodium salt dehydrate, ≥ 99 % | Carl-Roth GmbH | X986.2 |
| Fmoc chloride | Sigma-Aldrich Co. LLC. | 23186 |
| Glass beads, 0.1 mm | Carl-Roth GmbH | HH55.1 |
| Glass beads, 4 ± 0.3 mm | Carl-Roth GmbH | N029.1 |
| Glucose, α-D(+)-, monohydrate, ≥ 99.5 % | Carl-Roth GmbH | 6780.3 |
| Glutathione, L-, GSH, γ-L-glutamyl-L-cysteinyl-glycine, reduced, CELLPURE®, ≥ 99 % | Carl-Roth GmbH | 6832.2 |
| Glycerol, ≥ 98 % | Carl-Roth GmbH | 7530.1 |
| Hydrochloric acid, HCl, ≥ 32% | Sigma-Aldrich Co. LLC. | 84411 |
| Iron(II) sulfate heptahydrate, $FeSO_4 \cdot 7\ H_2O$, 99.0-103.4 % | Sigma-Aldrich Co. LLC. | 31236 |
| Isoleucine, L-, ≥ 99 % | Merck Chemicals GmbH | 1.05362.0025 |
| Kanamycin sulphate | Carl-Roth GmbH | T832 |
| Leucine, L-, ≥ 99 % | Merck Chemicals GmbH | 1.05360.0025 |
| Magnesium sulphate heptahydrate, $MgSO_4 \cdot 7\ H_2O$, ≥ 99 % | Carl-Roth GmbH | P027.3 |
| Manganese(II) sulfate monohydrate, $MnSO_4 \cdot H_2O$, ≥ 98 % | Sigma-Aldrich Co. LLC. | 63555 |
| Mercaptopropionic acid, 3-, ≥ 99 % | Sigma-Aldrich Co. LLC. | 63768 |
| Methanol | VWR International GmbH | 20864 320 |
| Morpholino propane sulphonic acid, 3-N-, MOPS, PUFFERAN®, ≥ 99.5 % | Carl-Roth GmbH | 6979.3 |
| Nickel(II) sulphate hexahydrate, $NiSO_4 \cdot 6\ H_2O$, ≥ 98 % | Carl-Roth GmbH | 7322.1 |
| Nicotinamide adenine dinucleotide phosphate disodium dihydrate, β-, NADP $Na_2$ | GERBU Biotechnik GmbH | 1014,1000 |
| Nicotinamide adenine dinucleotide, β-, NAD | GERBU Biotechnik GmbH | 1013,0001 |
| Perchloric acid, 70-72 % | Sigma-Aldrich Co. LLC. | 7601-90-3 |
| Phosphoric acid, *o*-, ROTIPURAN® ≥ 85 % | Carl-Roth GmbH | 6366.2 |
| Phthaldialdehyde, *o*- | Sigma-Aldrich Co. LLC. | 79760 |
| Potassium acetate, 99.0-100.5 % | Merck Chemicals GmbH | 1048201000 |
| Potassium dihydrogen phosphate, $KH_2PO_4$, ≥ 98 % | Carl-Roth GmbH | P018.5 |
| Potassium hydrogen phosphate, di-, $K_2HPO_4$, anhydrous, ≥ 98 % | Carl-Roth GmbH | 6875.3 |

| Product | Company | Cat. No. |
|---|---|---|
| Potassium hydrogen phthalate, 99.9-100.1 % | Merck Chemicals GmbH | 104874 |
| Potassium hydroxide, KOH, pellets, ≥ 85 % | Carl-Roth GmbH | 6751.2 |
| Protocatechuic acid, PCA, 3,4-dihydroxybenzoic acid, ≥ 97 % | Carl-Roth GmbH | 8274.1 |
| Sodium azide, $NaN_3$, ≥ 99.5 % | Sigma-Aldrich Co. LLC. | S2002 |
| Sodium carbonate, ≥ 99.5 % | Carl-Roth GmbH | A135.1 |
| Sodium chloride, NaCl, > 99.8 % | Carl-Roth GmbH | 9265.2 |
| Sodium hydroxide, NaOH, pearls, ≥ 99 % | Carl-Roth GmbH | 9356.2 |
| Sodium sulfite, ≥ 98 %, anhydrous | Carl-Roth GmbH | 8637.1 |
| Sodium tetraborate decahydrate, ≥ 99.5 % | Sigma-Aldrich Co. LLC. | S9640 |
| Sorbitol, D-, ≥ 98 % | Carl-Roth GmbH | 6213.1 |
| Spectinomycin dihydrochloride pentahydrate, ≥ 98 % | Sigma-Aldrich Co. LLC. | S9007-25G |
| Struktol™ J 647, 1015 kg $(m^3)^{-1}$, 500 mPa s, combination of polyglycol ethers and aliphatic alcohols, antifoam agent fermentation | Schill+Seilacher GmbH | |
| TRIS PUFFERAN®, ≥ 99,9 % | Carl-Roth GmbH | 4855.2 |
| Tryptone | Becton, Dickinson and Company | 211701 |
| Urea, ≥ 99 % | Sigma-Aldrich Co. LLC. | 51460 |
| Valine, L-, ≥ 99 % | Merck Chemicals GmbH | 1.08495.0025 |
| Water HiPerSolv CHROMANORM® | VWR International GmbH | 83645 320 |
| Xylene Cyanol FF | Sigma-Aldrich Co. LLC. | X4126 |
| Xylose, D-(+)-, ≥ 98.5 % | Carl-Roth GmbH | 5537.2 |
| Yeast extract | Becton, Dickinson and Company | 212730 |
| Zinc sulfate heptahydrate, $ZnSO_4 \cdot 7\ H_2O$, 99.0-103.0 % | Sigma-Aldrich Co. LLC. | 96501 |

## A2.4. Enzymes

**Table S 5. Enzymes and related buffers**.

| Product | Company | Purpose | Cat. No. |
|---|---|---|---|
| PCR | | | |
| Coral Red Buffer Dye solution, 10x | Genaxxon BioScience GmbH | Dye for colony PCR | M3309 |
| dATP Solution (100 mM) | Thermo Fisher Scientific Inc. | For equimolar dNTP mix for PCR | R0141 |
| dCTP Solution (100 mM) | Thermo Fisher Scientific Inc. | For equimolar dNTP mix for PCR | R0151 |

| Product | Company | Purpose | Cat. No. |
|---|---|---|---|
| dGTP Solution (100 mM) | Thermo Fisher Scientific Inc. | For equimolar dNTP mix for PCR | R0161 |
| dTTP Solution (100 mM) | Thermo Fisher Scientific Inc. | For equimolar dNTP mix for PCR | R0171 |
| PCR Buffer S complete, 10x | Genaxxon BioScience GmbH | Buffer for colony PCR | M3454.0015 |
| Phusion GC Buffer, 5x | Thermo Fisher Scientific Inc. | Buffer for standard PCR | F519 |
| Phusion Hot Start II HF DNA Polymerase, 100 U | Thermo Fisher Scientific Inc. | Standard polymerase used in PCR | F-549S |
| Taq DNA Polymerase S, 250 Units, 5 U $mL^{-1}$ | Genaxxon BioScience GmbH | Polymerase for colony PCR | M3001.0250 |
| Isothermal assembly and cloning | | | |
| FastAP Thermosensitive Alkaline Phosphatase, 1 U $mL^{-1}$ | Thermo Fisher Scientific Inc. | For dephosphorylation of DNA | EF0654 |
| T4 DNA Ligase Buffer, 10x | Thermo Fisher Scientific Inc. | Buffer for ligation | B69 |
| T4 DNA Ligase, 400,000 U $mL^{-1}$ | New England Biolabs | For isothermal assembly mix | M0202S |
| T4 DNA Ligase, LC, 1 U $\mu L^{-1}$ | Thermo Fisher Scientific Inc. | For ligation during plasmid cloning | EL0016 |
| T5 Exonuclease, 10,000 U $mL^{-1}$ | New England Biolabs | For isothermal assembly mix | M0363S |
| Restriction | | | |
| BamHI, 10 U $mL^{-1}$ | Thermo Fisher Scientific Inc. | Restriction digest | ER0051 |
| BamHI-Lsp1109I Buffer, 10x | Thermo Fisher Scientific Inc. | Reaction buffer | B57 |
| Buffer B, 10x | Thermo Fisher Scientific Inc. | Reaction buffer | BB5 |
| Buffer O, 10x | Thermo Fisher Scientific Inc. | Reaction buffer | BO5 |
| Buffer R, 10x | Thermo Fisher Scientific Inc. | Reaction buffer | BR5 |
| Buffer Tango, 10x | Thermo Fisher Scientific Inc. | Reaction buffer | BY5 |
| EcoRI Buffer, 10x | Thermo Fisher Scientific Inc. | Restriction digest | B12 |
| EcoRI, 10 U $mL^{-1}$ | Thermo Fisher Scientific Inc. | Restriction digest | ER0271 |
| HindIII, 10 U $mL^{-1}$ | Thermo Fisher Scientific Inc. | Restriction digest | ER0501 |
| NheI, 10 U $mL^{-1}$ | Thermo Fisher Scientific Inc. | Restriction digest | ER0971 |
| NotI, 10 U $mL^{-1}$ | Thermo Fisher Scientific Inc. | Restriction digest | ER0591 |
| PaeI (SphI), 10 U $mL^{-1}$ | Thermo Fisher Scientific Inc. | Restriction digest | ER0601 |
| SalI, 10 U $mL^{-1}$ | Thermo Fisher Scientific Inc. | Restriction digest | ER0641 |

| Product | Company | Purpose | Cat. No. |
|---|---|---|---|
| XbaI, 10 U $mL^{-1}$ | Thermo Fisher Scientific Inc. | Restriction digest | ER0681 |

## A2.5. Materials and apparatuses for agarose gel electrophoresis

**Table S 6. Materials and apparatuses for agarose gel electrophoresis**.

| Product | Company | Purpose | Cat. No. |
|---|---|---|---|
| 15-Well Comb | Bio-Rad Laboratories, Inc. | | 1704465 |
| 15-Well Comb | Bio-Rad Laboratories, Inc. | | 1704446 |
| 20-Well Comb | Bio-Rad Laboratories, Inc. | | 1704447 |
| 8-Well Comb | Bio-Rad Laboratories, Inc. | | 1704463 |
| Biozym LE Agarose | Biozym Scientific GmbH | | 840004 |
| GelRed Nucleic Acid Gel Stain, 10,000x in water, 0.5 mL | Biotinum | Agarose gel stain | 41003 |
| GeneRuler 1 kb Plus DNA Ladder | Thermo Fisher Scientific Inc. | DNA ladder | SM1331 |
| LAS-3000 Imager (Filter: 605DF40) | Fujifilm Medical Systems | Imaging of agarose gels at UV light (320 nm) | |
| Power Pack P25 | Biometra GmbH | Power source | 846-040-800 |
| Sub-Cell® GT Cell, Mini-Sub® Cell GT Cell, Wide Mini-Sub Cell GT Cell | Bio-Rad Laboratories, Inc. | Various chambers | |

## A2.6. Media and buffers

**Table S 7. 2x yeast extract tryptone (YT) complex medium** (Sambrook and Russell, 2001).

| Component | Amount |
|---|---|
| Tryptone | 16 g $L^{-1}$ |
| Yeast extract | 10 g $L^{-1}$ |
| NaCl | 5 g $L^{-1}$ |

**Table S 8. Brain heart infusion (BHI) medium for cultivation of *C. glutamicum*** (Eggeling and Reyes, 2005). For cultivation on semisolid medium 1.8 % (w/v) agar were added prior to autoclavation.

| Component | Amount |
|---|---|
| BHI | 37 g $L^{-1}$ |

**Table S 9 Brain heart infusion sorbitol (BHIS) medium** (Eggeling and Reyes, 2005). Cultivation of *C. glutamicum* for production of electro competent cells and to perform electroporation. BHI and sorbitol, solutions were autoclaved separately and subsequently mixed. For cultivation on semisolid medium 1.8 % (w/v) agar were added prior to autoclavation.

| Component | Amount |
|---|---|
| BHI | 18.5 g |
| ad $dH_2O$ | 300 mL |
| Sorbitol | 45.6 g |
| ad $dH_2O$ | 200 mL |

**Table S 10. $CGXII_S$ minimal medium literature comparison**. The medium was used as standard for defined cultivation of *C. glutamicum* in this study (Blombach IBVT). $CGXII_S$ represents a modified version using distinct features from published CGXII media. Specific modifications [underlined]. (Eikmanns *et al.*, 1991) *[italic].* (Keilhauer *et al.*, 1993) **[bold]**

| | Final concentrations | | |
|---|---|---|---|
| | **$CGXII_S$** (Blombach IBVT) | (Eikmanns *et al.*, 1991) | (Keilhauer *et al.*, 1993) |
| $(NH_4)_2SO_4$ | *5 g $L^{-1}$* | *5 g $L^{-1}$* | **20 g $L^{-1}$** |
| Urea | *5 g $L^{-1}$* | *5 g $L^{-1}$* | **5 g $L^{-1}$** |
| MOPS | *21 g $L^{-1}$* | *20.9 g $L^{-1}$* | **42 g $L^{-1}$** |
| $K_2HPO_4$ | **1 g $L^{-1}$** | *0.5 g $L^{-1}$* | **1 g $L^{-1}$** |
| $KH_2PO_4$ | **1 g $L^{-1}$** | *0.5 g $L^{-1}$* | **1 g $L^{-1}$** |
| $MgSO_4$ x 7 $H_2O$ | 0.25 g $L^{-1}$ | *0.25 g $L^{-1}$* | **0.25 g $L^{-1}$** |
| $CaCl_2$ | 0.01 g $L^{-1}$ | *0.01 g $L^{-1}$* | **0.01 g $L^{-1}$** |
| $FeSO_4$ x 7 $H_2O$ | 16.4 mg $L^{-1}$ | *10 mg $L^{-1}$* | **10 mg $L^{-1}$** |
| $MnSO_4$ x $H_2O$ | 10 mg $L^{-1}$ | *10 mg $L^{-1}$* | **10 mg $L^{-1}$** |
| $CuSO_4$ x 5 $H_2O$* | 0.2 mg $L^{-1}$ | *0.2 mg $L^{-1}$* | **0.2 mg $L^{-1}$** |
| $ZnSO_4$ x 7 $H_2O$ | 1 mg $L^{-1}$ | *1 mg $L^{-1}$* | **1 mg $L^{-1}$** |
| $NiCl_2$ x 6 $H_2O$ | **0.02 mg $L^{-1}$** | - | **0.02 mg $L^{-1}$** |
| Biotin | 0.2 mg $L^{-1}$ | *0.2 mg $L^{-1}$* | **0.2 mg $L^{-1}$** |
| PCA | - | - | **30 mg $L^{-1}$** |
| pH | 7.4 | *6.5* | **7** |

* Eikmanns *et al.* and Keilhauer *et al.* use water free $CuSO_4$

**Table S 11. CGXII$_S$ minimal medium**. $MgSO_4$, $CaCl_2$, TES and biotin were added after medium autoclavation from sterile filtered stock solutions freshly prior to cultivation. The pH was adjusted to 7.4 with 5 N KOH.

| Component | Stock concentration | Amount |
|---|---|---|
| $(NH_4)_2SO_4$ | - | 5 g $L^{-1}$ |
| Urea | - | 5 g $L^{-1}$ |
| MOPS | - | 21 g $L^{-1}$ |
| $K_2HPO_4$ | - | 1 g $L^{-1}$ |
| $KH_2PO_4$ | - | 1 g $L^{-1}$ |
| $MgSO_4$ x 7 $H_2O$ | 1000x (250 g $L^{-1}$) | 0.25 g $L^{-1}$ |
| $CaCl_2$ | 1000x (10 g $L^{-1}$) | 0.01 g $L^{-1}$ |
| TES | 1000x | 1 mL $L^{-1}$ |
| Biotin | 1000x (200 mg $L^{-1}$) | 0.2 mg $L^{-1}$ |
| PCA* | 1000x (30 g $L^{-1}$) | 30 mg $L^{-1}$ |

* protocatechuic acid (PCA) was optionally added as indicated in the respective experiments (e.g. $CGXII_{S+PCA}$, $CGXII_{2+PCA}$)

**Table S 12. 1000x trace elements solution (TES) for CGXII medium**. The pH was adjusted to 1 with 32 % (w/v) HCl for complete dissolution.

| Component | Amount |
|---|---|
| $FeSO_4$ x 7 $H_2O$ | 16.4 g $L^{-1}$ |
| $MnSO_4$ x $H_2O$ | 10 g $L^{-1}$ |
| $CuSO_4$ x 5 $H_2O$* | 0.2 g $L^{-1}$ |
| $ZnSO_4$ x 7 $H_2O$ | 1.0 g $L^{-1}$ |
| $NiCl_2$ x 6 $H_2O$ | 0.02 g $L^{-1}$ |

* original publications use water free $CuSO_4$ (Eikmanns *et al.*, 1991; Keilhauer *et al.*, 1993)

**Table S 13. 50x Tris-acetate and EDTA (TAE) buffer.** Dilution to the 1x working solution for agarose gel electrophoresis results in final concentrations of 40 mM Tris-acetate and 1 mM EDTA.

| Component | Amount |
|---|---|
| Tris base | 242 g |
| Acetic acid | 57.1 mL |
| EDTA (0.5 M, pH 8.0) | 100 mL |
| ad $dH_2O$ | 1 L |

**Table S 14. 5x Iso reaction buffer** for isothermal assembly after Gibson *et al.* (Gibson, 2011).

| Component | Amount |
|---|---|
| PEG-8000 | 1.5 g |
| Tris-HCl (1 M, pH 7.5) | 3 mL |
| $MgCl_2$ (2 M) | 150 µL |
| DTT (1 M) | 300 µL |
| dCTP (100 mM) | 60 µL |
| dATP (100 mM) | 60 µL |
| dTTP (100 mM) | 60 µL |
| dGTP (100 mM) | 60 µL |
| $NAD^+$ (100 mM) | 300 µL |

**Table S 15. Iso enzyme-reagent mix** for isothermal assembly after Gibson *et al.* (Gibson, 2011). The reagent was stored at -21 °C.

| Component | Amount |
|---|---|
| 5x Iso reaction buffer | 320 µL |
| T5 Exonuclease (10 U $mL^{-1}$) | 0.64 µL |
| T4 DNA Ligase (40 U $mL^{-1}$) | 160 µL |
| Phusion Hot Start II HF DNA Polymerase (2 U $mL^{-1}$) | 20 µL |
| ad $dH_2O$ | 1200 µL |

**Table S 16. 6x DNA loading dye** for agarose gel electrophoresis (Sambrook and Russell, 2001). Used 1x concentrated in DNA samples for loading.

| Component | Amount |
|---|---|
| Xylene cyanol FF | 0.075 g |
| Bromophenol blue | 0.075 g |
| Glycerol, ≥ 98 % | 15 mL |
| ad $dH_2O$ | 50 mL |

**Table S 17. Lysis buffer** used for cell disruption of *C. glutamicum* via glass beads in a Precellys®24 (Bertin Instruments, Montigny-le-Bretonneux, France). The pH was adjusted to 7.4 with HCl (cf. 3.11.1, p. 93).

| Component | Amount |
|---|---|
| Tris-HCl (pH 7.4) | 0.1 M |
| Glycerol | 10 % (v/v) |

**Table S 18. Analysis buffer** used for enzyme activity measurement of the glucose-6-phosphate dehydrogenase and the 6-phosphogluconate dehydrogenase (3.12.6, p. 97).

| Component | Amount |
|---|---|
| Tris-HCl (pH 7.5) | 50 mM |
| $MgCl_2$ | 10 mM |
| $NADP^+$ | 1 mM |

## A2.7. PCR

**Table S 19. Standard PCR**. **A**. Reaction batch composition with variable amounts (X) of the DNA template. **B**. Thermocycler program.

**A**

| DNA template | X µL |
|---|---|
| DMSO | 2 µL |
| Phusion Hot Start II HF | 1 µL |
| dNTP mix (10 mM) | 5 µL |
| Phusion GC Buffer (5x, + $MgCl_2$) | 10 µL |
| Primer (10 pmol $\mu L^{-1}$) | 2 µL |
| ad $dH_2O$ | 50 µL |

**B**

| | | | |
|---|---|---|---|
| Denaturation | 98 °C | 3 min | |
| Denaturation | 98 °C | 0.25 min | |
| Annealing | 55 °C | 0.5 min | 30-35 cycles |
| Elongation | 72 °C | 0.25 min per 1 kb | |
| Elongation | 72 °C | 5 min | |
| Hold | 4 °C | ∞ | |

**Table S 20. Colony PCR**. **A.** Reaction batch. **B**. Thermocycler program.

**A**

| Colony DNA template | 10 µL |
|---|---|
| DMSO | 1 µL |
| Taq DNA Polymerase | 0.5 µL |
| dNTP mix (10 mM) | 2.5 µL |
| PCR Buffer S complete (10x) | 2.5 µL |
| Coral Red Buffer Dye (10x) | 2.5 µL |
| Primer (10 pmol $\mu L^{-1}$) | 2 µL |
| $dH_2O$ | 4 µL |

**B**

| | | | |
|---|---|---|---|
| Denaturation | 95 °C | 5 min | |
| Denaturation | 95 °C | 0.5 min | |
| Annealing | 55 °C | 0.5 min | 30-35 cycles |
| Elongation | 72 °C | 1 min per 1 kb | |
| Elongation | 72 °C | 8 min | |
| Storing | 4 °C | ∞ | |

## A2.8. BSA calibration for protein quantification

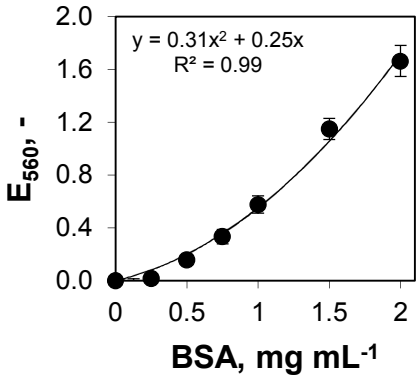


**Figure S 1. BSA calibration plot for protein quantification**. Quantification was accomplished with BCA Protein Assay Kit (Thermo Fisher Scientific Inc., Waltham, USA) by measuring a 9-level standard calibration curve of diluted albumin (BSA) at 560 nm in a Synergy 2 microplate reader (BioTek Instruments, Inc., Winooski, VT, USA).

## A2.9. CDW/$OD_{600}$ correlation

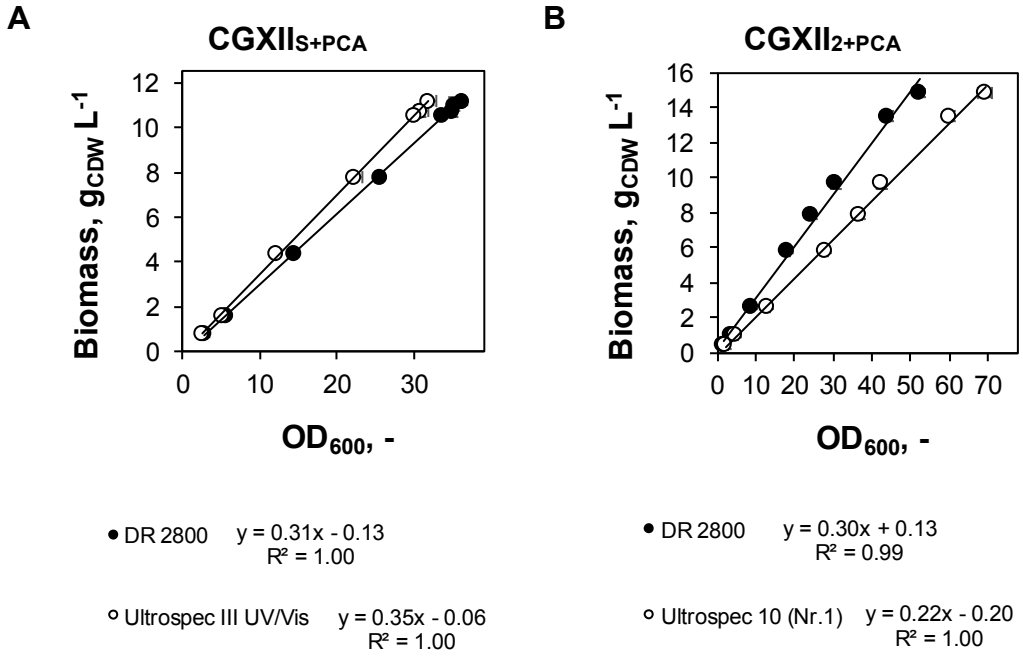

**Figure S 2. CDW/$OD_{600}$ correlation** (CDW [g $L^{-1}$] = α · $OD_{600}$). *C. glutamicum* WT was cultivated after Figure 3.1 D (p. 83) in the 30 L bioreactor triple-phase process in $CGXII_{S\ or\ 2+PCA}$ + 60 g glucose $L^{-1}$ minimal medium over a wide range of growth rates and oxygen availabilities (Figure 4.12, p. 143). Cell dry weight (CDW) concentrations and $OD_{600}$ biosuspension analysis was conducted and correlated. Two coefficients α in $CGXII_{S+PCA}$ medium of 0.35 g $L^{-1}$ (used for shaking flask experiments; Pharmacia LKB Ultrospec III UV/Vis spectrophotometer, GE Healthcare Europe GmbH, Freiburg, Germany) and 0.31 g $L^{-1}$ (used for bioreactor cultivations; DR 2800 Spectrophotometer, Hach Lange GmbH, Düsseldorf, Germany) and two coefficients α in $CGXII_{2+PCA}$ medium of 0.22 g $L^{-1}$ (used for shaking flask experiments; Ultrospec 10 Cell Density Meter, GE Healthcare Europe GmbH, Freiburg, Germany) and 0.30 g $L^{-1}$ (used for bioreactor cultivations; DR 2800 Spectrophotometer, Hach Lange GmbH, Düsseldorf, Germany) were calculated by linear regression. The respective line of best fit as well as corresponding linear equations and the coefficients of determination ($R^2$) are given. Error bars show SD of a technical triplicate of analysis.

## A2.10. Calibration of TC and TIC

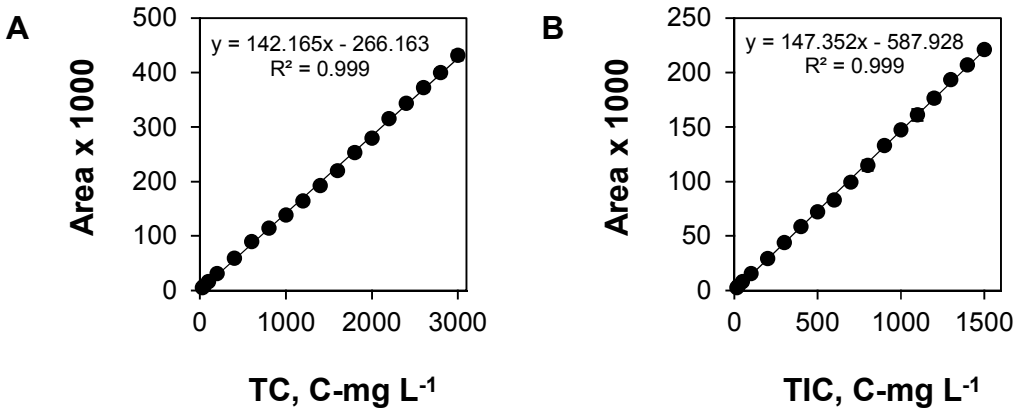


**Figure S 3. Calibration of total carbon (TC) and total inorganic carbon (TIC)** concentrations via 18-level external calibration with solutions comprising potassium hydrogen phthalate and sodium carbonate. The analyzed peak area is plotted over the applied carbon concentrations in carbon mg (C-mg) $L^{-1}$. Further description can be seen above (cf. 3.12.7, p. 98). The respective line of best fit as well as corresponding linear equations and the coefficients of determination ($R^2$) are given. SD of at least three technical replicates are shown.

## A2.11. Calibration HPLC Rezex™ ROA-Organic Acid

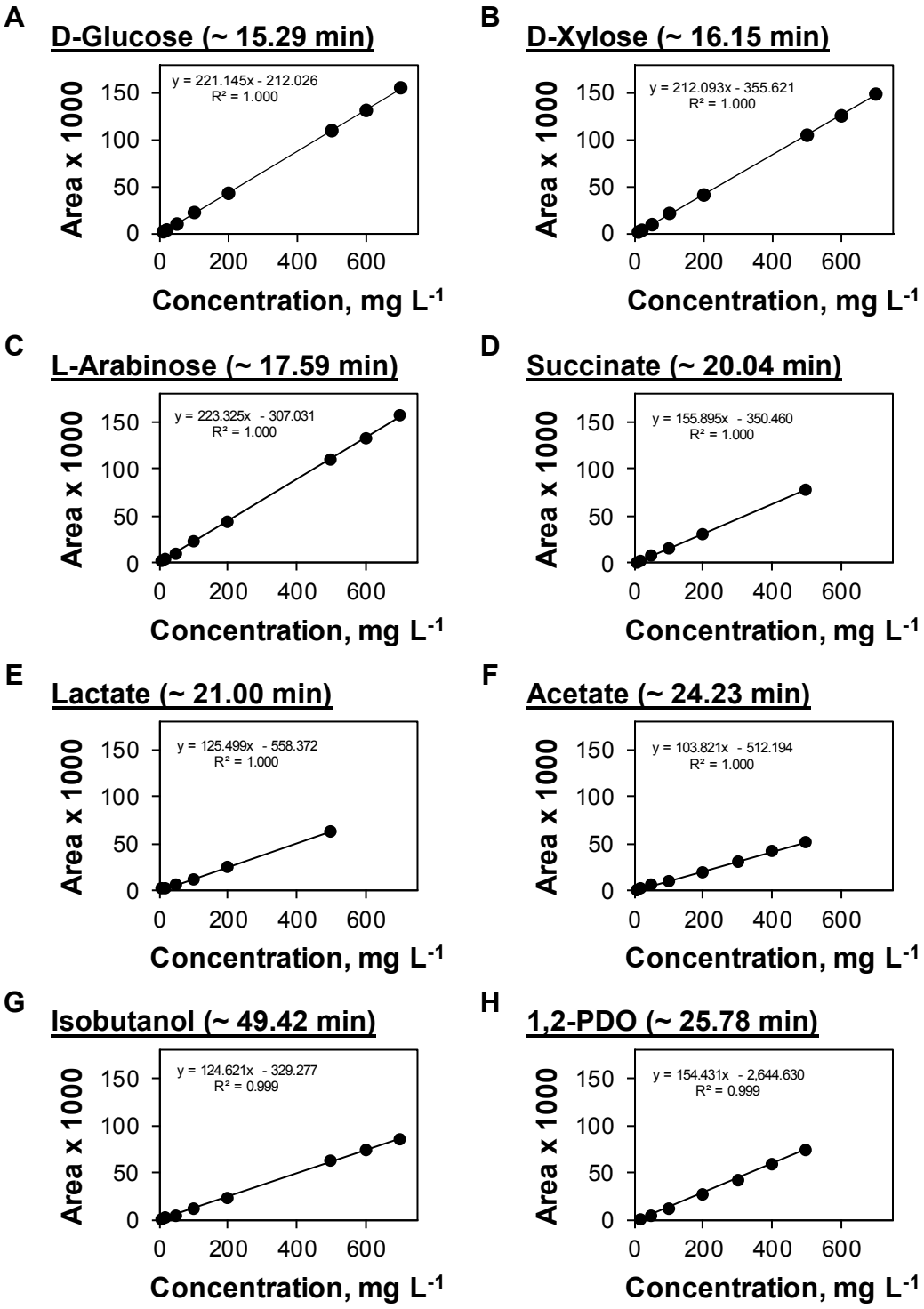

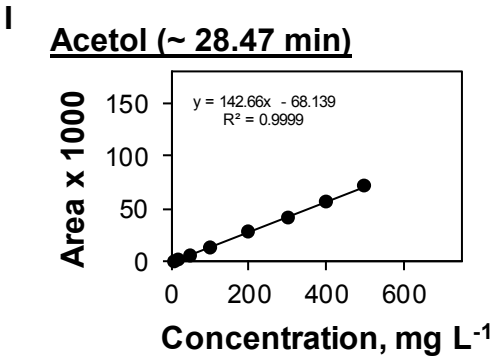


**Figure S 4. Calibration HPLC Rezex™ ROA-Organic Acid**. Exemplary calibration plots shown for the analyzed substances D-glucose (A), D-xylose (B), L-arabinose (C), succinate (D), lactate (E), acetate (F), isobutanol (G), 1,2-PDO (H), and acetol (I). The peak area is plotted over the final concentration in mg $L^{-1}$ that was loaded on the column. In parenthesis the retention time is given for analysis at 50 °C (A-G) or 20 °C (H, I). Further description can be seen above (cf. 3.12.5.1, p. 96). The respective line of best fit as well as corresponding linear equations and the coefficients of determination ($R^2$) are given.

# A3. Supplementary results

## A3.1. *C. glutamicum* PDO2 verification (colony PCR)

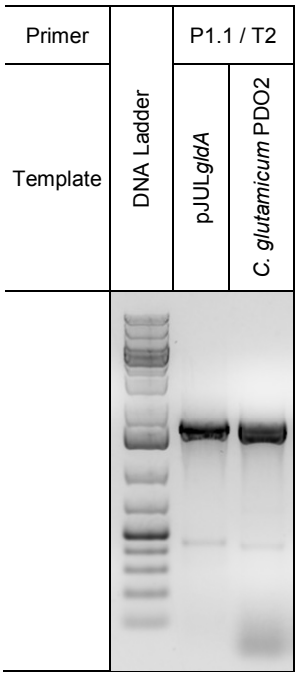


**Figure S 5. *C. glutamicum* PDO2 verification by colony PCR**. Inheritance of the plasmid pJUL*gldA* after transformation of *C. glutamicum* Δ*pqo* Δ*aceE* Δ*ldhA* Δ*mdh* is confirmed. As positive control purified plasmid was used during PCR. 1 % (w/v) agarose gel shown, where approximately 500 ng of the GeneRuler 1 kb Plus DNA Ladder (Thermo Fisher Scientific Inc., Waltham, USA) were loaded.

## A3.2. *C. glutamicum* Δ*pqo* Δ*ilvE* Δ*ldhA* Δ*mdh* verification (colony PCR)

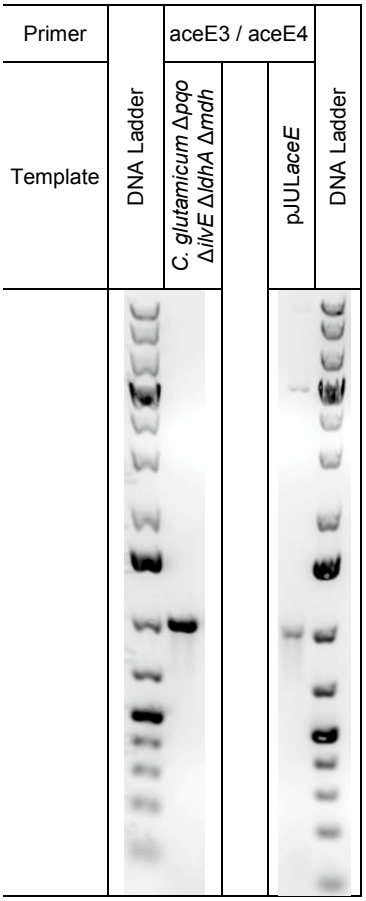


**Figure S 6. *C. glutamicum* Δ*pqo* Δ*ilvE* Δ*ldhA* Δ*mdh* verification by colony PCR**. Restoration of the *aceE* gene is confirmed. As positive control pJUL*aceE* was subjected to PCR as well (expected band size: 1002 bps). 1 % (w/v) agarose gel shown, where approximately 500 ng of the GeneRuler 1 kb Plus DNA Ladder (Thermo Fisher Scientific Inc., Waltham, USA) were loaded.

## A3.3. CArXy verification (colony PCR)

| Template | DNA Ladder | **CArXy** | | | | | | DNA Ladder |
|---|---|---|---|---|---|---|---|---|
| Genotype | | *C. glutamicum* Δ*pqo* Δ*ilvE* Δ*ldhA* Δ*mdh* CgLP4::($P_{tuf}$-*xylAB*-$T_{rrnB}$) CgLP12::($P_{tuf}$-*araBAD*-$T_{rrnB}$) | | | | | | |
| Primer | | ara1 / P2 | araseq3 / P1.2 | araseq6 / ara6 | xyl1 / P2 | xylseq4 / xyl6 | xylseq3 / xylseq5 | |
| Verified region | | Flank1-$P_{tuf}$ | $P_{tuf}$-*araB´* | *´araD*-Flank2 | Flank1-$P_{tuf}$ | *´xylB*-Flank2 | *´xylA*-*xylB´* | |
| Expected band size, bps | | 707 | 793 | 1143 | 717 | 1146 | 1400 | |

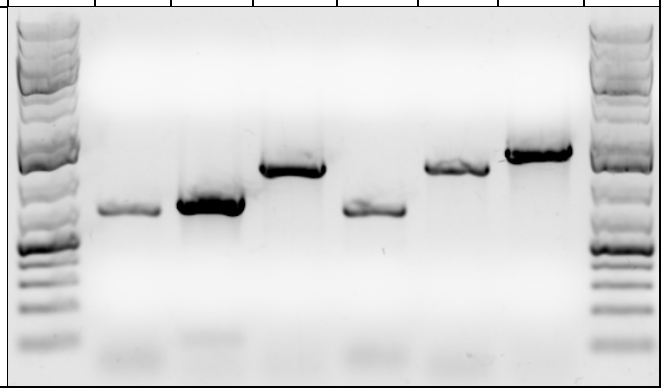

**Figure S 7. CArXy verification by colony PCR**. Complete integration of the synthetic operons for L-arabinose and D-xylose metabolization was confirmed. 1 % (w/v) agarose gel shown, where approximately 500 ng of the GeneRuler 1 kb Plus DNA Ladder (Thermo Fisher Scientific Inc., Waltham, USA) were loaded.

## A3.4. ClsArXy verification (colony PCR)

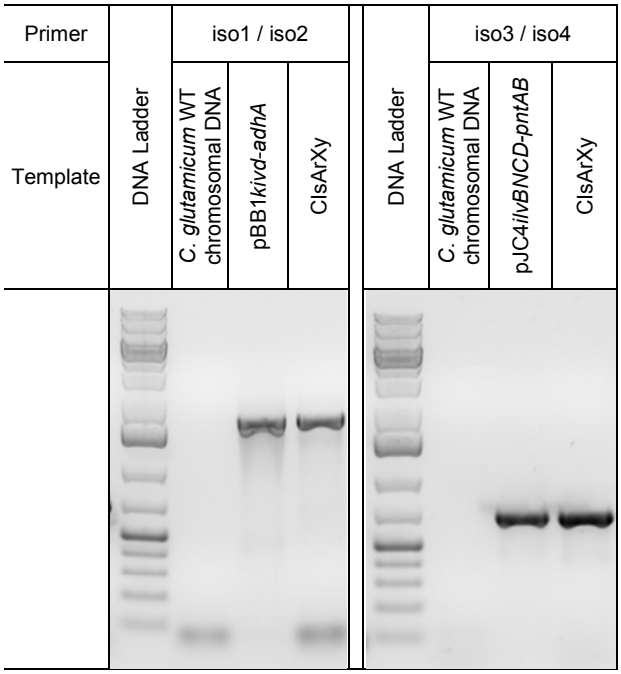


**Figure S 8. ClsArXy verification by colony PCR**. Inheritance of the two plasmids pJC4*ilvBNCD-pntAB* and pBB1*kivd-adhA* after transformation of CArXy is confirmed. As positive and negative control purified plasmid and chromosomal DNA was used during PCR, respectively. 1 % (w/v) agarose gel shown, where approximately 500 ng of the GeneRuler 1 kb Plus DNA Ladder (Thermo Fisher Scientific Inc., Waltham, USA) were loaded.

## A3.5. Pyrolysis water pretreatment

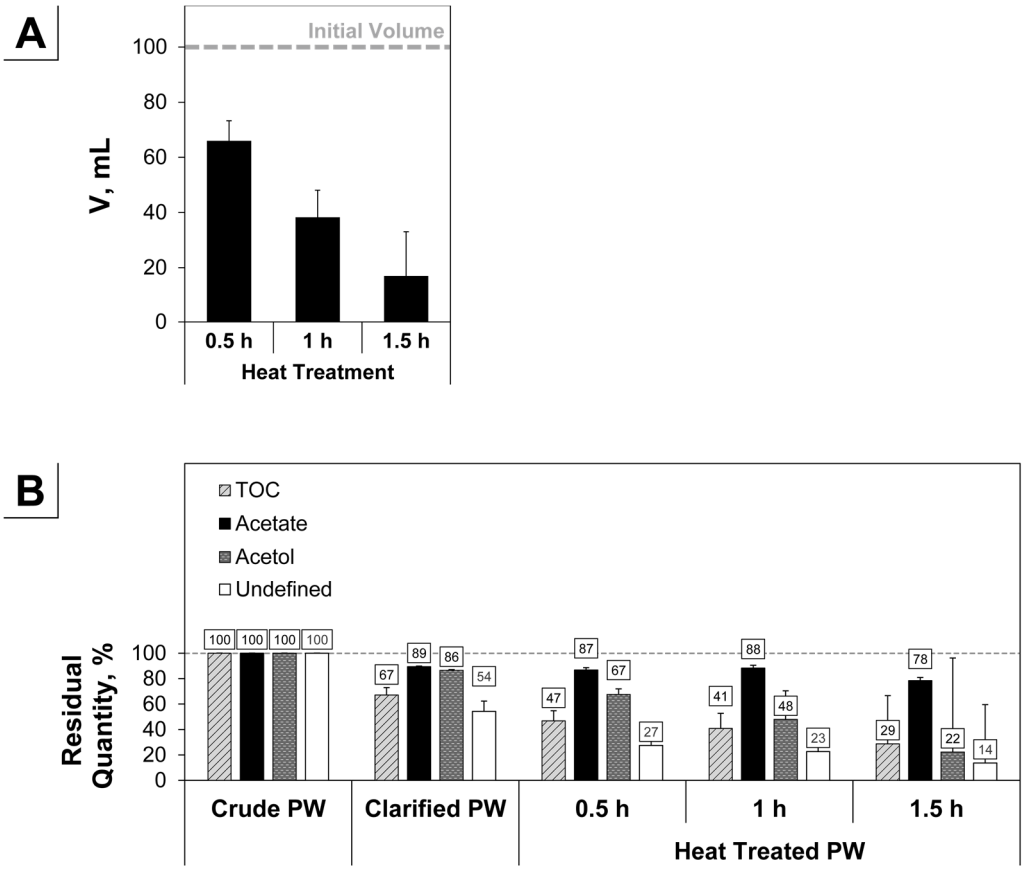


**Figure S 9. Volume reduction and residual quantities of TOC, acetate, acetol and unidentified entities during the applied pyrolysis water (PW) pretreatments**. **A**. Volume reduction of separate PW batches during heat treatment at 80 °C in open beakers. Depicted is the final volume after the respective time of exposure. The initial volume of 100 mL is indicated (dashed line). **B**. Residual quantities after the treatment are given in relative percent considering the volume loss and are based on total organic carbon (TOC) content, acetate, acetol and undefined entities in g carbon $L^{-1}$ (C-g $L^{-1}$). Error bars represent SD of ≥ 4 independent treatments and measurements. Graphic modified from publication (Lange, Müller, *et al.*, 2017).

## A3.6. Parallel metabolization of D-glucose and acetol

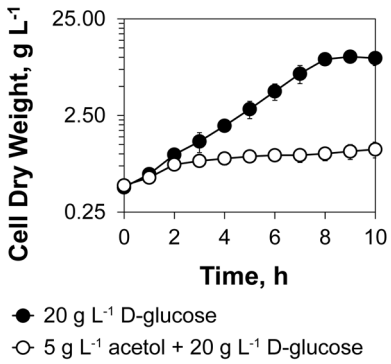


**Figure S 10. Parallel metabolization of D-glucose and acetol**. Shaking flask cultivation of *C. glutamicum* WT in CGXII$_1$ medium supplemented with either 20 g L$^{-1}$ D-glucose (black circles) or 20 g L$^{-1}$ D-glucose + 5 g L$^{-1}$ acetol. SD given for ≥ 3 independent experiments as error bars.

## A3.7. GSH effect on acetol metabolization

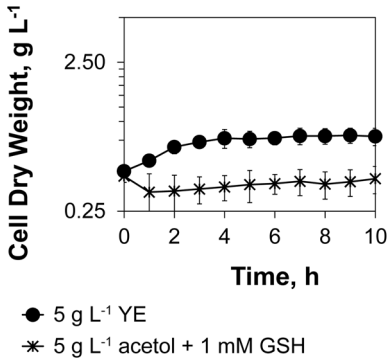


**Figure S 11. The effect of GSH supplementation to growth with acetol as sole carbon source**. Shaking flask experiments of *C. glutamicum* WT in CGXII$_1$ medium supplemented with either 5 g L$^{-1}$ yeast extract (YE, black circles) or 5 g L$^{-1}$ acetol + 1 mM reduced glutathione (GSH, crosses). SD given for ≥ 3 independent experiments as error bars.

## A3.8. Parameter comparison for growth and 1,2-PDO production based on pyrolysis water

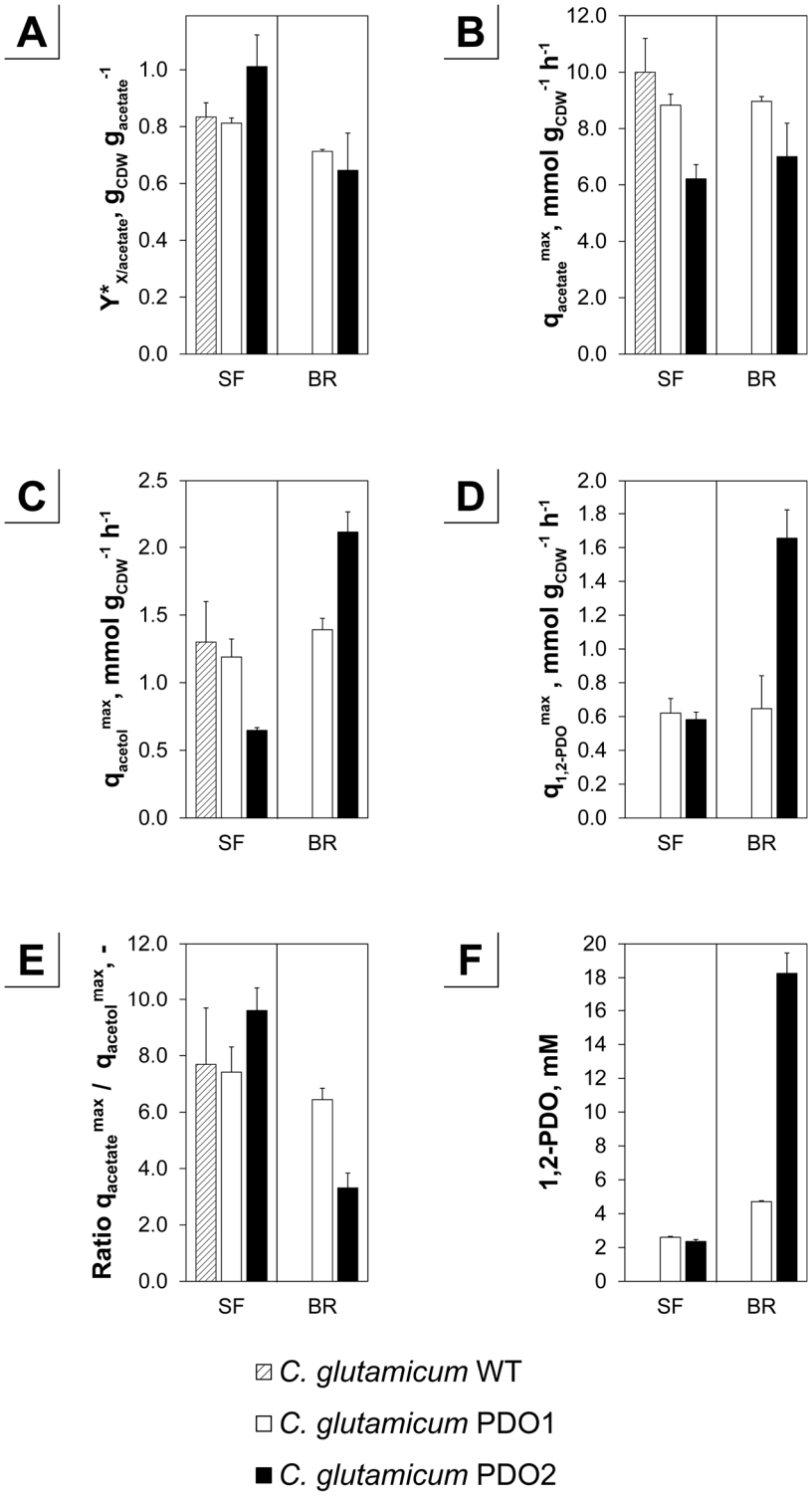

**Figure S 12. Comparison of parameters during cultivations on pyrolysis water**. *C. glutamicum* WT (shaded), *C. glutamicum* PDO1 (white; WT + pJUL*gldA*) and *C. glutamicum* PDO2 (black; Δ*pqo* Δ*aceE* Δ*ldhA* Δ*mdh* + pJUL*gldA*) was grown in shaking flasks (SF; $CGXII_1$ medium) and bioreactors (BR; $CGXII_2$ medium). Media were supplemented with 1 h HT PW (pyrolysis water clarified and exposed to 1 h heat treatment at 80 °C) and 5 g yeast extract (YE) $L^{-1}$. **A**. Apparent biomass yield ($Y_{X/S}$*) in g cell dry weight (CDW) per g acetate. For bioreactor cultivations the yield is given as an overall differential value. B-D. Biomass specific rates were calculated differentially within a 1 h timeframe and maximum values given over the period of the entire process: maximum biomass specific acetate uptake rate (**B**; $q_{acetate}^{max}$), maximum biomass specific acetol uptake rate (**C**; $q_{acetol}^{max}$), and maximum biomass specific 1,2-PDO production rate (**D**; $q_{1,2\text{-}PDO}^{max}$). **E**. Ratio of the respective maximum biomass specific uptake rates of acetate and acetol. **F**. Maximum titers of 1,2-PDO throughout the cultivation. Error bars represent SD of ≥ 3 independent experiments. Graphic modified from publication (Lange, Müller, *et al.*, 2017).

## A3.9. Cultivation of CArXy on hemicellulose fraction without yeast extract

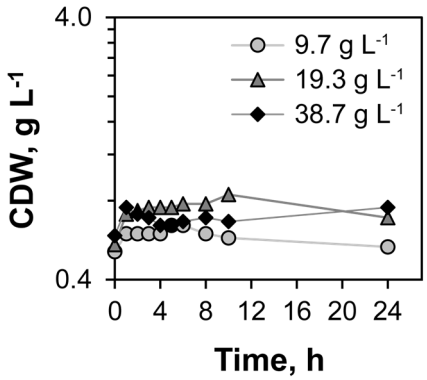


**Figure S 13. Shaking flask cultivations of the strain CArXy on hemicellulose fraction**. CArXy (*C. glutamicum* Δ*pqo* Δ*ilvE* Δ*ldhA* Δ*mdh* CgLP4::($P_{tuf}$-*xylAB*-$T_{rrnB}$) CgLP12::($P_{tuf}$-*araBAD*-$T_{rrnB}$)) was grown in $CGXII_S$ (+ 2 mM Val, Leu and Ile) with various concentrations of hemicellulose fraction (HF; 9.7 g HF $L^{-1}$ (circles), 19.3 g HF $L^{-1}$ (triangles) and 38.7 g HF $L^{-1}$ (diamonds)) and without yeast extract as additional supplement. Bacterial growth (cell dry weight, CDW) depicted over time. A representative single experiment is shown.

## A3.10. Cultivation of CArXy on hemicellulose fraction (various concentrations)

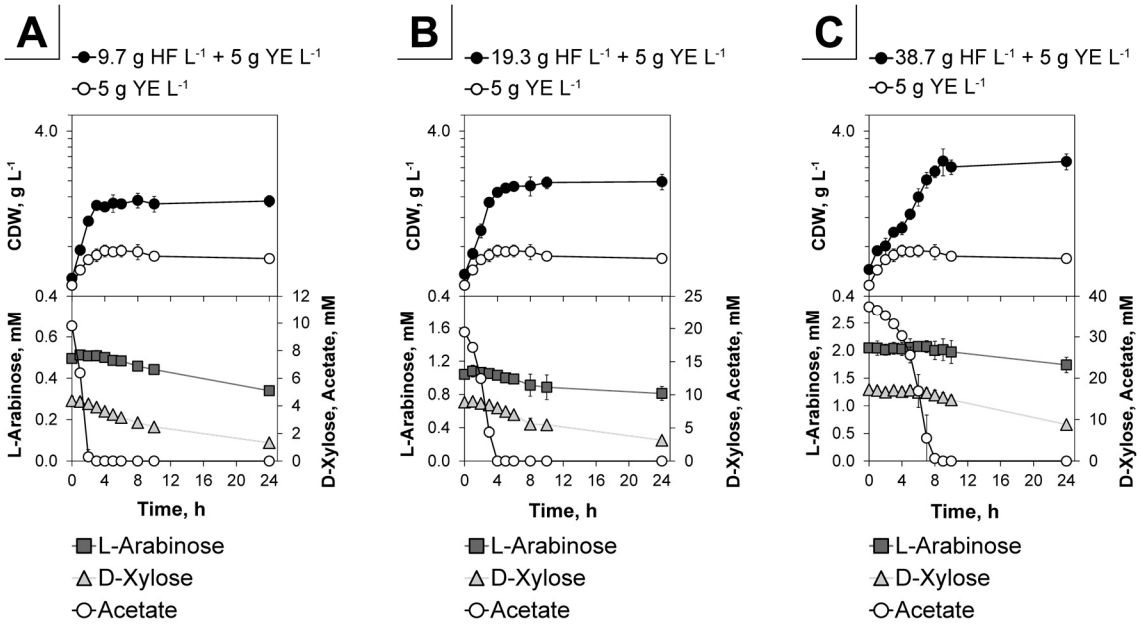


**Figure S 14. Cultivation of CArXy on various concentrations of hemicellulose fraction**. Aerobic cultivation of the strain CArXy (*C. glutamicum* Δ*pqo* Δ*ilvE* Δ*ldhA* Δ*mdh* CgLP4::($P_{tuf}$-*xylAB*-$T_{rrnB}$) CgLP12::($P_{tuf}$-*araBAD*-$T_{rrnB}$); Figure 3.1 A, p. 83). Cultivation was performed in $CGXII_S$ (+ 2 mM Val, Leu and Ile) minimal medium supplemented with 5 g YE $L^{-1}$ as reference (open circles) and variable concentrations of the hemicellulose fraction (HF) + 5 g YE $L^{-1}$: **A**. 9.7 g HF $L^{-1}$. **B**. 19.3 g HF $L^{-1}$. **C**. 38.7 g HF $L^{-1}$. The concentrations of acetate (circles), D-xylose (triangles) and L-arabinose (squares) are depicted. Analysis of the culture supernatants was conducted via HPLC (cf. 3.12.5.1, p. 96). Error bars represent SD of three independent experiments. Graphic modified from publication (Lange, J., Müller, F., *et al.*, 2018).

## A3.11. Two-stage isobutanol production

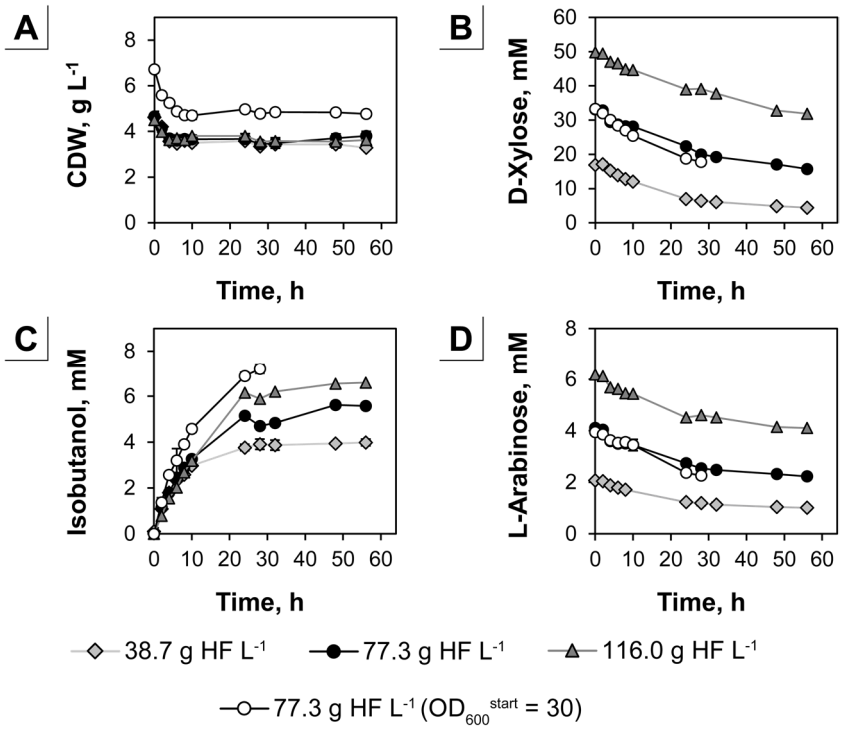


**Figure S 15. Two-stage isobutanol production with CIsArXy** (anaerobic stage shown). CIsArXy (CArXy harboring the plasmids pJC4*ilvBNCD-pntAB* and pBB1*kivd-adhA*) was cultivated in $CGXII_S$ (+ 2 mM Val, Leu and Ile + 50 µg Kan $mL^{-1}$ + 6 µg Cm $mL^{-1}$) minimal medium (Figure 3.1 B, p. 83) supplemented with 5 g YE $L^{-1}$ and variable concentrations of the hemicellulose fraction (HF) [38.7 g HF $L^{-1}$ (diamonds), 77.3 g HF $L^{-1}$ (circles and open circles) and 116.0 g HF $L^{-1}$ (triangles)]. Depicted are the concentrations of the cell dry weight (CDW) in g $L^{-1}$ (**A**) and D-xylose (**B**), isobutanol (**C**) and L-arabinose (**D**) in mM over the cultivation time. Various starting biomasses of 4.59 ± 0.14 g CDW $L^{-1}$ (diamonds, circles, triangles) and 6.72 ± 0.14 g CDW $L^{-1}$ (open circles) were used in the zero-growth production. Analysis of the culture supernatants was conducted via HPLC (cf. 3.12.5.1, p. 96). Error bars represent SD of three independent experiments (analysis of metabolites of selected experiments [circles and triangles] shown only for a single representative analysis).

## A3.12. Acetate behavior during isobutanol production with CIsArXy

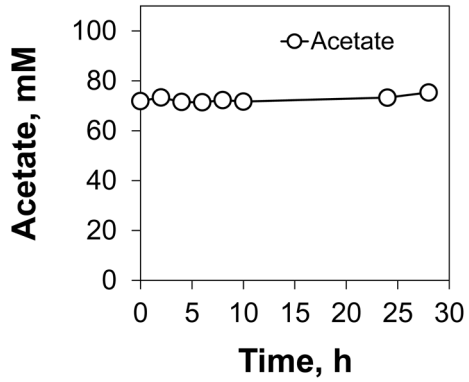


**Figure S 16. Course of acetate concentration during the anaerobic isobutanol production** with the strain CIsArXy (CArXy harboring pJC4*ilvBNCD-pntAB* and pBB1*kivd-adhA*) using the hemicellulose fraction (HF; corresponds to Figure 4.8 B, C; p. 132). Analysis of the culture supernatants was conducted via HPLC (cf. 3.12.5.1, p. 96). Error bars represent SD of three independent experiments. Graphic modified from publication (Lange, J., Müller, F., *et al.*, 2018).

## A3.13. Behavior of pH during aerobic/microaerobic (shaking flasks and bioreactor) and triple-phase bioreactor cultivations

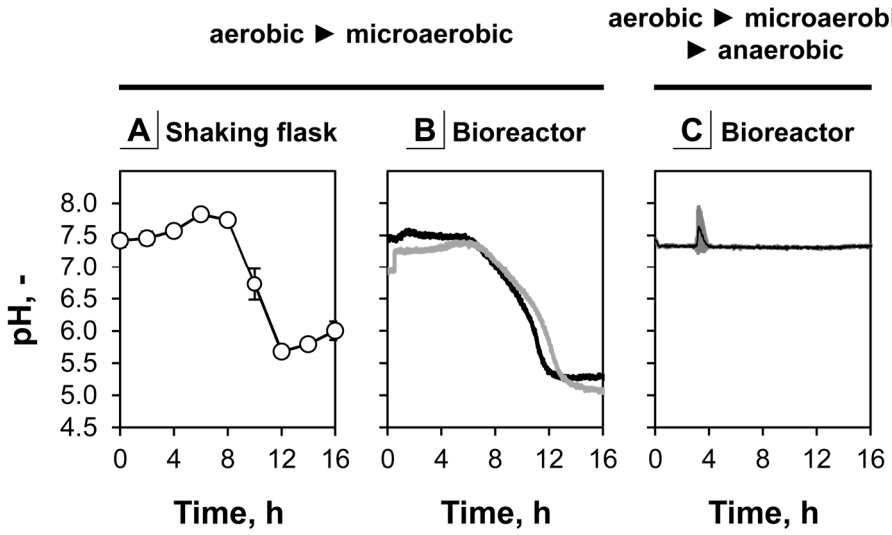


**Figure S 17. Delineation of the pH during cultivations at different oxygen availabilities**. Cultivations were performed with *C. glutamicum* WT in $CGXII_{S+PCA}$ (A, B; aerobic/microaerobic) or $CGXII_{2+PCA}$ (C; aerobic/microaerobic/anaerobic) + 60 g glucose $L^{-1}$ as substrate. The pH was uncontrolled in A and B and regulated by the addition of 25 % ammonium hydroxide solution in C. **A**. The pH in shaking flask cultivations was analyzed offline in the culture supernatant with a standard probe (refers to Figure 4.10 A, p. 138). Error bars show SD of five independent experiments. **B**. Two independent cultivations in the 30 L bioreactor (refers to Figure 4.10 B, p. 138). **C**. The triple-phase process with regulated pH (corresponds to Figure 4.12, p. 143). The peak of the pH in C was due to the application of antifoam and fast release of base that was retained in the foam. Shaded region indicates SD of four independent experiments.

## A3.14. $N_2$ gassing of headspace in the triple-phase batch fermentation

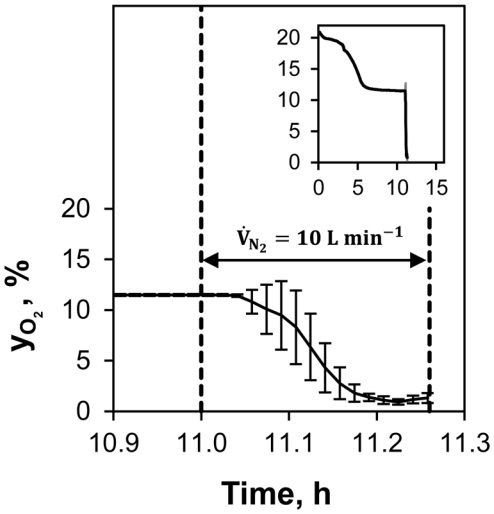


**Figure S 18. $N_2$ headspace gassing profile** for the initiation of the anaerobic phase in the triple-phase batch fermentation (cf. 4.11, p. 140; Figure 4.12, p. 143). Depicted is the analysis of the exhaust gas $O_2$ fraction ($y_{O2}$) in the exhaust gas over the cultivation time. Inset miniature diagram shows the entire cultivation period (off gas analysis stopped after 11.26 h to maintain the reactor pressure). Dashed lines border the 15 min of $N_2$ gassing with a volumetric flow of 10 L min$^{-1}$ in the extract of the overall experiment. Error bars in the main graph and grey shades in the miniature diagram represent SD of four independent experiments.

## A3.15. Differential substrate uptake and product formation rates during the triple-phase process

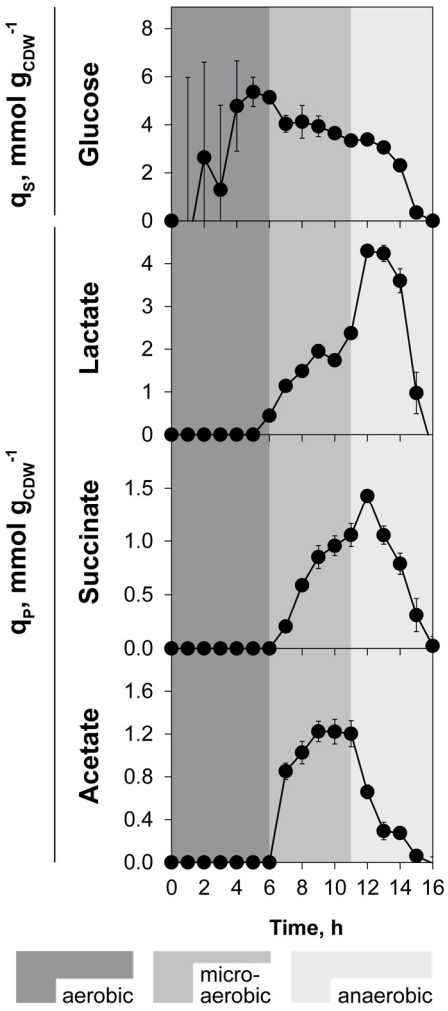


**Figure S 19. Differential biomass specific substrate uptake ($q_S$) and product formation ($q_P$) rates during the triple-phase process** (cf. 4.11, p. 140; Figure 4.12, p. 143). The aerobic (dark grey), microaerobic (grey) and anaerobic (light grey) phases are visualized. Error bars represent SD of four independent bioprocesses.

## A3.16. RNA isolation, processing and library preparation

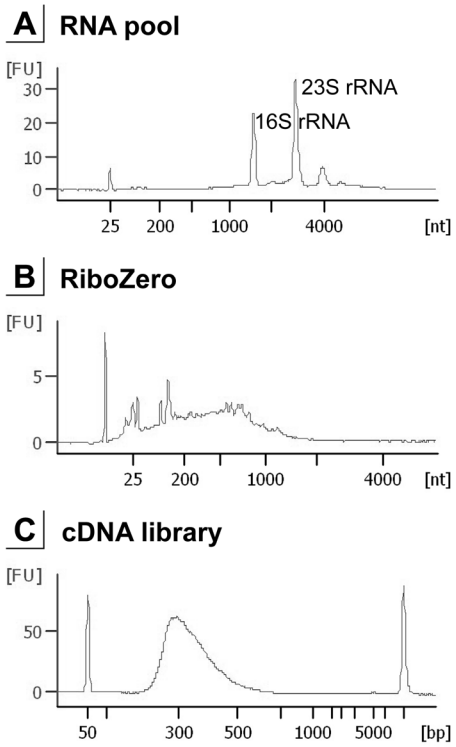


**Figure S 20. RNA isolation, processing and library preparation** for RNA-sequencing of the triple-phase process. **A**. Original pool of purified RNA (Agilent RNA 6000 Nano Kit). Peaks of the 16S and 23S RNA are labeled. **B**. RNA sample (Agilent RNA 6000 Pico Kit) after removal of rRNA with Ribo-Zero rRNA Removal Kit (Illumina, Inc., San Diego, USA). **C**. Final cDNA library prior to RNA-sequencing analysis (Agilent DNA 7500 Kit). Graphics correspond exemplarily to the sample ② during the triple-phase fermentation (cf. 4.11, p. 140; Figure 4.12, p. 143). Graphics were retrieved from the Agilent Technologies 2100 Expert software report of the chip analysis in the 2100 Bioanalyzer Instrument analysis.

## A3.17. Pearson correlation of RNA-sequencing data

| | ① | ② | ③ | ④ | ⑤ | ⑥ |
|---|---|---|---|---|---|---|
| ① | 1.00 | 0.98 | 0.92 | 0.90 | 0.88 | 0.80 |
| ② | | 1.00 | 0.93 | 0.91 | 0.89 | 0.82 |
| ③ | | | 1.00 | 0.98 | 0.96 | 0.90 |
| ④ | | | | 1.00 | 0.98 | 0.92 |
| ⑤ | | | | | 1.00 | 0.94 |
| ⑥ | | | | | | 1.00 |

**Figure S 21. Pearson correlation of RNA-sequencing data**. The $log_2$TPM values with the entire raw RNA-sequencing data were correlated (no significance constraints applied). Sample IDs of the triple-phase process (cf. 4.11, p. 140; Figure 4.12, p. 143) from left to right aerobiosis (①, ②), microaerobiosis (③, ④, ⑤) and anaerobiosis (⑥). Figure was analogously published (Lange, J., Münch, E., *et al.*, 2018).

## A3.18. Empirical $log_2$-fold change selection

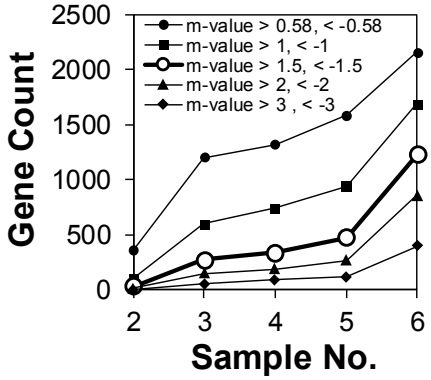


**Figure S 22. $Log_2$-fold change selection to determine a significance cutoff for the differentially transcribed genes within the RNA-sequencing of the triple-phase process** (cf. 4.11, p. 140; Figure 4.12, p. 143). The number of genes (gene count) that are differentially transcribed within the given m-value ($log_2$-fold change) range are depicted over the sample number. Open circles highlight the $log_2$-fold change (m-value > 1.50 and < -1.50) corresponding to a fold-change of 2.80 and 0.40, respectively. This cutoff was used for all RNA-sequencing data within this thesis. The selection was based on a clear separation of the three successive phases: aerobiosis, microaerobiosis and anaerobiosis.

## A3.19. Description of putatively oxygen responsive regulators

The following column graphs represent $log_2$-fold changes of enhanced (black) and reduced (grey) expression. Values outside the significance constraints (m-value > 1.50, < -1.50 and a-value > 1.00) are also shown (white). From left to right aerobiosis (②), microaerobiosis (③, ④, ⑤) and anaerobiosis (⑥) versus the aerobic reference (①; Figure 4.12, p. 143). Scaling of these graphs is variable and allows only qualitative comparisons. A quantitative comparison between different genes is therefore not legitimate.

The transcriptional regulator **SutR** (cg0993) belongs to the ArsR family is not described in literature in depth. It was shown for example to be upregulated under high $CO_2$ conditions (Buchholz, Graf, Freund, *et al.*, 2014).

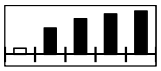

A putative transcriptional regulator **cg3303** (PadR-family) is activated towards microaerobiosis and anaerobiosis in the triple-phase process with a maximal enhancement of expression ~ 25-fold. This regulator is not functionally described in literature but was also upregulated in a *chrSA* deletion mutant (a two-component system involved in heme resistance) (Heyer *et al.*, 2012), in a Δ*ilvB* (acetolactate synthase) mutant of the lysine producer *C. glutamicum* DM1729 (Blombach, Hans, *et al.*, 2009) and upon heat shock (a homolog in *C. glutamicum* R (cgR_2866)) (Ehira, Teramoto, *et al.*, 2009) and repressed under stringent conditions in a *rel* mutant (Brockmann-Gretza and Kalinowski, 2006).

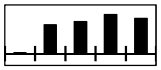

The gene **cg1327** encodes a putative transcriptional regulator. It represents one of three regulators of the Crp-Fnr protein family namely *glxR*, cg1327 and cg3291 (Kohl and Tauch, 2009). Therefore, cg1327 contains a predicted cAMP-binding domain. A nucleotide BLAST revealed its conservation amongst *Corynebacterium* sp., however it has not been further characterized in literature.

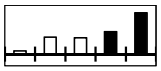

The transcriptional regulator **Znr** (cg2500, shown left) encodes a putative metal-sensing transcriptional regulator of the SmtB/ArsR family (Schröder *et al.*, 2010). It is located upstream of the *zur* regulator gene. A zinc dependent regulatory role was proposed previously (Schröder *et al.*, 2010). The genes *znr*, *zur* and a hypothetical protein (cg2504) are transcribed in a tricistronic operon (Pfeifer-Sancar *et al.*, 2013). We found that the zinc uptake regulator **Zur** (cg2502) is similarly enhanced

in transcription. Zur belongs to the subgroup of the ferric uptake regulators (Fur) and represses genes dependent on zinc as cofactor (Schröder *et al.*, 2010). Its homolog cgR_2151 is also described as zinc-dependent transcriptional regulator in *C. glutamicum* R (Teramoto *et al.*, 2012). Deletion of *zur* resulted in an enhanced expression of two Zn-inducible transporter genes (*zrf*, cgR_1359 and *zra*, cgR_0148).

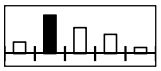

**FarR** (cg3202), a HutC/FarR-type regulator of the GntR family, was proposed to be involved with the amino acid biosynthesis. Especially, the arginine cluster and glutamate dehydrogenase gene (*gdh*) were found to be binding targets (Hänssler *et al.*, 2007). Upon its deletion genes such as of the succinate dehydrogenase (*sdhA*), malate synthase (*aceB*) and some structural genes of ribosomes were reduced in expression, whereas lactate dehydrogenase (*ldh*), phosphoenolpyruvate carboxykinase (*pck*) are transcribed at a higher level. As FarR depletes towards anaerobiosis, which fits to our transcriptional response assuming a repressing effect at the respective genes. However, a transcriptional response of the *gdh* gene could not be observed here and in literature (Hänssler *et al.*, 2007). The protein sequence of FarR contains two cysteine residues and besides a HTH superfamily DNA binding domain it shows a UTRA superfamily binding domain, which is associated with small molecule binding. Although an abundance of small molecules was tested (ammonium chloride, 2-oxoglutarate, glutamate, NADPH, $NADP^+$, arginine, ornithine, citrulline, glutamine, aspartate, asparagine, proline, urea, nitrate, glucose, fructose, oxaloacetate, malate, citrate, acetate, pyruvate, myristate, palmitate, NADH, AMP, and ATP), a hampering of DNA binding could not be shown specifically (Hänssler *et al.*, 2007). Its regulatory mechanism is therefore still quite vague.

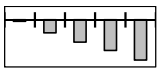

Important for iron homeostasis is the regulator **RipA** (cg1120) (regulator of iron proteins) (Wennerhold *et al.*, 2005; Frunzke and Bott, 2008). It is transcribed in a bicistronic operon (*ripA*-cg1121) (Pfeifer-Sancar *et al.*, 2013). The gene cg1121 encodes an undescribed permease of the major facilitator superfamily and is not differentially expressed in our experiments. RipA has been shown to repress important iron containing proteins of *C. glutamicum*, like the aconitase, succinate dehydrogenase or catalase (Frunzke and Bott, 2008). However, in our data the regulon response was low towards the reduced expression of *ripA*. Selected targets of

RipA are the *narKGHJI* operon (respiratory nitrate reductase) showing an increased transcription only under aerobiosis (②) or the *leuCD* operon (3-Isopropylmalate dehydratase) being reduced in expression upon complete anaerobiosis (⑥). As terminal oxidases also contain iron as cofactor, RipA may be additionally involved in adaptation towards anaerobiosis.

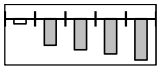

A potential activator of phenol pathway genes **cg2965** (AraC-family) shows reduced transcription in the triple-phase process. It was described to activate the utilization of phenol (Brinkrolf *et al.*, 2006) is only conserved among *Corynebacteria* (cgR_2584 in *C. glutamicum* R) but was not described in recent studies (Kallscheuer *et al.*, 2015, 2016). In the triple-phase process the putative phenol 2-monooxygenase (cg2966) encoded in the same operon (Pfeifer-Sancar *et al.*, 2013) showed a similarly decreased expression level.

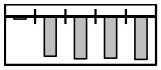

The master regulator of carbon metabolism **RamB** (cg0444) (regulator of acetate metabolism) (Gerstmeir *et al.*, 2004) is highly downregulated towards oxygen scarcity. Gerstmeir *et al.* deleted RamB, which resulted in an enhancement of the acetate kinase (*ackA*), phosphotransacetylase (*pta*), isocitrate lyase (*aceA*), and malate synthase (*aceB*) even in the absence of acetate as substrate. About 30 % of the genes assigned to its regulon (Schröder and Tauch, 2010) (16 out of 53 genes in total) were also differentially transcribed within the triple-phase process and mostly downregulated. Among these are also the *aceA* (isocitrate lyase), *aceB* (malate synthase), *malE* (malic enzyme), *pyc* (pyruvate carboxylase), *sucCD* (succinyl-CoA synthetase) and others. A study of RamA and RamB regulons including transcriptome analysis is available (Auchter *et al.*, 2011).

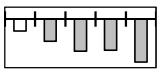

The putative transcriptional regulator **cg2320** (ArsR-family) shows reduced transcription in the triple-phase process. It was shown to be: upregulated upon biotin limitation (Schneider *et al.*, 2012), in a Δ*ilvB* mutant of the lysine producer *C. glutamicum* DM1729 (Blombach, Hans, *et al.*, 2009) and at pH 9, and downregulated at pH 6 (Follmann *et al.*, 2009), compared to Δ*sugR* (transcriptional regulators of sugar metabolism) (Gaigalat *et al.*, 2007) and upon heat shock (Barreiro *et al.*, 2009). Its cysteine residue at the N-terminus has a proposed regulatory role (Ehira, Ogino, *et al.*, 2009) but was not yet studied.

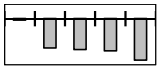

The putative sugar diacid utilization regulator **cg2746** was downregulated towards oxygen deprivation. It was shown to be enhanced in expression in a Δ*nanR* (amino sugar utilization regulator) strain (Uhde, 2014). Its homolog in *C. glutamicum* R (cgR_2412) was described as being regulated by SigC in *C. glutamicum* R (Toyoda and Inui, 2016b).

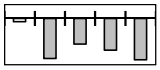

The putative bacterial regulator (ArsR-family) gene **cg2648** has a homolog in *C. glutamicum* R (cgR_2310) but both were not yet studied.

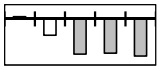

The transcriptional activator of putative hydroxyquinol pathway genes **IclR** (cg3388) is reduced in expression towards anaerobiosis (IlcR family). Most likely, this activator is involved in the regulation of resorcinol and 2,4-dihydroxybenzoate (Brinkrolf *et al.*, 2006) or myo-inositol catabolism (Schröder and Tauch, 2010). Recently, as result of adaptive evolution for improval of the *Weimberg* pathway for D-xylose utilization, *iclR* was target for disruptive mutation (Radek *et al.*, 2017). A homolog was additionally found in *C. glutamicum* R (cgR_2944) but the comprehensive function in both organisms is not known to date.

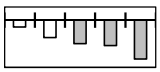

**CspA** (cg0215) belonging to the cold-shock protein family was described as one of the major secreted proteins of *C. glutamicum* (Joliff *et al.*, 1992; Kikuchi *et al.*, 2003) but also as repressor of the malate synthase (*aceB*) as sole target (Kim *et al.*, 2007; Schröder and Tauch, 2010).

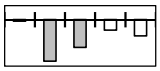

The Repressor of ribose uptake and uridine utilization genes **RbsR** (cg1410, LacI/GalR family) was investigated previously in literature (Nentwich *et al.*, 2009). A deletion showed indeed the increase of expression of the entire *rbsRACBD* operon encoding a ribose-specific ATP-binding cassette (ABC) transport system (Nentwich *et al.*, 2009). Further known targets of RbsR are the *uriR-rbsK1-uriT-uriH* operon encoding genes linked to transport and metabolization of the nucleoside uridine and the ribokinase gene *rbsK2* (Brinkrolf *et al.*, 2008; Nentwich *et al.*, 2009).

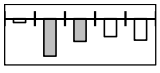

The described activator of the gentisate pathway **GenR** (cg3352, IclR-family) regulates the mycothiol-dependent gentisate pathway genes (Schröder and Tauch, 2010). A disruption of *genR* resulted in a loss of ability to proliferate on 3-hydroxybenzoate or gentisate as sole carbon sources (Shen *et al.*, 2005; Feng *et al.*, 2006). An involvement in the regulation of oxygen dependent phenotypes of

*C. glutamicum* may not be very likely.

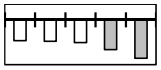

Unknown is the function of **cg0150** a putative transcriptional regulatory protein (Fic/Doc family). The homologous protein in *C. glutamicum* R (cgR_0191) was not investigated as well. Recently, it was shown that CgpS, a xenogenic silencer, binds to the promoter region of cg0150 (Pfeifer *et al.*, 2016).

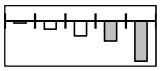

The decreasing expression of a putative transcriptional regulator **MmpLR** (cg1053, TetR-family) makes it also an interesting candidate for deletion. In *Corynebacterium jeikeium* K411 it was by genomic context classified as being involved in regulation of Rnd-family drug exporter gene *mmpL2* (Barzantny *et al.*, 2012) and proposed as repressor of MmpL-type transporter gene in *C. glutamicum* (Brinkrolf *et al.*, 2010). It comprises two cysteine residues and an ArcR domain.

## A3.20. Deletion of putatively oxygen responsive regulators

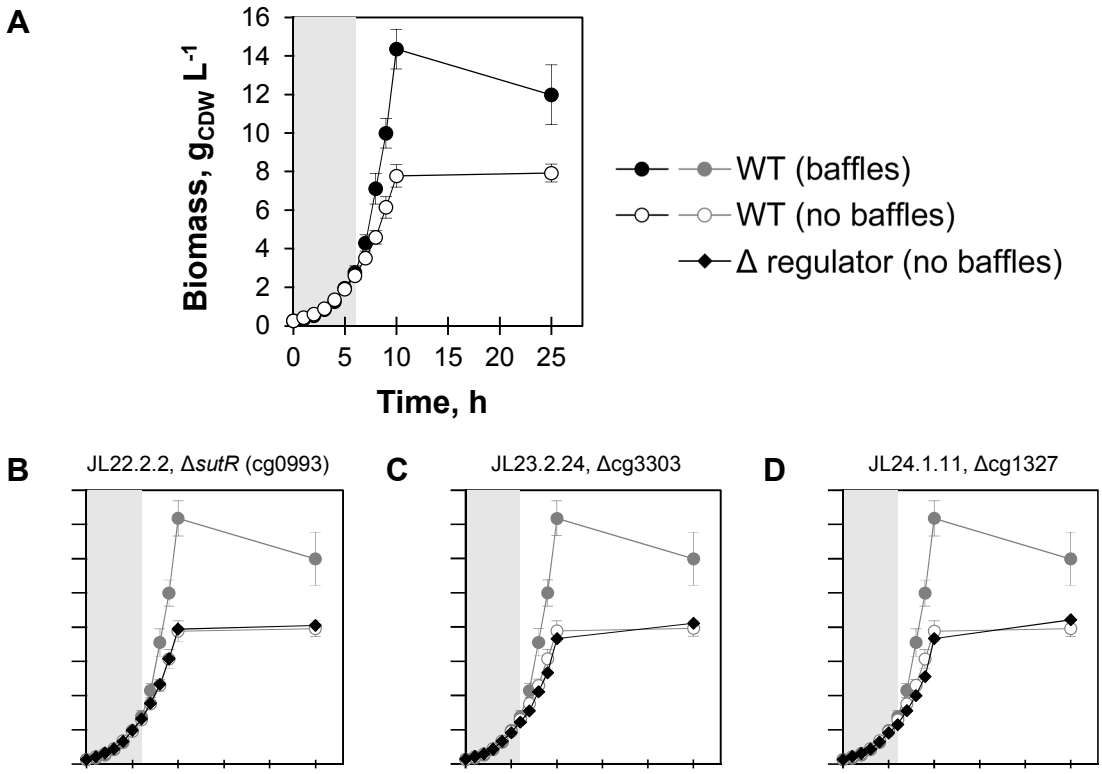

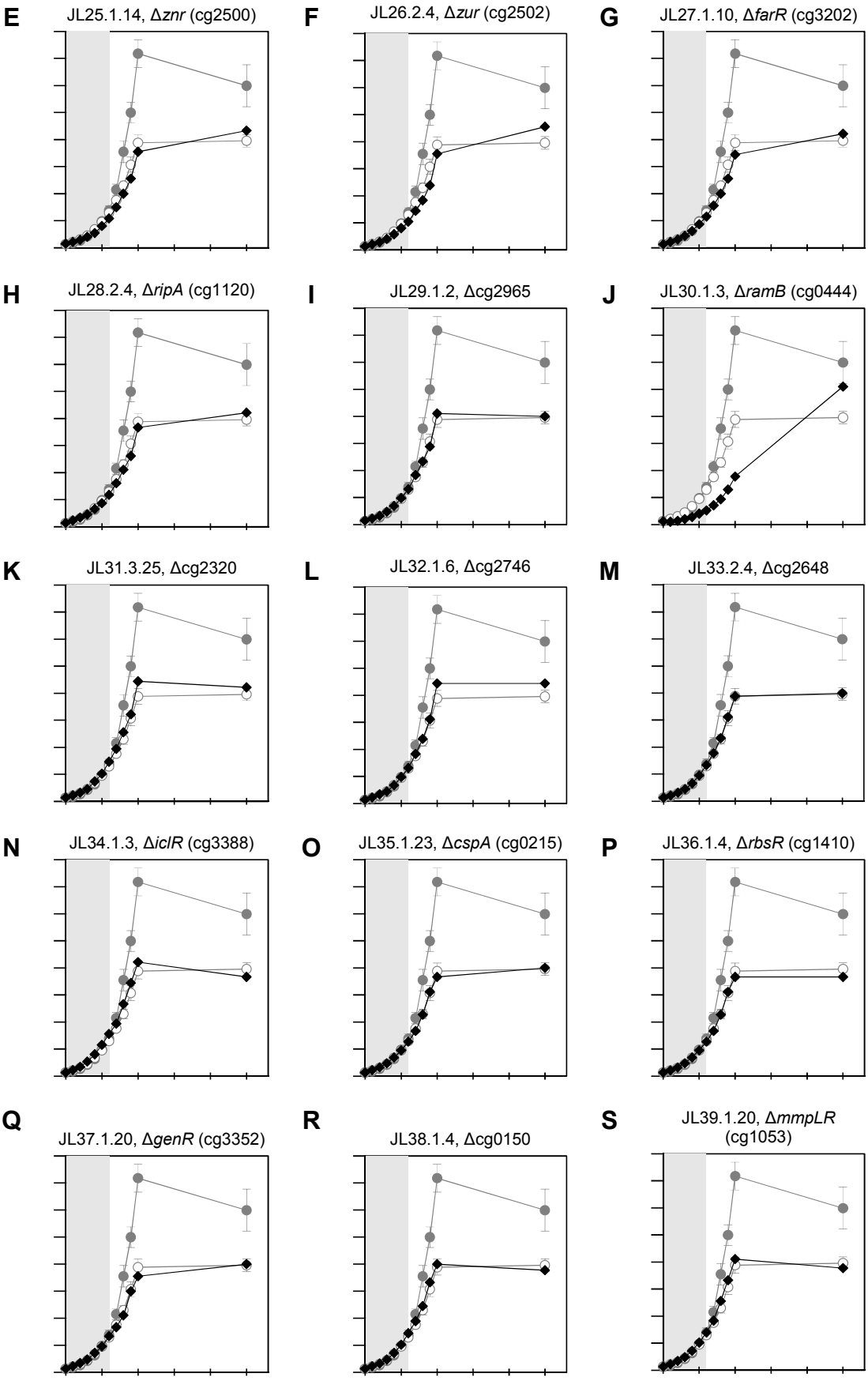
E
JL25.1.14, Δznr (cg2500)
F
JL26.2.4, Δzur (cg2502)
G
JL27.1.10, ΔfarR (cg3202)
H
JL28.2.4, ΔripA (cg1120)
I
JL29.1.2, Δcg2965
J
JL30.1.3, ΔramB (cg0444)
K
JL31.3.25, Δcg2320
L
JL32.1.6, Δcg2746
M
JL33.2.4, Δcg2648
N
JL34.1.3, ΔiclR (cg3388)
O
JL35.1.23, ΔcspA (cg0215)
P
JL36.1.4, ΔrbsR (cg1410)
Q
JL37.1.20, ΔgenR (cg3352)
R
JL38.1.4, Δcg0150
S
JL39.1.20, ΔmmpLR (cg1053)

**Figure S 23. Shaking flask cultivations of *C. glutamicum* with deleted putatively oxygen responsive regulators**. All cultivations were performed in $CGXII_{S+PCA}$ minimal medium including 40 g glucose $L^{-1}$ and supplemented with 30 mg protocatechuate $L^{-1}$. Graphs delineate behavior of the biomass concentration ($g_{CDW}$ $L^{-1}$) over the incubation time (scaling is identical in all graphs). **A.** Reference cultivations of *C. glutamicum* WT in shaking flasks with baffles (filled circles) and without baffles (open circles) was conducted as independent triplicates (shown in grey color in all other graphs for comparison). The grey area indicates a period (0-6 h) with similar growth behavior in baffled and non-baffled flask. An enhanced oxygen limitation in unbaffled flasks that negatively affects growth initiates at this point in time. **B-S.** Cultivation of the *C. glutamicum* strains JL with given chromosomal gene deletions (diamonds, a representative single cultivation is depicted). SD given for triplicate experiments as error bars.

# A4. Pyrolysis water GC analysis

**Table S 21. GC-MS analysis of pyrolysis water**. The following GC-MS analysis of pyrolysis water was performed by the Johann Heinrich von Thünen-Institut (Braunschweig, Germany) and prompted by Prof. Dr. Nicolaus Dahmen (Institute for Catalysis Research and Technology, Karlsruhe Institute of Technology (KIT), Eggenstein-Leopoldshafen, Germany), who obtained the pyrolysis fractions from the bioliq® plant of the KIT. Analysis was executed by Ingrid Fortmann and Dr. Meier (dietrich.meier@ti.bund.de) at the Johann Heinrich von Thünen-Institut. The pyrolysis water LOT can be issued under the following sample description*: KIT 14a: Schwelwasser 1303* (sample received: 27.05.2014; date of analysis: 10.06.2014). For the analysis the apparatus was equipped with an Agilent J&W VF-1701ms GC Column (60 m, 0.25 mm, 0.25 µM, 7 inch cage) and FID and MS for quantification and identification. 1900 µL sample were supplemented with 100 µL 1,2-diethoxyethane as internal standard and loaded as liquid into the injector. A water content of 81.9 % (w/v) of pyrolysis water was determined. Of the total peak area, 69.0 % could be allocated to specific substances, while 31.0 % remained unquantified. A recalculation showed that 14.3 % (w/v) of pyrolysis water were quantified as organic substances, whereas the remainder 3.7 % (w/v) were not analyzable.

| Compound | % (w/w) | |
|---|---|---|
| **NON-AROMATIC COMPOUNDS** | | |
| Acids | 4.99 | |
| Acetic acid | 4.492 | c |
| Propionic acid | 0.404 | c |
| Pentanoic acid (NIST MQ 87) | 0.055 | # |
| Hexanoic acid | 0.015 | # |
| 2-Butenoic acid, (E)- (NIST MQ 82) | 0.024 | # |
| Non-aromatic alcohols | 2.13 | |
| Methanol | 1.689 | # |
| Ethylene glycol | 0.437 | c |
| Non-aromatic aldehydes | 0.16 | |
| poss: 2-Butenal, 2-methyl- (NIST MQ 82) | 0.019 | # |
| Crotonaldehyde, trans | 0.142 | c |

| Compound | % (w/w) | |
|---|---|---|
| Non-aromatic ketones | 5.68 | |
| Acetol (Hydroxypropanone) | 3.484 | c |
| Butanone, 1-hydroxy-2- | 0.490 | c |
| Butandione, 2,3- (Diacetyl) | 0.430 | c |
| Acetoin (Hydroxy-2-butanone, 3-) | 0.095 | # |
| Propanone, acetyloxy-2- | 0.125 | c |
| 3-Buten-2-one, 3-methyl- (NIST MQ 88) | 0.026 | # |
| poss: 2,3-Pentanedione (NIST MQ 87) | 0.054 | # |
| 3-Penten-2-one | 0.125 | # |
| 4-Hexen-3-one (NIST MQ 82) | 0.009 | # |
| poss: 3-Hexen-2-one (NIST MQ 82) | 0.014 | # |
| 2-Butanone, 1-hydroxy-3-methyl- (NIST MQ 82) | 0.023 | # |
| Cyclopentanone | 0.074 | c |
| Cyclopenten-1-one, 2- | 0.262 | # |
| Cyclopenten-1-one, 2,3-dimethyl-2- | 0.045 | # |
| Cyclopenten-1-one, 2-methyl-2- | 0.125 | c |
| Cyclopenten-1-one, 3-methyl-2- | 0.058 | c |
| Cyclopenten-3-one, 2-hydroxy-1-methyl-1- | 0.093 | c |
| Cyclopenten-1-one, 3-ethyl-2-hydroxy-2- | 0.021 | c |
| Cyclopentanone, 2-methyl- (NIST MQ 87) | 0.019 | # |
| Cyclopentanone, 3-methyl- (NIST MQ 90) | 0.010 | # |
| Isomere of 2-Cyclopenten-1-one, 3methyl- | 0.020 | # |
| poss: 2-Cyclopenten-1-one, 3,4-dimethyl- (NIST MQ 87) | 0.021 | # |
| 2-Cyclopenten-1-one, 3,4-dimethyl- (NIST MQ 92) | 0.020 | # |
| 2-Cyclopenten-1-one, 2,3,4-trimethyl- (NIST MQ 88) | 0.010 | # |
| 2-Cyclohexene-1,4-dione (NIST MQ 78) | 0.008 | # |
| 2-Cyclopenten-1-one, 2-hydroxy-3,4-dimethyl- (NIST MQ 80) | 0.023 | # |
| **HETEROCYCLIC COMPOUNDS** | | |
| Furans | 0.58 | |
| Furfuryl alcohol, 2- | 0.020 | # |
| Furanone, 2(5H)- | 0.027 | c |
| Furaldehyde, 2- | 0.281 | c |
| Furaldehyde, 3- | 0.057 | c |
| Furaldehyde, 5-methyl-2- | 0.016 | c |
| Ethanone, 1-(2-furanyl)- | 0.043 | c |
| Furan-2-one, 3-methyl-, (5H)- | 0.024 | c |
| Butyrolactone, γ- | 0.115 | c |
| **CARBOHYDRATES** | n.i. | |
| **AROMATIC COMPOUNDS** | | |
| Catechols | n.q. | |

| Compound | % (w/w) | |
|---|---|---|
| Aromatic ketones | 0.01 | |
| Acetophenone | 0.010 | c |
| Lignin-derived phenols | 0.11 | |
| Phenol | 0.041 | c |
| Cresol, o- | 0.031 | c |
| Cresol, p- | 0.015 | c |
| Cresol, m- | 0.012 | c |
| Phenol, 2,6-dimethyl- | 0.005 | c |
| Phenol, 4-ethyl- | 0.008 | c |
| Guaiacols (methoxy phenols) | 0.14 | |
| Guaiacol | 0.104 | c |
| Guaiacol, 3-methyl | 0.005 | # |
| Guaiacol, 4-methyl- | 0.019 | c |
| Guaiacol, 4-ethyl- | 0.009 | c |
| Guaiacol, 4-vinyl- | 0.003 | # |
| Syringols (dimethoxy phenols) | 0.01 | |
| Syringol | 0.011 | c |
| **OTHER ORGANIC COMPOUNDS** | | |
| Non-aromatic esters | 0.13 | |
| Acetic acid 2-hydroxyethyl ester | 0.128 | c |
| N-Compounds | 0.07 | |
| Pyridine | 0.020 | # |
| Acetonitrile (NIST MQ 95) | 0.039 | # |
| Pyridine, 2-methyl- (NIST MQ 92) | 0.010 | # |
| Unknown compounds | 0.31 | |
| unknown overlapping compounds | 0.030 | # |
| overlapping not identifiable compound MW=? | 0.221 | # |
| unknown not identifiable compound (unspecific spectrum) (no NIST spectrum found) | 0.019 | # |
| overlapping not identifiable compound MW=? | 0.031 | # |
| unknown compound (unspecific spectrum) (no NIST spectrum found) | 0.009 | # |

c = calibrated compound
n.i. = not identified
n.q. = not quantifiable compound
# = estimated response factor

# A5. RNA-sequencing data

A complete list of differentially expressed genes throughout the triple-phase process (Figure 4.12, p. 143) according to criteria specified above (cf. 3.13.3, p. 100) is attached to this thesis as data CD including a Microsoft Excel editable data file (A5_RNA-Seq-Data.xlsx).

**Table A5. (attached as data CD including file A5_RNA-Seq-Data.xlsx) RNA-sequencing analysis of the triple-phase process**. The RNA-sequencing yielded a total of 28,720,937 reads as assignable and unique mapping events. Differential gene expression calculations were performed applying RPKM (reads per kilobase) and TPM (transcripts per million) normalization. The strict aerobic state of sample ① served as reference for all following analysis. We defined a significance level at an empirical log2-fold change (m-value) of > 1.50 and < -1.50 (corresponding to a fold-change of 2.80 and 0.40, respectively) and an average value (a-value ) > 1.00 to exclude results that are derived from very few reads. Differentially expressed genes are given within the aerobic (②), microaerobic (③, ④, ⑤) and anaerobic (⑥) phase. Values within the significance constraints were highlighted as significantly up- (black) or downregulated (grey) genes. The locus, feature, product and major COG class is given.

| | | | | m-values | | | | |
|---|---|---|---|---|---|---|---|---|
| Locus | Feature | Product | COG | ② vs. ① | ③ vs. ① | ④ vs. ① | ⑤ vs. ① | ⑥ vs. ① |
| cg0001 | *dnaA* | Chromosomal replication initiator protein DnaA | L | -0.07 | -0.32 | -0.33 | -0.16 | -1.56 |
| cg0005 | *recF* | DNA replication and repair protein RecF | L | 0.11 | 0.01 | -0.47 | -0.69 | -1.83 |
| cg0007 | *gyrB* | DNA gyrase subunit B | L | 0.06 | -0.19 | -0.64 | -0.53 | -1.80 |
| cg0009 | - | Putative membrane protein | - | -0.44 | -0.78 | -1.04 | -1.11 | -2.99 |

…

For full data please refer to the attached data CD.